Time-course of kinetic and kinematic changes in cyclists' pedalling technique with fatigue

Jon Kelly

PhD Thesis

University of Edinburgh

2007

Abstract

The limited research to date that has examined the biomechanical responses that occur with fatigue has been restricted to examining limited discrete time points. Whilst this indicates that changes occur, it does not elucidate their time course. This research therefore seeks to redress this by using continuous collection of kinetic and multiple time windows of kinematic data in the context of cycling. To this end, a unique design of force instrumented pedals were developed and validated against a criterion measures (SRM Power Measuring Crankset) and two methodologies that attempt to increase the accuracy of kinematic data were investigated. Adaptations with fatigue were investigated utilising these equipment and methodologies using a high and a low-fatigue trial both with identical initial stages ending in a ramp up to 95% of maximal minute power (MMP). In the high fatigue trial, the subjects then maintained this power output till failure whilst in the low fatigue trial, power output was returned to 50% MMP and maintained at this level. Results showed significant ($p < 0.05$) trial and time interactions indicating fatigue related changes in the mean Instantaneous Index of Effectiveness (IIE), the crank angle at which positive work started and at which maximum foot angle occurred, as well as minimum knee and maximum hip angular velocities. Within trial analysis of the complete 95% MMP section of the high fatigue trial showed significant effects for the magnitude of peak resultant and ineffective forces and for the crank angle at which peak effective and ineffective forces occurred. Significant changes were also shown for mean IIE, mean power, total work and the crank angle at which positive work started. In the kinematic data, significant effects were also shown in foot minimum and maximum angles, angle of peak knee extension, the crank angle at which maximum hip extension occurred and the maximum hip and knee and minimum knee angular velocities. Post-hoc analyses of these data indicated that the changes in some of the kinetic variables appeared to occur in stages (Instantaneous Index of Effectiveness and the crank angles at the start of positive work and at peak effective force) with similar staged responses also being apparent in the performance measure (power output), with some evidence of possible temporal alignment in the changes in the different parameters. However, stages in the changes observed in the kinematic

variables could not be established. It is concluded that changes do occur with fatigue in cyclist's pedalling techniques and that the time course of these may not be linear or uniform across biomechanical parameters.

Table of contents

Section 1: Technical

Section 2: Kinetic and kinematic changes with fatigue

List of tables

List of figures

List of abbreviations

α	*Alpha* level
η_p^2	Estimated effect size (partial eta squared)
%TTF	Percentage time to failure
Δ	Change in
π	*pi* (3.1415927)
Σ	Sum of
ω_c	Crank angular velocity
(I)IE	(Instantaneous) Index of Effectiveness
ℓ, ℓ_c	Length, of crank
+ve	Positive
AD	Automatic digitising
ANOVA	Analysis of Variance
ASIS	Anterior superior iliac spine
BDC	Bottom dead centre
BON	Bonferroni correction
C, UC	Corrected/ uncorrected
df	Degrees of freedom
EMG	Electromyography
F	F statistic from ANOVA
F_{eff}	Effective force
F_{ineff}	Ineffective force
fps	Frames per second
F_r	Resultant force
FSD	Full scale deflection
F_x, F_y, F_z	Force components acting on the pedals
HF	High fatigue
HJC	Hip joint centre
Hz	Hertz
ICC	Intra-class Correlation Coefficient
J	Joules
Kg	Kilograms
LF	Low fatigue
LSD	Least significant difference
m	Metres
MD	Manual digitising
mm	Millimetres

MMP	Maximal minute power
MS	Mean squares
M_x, M_y, M_z	Moment components acting on the pedals
N	Newtons
P	Power
p	Probability level
PI	Performance index
$\overline{P}_p, P_p$	Mean, power as measured by instrumented pedals
$\overline{P}_s, P_s$	Mean, power as measured by SRM Crankset
R(1/2)	Ramp 1, 2
RA	Relative angle
RMS	Root mean square
s	Seconds
SD	Standard deviation
SPS	Smart position sensor
SRM	Schoberer Rad Meβtechnik, manufacturers of power measuring crankset
SS(1,2-1,2-2)	Steady state 1, 2-1, 2-2
t	Time
TDC	Top dead centre
TE	Typical error
u, v	Coordinates on video image
VA	Angle to the vertical
Var	Variance
-ve	Negative
W	Watts
ε	Epsilon
θ, θ_c	Angular displacement, of crank

Dedication

This thesis is dedicated to my son, Ciarán. You were not born when it began, and it is only the thought of a better life with you when it was all over that kept a light on at the end of the tunnel. Maybe, if one day it inspires you to pursue your dreams, it will have been worth it!

Acknowledgements

Firstly, my sincere thanks must go to my supervisor, Dr Simon Coleman. His guidance and feedback has turned the efforts of an infinite number of monkeys into the work now before you. Without him, this work would simply never have reached completion. My deep gratitude also goes to Ian Hamilton, whose blether eased the long-road and whose creative methods ensured the means were there to make this research possible. Thanks also to Professor Sandy Nicol and John MacLean at The University of Strathclyde for the pedals, other promised, they produced!

The wilderness of a PhD is a lonely place and I am glad not to have walked it alone. For which my heartfelt thanks go to Chris Connaboy and Mandy Winterton who have shared so much of the joy, despair, anger, frustration and apathy along the way and who will both hopefully soon gain those three magical letters after their names, they will be well deserved! My thanks also to those that stuck with me long enough to still be here when I reach the end of the tunnel, despite me never being around, thank you for never stopping believing in me. My gratitude also to my father, who has done much to ensure that there was always food on our table and a roof over our heads and to my Ma, for the example that she set and for always being there for me.

Thanks also of course to the subjects, who gave of their time, energy, sweat and pain to give me the numbers to crunch. Without all of these people, there would be no thesis.

I, Jan Kelly, hereby certify that this doctoral thesis has been composed by me, that it is my own work and that it has not been submitted for any other degree or professional qualification

09/08/07

Chapter 1: Introduction

Biomechanics is the '*application of mechanical laws to living structures, specifically to the locomotor system of the human body*' (Hay, 1993) and, in this respect, is no different to the study of the mechanics of any other system. However, the behaviour of the human performer is dependent upon the biological processes that underlie the function of the system and the complex interactions with the environment in which it operates. The importance of such factors may be most apparent in the field of sports biomechanics, where the techniques examined must be enacted in the high stress environment of competition. Indeed it is this ability to perform in the appropriate situation that distinguishes skill from technique (Sharp, 1992). One such stressor, common in the competitive environment, but absent in the majority of biomechanical studies, is fatigue.

One of the problems encountered in the study of fatigue is the inconsistency with which the term is used. Fatigue has been variously defined as a '*failure to maintain the required or expected power output*' (Edwards, 1983) or, '*the decline in muscle tension capacity with repeated stimulation*' (McArdle *et al.*, 1996). Both of these definitions suggest that fatigue is indicated by a performance decrement. Enoka and Stuart (1985) add to this description an inclusion of increased effort, defining fatigue as '*a progressive increase in the effort required to exert a desired force and the progressive inability to maintain this force in sustained or repeated contractions*'. However, such definitions ignore the fact that the physiological processes associated with fatigue (e.g. substrate depletion, neural fatigue, ionic imbalances, elevated core temperature (Abbiss and Laursen, 2005; Noakes, 2000)) can be shown to begin to occur prior to the manifestation of these deleterious effects. Such definitions also do not concur with the way the term is used in other sciences, such as physics or engineering. Here fatigue is defined as '*the progressive failure of a material due to changes in material properties resulting from repeated stress*' (Morris, 1992). Hence fatigue is regarded as on-going process where an outward manifestation may only be apparent when failure point is reached. Such an approach towards fatigue is also supported by one of the few studies to have examined its effects on the biomechanics of cycling (Black, 1994) who stated that, '*fatigue should... be thought of as a*

continuous slope where at some point the athlete can no longer overcome the effects of fatigue and cessation of the activity occurs'. Indeed, technique changes in fatiguing exercise could occur at one or more of three stages; firstly, prior to the outward manifestation of fatigue, acting to modulate the development of the physiological and/or psychological processes, secondly, as the deleterious effects become manifest to allow the task to be maintained and finally, as the body ceases to be able to continue the task and the ultimate failure point is reached. Therefore, for the purposes of this study, fatigue will be defined as;

> *"a time and intensity-dependent process associated with repetitive or sustained contractions that will, if sustained, lead to enforced performance decrement, technique modification and/or increased mental effort".*

It should be noted from this definition that a lack of psychological or biomechanical changes does not preclude the presence of fatigue. The term 'failure' will be used throughout this study to refer to the point of exercise cessation that ultimately occurs with on-going fatigue.

Whilst there is an extensive body of research regarding the physiological basis of fatigue, the potential effects upon technique have received much less investigation, although this could have important implications for performance or injury (Johnston *et al.*, 1998; Nyland *et al.*, 1999). Previous research has shown that biomechanical changes are apparent with fatigue in various sports including running (Bates *et al.*, 1977; Brüggerman and Arndt, 1994; Chapman, 1982; Chapman and Medhurst, 1981; Elliott and Ackland, 1981; Elliott and Roberts, 1980; Siler and Martin, 1991; Sprague and Mann, 1983; Williams *et al.*, 1991), walking (Winter, 1984) and cycling (Amoroso *et al.*, 1993a,b Black, 1994; Black *et al.*, 1993b; Black *et al.*, 1994; Delextrat *et al.*, 2005; Sanderson and Black, 2003; Sarre *et al.*, 2005) but there remain key questions to be addressed. Those focusing on cycling have shown effects in both the magnitude and timing of forces within the crank cycle, (Amoroso *et al.*, 1993a, b Black *et al.*, 1994), angular impulse (Black *et al.*, 1994) and joint (Amoroso *et al.*, 1993b; Black *et al.*, 1994) and segment (Black *et al.*, 1994) angles, although, Sarre *et al.* (2005) found no changes in work.

Most of the research to date in this area has relied upon comparisons of biomechanical parameters taken close to the start and end points of the trials. However, with this type of analysis, changes that occur within the trial cannot be separated from those that occur immediately prior to task failure. Therefore, the differences identified may only reflect the changes in techniques that occurred as the subjects' ability to maintain an effective technique failed. Consequently, technique adaptations within the trials, which may have served to modulate the deleterious effects of fatigue, could have been missed. Since, it is this potential to limit the effects of fatigue on performance that may be of primary interest to performers, such information may be most germane. Even where more than two time points have been examined, either the number of points or the analysis has been limited and so has provided little information on the time course of changes. Hence, it is not possible to determine whether the changes are progressive, (e.g. linear or exponential) or whether there are some kind of threshold responses, where the athlete's technique 'switches' or whether there are multiple stages of change. Additionally, many of these studies also use protocols with non-constant power outputs (Black *et al.*, 1993b) or running speeds (Adrian and Kreighbaum, 1973; Bates and Haven, 1974; Chapman, 1982; Chapman and Medhurst, 1981; Elliot and Ackland, 1981; Sprague and Mann, 1983), therefore confounding the attempt to isolate the responses with fatigue. Comparisons have also generally been made within a single trial and thus any fatigue related changes cannot be separated from other time dependent processes such as 'warm-up'. The present study will therefore attempt to redress these short-comings by making multiple time comparisons between high and low fatigue protocols.

The current study aims to examine both how the output of the human system changes in its ability to effectively produce the power output required to propel the cycle by examining the applied pedal forces and the outward manifestation of the changes through kinematic parameters. Both of these present technical challenges if the identification of the potentially small changes that occur with fatigue is to be successfully achieved over small time periods.

The study of kinetic changes with fatigue in cycling poses the same technical challenge that have been faced by other investigators examining the kinetics of cycling, namely, that in order to be able to analyse the application of the propulsive forces, specialist equipment is required. Whilst various commercial systems are available which are capable of measuring the applied torque or power output (e.g. SRM Powermeter (Schoberer Rad Meßtechnik, Jülich, Germany), Ergomo Powermeter (SG Sensortechnik, Mörfelden-Walldorf, Germany), Lode Excalibur Sport ergometer (Lode BV, Groningen, The Netherlands), PowerTap hub (Saris/ Cycleops, Madison, USA)) these are not capable of measuring the orthogonal components of the forces applied to each pedal. They therefore have limited value in investigating the responses with fatigue since although only the forces normal to the crank can contribute to its rotation and therefore propulsion of the bicycle, other components of the applied forces may change with fatigue indicating possible changes in the efficacy of force application. Researchers investigating these forces have thus sought to develop systems capable of such measurement with various designs reported capable of measuring either the two force components parallel to the crank rotation (Álvarez and Vinyolas, 1996; Bremble and Brown, 1985; Dal Monte *et al.*, 1973; Gregor *et al.*, 1985; Harman *et al.*, 1987; Newmiller *et al.*, 1988; Soden and Adeyefa, 1979), all three force vectors (Bratt and Ericson, 1985; Coleman and Hale, 1998) or all six forces and moments (Boyd *et al.*, 1996; Broker and Gregor, 1990; Hull and Davis, 1981; Newmiller *et al.*, 1988; Wheeler *et al.*, 1992). For the purposes of the current research, a new design will be presented that is capable of measuring the pedal forces parallel to the crank rotation. Whilst there may be alterations with fatigue in the other force components, only those acting parallel to the rotation of the cranks can affect the propulsion of the bicycle and thereby performance, so for this study the analysis and therefore the pedal design will be restricted to these elements.

Investigation of the kinematic changes that occur with fatigue in cycling also presents methodological challenges since the action is constrained by the rider's attachment to the cycle. There is therefore less scope for gross changes with fatigue than may be observed with other techniques such as running. This is supported by the only study of kinematic changes with fatigue in cycling to have used low/high

fatigue trial comparisons (Sanderson and Black, 2003). This showed that, although there were differences between the start and end of the trial, these were not significantly different in a low or high fatigue trial. Therefore, the successful detection of potentially small changes with fatigue will be dependent upon the minimisation of measurement error. This study will therefore make use of techniques, including a new method, aimed at reducing errors in the calibration process in the kinematic data.

In conclusion, the study of the time course of the changes that occur with fatigue in cycling presents a series of methodological challenges. However, if these can be successfully addressed, it may provide a deeper understanding of how the human body responds in attempting to maintain a sporting technique during conditions of underlying physiological change with fatigue.

1.1: Statement of the problem

Although there exists a substantial body of research on the biomechanics of pedalling techniques in cycling, there is little work examining how it is affected by fatigue. Cycling is a sport where the athlete must continue to perform with high levels of fatigue, sometimes for prolonged periods. Therefore, a greater understanding of any such changes that occur may enhance the knowledge of the manner in which the technique is executed in competition. There has been a small body of work that has examined technique adaptations with fatigue, but this work has yet to elucidate the time course of such changes.

1.2: Aims of the study

The aims of this study are to determine the time course of kinetic and kinematic changes that occur in cyclists' pedalling techniques under conditions of short-term fatigue. It is therefore intended to address the following research questions:

1) During fatiguing, high-intensity, cycling exercise, what changes occur in the magnitude of specific kinetic and kinematic parameters or their relative timing within the crank cycle?

2) What differences are apparent in these parameters in comparison to those that occur within the same time frame in similar lower intensity exercise?

3) What are the time-courses of any such changes?

In order to be able to answer these questions, equipment and techniques are required that are capable of measuring the potentially small changes that occur in these parameters within each time period. Additionally, the collection of the kinetic data will also be dependent upon the use of equipment capable of measuring relatively high pedal forces in the prolonged protocols required. Therefore, a secondary aim of this study is to develop the technical innovations that will be required to answer the primary research questions.

Chapter 2: Biomechanical changes with fatigue; review of literature

Competition introduces many situational factors that are absent during practice which may increase the challenges to performers' skills and therefore may modify the manner in which techniques are executed. One major factor, common within endurance sports, is fatigue. However, the vast majority of research concerning the biomechanics of sports techniques has been conducted in the absence of this stressor and so its effects remain to be fully explored.

The biomechanical changes occurring with fatigue that are the focus of the current research are thought to be responses to underlying psychological or physiological processes. Thus, although the physiological determinants of fatigue are of secondary interest to the current work, some understanding of these mechanisms is required to inform the design and interpretation of the results of the present study and to be able to compare them to the work of previous investigators. Therefore, in addition to the biomechanical changes with fatigue, the physiology of fatigue will also be briefly reviewed.

2.1: Physiology of fatigue

Various models have been proposed to explain the mechanisms by which fatigue occurs during exercise. These include: cardiovascular/ anaerobic; energy supply/ energy depletion; neuromuscular fatigue; muscle trauma; biomechanical; thermoregulatory; psychological/ motivational and central governor which has more recently been expanded as an integrative complex system model (Abbiss and Laursen, 2005).

Examining firstly the cardiovascular/ anaerobic model; this suggests that exercise performance is limited by both the ability of the heart to supply sufficient oxygenated blood to the working muscles and the ability of the cardiovascular system to remove accumulated metabolites. The key criticism levelled at this theory is that the first organ to be affected by the postulated oxygen deficit would be the heart, not the skeletal muscles (Noakes, 2000). The related energy supply/ energy depletion model

attributes fatigue to an inadequate supply of adenosine triphosphate (ATP) to the working muscles. It is suggested that this may arise either from a depletion of substrates (muscle and liver glycogen and glucose) or restrictions in the oxidative or glycolytic energy supply pathways (Abbiss and Laursen, 2005).

Conversely, in the muscle trauma model of fatigue, it is proposed that prolonged exercise may result in physical damage to the muscles, causing significant disruption of the muscle and resulting in changes to the intramuscular chemical homeostasis and activation of pain receptors. This nociceptive neural activation may in turn lead to reduced neuromuscular activation or a reduction in force production by the muscle. (Abbiss and Laursen, 2005)

Proponents of the biomechanical model of fatigue suggest that fatigue is elicited by interaction with some of the processes suggested by the other models. They propose that fatigue leads to deterioration in the co-ordination of the movements resulting in increased metabolic energy requirements for the same intensity. Thus greater demands are placed upon other physiological mechanisms leading to the changes suggested by the other models. (Noakes, 2000)

Advocates of the thermoregulatory model suggest that fatigue results from the increased core temperature that occurs with prolonged exercise. This elevation in temperature is thought to increase the physiological demands placed upon other systems and thus, similarly to the biomechanical model, lead to changes via the mechanisms suggested by some of the other models (Gonzalez-Alonso *et al.*, 1999).

The psychological/ motivational model suggests that rather than the performance of the task being limited by physiological mechanisms, it is a psychological phenomenon mediated by physiological inputs. Support for this theory stems from the fact that there is no apparent single physiological variable that can be demonstrated to be responsible for the alterations in motor unit response to afferent signals (Abbiss and Laursen, 2005). It is therefore suggested that several physiological mechanisms lead to psychological changes in central activation and perceived exertion. These, in turn, determine the unconscious perception of fatigue, leading to reductions in the intensity of activity that is maintained and, potentially,

the attainment of a point of exhaustion (Noakes, 2000). Similarly, the central governor model suggests that peripheral inputs from the active muscles, chemo and thermoreceptors and other areas are integrated by a central mechanism and exercise intensity mediated to either optimise exercise performance (Ulmer, 1996) or protect vital organ functions (Hampson *et al.*, 2001).

However, as Noakes (2000) stated, '*it is highly improbable that the factors explaining human exercise performance under all conditions are restricted to one physiological system... Thus, human performance is unlikely to be adequately defined by any of these unitary models*'. In attempt to address this quandary, a complex systems model of fatigue has been proposed. This suggests that exercise performance is continuously manipulated in response to the interaction of numerous physiological systems that are monitored via constant feed-backwards and feed-forward loops (Figure 2-1). The exercise is therefore continually regulated to achieve the objective task, for example, maintaining the power output for as long as possible, whilst avoiding pushing any of the peripheral systems beyond homeostatic limits.

It is not within the scope of the present study to attempt to evaluate these various theoretical models or indeed to ascertain which are pertinent to the present and reviewed research. Indeed, any such attempt would be problematic since, as Noakes (2000) stated, '*an important weakness in our current thinking in exercise physiology is that we lack certain knowledge of the precise factors that determine fatigue and hence limit performance in different types of exercise under a range of environmental conditions*'.

However, perhaps of more importance to the present study, is an understanding of the various time courses over which the effects of fatigue may be manifest. These can be broadly defined as short (up to 30 seconds), intermediate (up to 10 minutes) and prolonged (30 to 180 minutes) (Maughan and Gleeson, 2004). Thus, although the underpinning mechanisms may not be clear, it is likely that subjects performing exercise tasks of a similar nature and duration that fit within these time brackets are likely to possess similar fatigue responses and should therefore be comparable in terms of technique responses. However, the mechanisms which contribute to fatigue are influenced by the type and intensity of the exercise, the muscle group involved

and the physical environment in which the task is performed, so that, '*even relatively subtle variations in task can be associated with marked difference in the time to task failure*' (Hunter *et al.*, 2004).

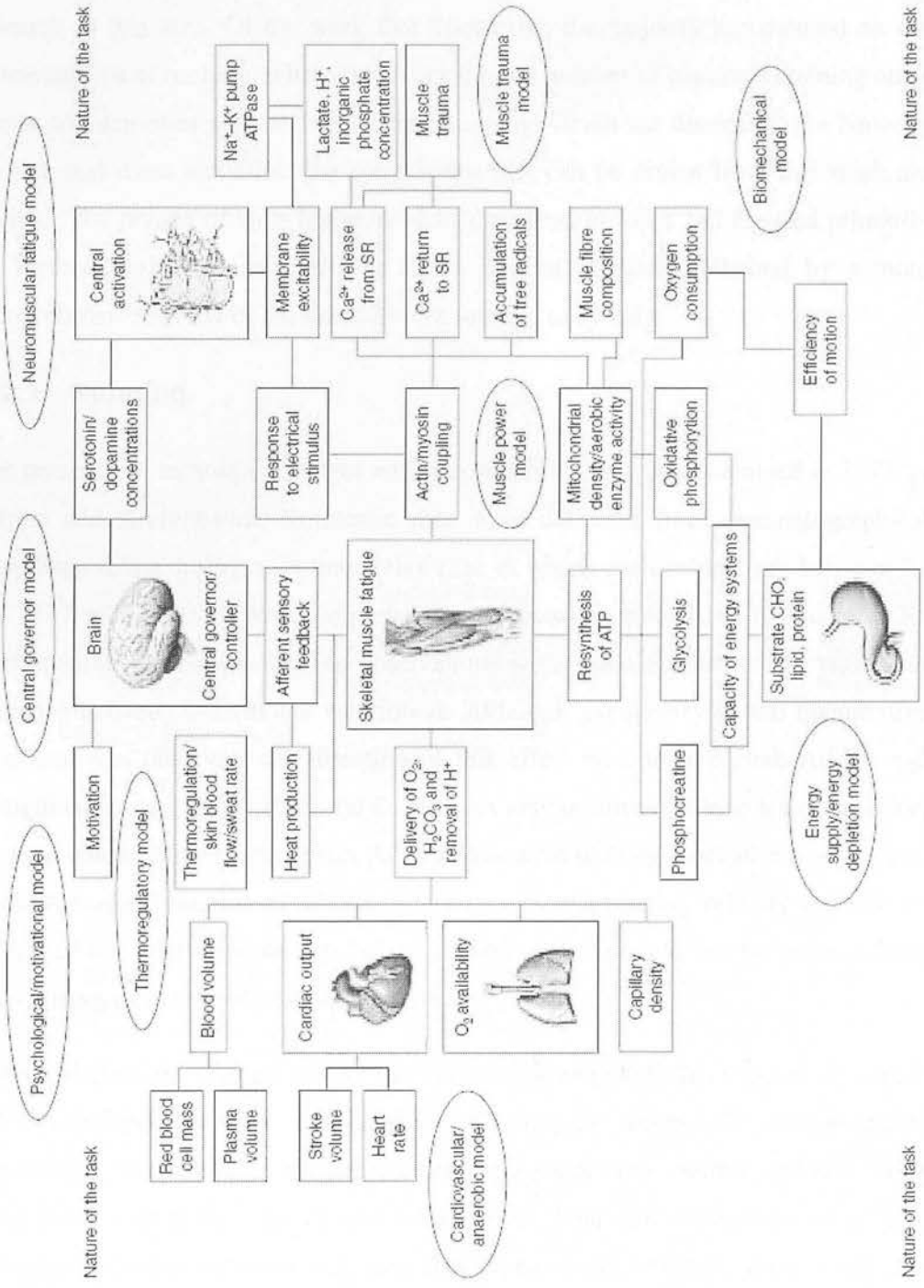

Figure 2-1: Schematic representation of complex systems model. ATP: adenosine triphosphate, ATPase adenosine triphosphatase, CHO: carbohydrate, SR: sarcoplasmic reticulum (Abbiss and Laursen, 2005)

2.2: Biomechanical changes with fatigue

Although it has been recognised by researchers for over thirty years that athletes' techniques are subject to change as they become fatigued, there is still a sparsity of research in this area. Of the work that does exist, the majority has focused on the biomechanics of running, with only a very limited number of papers examining other sports and activities such as rowing and jumping. Given the dissimilarities between cycling and these activities, the conclusions that can be drawn from this work are limited. The review of such literature shall therefore, be brief and focused primarily on methodological issues pertinent to the current research, followed by a more comprehensive review of the limited work relating to cycling.

2.2.1: Running

The presence of technique changes within competition was first examined in 1973 by Adrian and Kreighbaum. Kinematic data were collected from cinematographical recordings taken during a 24 hour relay race in which each subject ran between 27 and 31, 1-mile intervals with comparisons made between miles 10 to 12 and 28 to 30. Both qualitative and quantitative observations were made but little clear pattern of response between individuals was found. Although asymmetry in the quantitative measures was observed, the direction of this effect was not reported. Adrian and Kreighbaum noted that such lateral differences may be attributable to leg dominance, postural abnormalities and the fact that subjects were running clockwise on a circular track. A major limitation of this study however, is that running velocity was neither measured nor controlled so any fatigue related changes could not be isolated from ones arising from altered running velocity.

Bates and Haven published a paper the following year (1974) that focused on female runners competing in a 4x440 yard (402 metres) event. Cinematographical recordings were obtained at approximately 185 yards (169 metres) and 405 yards (370 metres) from the starting line with various kinematic parameters examined. Although changes between the two conditions were reported, these were not statistically analysed. Also, running velocity was again neither measured nor controlled and no indication of inter-subject differences, such as those reported by

Adrian and Kreighbaum, were given. One of these limitations was redressed by a later presentation of the same data (Bates *et al.*, 1977) which showed statistically significant changes in some of both the temporal and kinematic variables and provided evidence of bilateral asymmetry. The authors thus concluded that, '*fatigue does not simply produce a consistent uniform reduction in the components of the movement pattern but rather changes their relationship completely*".

The work of Elliott and Roberts (1980) was the first to attempt to control running velocity and thus prevent introducing a confounding variable. To achieve this, their subjects ran a 3000 metre timed effort with markers placed around the track with an auditory signal provided to allow the subjects to regulate their pace. This methodology was successful in that no statistically significant differences were found between horizontal velocities at each of the four stages (500, 1300, 2100 and 2900 metres). This research therefore also represented an advance by using analysis at multiple time points rather than the simple low/ high fatigue comparisons previously conducted. However, although statistically significant results were reported between variables at the 2900 metres point and several of the three other stages, these were obtained with Newman-Keuls post-hoc tests with α set at 0.1. These procedures are sometimes considered too liberal and do not fully control for the experiment-wise error (Field, 2000), which, combined with the high α-level, makes the results susceptible to type I errors. Also, the authors erroneously conclude that '*as there were no statistical*[ly significant] *differences in velocity over the four stages of the trial, any variations in the biomechanical variables measured* [can] *be attributed to the fatigue effects of the race effort*'. Indeed, whilst high levels of fatigue may be assumed for the type of effort undertaken, the absence of a performance decrement throughout the trial removed the study's only positive indication of fatigue. Thus, time related effects such as 'warm-up' cannot be discounted (Mohr *et al.*, 2005) or inferences about causality made.

A later paper by Elliott and Ackland (1981) examined change in running technique during the course of a 10 kilometre race, again examining four stages (780, 3980, 6790 and 9580 metres). However, since data were obtained from a competitive event, horizontal velocity could not be controlled and significant differences were shown

during the course of the race. Significant differences were also found in the kinematic variables examined with the trend of the changes shown to be linear or quadratic in nature.

Chapman and Medhurst (1981) showed inter-individual differences in modification of technique with fatigue in runners, but noted that '*individual fatigued running styles are just as repeatable as are normal un*[-]*fatigued styles*'. In a subsequent paper Chapman also reported an attempt to establish a hierarchical structure of the same data, i.e. to establish which were primary changes and which were secondary effects of the primary changes (Chapman, 1982). This indicated that, even where changes in overall parameters (e.g. cycle time) were consistent across the group, there were individual responses in their components (e.g. stance and recovery time). The authors thus concluded that, '*the individual directional nature of temporal and kinematic changes can lead to an absence of a change when the subjects are considered as a group*'. However, again, running velocity was not constant between the two conditions and the 'fatigued' observations were taken whilst the subject ran against a pacer towards the end of the 400 metres, whilst the 'non-fatigued' condition was recorded at the start of the run whilst the subject ran alone. All of these factors might produce kinematic changes that could thus be falsely attributed to fatigue effects.

The following year, Sprague and Mann (1983) added to the understanding of the effects of fatigue on running by including both kinetic and kinematic variables in their study. The fatigue trial used a 400 metre run with data collected at 40 and 380 metres. The investigators showed significant changes in kinematic parameters and also linked these changes to alterations observed in joint moments related to the subjects' change in centre of mass velocity. As noted previously, since running velocity was not held constant in the two conditions and was shown to vary considerably, the effects may not be attributable solely to fatigue. Although the authors report that the kinetic variables during the 'fatigued' state were 'unlike' those observed in research with the same subjects in a 'non-fatigued' state (Mann *et al.*, 1980), without indications of the reliability of the data and a statistical analysis this cannot be taken as supporting the attribution of the changes to fatigue. The research was also limited in that ground reaction force components were derived from centre

of mass accelerations and therefore there may have been errors in the estimation of these forces. Further, unilateral video analysis was used and therefore, possible asymmetry could not be examined. Indeed the authors do not report which side was examined or whether this was the same in all cases.

Siler and Martin (1991) attempted to achieve standardisation of running velocity by conducting their testing using a treadmill with the speed set to attempt to replicate the subjects' 10 kilometre race pace according to their most recent time for that event and prior $\dot{V}O_2max$ and physiological economy tests. For the 'slow' and 'fast' groups investigated, this resulted in intensities equivalent to 81% and 87% of the runners' $\dot{V}O_2max$ and times to volitional exhaustion of around 43 and 35 minutes for the 'slow' and 'fast' groups respectively. Kinematic parameters were recorded and also used to estimate mechanical power. Siler and Martin reported that the changes relative to baseline commonly occurred at 70% or later of time to failure with limited indication of differences in the responses between the two groups. The authors also noted substantial individual differences in these changes. However, since a lower fatigue trial was not included, changes cannot be definitively attributed to fatigue rather than time. Also, kinematic data were collected at fixed time points and then linear interpolation used to calculate these variables at points relative to the time of volitional exhaustion. This assumed that the changes are linear throughout the trial which may not be valid and the authors do not report any attempt to verify this.

Williams *et al.* (1991) made use of both treadmill and track running, with the outdoor runs being recorded for both competitive and non-competitive runs. The kinematic data obtained at four time points within each of the track runs and every '*one or two minutes*' of the treadmill run, were compared to that obtained from a series of short 'rested' trials with linear interpolation being used to match the running speeds of the 'fatigue' trials. Unlike Siler and Martin's (1991) work, the interpolation procedure was selected on the basis of previous pilot work that indicated data were best approximated using a linear fit. However, the authors found that significant differences existed between the rested data and that from the initial stages of the 'fatigue' trials and again used interpolation to correct for these, for which no validation was reported. The authors found little apparent differences between the

three fatigue trials but stated that, although significant differences were found in some of the dependent variables, '*fatigue did not result in marked changes in kinematics for the group as a whole* [but], *changes for individuals were at times large*'.

Darras and Burden (1994) also used a treadmill with constant running velocities set to elicit 90% of $\dot{V}O_2$max. This brought subjects to volitional exhaustion at around 18 minutes. The kinematic measure used by the researchers was the three-dimensional linear range of motion which the authors defined as '*the volume... which enclosed the path of the body landmark* [i.e. joint centre,] *during a complete stride*'. Why these measures were used was not indicated and no significant changes were found compared to the baseline at each of the time points used (60%, 75%, 90% or 100% of time to failure). This may be partly attributable to the very low subject numbers (n = 4), especially when, as the authors note, '*analysis of each individual athlete's response to fatigue revealed very distinctive kinematic adaptations*'.

The work by Evans *et al.* (1994), also used a treadmill to control running speed. The female athletes used were required to run at a treadmill speed set to elicit approximately 75% of the subjects' $\dot{V}O_2$max with video data recorded every five minutes. However, time to failure was not reported. The authors adopted a novel approach to the analysis of the kinematic data by utilising phase plane plots (joint angular velocity plotted against joint angle) and showed significant changes in the area under the phase plane plot curves with fatigue. Whilst such changes may be taken as indicative of intra-cycle velocity changes, their mechanical basis or impact was not discussed.

Brüeggemann and Arndt (1994) used an instrumented treadmill and measured kinetic, kinematic and EMG parameters. This work was also of note in that two different types of fatigue were distinguished; aerobic and local muscular fatigue. Whilst these were not defined, it was reported that the aerobic fatigue was induced by running for 45 minutes at 3.5 $m.s^{-1}$. However, although the authors stated that a foot muscular training device was used to produce the local muscular fatigue, details such as intensity and duration were not given. Differences in comparison with the pre-fatigue running techniques were shown for kinematic parameters for the local

muscular fatigue trial and for both kinematic and kinetic measures in the aerobic fatigue trial. However, details of the protocol used for collecting the kinematic data were not given, so it is not possible to determine whether observed changes are attributable to 'warm-up' effects or can be asserted to be fatigue-related. The indigent reporting of the study also omits details of which parameters were actually examined and whether both sides of the body were analysed.

Kinetic changes with fatigue were also investigated by Nummela *et al* (1994), as well as EMG. Their protocol involved three separate trials; a maximal 20 metre sprint, a 400 metre timed run and sub-maximal runs at the average speed of the first 100 metres of the 400 metre run. Data were collected from a 4 metre long force platform system positioned at 6 to 10 metres before the end of each distance. Significant differences were found in the ground reaction forces between both the maximal and sub-maximal 20 metre runs and the end of the 400 metre trial. These differences were most apparent in the braking phase of the stride where the authors noted that the contractions of the leg-extensors were mainly eccentric. Nummela *et al.* therefore attributed this to altered stiffness characteristics of the muscle resulting in reduced elastic energy storage.

No further research detailing kinetic or kinematic changes in running were published until Christina *et al.* (2001). This showed significant changes in ground reaction forces and leg kinematics with localized fatiguing of the dorsiflexors or the invertors of the foot. However, the applicability of the findings of such research, where isolated muscles are fatigued, rather than the more generalized fatigue associated with gross dynamic movements of the type to be used in the current research, may be limited.

Recently, Gerlach *et al.* (2005) showed changes in kinetic impact parameters following an exhaustive treadmill run for female athletes running at their approximate 5 km race velocity. Contrary to the finding of some of the previous work examining kinematic parameters, the authors reported that bilateral differences were not apparent in the kinetic data. However, this finding cannot be related to the other studies to have examined kinetic parameters in running since these have either not measured or not reported asymmetries. Data were obtained for the first six strides

in the pre and post fatigue trials and so no time course of fatigue related changes could be ascertained and any such effects cannot be separated from possible time related changes.

2.2.2: Other sport techniques

In addition to the research examining running, there is a limited body of work investigating other activities. For example, rowing was examined by O'Donovan and Anderson (2000). The authors investigated the kinematic changes that occurred during the course of a 2000 metre ergometer row with data taken at 150, 500, 1000, 1500 and 1950 metres using both standard kinematic variables and angle-angle plots (knee angle against elbow angle). Comparisons were then made between the technique at 150 metres and all other distances. Although significant effects were shown in all of the parameters within the trial, little information was given as to the time-course of these changes. The other key methodological flaw was the use of the technique at 150 metre as the '*prototypical stroke*'. The inter and intra-trial reliability of this technique was not established in reduced fatigue conditions (Anderson, 2002) so it is unknown if this could be taken as representative of a low-fatigue technique. Therefore, other time related effects cannot be discounted and so attribution of the observed changes to fatigue could be erroneous. The authors also only standardised the estimated distance covered by the subjects and did not report the duration of the trials or estimated velocities. Therefore, it is not possible to determine if all subjects were likely to be influenced by the same fatigue mechanisms. Further, the identification of fatigue related changes may have been confounded by the presence of technique alterations with velocity changes.

Jumping tasks have come under investigation by Chappell *et al.* (2005) and Rodacki *et al.* (2001), both of whom examined both kinetic and kinematic parameters with Rodacki *et al.* also including EMG data. Rodacki *et al.* used a vertical jumping task with exercise in a knee flexor/ extensor 'weight machine' used to induce fatigue, whilst Chappell *et al.* used stop-jump tasks and developed fatigue with a combination of vertical jumps and 30 metre sprint runs. Both works reported fatigue effects in kinetic and kinematic parameters, however, Rodacki *et al.* found that these were only apparent when the knee extensors rather then knee flexor muscles were fatigued.

However, the key flaw in the fatigue protocol used by Rodacki *et al.* is that biarticular muscles complicate attempts to isolate the muscles associated with a particular task. For example, although the hamstrings group (m. biceps femoris, m. semitendinosus, m. semimembranosus) act to both flex the knee and extend the hip and therefore their fatigue could affect the execution of the task The authors themselves noted '*gluteus maximus, which was not fatigued in* [the] *study, is the strongest hip joint extensor and performs most work necessary to extend the hip joint*'. Therefore, unlike for the knee extensor trial, in the knee flexor fatigue trial, the primary task specific muscles were not fatigued and this therefore actually represented an effectively lower-fatigue state. Both papers also only compare 'non-fatigued' and 'fatigued' conditions and therefore do not illuminate the time course of changes.

In summary, although the finding of the research that currently exists on biomechanical changes with fatigue in other sports and activities do not directly inform the present study, examination of the limitations of the work can help to inform the approaches of the present study. The first common limitation is that much of the research has been restricted to limited time points therefore not allowing the process of change to be examined. Even in the studies that have collected data from multiple time points, these have presented only limited explorations of this information. Secondly, data have not been collected for sufficient times prior to the fatiguing activity, so it is not possible to determine if a stable technique had been obtained prior to the development of increased fatigue and so time related changes cannot be discounted as an explanation of any changes observed rather than fatigue. Thirdly, the durations and intensities of the activities used by the various researchers to elicit high fatigue levels have varied greatly and so physiological fatigue mechanisms and therefore biomechanical responses to them may vary, thus making comparisons between studies problematic. Fourthly, despite clear indications of asymmetry in kinematic responses to fatigue, several of the studies have been restricted to unilateral data collection. The final general criticism that can be levelled at much of this work is the failure to control confounding variables such as horizontal velocity and, in almost all of the work to date, a failure to isolate fatigue related effects from other time related changes. This deficit is compounded by a

common potentially erroneous attribution of observed changes to fatigue. As previously discussed, the mechanisms of fatigue are uncertain and highly task dependent and therefore quantifying levels of fatigue or the time-course of its development is highly problematic. Therefore, since the presence of fatigue can only be implicitly indicated, and other time related parameters may be involved, statements regarding the causality of changes should not be made. Thus, whilst indirect indicators of fatigue, such as a decrement or cessation of performance, may legitimate describing biomechanical changes as 'occurring with' fatigue, it does not allow these effects to be appropriately described as 'caused by' fatigue.

The studies reviewed also indicate that, to eliminate the need to use interpolation in order to obtain data at times relative to failure point, data collection should ideally be continuous. Further, the individual differences in the response to fatigue suggest potential problems in the statistical analysis of group data.

2.2.3: Cycling

Unlike the case of running, the changes that occur with fatigue in cycling have only come under investigation in recent years. The first of these studies was that of Amoroso *et al.* (1993b) who used a trial where both power output and cadence were controlled. The authors reported significant differences in peak normal (339.4 N, 370 N) and shear forces (79 N, 68 N, both 'non-fatigue' and 'fatigue' respectively) as well as the crank angle at which these occurred, although details of these changes were not reported. They also found differences in the kinematic parameters including maximum hip flexion (105°, 106°) and extension angles (145°, 147°), and ankle dorsiflexion (85°, 90°) and plantar-flexion (108°, 112°, all 'non-fatigue' and 'fatigue' respectively) angle. However, the work was only published as an abstract and so further details of the research, such as the pedal instrumentation or whether bilateral data were obtained was not reported.

Black *et al.* (1993b) utilised both video recording and an instrumented pedal to obtain kinematic and kinetic changes during a cycling $\dot{V}O_2$max test. Comparisons between the initial and final minutes of the trial showed greater forces at the end of the incremental test and changes in the crank angles at which maximum resultant

force, as well as its components (F_z and F_y), were applied. In each case, this trend was for the forces to be applied earlier in the pedal cycle. Black et al. also reported that the mean Index of Effectiveness (i.e. the ratio of the force normal to the crank to the resultant force) increased from 0.30 (30%) in the first minute to 0.60 (60%) in the final minute. The authors showed significant differences in the kinematic parameters with the ankle becoming significantly more dorsiflexed and concurrent changes occurring at both the knee and the hip joint as well, although details of these were not reported. There are however three key limitations of this work. Firstly, the analysis was unilateral and therefore whether or not asymmetries similar to those identified in several of the running papers were present cannot be ascertained. Secondly, since only start and end points were examined, the time course of the changes is unknown and no indication as to whether a stable technique had been achieved in the first minute is available. The final criticism is the use of non-constant power output since, as Black later acknowledged, '*the changes in ... the incremental exercise could be a result of increased power output, a result of fatigue or some combination of the two*' (Black, 1994). Indeed, some of the changes, i.e. increases in the magnitude of the forces would clearly be expected with the differences in power output between the two sections.

This limitation was redressed by the authors in a subsequent paper (Sanderson and Black, 2003) by using two constant power trials. The first of these was designed to elicit high level of fatigue by requiring subjects to maintain 80% of their maximal minute power (MMP) whilst the second, which was of equal duration, only required 30% MMP to be maintained. As for Black *et al.* (1993), kinetic and kinematic data were again compared for first and final minute of the trials. Sanderson and Black reported that minimum effective force (i.e. that acting perpendicularly to the crank in a plane parallel to the crank rotation), positive angular impulse, minimum thigh and shank segment angles, maximum ankle plantar-flexion, knee flexor and hip extensor moments all differ significantly between the first and final minute of the 80% MMP trial. The authors further stated that no significant differences between the two time points were found in the 30% MMP trial. However, the research was based upon the thesis of Black (Black, 1994) which included other variables in its analysis and showed significant changes in many of these within the 30% MMP trial specifically;

maximum hip extension, knee flexion, ankle dorsiflexion, mean index of effectiveness, total angular impulse, negative impulse, maximum ankle plantar-flexor, knee and hip flexor moments. As well as differences in the crank angle at which maximum knee extension, maximum resultant forces and force normal to the pedals, start of negative impulse, maximum hip flexor and ankle plantar-flexor moment occurred. Thus, the results of the two reports of the same research are in some cases contrary (mean Index of Effectiveness, negative impulse, maximum ankle plantar-flexor, and knee and hip flexor moments) and in the remainder, omit findings which could alter the impression given of the data. It is thus unclear if the original work is incorrect or its subsequent published form or why potentially relevant findings were excluded. The limitations previously identified of Black *et al.* (1993b) in regard to examining only start and end points and the use of unilateral analysis clearly also apply to these works.

Recently, Sarre *et al.*(2005) investigated the effects of cadence upon kinetic as well as EMG parameters during a one hour ride at 65% of the subjects' maximal aerobic power (maximal minute power). The authors reported that although significant differences were found between cadences for positive and negative work as well as peak torque, no such effects were apparent over time, i.e. there was no indication of kinetic changes with fatigue. However, this may be attributable to the limitations of the equipment used, i.e. strain-gauge instrumented cranks (LODE Excalibur) which are not capable of resolving the orthogonal vector components of the applied forces which may have revealed more changes. The authors also stated that measurements were made for the right leg only. However, unilateral measurements are not possible with the instrumentation applied to the cranks since torques will be transmitted from the opposite crank via the crank bearings. It may also be that the intensity was insufficient to produce sufficient fatigue within the trial to elicit significant effects. Although, the authors do report that all participants perceived the higher cadence trial to be '*a very intense effort, which could not have been sustained for much longer*'. Since the previous works investigating cycling have only examined start and end points, it is not possible to ascertain whether these apparent contradictions are due to technique alterations only occurring immediately prior to failure or whether this is

indicative of specific intensity/ duration effects. In either case, this is contrary to the findings of some of the running related research.

Delextrat *et al.* (2005) examined the biomechanical effects of fatigue in triathlon and focused upon the effects of fatigue resulting from swimming on subsequent cycling technique. The cycling trial consisted of a 10 minute ride at 75% of maximal aerobic power (maximal minute power) on a cycle ergometer immediately preceded by either a 750 metre swim at competition pace with or without drafting, or cycling at 30% maximal minute power for the same duration. Results did not indicate any significant differences in the kinetic parameters between the low intensity cycle trial and the swim trial with drafting. However, significant differences were shown in cadence and mean torque for both where the dominant and non-dominant legs were on the down-stroke of the crank cycle and the peak torque during the down-stroke of the non-dominant leg. These results are therefore contrary to the findings of Sarre *et al.*(2005). However, the same technical limitation that was apparent in Sarre *et al.*'s work was also apparent in that of Delextrat *et al.* in that orthogonal force components could not be resolved nor each side measured independently. A further limitation of the work is that, although the authors report that kinetic parameters were recorded for the last 30 seconds of each minute, no time course of change was reported, nor indeed at what time the significant differences were found. It should also be noted that the changes in torque reported were all toward higher magnitudes in the non-drafting trial which are therefore also at least partly explicable by the concomitant decrease in cadence.

The paucity of research in this area therefore leaves many questions unanswered. All of the limitations previously noted with the review of studies relating to running and other activities, are also applicable to those related to cycling. Firstly, time, power output and cadence have not been controlled thus introducing confounding variables and again, potentially erroneous attributions to fatigue have been made. Secondly, that unilateral analyses have been used despite much of the running related research indicating that this may not be appropriate. Finally, to date, no research has explored the time course of the changes that have been observed. Without this information, it is difficult to ascertain whether fatigue related changes in technique occur

progressively during exercise which elicits high levels of fatigue or merely represent the disintegration of technique immediately prior to task failure. Without this knowledge, it is not apparent whether interventions could productively alter cyclists' biomechanical responses with fatigue and thus offer performance benefits. Therefore, the work that exists to date possesses limitations and methodological flaws and therefore further investigations in this area are warranted.

Chapter 3: Kinetics and kinematics of cycling; review of literature

Although the biomechanics literature is largely devoid of work concerning the effects of fatigue in cycling, there is a wealth of research investigating other biomechanical aspects relevant to the sport. However, not all of this broad range of research is pertinent to the current investigation and so will not be reviewed here. Areas that will be largely omitted include those focused on clinical applications and those investigating the effects of an incline or riding out of the saddle or in a recumbent position. The former will be omitted since, although biomechanical changes with fatigue may have clinical implications, this is not within the scope of the current work and findings from this work are unlikely to be directly applicable to the non-clinical competitive populations to be used in the current investigation. Further, since research into biomechanical changes with fatigue in cycling is very much in its infancy, the latter may be regarded as a special case and therefore will also be excluded, though such situations may be appropriate for later investigators. However, where research in either of the aforementioned areas does overlap with the current work, it will be included.

This review will therefore focus on research that is most pertinent to the current work. This can broadly be categorised as that which has examined the effects of different task attributes, subject characteristics and bicycle configurations upon technique. Also, a range of papers exploring the theoretical basis for interpreting the biomechanical parameters will be reviewed. Whilst there is a degree of overlap in some of the work between these areas, to facilitate the clarity of the review of literature, the research will be examined under these headings.

3.1: Task attributes

Whilst the constrained nature of the pedalling technique in cycling may make it an apparently simple task, there are a host of parameters that can be manipulated that may influence the manner in which it is executed. These include the prescribed cadence and power outputs as well as the nature of the equipment which the subjects

are required to ride. Thus it is necessary to understand the effects of such parameters if their effects are not to confound those related to fatigue.

3.1.1: Effects of cadence

One of the key parameters that a rider is normally free to manipulate in order to respond to changes in the requirements of the pedalling task, such as changes of gradient, power output or fatigue levels, is cadence. This has therefore been the subject of several investigations. Ericson (1986) showed hip flexion and extension moments and knee extension moments to increase with cadence across the range tested (40, 60, 80 and 100 rev.min^{-1}). However, this study simultaneously manipulated power output and so the observed differences may not necessarily be attributable to the effects of cadence

In the same year, Sargeant and Greig (1988) examined maximum leg force and its proportional utilisation in cycling using instrumented pedals. The maximal peak forces were established by connecting the cycle ergometer to an isokinetic drive mechanism. The subjects were then asked to pedal at a maximal intensity for twenty seconds at the set cadence. The pedal forces were also measured during a progressive exercise test. The results indicated that, for both tests, peak pedal forces decreased with increasing cadence. Although this may expected given that power is the product of force and velocity. They also observed that the proportion of the maximal force required at any given level of exercise also fell with increased pedal rate (62% at 45 rev.min^{-1}, 50% at 75 rev.min^{-1}, 44% at 100 rev.min^{-1}). From this observation they stated that '*the greater reserve of force generating capability at the higher pedalling rates suggests a lower peripheral (muscle) stress and this could be an important factor in delaying the onset of fatigue during sustained activity*'. It was further suggested that this may be related to the selection of higher cadences by competitive cyclists.

Takaishi et al. (1998) combined force pedal and EMG data in an attempt to clarify why trained cyclists tend to prefer higher cadences than non-cyclists. They reported that the peak pedal forces were higher in the non-cycling athletes compared to the cyclists at each of the power outputs and cadences set. From this, together with EMG

data, they concluded that '*cyclists have a certain pedalling technique for positive utilisation of the knee flexors to decrease peak pedal force and alleviate muscle activity for the knee extensors*'. They further speculated that '*pedalling skills that decrease muscle stress influence the preferred cadence selection, contributing to recruitment of* [slow twitch] *ST muscle fibres with fatigue resistance and high*[er] *mechanical efficiency*'.

More recently Marsh *et al.* (2000) used a moment based cost function to look at the relationships between preferred cadence, power output and cycling experience. The sum of the average absolute joint moments at the hip, knee and ankle was taken as a cost function for each cadence and power output. The cadence at which this was lowest was defined as the cost function cadence. This was shown to increase with power output but was not different across the three subject groups (cyclists, runners and less trained non-cyclists) for each of the power outputs. Also, the correlations between the cost function cadence and the preferred cadence at each of the power outputs were not found to be significant. However, as noted by Kautz and Hull (1995), joint moment cost functions do not necessarily reflect optimisation in terms of muscle energetics and so may give an incomplete picture of optimisation.

Efficiency has also been reported to decrease with increasing cadence (Black *et al.*, 1993a) as measured by the Index of Effectiveness (IE). This measures the percentage of the applied linear impulse that is used to generate angular impulse, i.e. the 'effective' component, as;

$$IE = \frac{\int_{t_0}^{t_1} F_{eff}\,dt}{\int_{t_0}^{t_1} F_r\,dt} \times 100$$

Equation 3-1 (Black, 1994)

Where F_{eff} is the effective force (i.e. that normal to the crank), F_r the resultant and t_0 and t_1 the start and end times of the integration. This is thus analogous to the Instantaneous Index of Effectiveness used in the present thesis. Bertucci *et al.* (2005) have also shown that in on-road riding, in addition to the expected increase in torque with reduced cadence, torque minimas also occurred earlier in the crank cycle. This latter effect, the authors attribute to differences in the crank inertial load.

It is therefore clear that cadence affects a broad range of biomechanical parameters and therefore must be controlled if fatigue related changes are not to be obscured.

3.1.2: Effects of power

Much of the research that has been conducted upon biomechanical changes with fatigue has used either non-constant power outputs, or related parameters such as running velocity, in the fatiguing exercise. However, non-fatigue specific research has shown that power output effects in both kinetic and kinematic parameters. Soden and Adeyefa (1979) showed that although force production patterns were similar at various power outputs, peak forces increased with power output (450 N at 434 W and 90 rev.min^{-1}, 580 N at 772 W at 130 rev.min^{-1}). At the higher power outputs, the negative torque during the upstroke also became positive, rising to ~100 N at 906 W at 130 rev.min^{-1}. However, a number of criticisms can be made of this study. Firstly, the pedal angles were not recorded but assumed to remain horizontal, therefore the normal and tangential forces could be in substantial error. The authors themselves noted that measurements taken from the cine recordings showed pedal angles of up to 50°. The overall presentation of results was also unclear. For example, there was no table of data and results are inconsistently given as group means or individual scores and both normal and tangential values are not always included in the text. Also, it was often not stated whether the forces being reported were normal, tangential of resultant. Finally, the workload settings on the ergometer also appear questionably high. These reached 906 W which, although possible for short durations, would probably be equivalent to in excess of the twice the subject's power output at $\dot{V}O_2max$ (Arts and Kuipers, 1994).

Davis and Hull (1981) later presented research showing that pedalling efficiency increases with power level. The authors defined efficiency according to a performance index (PI) scale as;

$$PI = \left(\frac{1}{360 F_{max}} \sum_{\theta_c=1}^{360} T(\theta_c) \right) \frac{1}{\ell_c}$$

Equation 3-2 (adapted from Davis and Hull (1981))

where F_{max} is the maximum resultant force in the plane parallel to the crank rotation, T is crank torque, θ_c is the crank angle and ℓ_c is the crank length. Although, this conclusion was based upon a single subject and must therefore be treated with caution, it was supported by the work of Black *et al.* (1993a) who used a greater number of subjects, although using a different measure of efficiency (IE see Equation 3-1).

The effect of manipulating power output whilst maintaining a constant cadence was examined by Kautz *et al.* (1991). Their subjects were elite male time-trialists who rode at a range of power outputs that increased from '*similar to an easy training ride to similar to a 40 km competition*' (time-trial). Results showed that amongst the subjects, there were two techniques for responding to the increasing demands. For some of the subjects the pedal orientation was largely unaltered with the higher power outputs being achieved largely by increasing the magnitude of the vertical force component in the down-stroke. Conversely, the other subjects, whilst also increasing the down-stroke vertical component, also increased the horizontal component between 0° and 90°. Additionally, they reported that, whilst at low workloads the torque about the bottom bracket was negative during the upstroke, this generally became positive as the workload increased. However, this did not contribute to the external work serving only to reduce the total work required during the down-stroke.

The research thus evidences substantial effects of power upon the biomechanics of the pedalling technique. This creates a quandary for research investigating the effects of fatigue since, if trials are to elicit different levels of fatigue, then either time or power must be manipulated and therefore either a known or postulated confounding variable will be introduced. How this challenge will be addressed will be discussed in Chapter 8.

3.1.3: Ecological validity of ergometry

Due to the technical challenges associated with kinetic or kinematic data collection outside of the laboratory, the vast majority of studies to date have examined the biomechanics of cycling using a stationary ergometer. However, discrepancies are known to exist between performance parameters (e.g. speed) in the laboratory and on-road (Jobson *et al.*, 2006; Palmer *et al.*, 1996). Whilst Jobson *et al.* (2006) have indicated that the effects of body mass may be a factor in this, the biomechanical differences are yet to be investigated. Where testing has been conducted with either the bicycle unsupported on rollers (Davis and Hull, 1981) or a treadmill (Stone and Hull, 1993), or on-road (Álvarez and Vinyolas, 1996; Soden and Adeyefa, 1979) or off-road (Rowe *et al.*, 1998), comparisons to ergometer riding have not been made. The only element within the ergometer characteristics to have received investigation is crank inertia. This can vary widely in on-road riding conditions, so the manner in which this is reflected in the inertial characteristics of the ergometer may affect the extent to which particular conditions are replicated. Comparisons of high and low inertial loads by Fregly et al (1996) showed little difference in terms of net hip, knee or ankle joint torques but significantly higher crank kinematic variability in the low inertia trial both between and within crank cycles. Hansen *et al.* (2002) have also shown subjects to adopt lower freely chosen cadence, increase gross efficiency and reduce peak crank torques at lower inertial loads.

Thus, although it may be reasonable to suppose that the mechanical differences that are apparent between ergometer and road cycling could impact upon riders' pedalling techniques, it has yet to be sufficiently explored by research. Therefore, since this factor is beyond the scope of the current work, it must be assumed that riders' techniques and their adaptations with fatigue in ergometer riding are representative of those outside of the laboratory.

3.2: Subject characteristics

In common with other sports techniques, the pedalling action of cyclists will become ingrained through thousands of hours of repetition. In this it should be noted that Dynamical Systems Theory suggests that, whilst outcome variability would be

expected to be lower with more experienced performers, they may be able to utilise higher degrees of freedom to achieve these outcomes and thus display greater movement variability (Davids *et al.*, 2003). It may also be supposed that the level of experience would affect the movement and outcome variability displayed in response to fatigue. Additionally, in some cycling disciplines, race distances normally increase with the level of competition (see for example British Cycling's road race event classification system) and so techniques may vary with the specific nature of each event. Takaishi *et al.* (1998) have shown differences in peak pedal forces between cyclists and non-cycling athletes although Marsh *et al.* (2000) did not show differences in moment based cost functions. Additionally, Coyle *et al.* (1991) reported that in a 40 kilometre time-trial, elite-national class cyclists produced higher performance power output compared to good-state class group (346 W national; 311 W state). The authors attributed this primarily to the national class riders producing higher peak torques about the centre of the crank (77 Nm national, 63 Nm state) and by applying larger vertical forces to the crank arm during the down-stroke (–456 N national, -369 N state). This was true even when both groups were cycling at the same absolute power output.

The limited research to have directly investigated biomechanical differences with experience or competitive level have thus produced equivocal results. However, it does appear that homogeneity of the subject group may be important in reducing variability and that conclusions from research should perhaps be restricted to comparable populations. Other areas that remain to be investigated by research include differences associated with gender, morphology and intra-discipline specialism of the subjects (for example, sprinting, time-trialling of climbing).

3.3: Bicycle configurations

For the majority of the time, riders are in contact with the cycle at five points (both hands on the handlebars, both feet on the pedals and bottom on saddle) and their movements are therefore constrained and guided by the machine to an extent unique in sport. This interface therefore plays a major role in determining the manner in

which the pedalling technique is executed and thus has been the subject of much research.

3.3.1: Saddle height

Research has shown that changes in this parameter can have large effects on physiological parameters (Hamley and Thomas, 1976; Shennum and DeVries, 1976) and experienced riders will commonly set this dimension to an accuracy of a few millimetres. It is therefore clearly an important element of the rider/ cycle interface and its implications for pedalling technique has thus been the subject of several investigations. Saddle height is normally measured between the pedal surface and saddle. However, comparison of saddle heights between studies is problematic since there has been inconsistency in the anatomical reference points and the exact points on the cycle used. Indeed the works by Ericson and colleagues are the only ones to detail the measurement points on the cycle, but the measure they used was problematic, '*saddle surface... in a straight line along saddle pillar and crank*' (Ericson, 1986). This was therefore relative to the arbitrary geometry of the ergometer and not to the riders' point of contact and thus may vary between ergometers and therefore between studies.

Some of the earliest works on the biomechanics of cycling showed that kinematic effects were apparent with altered seat height. Houtz and Fischer (1959) reported that mean hip range of motion (ROM) was higher at the lower saddle setting (25° at 25" (0.635 metres), 34° at 21" (0.533 metres)), although mean knee ROM was unchanged (55°). However, several limitations are apparent with this paper. Firstly, absolute saddle heights were used rather than setting them relative to the subject's leg length. Secondly, cadence was neither controlled nor reported, so that, although subjects exercised with the same resistance, their power outputs could have varied substantially.

The paper of Despires (1974) also used a 'low' and a 'high' saddle height (95 and 105% of the subject's pubic symphis height respectively). Their results indicated that ankle plantar flexion was significantly affected by changes in saddle height (ankle ROM: 66 to 103° low, 64 to 137° high). However, this work must be criticised

because, although cinematographic techniques were used, these were only used to record pulses to synchronise foot positions with electrogoniograms. It may have been better to use these recording to calculate the joint angles since this would have provided less encumbrance to the riders' techniques than electrogoniograms. Finally, the paper may be criticised due to the small sample (n=3).

Rugg and Gregor (1987) also showed saddle height to affect muscle lengths with the absolute lengths for the vasti (*m. vastus medialis, lateralis and intermedius*) and *m. soleus* tending to decrease whilst the hamstrings (*m. semitendinosus*, *m. semimembranosus* and *m. biceps femoris*) and *m. gastrocnemius* lengths increased with greater saddle heights. The authors also showed average moment arm lengths for the vasti and hamstrings to be increased with greater saddle height.

More recently, Price and Donne (1997) reported increased maximum ankle angle (32°, 37° and 46° at 96, 100 and 104% of trochanteric height respectively), decreased maximum and minimum knee angles (109°, 44°; 104°, 34° and 99°, 22° maximum and minimum respectively) and minimum hip angle (54°, 52°, 50°) with increased saddle height.

Joint force and moment patterns have also been shown to be affected by alterations in saddle height in various works by Ercison and colleagues (Ericson, 1986; Ericson *et al.*, 1986; Ericson *et al.*, 1985a). These have shown hip extensor moments to decrease with increased saddle height, whilst knee extensor moments increased and flexor moments decreased (Ericson, 1986; Ericson *et al.*, 1986) and ankle dorsiflexor moments either increased (Ericson *et al.*, 1985a) or remained unchanged (Ericson *et al.*, 1986). However, Browning *et al.* (1988) reported exactly opposite findings. Browning et al.'s work was only published as an abstract and so does not include a discussion of its comparisons to previous work, so no explanation of this contradiction is given. Given the similarity of protocols used and the exact opposition of the findings, it may be questioned whether the findings or Browning *et al.* are misreported and actually refer to decreased saddle heights.

3.3.2: Seat tube angle

The seat tube angle is the angle with respect to the vertical formed by the line between the centre of crank rotation and the saddle. However, similarly to the research investigating saddle height, the only paper to attempt to experimentally measure the effect of seat tube angle (Price and Donne, 1997) did not detail how this was measured. As well as the effects of saddle height already discussed, Price and Donne also showed changes in seat tube angle (STA) to only significantly affect maximum and minimum hip angles (80° STA 88°, 48°; 74° STA 96°, 53°; 68° STA 100°, 56° maximum and minimum at a seat height of 100% of trochanteric height). From physiological data they suggested that the steeper seat tube angles (i.e. the saddle further forward relative to the centre of crank rotation) increased efficiency and that this was related to altered patterns of ankle plantar-flexion and dorsiflexion.

3.3.3: Crank length

Since, for any given effective force, torque will increase with crank length but so will the length of the path described by the pedal, there is a compromise in power development between longer cranks for increased torque and shorted cranks for decreased joint angular velocities. Various researchers have thus sought to establish an optimal length. Inbar *et al.* (1983) calculated optimal crank lengths based on the maximisation of mean and peak power during a 30-s Wingate Anaerobic test. They calculated from the range of crank arm lengths tested (125, 150, 175, 200 and 225 mm) that maximum peak power and mean power would occur at crank lengths of 164 and 166 mm respectively and noted that this varied as a function of the subject's leg length. However, sensitivity within the range of crank lengths commonly used by cyclists (16.5 to 18.0 cm) was low. However, uncorrected power outputs were used which produce inaccurate peak power values (Coleman, 1994). In a similar investigation, Too and Landwer (2000) reported similar optimal crank lengths for peak power (164 mm) but substantially longer optimal lengths for mean power (200 mm). They suggested that this could be attributable to either differences in the loads used (7.5% and 8.5% body mass, Inbar *et al.* and Too and Landwer respectively) or the subjects' anthropometric characteristics. Too and Landwer also included

kinematic analysis and reported that with increasing crank length, minimum hip and knee angles decreased and hip ROM increased. Knee ROM also increased with increasing crank length with the exception of values between 100 mm and 145 mm.

3.3.4: Shoe/ pedal interface

Since, the majority of propulsive force is applied to the bicycle through the pedals, the interface between the bike and rider at these points is clearly important. In 1981 Davis and Hull reported research using the pedal design they had previously presented (Hull and Davis, 1981) to investigate the effects of altering the shoe/pedal interface. They concluded that the use of cleated shoes increased efficiency (Equation 3-1), reduced maximum torque and the proportion of the crank cycle over which negative torque is applied. However, as previously mentioned, the results from this paper must be treated with caution since a single subject was used. Increased Index of Effectiveness (Equation 3-1) with the use of cleated shoes (MCS) were also shown by Lafortune and Cavanagh (1983) with a concomitant reduction in lower oxygen consumption. However, the authors also reported that the normal component of the Index of Effectiveness, (the percentage of the linear impulse of the force normal to the pedal surface) used to produce angular impulse was significantly higher for the condition without toe-clips and a soft soled shoe (RLS) (48% RLS, 46% MCS), but that the tangential component (percentage of the linear impulse of the force tangential to the pedal surface used to produce angular impulse) was significantly lower (13% RLS, 23% MCS).

As well as the effects of physical properties of the shoe-pedal interface itself, the angle and movement of the foot with respect to the plane parallel to crank rotation has also been the subject of a number of investigations. Knutzen and Schot (1987) used electrogoniometry to investigate the effects of foot position on knee kinematics. Three randomly ordered foot positions were used; 10° of toe-in, 10° of toe-out and with the foot perpendicular to the pedal. Significant differences were shown for maximum values for flexion (92°, 92°, 86°), abduction (-16°, -17°, -14°), adduction (-6°, -6°, -5°), internal rotation (13°, 18°, 11°), total abduction/ adduction (10°, 12°, 9°) and total rotation (14°, 16°, 13° all normal, toe-out and toe-in respectively) across the three conditions. The authors concluded this that '*by establishing a toed-in position*

the cyclist may reduce movement parameters associated with knee strain and instability' and therefore, '*any foot position alteration should be made in the medial direction*'. However, this negates inter-individual anatomical differences and the fact that the knee joint is not a plain hinge. Therefore, positioning the foot to minimise movement parameters may actually increase knee stress by constraining the joint's 'natural' movement. The methodology of this study may also be questioned in that the data were based on one 'representative' leg cycle. However, the basis for this selection was not stated and it may be questioned whether conclusions can be generalised from a single crank cycle. Additionally, the use of electrogoniometry is problematic since it may constrain the subjects' pedalling action and, when fixated over soft tissue, the artefacts may be substantial where small angle changes are observed, such as shown in the frontal plane at the knee.

In recent years, toe-clips have largely been abandoned and 'clipless' pedal designs become ubiquitous amongst those involved in competitive cycling. These systems are similar to ski-binding mechanisms consisting of a cleat attached to the sole of the shoe which locks into the pedal, thus obviating the need for toe-clips. The early designs were built with rigid attachment of the foot to the pedal, which, due to the rotational movement observed by Knutzen and Schot (1987) and shown in the force pedal data of Wheeler *et al.* (1995), were thought to create torsional loads on the knee joint when the foot position was constrained. Therefore, designs subsequently emerged that incorporated a certain amount of 'float' i.e. rotation about the vertical axis. The effects of such 'floating' pedal was investigated by Fecteau and Smith (1992). Mean maximum knee angles recorded were 2° adduction and 8° abduction. However, there were substantial differences between subjects with abduction/ adduction movement ranging from 6° to 18°. The results indicated that, for the five rotational options tested (no motion, ±3°, ±5°, -1° to +5° and -5° to 1°), frontal plane leg kinematics were unaffected. The kinetics and knee injuries associated with the use of such 'floating' designs were also investigated by Wheeler *et al.* (1995). Three shoe/pedal interface systems were used (toe-clips and straps, clipless fixed and clipless float) for two subject groups; one that was free from knee pain and another with cycling related pain. Of the three interfaces, it was found that the largest applied moments (M_z, i.e. moments about an axis normal to the pedal surface) were observed

with the fixed clipless system whilst the float system attenuated the moment (peak ~1.0 Nm fixed, ~0.6 Nm float and toe-strap). However, the 'floating' design did not compromise the power transmitted to the bike (as assessed by effective force patterns). Interestingly, marked differences were observed in the M_z patterns between the two subject groups. Wheeler *et al.* took this as '*supporting the theory that relatively high moments, particularly internally applied moments during the power phase, may be related to knee loads and subsequently overuse injuries*'.

3.3.5: Aerodynamic position/ Body orientation

In addition to making positional modifications to try to optimise the efficiency of a rider's position in terms of propulsive forces, these are also made to try to reduce the resistive forces associated with the rider's aerodynamic drag. The effects of this on lower-limb kinetics were examined by Browning *et al.* (1992). Three positions were examined, termed '*conventional*', '*aerodynamic*' and '*advanced aerodynamic*'. However, the work was only published as an abstract so details of the three positions were not given. Results showed that, during the power phase, the aerodynamic position resulted in greater hip extensor moments whilst the advanced aerodynamic position resulted in greater knee extensor moments. Additionally, a total joint moment integral was calculated for each of the three positions. These were 3% and 12% lower in the advanced aerodynamic position and the aerodynamic position respectively, compared to the conventional one. From this Browning *et al.* concluded that the benefits of the aerodynamic positions in reducing drag are not outweighed by increased joint moments and that '*in fact the advanced-aerodynamic position may even enhance cycling mechanics in elite athletes*'. It should be noted however, that subjects were free to select their own cadence and no indication was provided as to the standardisation of this over the three positions.

3.3.6: Use of mathematical modelling in studies of bicycle configuration

Attempts to measure experimentally the effects of manipulating multiple parameters face the practical challenges of the volume of data collection and the potential interaction of the independent variables. These problems are obviated by the use of

mathematical modelling techniques and these have been adopted by various researchers investigating optimisation of the bicycle/rider interface. One of the earliest works to use this type of approach is that of Nordeen and Cavanagh (1976). They used a two-bar linkage model with movement of the hip and foot calculated as a function of crank ankle. They reported that this model was '*in fairly good agreement*' with the experimental data (at least for the hip and knee angles) with maximum differences being in the order of seven degrees. The results for the ankle however, were '*less satisfactory*'. The study also reported that '*seat height has a minimal effect on the pattern of foot movement*'. The key problem with this study was that results were inadequately reported and statistical analysis omitted. For example, although it was reported that experimental and modelled data were '*in good agreement*', there was no attempt to test whether they were significantly different. Since no data was presented in this regard, the reader is therefore unable to form an opinion of the model and the worth of this technique cannot be evaluated without replicating the research.

Hull and Gonzalez (1988) used a five-bar linkage model in an attempt to determine optimal cadence and crank length using bivariate analysis. These optimisations were based upon cost function analysis of the ankle, knee and hip moments. It was shown that, averaged over the crank cycle, hip moment was considerably more sensitive to both pedalling rate and crank length than the knee or the ankle. The hip moments also showed a clear optimal cadence and a relationship to crank length opposite to those of the ankle and knee. These differences, it was suggested, arose from the relative contributions of static and kinematic moments. It was also suggested that, for the 'average man', the optimal cadence and crank length combination was 110 $rev.min^{-1}$ and 145 mm. However, this was shown to vary with the size of the subject, with optimal values increasing for crank length and decreasing for cadence with increased subject size. However, the optimal cadences and crank length suggested by this study do not tally with those used in practice by cyclists. This may suggest that the cost function analysis represents an incomplete picture of optimisation. It would therefore have been useful to verify these results with experimentally derived data. This work was later extended by Gonzalez and Hull (1989) to a multivariate optimisation analysis incorporating five variables (cadence, crank length, seat tube

angle, seat height and longitudinal foot position relative to the pedal). Their results indicated that all of the variables had a significant effect on the joint moment cost function except foot position, although the degree of sensitivity differed. They also showed that all of the variables interacted, so that in order to determine optimal parameters they all must be considered simultaneously. Additionally, there was an interaction with the anthropometric characteristics of the rider so that optimal crank length, seat height and foot position increased with increased rider height whilst seat tube angle and pedalling rate decreased. Additionally, force pedal data was included in the study to determine the validity of the pedal force scaling method. The results indicated that the calculated figures did not duplicate the experimental force profiles and, although the percentage deviation increased with cadence for both methods, it was consistently greater for the scaled profiles.

Hull and Gonzalez (1990) also used modelling techniques to examine the effect of pedal platform height on inter-segmental moments. Their results indicated that the moment of the hip was most affected over the range of heights used (±4 cm), displaying a 13% change. However, the ankle and knee also showed ranges of ±6%. The optimal platform height was therefore determined to be around 2 cm. However, substantial interaction with cadence was shown such that optimal heights could be substantially higher or lower than this depending upon cadence. Clearly, these finding have important implications for the design of not only instrumented pedals such as those used in the present study, but for those intended for normal use. However, although various commercial manufacturers report the importance of minimising this dimension (Time Sport International, Varennes-Vauzelles, France, Crank Brothers, California, U.S.A., Shimano Europe, Nunspeet, The Netherlands), no research has yet been published to verify Hull and Gonzalez's finding and support the manufacturers' claims.

Yoshihuku and Herzog (1990) also used a five-bar linkage model and also included seven functional muscle groups based on Hill's equations. Using this they determined optimal parameters for crank length, pelvic inclination, saddle height and cadence. They reported that, whilst pelvic inclination and saddle height showed little sensitivity to crank length, this was not the case for cadence. They also stated that

deviations in cadence away from the optimal values caused large changes in the instantaneous power of muscle groups both individually and for the leg as a whole.

Kautz and Hull (1995) also used this approach to attempt to optimise the shape of the chainring. They used dynamic optimisation procedures and produced a chainring shape that reduced the cost of cycling as calculated from joint moments. However, the authors also noted that this optimisation increased peak joint moments and thus it did not appear to be optimal from a muscle energetics perspective, although this was not assessed. They therefore suggested that their findings emphasized the need to consider individual muscle co-ordination rather than net joint moment co-ordination. Such an approach integrating a musculoskeletal model with the dynamic optimisation analysis was recently adopted by Vilimek (2006) to show that higher cadences may be preferable in eliciting a better ratio between metabolic energy consumption and power output. However, this work was only published as an abstract and so no other details were given.

The use of mathematical modelling has thus enabled the investigation of a host of independent variables whose impact and interaction would not be readily open to physical experimentation. However, whilst these works have provided useful information, they do not account for the effects of alterations in neuromuscular co-ordination elicited by the changes and so some areas, in particular the effect of pedal platform height, warrant an experimental confirmation that has, as yet, to be conducted.

3.4: Task demands and the functional roles of musculoskeletal system in meeting them

Cycling has been the exercise modality of choice for numerous investigators because of the constrained nature of the action that simplifies modelling of the task and because of the relative ease with which the principal forces can be measured throughout the action. However, even in this constrained task, researchers have found complexity in the nature and co-ordination of the technique. Thus, whilst technological innovations have allowed the accurate measurement of the external work on the pedals, this has been shown to be only part of the story in understanding

the demands that the body must meet. For example, Kaneko and Yamazaki (1978) showed that the velocity changes in the lower limb during cycling resulted in substantial internal mechanical work, i.e. in addition to the work done on the pedals. They also showed that the magnitude of this work varied throughout the crank cycle (see Figure 3-1), and that, although for the loads up to 3 kiloponds (kp) (~165 W), the internal work remained relatively constant, for subsequent increases in load it increased appreciably (84, 83, 86, 100 and 108 $kg.m.min^{-1}$ for 1, 2, 3,4 and 5 kp (~56, ~111, ~167, ~222, ~278 W) respectively). This increment was attributed to the '*increased amplitude of velocity change caused by a hard push followed by a quick deceleration in the leg movement*'. Why this apparent change in levels of acceleration and deceleration should occur, however, was not discussed, though it may be related to the changes in the negative torques patterns during the upstroke observed by Kautz *et al.* (1991).

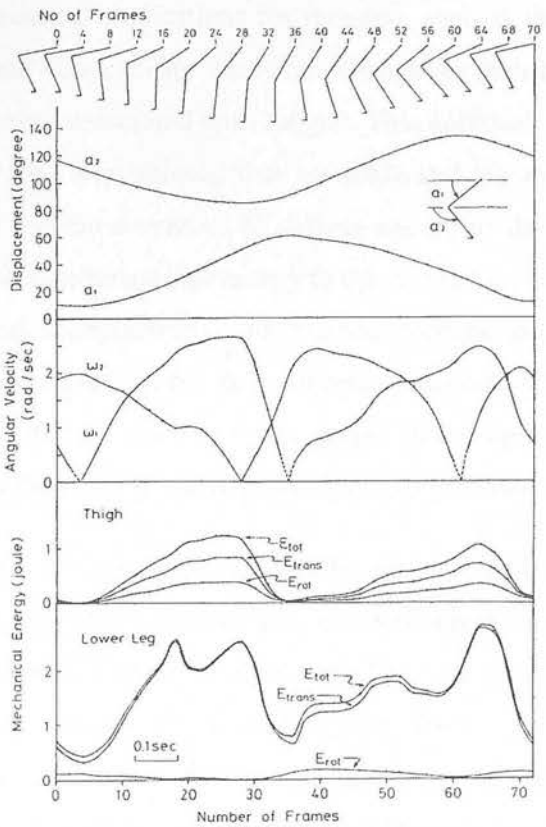

Figure 3-1: Time course of joint angle, angular velocity and rotational (E-rot), Translational (E-trans) and total kinetic energy (E-tot) over one crank cycle. (Kaneko and Yamazaki, 1978)

Until relatively recently, it was assumed in the much of the biomechanics of cycling literature that force application would be optimal if all of the applied force acted perpendicularly to the crank and in the direction of desired crank rotation (see for example, Lafortune and Cavanagh, 1980; Sanderson and Cavanagh, 1990). However, in 1993, Kautz and Hull presented a theoretical basis by which the pedal forces could be decomposed into their muscular and non-muscular (gravitational and inertial effects) components. The non-muscular component was shown to make significant contributions to the pedal forces and predominated in the horizontal component of the force. The authors noted that, contrary to what had been previously assumed, '*more muscular effort is likely to be required to produce an applied pedal force orientated only perpendicular to the crank*'. They thus concluded that the '*quantifying pedalling effectiveness through indices that only consider the orientation of the applied force provides a misleading measure of the true pedalling effectiveness because the non-muscular component of the applied force is ignored*'. This clearly has important implications for research, such as the present study, that attempts to understand how cyclists' technique changes as their bodies respond to the physiological challenges associated with fatigue. This approach was also adopted by Fregly and Zajac (1996) who showed that net ankle and hip extensor torques acted synergistically with the hip extensors to deliver energy to the limb whilst the net ankle extensor torque transferred this energy to the crank. However, the knee torques were reported to work independently with extensor torques delivering energy to the crank around top dead centre whilst flexor torques delivered it around bottom dead centre. Additionally, the net ankle extensor torque in the upstroke was reported to transfer energy from the crank to the limb to restore its potential energy.

The recent work of Zameziati *et al.* (2006) utilised both biomechanical and physiological indicators of efficiency. The biomechanical measure used was the Index of Effectiveness (IE) which was calculated for the upstroke and downstroke separately as well as for the whole crank cycle. They reported that, during an incremental test to exhaustion, IE for the upstroke and complete cycle were significantly correlated with the physiological efficiency measures (gross and net efficiency), although this was not the case for the downstoke. However, force data were obtained using the force-plate based method of Mornieux *et al.* (2006), which

has yet to be validated against instrumented pedals (see Chapter 4). Also, it should be noted that, since IE expresses the ratio between resultant and effective forces, it is more sensitive to changes in ineffective forces where effective forces are lower, e.g. in the upstroke. Hence, this portion of the crank cycle would be more sensitive to IE changes. Further, the work of Kautz and Hull (1993) and Fregly and Zajac (1996) have shown that optimal efficiency cannot be determined purely on the basis of pedal forces relative to the crank.

These works therefore elucidate the complex nature of the task demands of the pedalling techniques. Other investigators have attempted to develop a deeper understanding of the musculoskeletal co-ordination that contributes to meeting these demands. The paper of Gregor *et al. (1985)* attempted to explain the phenomenon commonly referred to as Lombard's paradox where the moment required at a joint for an action is opposite to that which can be produced by the activity of a biarticular muscle that crosses it. In cycling, the biarticular muscles of the quadriceps group act agonistically to extend the knee but also have an apparently paradoxical action in acting to antagonistically flex the extending hip. Gregor *et al.* confirmed that antagonistic muscle action was indeed shown, in that the activity of the quadriceps electrode site was always accompanied by activity at the hamstring location. However, a combination of the data sources (pedal forces, EMG and joint moments) offered a potential solution to this apparent paradox. Data showed that knee flexor moment occurred during the propulsive phase although the knee was extending. This extension, as well as being observed in the kinematic data, would be expected from the line of the resultant pedal force, which passed in front of the knee, creating an extensor moment. The flexor moment at the knee therefore was determined to be acting to control this with the muscles contracting in an eccentric manner. Broker and Gregor (1994) have also established the role of biarticular muscles in mechanical energy management (MEE) using inverse dynamic solutions. They concluded that including inter-compensating multi-joint muscles into the energy management analysis indicated a marked reduction in mechanical work relative to single-joint muscle operation alone. They also noted that this effect was increased at higher power outputs.

The role of biarticular muscles was also investigated by Prilutsky *et al.* (1997) in an attempt to determine if the muscle co-ordination pattern used in pedalling by either pushing or pulling the pedal corresponded with the strategy that minimised muscle fatigue. Muscle forces were calculated for each trial using a musculoskeletal model with a standard static optimisation and the criterion of minimised fatigue, as defined as the sum of muscle stresses cubed (Crowninshield and Brand, 1981). Force and EMG peaks were reported to be higher for the single joint extensors (*m. soleus*, *m. vastus medialis* and *m. gluteus maximus*) in pushing compared to pulling whilst the reverse was true for the ankle, knee and hip flexors (*m. tibialis anterior*, *m. semimembranosus* and *m. rectus femoris*). EMG and predicted forces of two joint muscles were reported to be greater when they acted as agonists at both joints that they crossed compared to when they acted agonistically at one joint and antagonistically at the other. However, the lowest activity and predicted forces was reported to be when the muscles acted antagonistically at both joints that they cross.

Other researchers have attempted to better understand the pedalling technique by investigating the effect of altering the nature of the task. For example, Pierson-Carey *et al.* (1997) examined the effects of ankle immobilisation on pedalling technique. They showed that the magnitude of the resultant pedal forces were reduced when the ankles were locked in a neutral position by ankle braces although the direction of the forces was largely unchanged. From this they suggested that the normal plantar flexion that occurs during unconstrained pedalling might be a strategy for effectively transferring power from the hip and knee muscles to the foot/pedal interface.

Neptune *et al.* (2000) altered the pedalling task by comparing the biomechanical functions of the muscles in backward versus forward pedalling. Results showed that, in both backwards and forwards pedalling, muscles contributed to the same primary biomechanical functions. In accelerating the crank, *m. gluteus maximus* was shown to work synergistically with *m. soleus*, the hip flexors (*m. iliopsoas*, *m. pectineus*, *m. rectus femoris*, *m. sartorius, m. tensor fasciae latae*) to work synergistically with m. tibialis anterior and the vasti (*m. vastus medialis*, *lateralis and intermedius*) and hamstrings (*m. semitendinosus*, *m. semimembranosus* and *m. biceps femoris*) to work independently. Further, the *m. rectus femoris* was shown to utilise complex

biomechanical mechanisms to accelerate the crank. This included negative work being used to transfer energy generated elsewhere (primarily from other muscles) to the pedal reaction force in order to accelerate the crank. Similarly, Neptune and Herzog (2000) used circular and elliptical chainrings to examine muscle co-ordination pattern changes with altered task mechanics and concluded that '*the nervous system used adaptations to the muscle EMG magnitude, rather than timing, to adapt to* [the] *altered task mechanics*'.

The research reviewed thus indicates the underlying complexity of the overtly simple pedalling technique. It may be further speculated that further complexity is introduced as riders respond to the stressors of fatigue.

3.5: Methodological issues

All biomechanics research presents methodological and technological demands that must be met if valid and reliable data are to be obtained. This is no less true for research focusing on the biomechanics of cycling and so, in addition to the sources reviewed in Chapter 3, other research investigating methodological issues particular to the investigation of cycling will be reviewed in this section.

In any biomechanical study, the accuracy of any kinematic data is dependent upon the correct identification and tracking of joint centres. This can be problematic since the joints' centres of rotation may not be readily apparent from surface landmarks. This issue was addressed with specific reference to the hip joint centre in cycling in a single subject case study by Neptune and Hull (1995). The study compared four methods for identifying the hip joint centre (HJC); i) a marker placed over the superior aspect of the greater trochanter (TRO), ii) assuming the HJC was fixed and taking its position from anthropometric measurements relative to a laboratory co-ordinate system, iii) using a vector of fixed magnitude and orientation (based upon an averaging of the relative locations of the two landmarks) to locate the HJC relative to the anterior-superior iliac spine (ASIS) and iv) a reference method based on a intracortical pin being placed into the lateral iliac crest with an attached triad of reflective markers (STD). Additionally, Neptune and Hull collected force data using the instrumented pedals of Newmiller *et al.* (1988) (modified for use with 'clip-in'

cycling shoes) to determine the effects of inaccuracies in identifying the HJC on inverse dynamic solutions. The range of total errors was greatest for the TRO in both the X and Z directions (2.7 and 3.6 cm respectively) whilst the lowest errors were recorded for ASIS in the X- direction (0.5 cm) and for FIX in the Z-direction (0.9 cm). It was also shown that ASIS produced similar movement in both magnitude and phase as STD whereas TRO yielded both magnitude and phase differences. The inaccuracies in HJC identification were also reflected in sizeable errors in the resulting inverse dynamic solutions. For example, TRO caused a 254% error in calculations of hip joint power (12 W STD, 42 W TRO) and a 384% error in hip joint force work (3 J STD and 12 J TRO, 225 W at 90 rev.min^{-1}). However, whether the FIX or ASIS methods produced the most accurate results was dependent upon the kinetic variable under examination. Neptune and Hull therefore concluded that 'the method used to track the HJC... should depend on the biomechanical quantity of interest'. The major weakness of this study was the size of the sample, which the authors acknowledged '*present*[ed] *an immediate limitation of the applicability of the results to the general population of cyclists*' (Neptune and Hull, 1995). However, using a larger sample in this case was clearly problematic given the invasive nature of the STD method. Neptune and Hull therefore published another paper the following year (Neptune and Hull, 1996) comparing the TRO and ASIS methods with a larger sample (n=7). The results indicated significant differences between the two techniques with the ASIS method showing a two-cycle pattern in the fore-aft direction while the TRO only showed one. The movement range of the TRO was also around 50% greater than the ASIS. In the vertical direction, the movement patterns were similar in both cases although, the magnitude obtained via TRO was around 150% of that from ASIS. These differences also resulted in significantly different results for the power and work calculations. The authors also noted that at naturally preferred pedalling rates (~90 rev.min^{-1}) and lower power outputs (<225 W), the hip joint movement was minimal. Therefore the assumption of a fixed hip often used in inverse dynamic solutions is least prone to error under these conditions.

Many of the works on the biomechanics of cycling have calculated joint moments. However, the work of Broker and Gregor (1990) and Gregersen and Hull (2003) have shown that accurate calculation of these variables presents methodological

challenges since the centre of pressure moves substantially during the crank cycle (this is discussed further in Chapter 4). This can have a significant effect on the calculated pedal moment thus creating questions over the validity of inverse dynamic models that do not reflect this in their inputs (Broker and Gregor, 1990). In addition to this, Gregersen and Hull reported that the three dimensional orientation of the shank segment has a major affect on the computation of the non-propulsive knee moments. Whether or not these findings are also applicable to the ankle and hip joints was not the subject of Gregersen and Hull's investigation and so remains unknown.

Thus, even in the constrained, comparatively planar task of cycling where force inputs to inverse dynamic solutions are relatively easy to measure, the calculation of such parameters presents technical and methodological challenges.

3.5.1: Use of biomechanics to modify riders' techniques

Although the wealth of research into the biomechanics of cycling has done much to illuminate our understanding of the technique, its application is dependent upon the ability to utilise this knowledge in improving the manner in which the technique is executed. Sanderson (1986) and Broker *et al.* (1993) have both demonstrated the efficacy of using the real-time kinetic feedback made possible with instrumented pedals to modify subjects' technique. However, neither study made use of a control group so the modifications cannot be unequivocally attributed to the provision of feedback. There is therefore, more research required in this area and this may present a major challenge to researchers because of the complexity of establishing an 'optimal' criterion measure that has been shown by the other research in this area.

3.6: Miscellaneous research

Various other investigations have been conducted into the biomechanics of cycling that do not fit readily with other research but are still pertinent to the present work. For example, one of the early investigations to have measured kinetic parameters in cycling indicated the potential for substantial asymmetry (Sargeant and Davies, 1977) to exist in applied pedal forces. They showed that, although no significant

asymmetry was shown between the mean peak forces as applied by the left and right legs during one leg cycling, when both legs were used together, a consistent and significant trend was shown for the right leg to apply greater peak forces than the left (~3%). However, the cadence selected for this study (50 rev.min^{-1}) is well below that commonly chosen by experienced cyclists (>90 rev.min^{-1}), therefore, it is unclear the extent to which these findings can be applied to such groups.

3.7: Conclusions

In conclusion, the preceding research highlights an array of parameters that may influence the execution of the pedalling technique and therefore must be controlled if their effects are not to obviate the attempt to identify fatigue-related changes. These include the effects of differences in power output and cadence, subject experience and bicycle and ergometer configurations. Whilst most of these are relatively easily controlled by subject selection and equipment set up, since power output will determine the rate at which fatigue occurs, this must be varied between trials. Consideration of these reported effects will therefore be required in the design of the protocol and the interpretation of the findings in the current research.

This review has also highlighted areas where more work is required, such as into the ecological validity of the use of ergometers and experimental verification of some of the findings derived from mathematical techniques. In these areas, certain assumptions will therefore have to be made in the present study. This review has also identified methodological issues pertinent to research in this area; specifically with regard to marker set up to accurately track the hip joint centres and the movement of the centre of pressure on the pedal. Since errors in either joint centre location of assumed point of force application will both create compound errors in joint moment and power calculations, especially for joints distal from the point of force application, these findings highlight the problematic nature of obtaining sufficiently accurate inputs for such calculations.

This review therefore, highlights a host of technical and methodological considerations that must be taken into account in the design of the current research and the interpretation of its findings.

Section 1: Technical

Chapter 4: Instrumentation of pedal for force measurement; review of literature

For researchers wishing to investigate the application of propulsive forces, cycling offers the advantage over many cyclical activities that these are continuously applied to the same points on the equipment throughout the action (i.e. the pedals). Thus instrumentation of the pedals allows for all of the propulsive forces to be measured continuously. However, although equipment is now commercially available that allows the measurement of torque or power (see introduction), such systems are not capable of measuring the orthogonal force components separately. Although the forces parallel to the crank will not affect the propulsion of the bicycle, they will contribute to the energy costs of the activity. The work of Kautz and Hull (1993) has also suggests that optimal efficiency is not achieved by all forces being applied perpendicularly to the crank arm. Since, these are areas that may be affected by fatigue, only designs capable of measuring all of the major force components (i.e. those in the plane parallel to crank rotation) will be of relevance to the present study. Therefore, research that has applied the instrumentation only to the crank will not be reviewed. Also, this review of the literature will be restricted to the design, calibration and validation of the equipment itself. Discussion of the application of the devices has already been undertaken in Chapter 3, therefore this review will be restricted to examining their applicability to the present study.

In order to elucidate the review of the various pedal designs, it is necessary to understand the nature of the forces that they have been created to attempt to measure. Since the instrumentation applied to the pedals provides these measurements with respect to the object to which it is applied, i.e. the pedals themselves, the forces are initially obtained relative to the pedal as a rotating reference frame. Although there has been some variation in the terminology used in the research to describe these forces, for clarity, this review will adopt the conventions most regularly used. Specifically, that the force normal to the pedal platform is termed F_z, that acting in the fore-aft direction, F_x and that acting parallel to the pedal axis, F_y (Figure 4-1). For some of the simpler designs, resolution of these vectors was not possible and only the resultant forces (F_r) were given. Where moments have also been measured, these will

follow the same convention, e.g. that M_x will refer to rotation around a fore-aft axis i.e. the direction of the F_x vector and so forth. However, although forces are usually measured relative to the pedal, it is only the components of the force that act perpendicularly to the cranks that will contribute to the development of torque about the centre of the cranks and therefore propulsion of the bicycle. It is generally necessary therefore, to convert between the two frames of reference. In order to do this, it is necessary to know the orientation of the pedals with respect to the cranks, i.e. the pedal angle. Since only the component of the applied force which acts normal to the crank will contribute to production of torque about the axis of the cranks and therefore propulsion of the bicycle, this has been termed the effective force (F_{eff}), whilst that which acts along the longitudinal axis of the crank is referred to as the ineffective forces (F_{ineff}). However, it should be noted that the terms 'effective' and 'ineffective' in this context only refers to the forces tendency to create torque and are not indicative of 'optimal' force application. Crank angle is also usually measured so that measured forces can be attributed to where they occur within the cycle. By convention, the zero point is usually with the right crank at top dead centre (TDC).

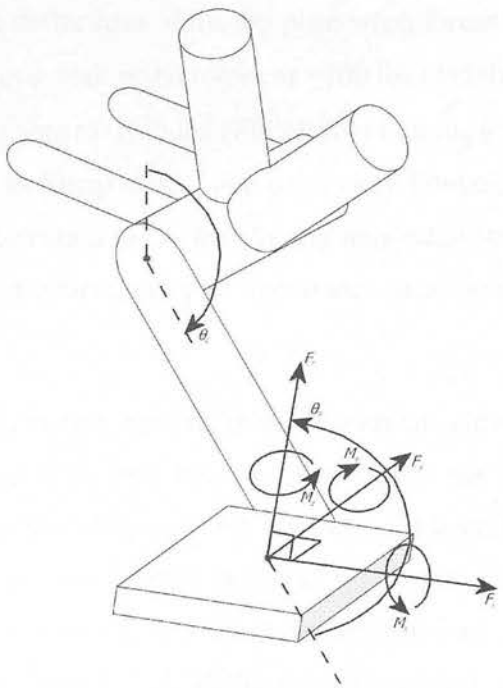

Figure 4-1: Definition of foot-pedal reactive load components and crank and pedal angles

One point to note in reviewing the literature on pedal design is that several of the researchers have chosen to instrument only one pedal. However, asymmetry has been shown in right to left ratios of up to 85% (15%) for net F_{eff} (Briggs *et al.*, 1987), around 3% for peak F_{eff} (Sargeant and Davies, 1977) and significant differences in peak M_z (Wheeler *et al.*, 1995) with exemplar data indicating peak M_z at the left pedal of 2.5 Nm and 1.25 Nm at the right (Wheeler *et al.*, 1992). Smak *et al.* (1999) have also shown significant asymmetry in average positive (from 1.8% at 118.3 rev.min^{-1} to 2.4% at 88.8 rev.min^{-1}) and total power (from 1.3% at 118.3 rev.min^{-1} to 2.14 at 64.6 rev.min^{-1}) as well as significant interactions between average negative power asymmetry and pedalling rate (from 10.1% at 118.3 rev.min^{-1} to 29.1% at 64.6 rev.min^{-1}). Thus the assumptions of symmetry associated with the instrumentation of only one pedal are not valid.

One of the earliest investigations of the biomechanics of cycling was that reported by Sharp in his book 'Bicycles and Tricycles' originally published in (Sharp, 1896). This described a pedal used by Scott (1889) called a 'cyclograph' which consisted of a pedal with a sprung top plate connected to a pencil on a rotating, paper covered drum. This recorded the deflections of the top plate when forces were applied. Using this device, Scott measured peak pedal forces of ~100 lbs (445N) for a cyclists riding at 18 mph (8.05 m.s-1) rising to ~175 lbs (779 N) for climbing a 1 in 10 hill at 4 mph (1.79 m.s^{-1}). However, as Sharp stated, one of the key limitations with this design was that it gave no information 'as to the varying *tangential* (original italics) effort on the crank, which is of course, of more importance than the total pressure on the pedal'.

More sophisticated designs only became possible with advances in electronic force measurement technology. This may help to explain why the late 1960's to early 1990's was such a fertile period for research involving the instrumentation of pedals, whilst the publication of new designs in the last 10 years has been sparse. The increasing availability of commercially available systems such as the SRM Power Measuring Crankset (Schoberer Rad Meβtechnik, Germany) may have also have removed some of the impetus for the development of pedal instrumentation since they offer an 'off-the-peg' solution suitable for some support and research work. For

the vast majority of the designs to have been presented, the instrumentation has been achieved either through the application of strain-gauges of piezoelectric devices. Since these each present different strengths and weaknesses and present different design requirements, they shall be reviewed separately, before a brief discussion of the few designs to have used other technologies. The sections on strain gauges and piezoelectric devices will also be prefaced by a brief review of the technologies.

4.1: Designs using strain gauges

When stress is applied to a material, this tends to cause deformation or strain. By attaching strain-gauges to the surface of the deforming object, this deformation can be measured. Strain gauges are based around the principle that conductive materials change their resistance as they are deformed. By selecting materials that exhibit larger change in resistivity for a given strain and forming them into a grid (see Figure 4-2) this property can be exploited to yield measurable changes in electrical resistance as the material to which the gauge is attached is distorted.

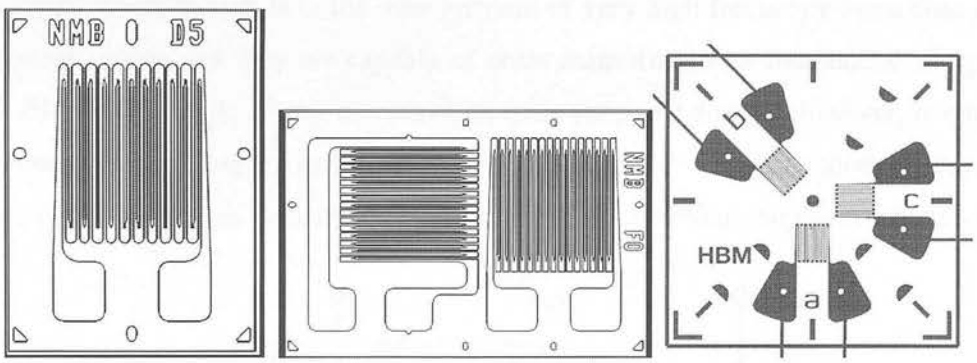

Figure 4-2: Left: Single measuring grid linear strain gauge. NMB: Minebea, Tokyo, Japan, Middle: Two measuring grid 'T' strain gauge, NMB: Minebea, Tokyo, Japan, Right: Three measuring grid 120° rosette strain gauge. HMB, Darmstadt, Germany

Modern strain gauges are normally of the foil type and, if properly installed deviations from linearity will generally be between 0.05% and 0.1% and hysteresis and zero shift less than 0.2% of the maximum strain (Chalmers, 1992). They do however, also possess some sensitivity to strain that is at 90° to the strain of interest. This occurs since part of their conducting path is in that direction and because of the complex nature of strain (Noltingk, 1996); however, particularly for foil gauges, this is very small. Conversely, the cross effects that are introduced by errors in gauge

alignment with respect to the strain of interest may be larger and so must be accounted for in the calibration process.

Another major undesirable characteristic of strain-gauges is that their resistance changes with temperature as well as elongation. As Pope (Pope, 1979 p. 46) noted, '*unless this effect is accounted for, large errors will be introduced in the strain measurement*'. This is one of the key reasons why they are generally used in a Wheatstone bridge configuration. In the case of instrumented pedals, these are usually fully active symmetrical bridges, i.e. strain gauges with the same resistance forming all 4 resistors on the bridge (Figure 4-3). Wheatstone bridges also have the advantage that their output is zero at zero load. However, this can change over time due to changes in temperature or creep in the cement so, for accurate measurement, the bridge should be re-zeroed before data each data collection. However, unlike piezoelectric devices, even with static loading, their zero output remains stable over time and so are suited to prolonged data collections, such as in the present research, with quasi-static loading such as experienced in pedalling. Where strain gauges are less well suited though is in the measurement of very high frequency force changes, although, given that they are capable of point measurement at frequencies of up to 10-20 kHz (Noltingk, 1996), this is not an issue for pedal design. However, one area pertinent in applying gauges to pedals is the effect of applying them to curved surfaces. This creates differences in apparent strain, including apparent temperature

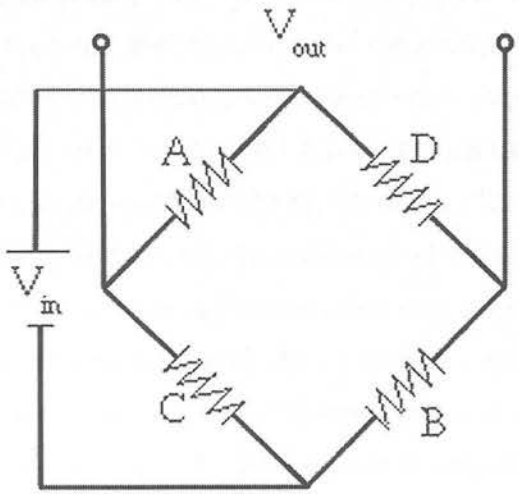

Figure 4-3: Wheatstone Bridge: A to D all strain gauges in fully-active symmetrical bridge

strain, than if they are applied to a flat surface (Pope, 1979). Thus if they are to be applied to curved surfaces, such as around pedal axles, then all gauges in the bridge must be applied to surfaces with equal curvatures.

In order to measure the strains of interest that occur in more than one direction, as is generally the case with instrumented pedals, multiple gauges are required. In order to simplify gauge application and allow multiple gauges to be located in a small area, gauges possessing either two (Figure 4-2) or 3 measuring grids (i.e. rosettes) (Figure 4-2) are commonly used with their grids aligned at 45°, 60°, 90° or 120° to each other. Thus their compact size, versatility of application and relative ease of use makes strain gauges well suited to the development of designs of force instrumented pedals and have thus been the most commonly adopted technology for researchers in this area.

One of the earliest studies to use such electronic devices in measuring pedal loads was that of Hoes *et al.* (1968). As well as applying strain-gauges to the cranks, they also presented the design of a pedal with strain-gauges applied to a cage supporting the pedal top-plate, attached to the pedal spindle. Crank position was recorded by an induction coil attached to the ergometer which was activated by 8 magnets attached to an aluminium disc fastened to the crank. Hoes stated that positioning of these '*had a maximal deviation of 0.01 sec.*', which at the cadence they mostly used (60 rev.min^{-1}) would give an accuracy of 3.6 degrees. However, since only 8 points on the crank cycle were recorded, the resolution was substantially less than this (45° ± 3.6°). Details of the calibration procedures used were scant, other than that the pedals were loaded with masses up to 100 Kg (981 N), which substantially exceeded peak experimental force reported (~560N at 400 W, 60 rev.min^{-1}). There were however, several limitations of this work. Firstly that, although identical pedals were used on both sides, only the right pedal was instrumented, thus assuming symmetry. The pedal was also not capable of measuring the separate force components. It would have been possible to calculate these from the crank and pedal forces if pedal angles were obtained, but this was not done, therefore substantially constraining the information that could be obtained. Secondly, the design also placed the surface of the top-plate substantially (40 mm) above the axis of the pedal spindle, which has

been subsequently shown to alter the joint mechanics (Hull and Gonzalez, 1990). Indeed, although only presented graphically, there appear to be differences in the force traces presented by Hoes from data obtained from the cranks with the instrumented pedals and normal pedal, especially from BDC to TDC (Figure 4-4). Finally, the authors also do not report any validation of the data obtained from the pedals so the magnitude of any errors in unknown.

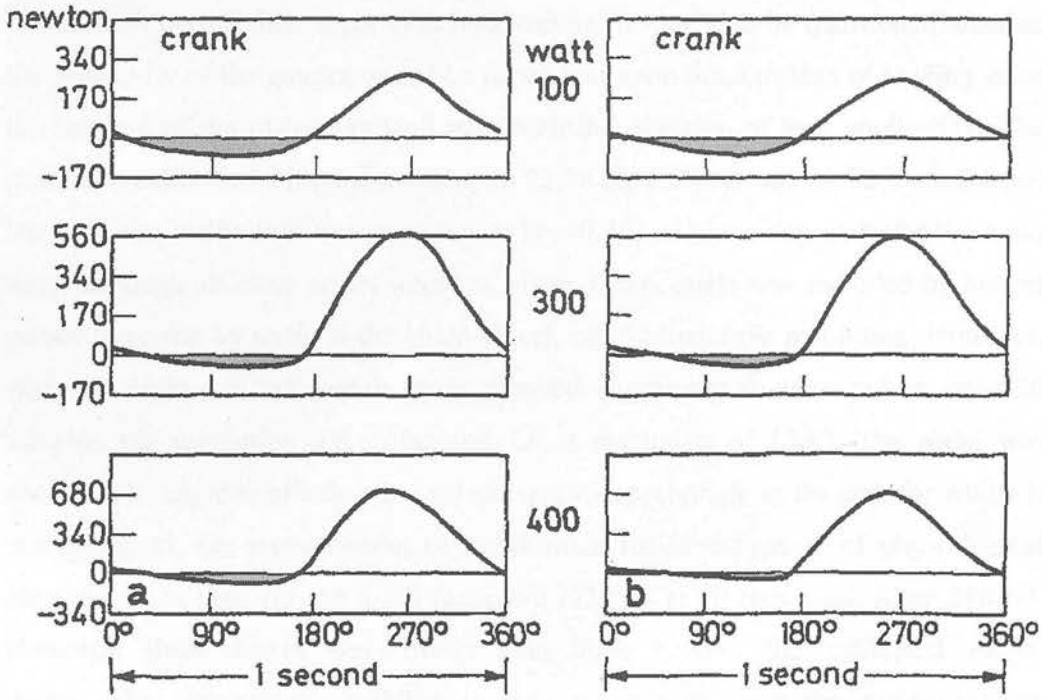

Figure 4-4: Force exertion on the crank while cycling with the measuring pedal (a) and the normal pedal (b) at loads of (top to bottom) 100, 300 and 400 Watts and 60 rev.min^{-1} (Adapted from Hoes *et al.* 1968)

The pedal design of Adeyefa (Soden and Adeyefa, 1979) used two crossed beams to transmit loads to the pedal platform with four strain-gauges attached to each beam. These were arranged into Wheatstone bridge circuits to allow the measurement of forces normal and tangential to the pedal platform. Crank position data were obtained via an aluminium disc with teeth cut into it attached to the chain wheel that activated a micro-switch with pulses being recorded on a UV recorder along with the force data. However, pedal angles were not measured meaning that forces could not be calculated relative to the crank. This is critical given that it is the direction as well as the magnitude of the force vector relative to the crank, not the pedal, that will determine the effect of the applied loads upon the bicycle's propulsion. The design

was also limited in that the toothed wheel used in measuring crank position had only 9 teeth and therefore, could only resolve crank angle to ± 20°.

A simple design was presented by (Brooke *et al.*, 1981) based around a rolled steel plate, the upper surface of which formed the pedal top-plate and the lower section attached to the base of a normal pedal. Two strain gauges bonded to the inside and outside of the curves of the plate allowed the measurement of applied forces although this did not permit their separation into vectors. It may also be questioned whether the sensitivity of the gauges would be dependent upon the direction of loading since the bending of the plate may well vary with the direction of load application. The pedal was calibrated with masses of up to 22.78 Kg (224 N) and the 95% confidence band for the calibration was reported to be ±0.2% within a day and ±0.6% across days, although absolute errors were not given. Crank angle was recorded by optical pulses triggered by teeth of the chain wheel, i.e. 52 times per revolution. However, since the right and left pedals were sampled alternately at these pulses, only 26 samples per revolution were obtained, i.e. a resolution of 13.8°. The pedal was shown to be capable of achieving measurements appropriate to the task for which it was designed, i.e. measurement of pedal force for investigation of physiological phenomena, at least for the loads measured (150 W at 60 rpm, peak force 348 N). However, these forces were more than 50% beyond the calibrated range. Additionally, the designs' inability to independently measure the components of propulsive force makes it unsuitable for the present study.

In 1981 two papers were published on a pedal design that would be subsequently much used in research on the biomechanics of cycling (Davis and Hull, 1981; Hull and Davis, 1981) (Figure 4-5). The design used thirty-two strain gauges connected into eight Wheatstone bridge circuits, thus forming four octagonal strain-rings. This was thus a substantial advance on previous designs in that it allowed the measurement of all of the six foot-pedal load components (F_X, F_Y, F_Z forces and M_X, M_Y, M_Z moments). The pedal was also designed in such a manner that the geometry of the instrumented pedal closely matched that of a typical pedal. This had been an issue for previous designs since, the decoupling the pedal surface and axle requires clearance to be left between the two, which is difficult to achieve without increasing

the height of the pedal platform relative the axle in comparison to conventional pedals. Pedal and crank angles were obtained using linear continuous turn potentiometers. In the case of the pedal angles, these were simply attached to the body of the pedal with the potentiometer shaft attached to the pedal spindle. Crank angle was obtained using two identical meshing gears, one attached to the chainring of the bicycle and the other to the shaft of the potentiometer, which was mounted to the bicycle frame. This was thus a further innovation in that it allowed direct recording of the crank and pedal angles rather than reliance on video or film recordings.

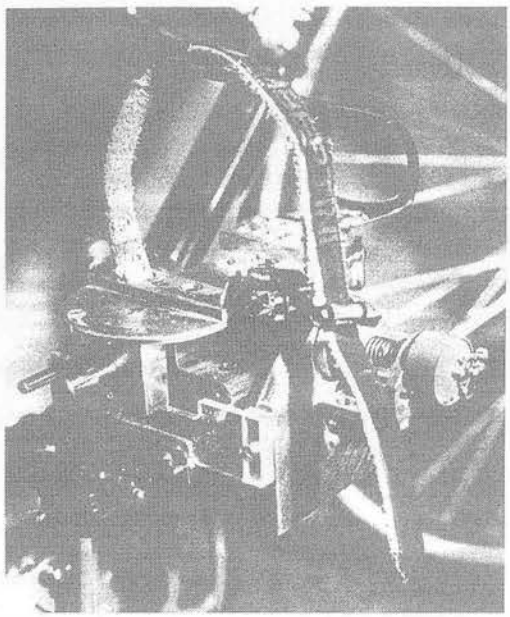

Figure 4-5: 6-Axis dynamometer of Hull and Davis (1981)

Precision calibration equipment was used to statically load the pedal over one complete loading cycle (positive loading, positive unloading, negative loading, and negative unloading) for each of the force components. From this a 6x6 calibration matrix was produced of the direct and cross-sensitivity coefficients. This reveals that substantial cross effects were present, especially for force measurements when moments were applied. Although the accuracy of the resulting measurements was not indicated, it was reported that the pedal met the stated design criteria which includes that '*the complete, 6-axis loading must be measured with full scale accuracy of ± 0.5%*'. The pedal was successfully used in a series of trails by Davis and Hull (Davis

and Hull, 1981) with single leg power outputs of up to 200 W with a cadence of 76 rev.min^{-1} (Peak F_x ~125 N, F_y ~120 N, F_z ~450 N). However, although the design offered many innovations, a key limitation was that only one pedal was instrumented and, as has been discussed, it is known that substantial bilateral asymmetries may exist. Adoption of this design also presents difficulties in the calibration requirements necessary to address the potential cross-sensitivity. As (Gregor *et al.*, 1991) noted, '*the use of this pedal may be restricted to laboratories equipped with the elaborate calibration equipment and procedures necessary to develop the 6 x 6 coefficient sensitivity matrix employed in the derivation of the applied moments and loads.*'

Gregor *et al.* (1985) presented details of a design using eight strain-gauges to measure the normal and fore-aft forces applied to the pedal surface. Four were bonded to a 'force cube' at the centre of the pedal that allowed the measurement of forces normal to the pedal surface whilst the remainder were attached to the beams of the pedal allowing measurement of the tangential forces. Crank and pedal positions were measured with linear continuous turn potentiometers. Little detail of the calibration procedures were given other than they were calibrated with specially designed apparatus through a range of 1-1000 N in the normal direction and 0-250 N in the tangential direction and that cross-sensitivity was less than 5%. The advantage of Gregor *et al*'s work over that of Hull and Davis (Hull and Davis, 1981) is that both pedals were instrumented. However, without further information on the accuracy of the data produced by the two designs, little comparison can be made of the relative merits of the actual pedals' design.

A design combining a load cell in the pedal top-plate to measure vertical force and strain gauges bonded to a cantilever sleeve attached to the pedal spindle to measure the horizontal force components was presented by Bremble and Brown (1985). They measured crank angle using a photocell triggered by strips of tape attached to the spokes of the rear wheel. Pedal angle was measured with a linear continuous turn potentiometer. Calibration was conducted by applying known masses to the pedals, but further details of this, including the range of loads applied, was not given. No validation of the pedals was described thus the effectiveness of the design cannot be

evaluated. The exemplar data given was also minimal. Peak forces of around 22Kg (216 N) were indicated at a cadence of around 4.6 $rad.s^{-1}$ (44 $rev.min^{-1}$), but the exercise protocol used to achieve these was not stated. Additionally, one potential source of error was the use of wheel position to measure crank angle. This could be affected by changes in chain length under loading and movement of the freewheel mechanism.

Harman *et al. (1987)* produced a pedal design with the specific objective of producing a device that was capable of measuring the high forces exerted during maximal power cycling. This used a pair of four-arm strain gauge bridges to measure forces in the plane normal to the pedal spindle, both normal and tangential to the pedal surface. Pedal angles were measured using sine-wave potentiometers mounted in a similar manner to the design of Hull and Davis' (1981). These have the advantage that they do not produce the voltage transients at the border between the highest and lowest resistance which occurs with linear potentiometers due to a gap in the resistive tracking. This normally has to be filled with linear interpolation. However, a linear potentiometer was used for crank angle measurement. This, the authors report as being adequate since crank angle '*increases steadily during pedalling, producing a saw-toothed waveform*'. However, the rotation of the crank arm was transmitted to the potentiometer by means of a plastic chain and it is possible that this could distort during pedalling resulting in an error in the calculated crank angles. Calibration of the pedals was conducted on each day of their usage by suspending known masses from them giving a linearity of <1%. However, no quantification of measurement error or sensitivity to cross effects was presented. Also, since data were collected at 100 samples per revolution per channel (i.e. 100 Hz at the cadence chosen, 60 $rev.min^{-1}$) this only represents a resolution of 3.6 degrees. Further, although the power output achieved by the subjects was not stated, the power output indicated in the exemplar data (average power output across the pedal cycle of 485 W, 60 $rev.min^{-1}$) was relatively low (at least for experienced cyclists) for the 5 s of maximal riding used. It was also not substantially higher than some of those achieved in some of the other studies that have not been specifically aimed at examining '*maximal power cycling*'. The peak force indicated therefore

were also not substantially higher than those in some other studies (F_x ~125 N and F_z ~780 N).

Newmiller *et al.* (1988) criticised previous studies for a failure to report the sensitivity of their designs to out-of plane loadings. Newmiller *et al.* noted that Davis and Hull (1981) had demonstrated such effects and stated that '*electrical decoupling by element orientation, gauge placement and interconnection is not especially effective where out-of-plane loads are concerned*'. The design they presented sought to address this issue by using both mechanical and electrical decoupling. To achieve this, their dynamometer used a single octagonal strain ring that was mechanically constrained so that deformation would only occur with the application of normal or tangential forces. Thrust bearings were then used between the inner and outer plates to achieve mechanical decoupling (see Figure 4-6) and pedal and crank angles determined with continuous turn linear potentiometers. The efficacy of the mechanical decoupling was indicted by conducting calibration with this in place and without (using the apparatus and procedures of Hull and Davis (1981)). With mechanical decoupling direct to cross sensitivity ratios were < 0.6% for F_x and < 2.6% for F_z but increased 4.5 times for F_x (2.5%) and 3.5 times for F_z (8.79%) without it. However, even with mechanical decoupling, sensitivity to moments were still apparent (F_x sensitivity: M_x 7.06%, M_z 8.22%, F_z sensitivity: M_x 17.9%, M_z

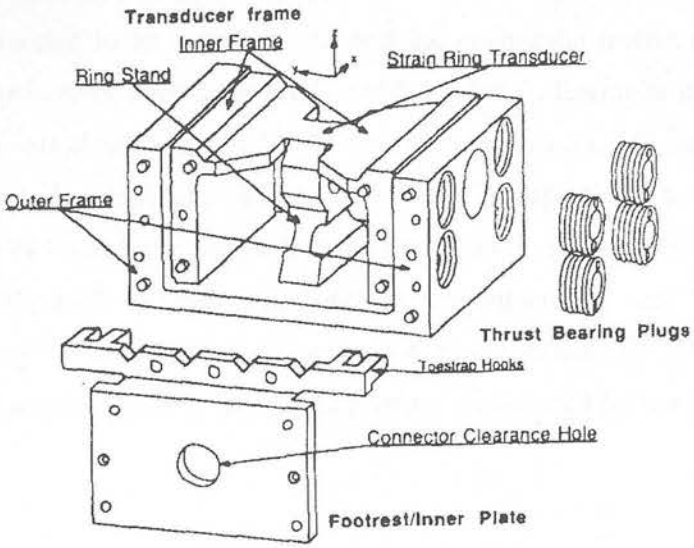

Figure 4-6: Schematic representation of pedal of Newmiller *et al.* (1988)

9.00%) although this did increase around 9 fold without it. However, in practice the errors associated with cross-effects from moments were relatively small due to their comparatively small magnitude in pedalling. With both the mechanical and electrical decoupling absolute error was shown to be within ± 5 N for the range tested. This would equate to errors of 3% for F_x and 1% for F_z for expected maximum loads (150 N and 500 N respectively). However, whilst these measurement ranges were appropriate to the exemplar data given (subject riding at 92 W single leg power at 63, 80 and 100 rev.min^{-1}, peak F_x ~ 85 N, F_z ~ 350 N), it was below what may be expected for the present study and so it is unclear whether this type of design would be appropriate.

A step towards greater ecological validity was made by Álvarez and Vinyolas (1996) by designing an instrumented pedal system that could be used with outdoor cycling. This took a completely novel approach to the design of such pedals. Rather than allowing the pedal to rotate about the spindle and decoupling the pedal top-plate and axle as had been previously done, Álvarez and Vinyolas rigidly mounted the pedal body onto the pedal spindle and moved the bearings into the crank arm. Eight strain-gauges were bonded between the pedal body and spindle which, allowed the measurement of both orthogonal force components in the plane normal to the crank spindle. The data were then transmitted, via a telemetric system, to a vehicle that followed the rider. Little detail was given of the calibration procedure, but maximum errors were reported to be less than 2% and the calibration matrix indicated that cross/direct sensitivities were 2.1% for F_x and 5.3% for F_z. Exemplar data was given for both riding seated on the flat at 390 W and standing on a 8 to 9% incline at 415W and the relatively low cadences (65 and 61 rev.min^{-1}) respectively thus elicits high peak forces (0.74 times body weight (545 N) and 1130 N respectively). Whilst these forces were comparable to those expected in the present study, it may be questioned whether housing the bearings in the crank would prove sufficiently robust if similar power outputs were maintained for several minutes as, required for the present study.

In 1996, Boyd *et al.* reported a design that was capable of interfacing with multiple pedal platforms of varying heights, whilst maintaining a desired elevation of the foot above the pedal spindle. The dynamometer was designed for substantial maximum loads (F_x 525 N, F_y 175N, F_z 1925 N, M_x 7 Nm, M_y 7 Nm, M_z 5 Nm) and used seven elements with thin cross-sections termed 'shear panel elements (SPEs)'. These were aligned such that four SPEs supported and measured the strain in the Z direction, two in the x direction and one in the y direction (see Figure 4-7). Measurement of the pedal loading was achieved by attaching two 90 degree strain-gauge rosettes aligned to the axis of principal strain to each face of the SPEs. These were wired into a full Wheatstone bridge configuration, thus making them insensitive to bending and axial strain with respect to the SPE orientation. Independent measurement from each of the SPEs thus allowed all 6 load components to be measured. The dynamometer was calibrated using the apparatus described by Hull and Davis (1981) and was shown to produce hysteresis of less than 0.5 N for all of the forces and 0.1 Nm for all of the moments (forces <0.3%. moments <2% relative to maximal design loads). Maximum errors were reported to be <6.5 N for forces and <0.45 Nm for moments (relative to maximal design loads F_x 1.16%, F_y 3.66%, F_z 0.02%, M_x 6.00%, M_y 3.29%, M_z 8.80%). However, similarly to the design of Davis and Hull (Davis and Hull, 1981; Hull and Davis, 1981), whilst the design produced accurate measurements of applied loads, its use was contingent upon the same complex calibration procedures and apparatus. This type of design may also not be suitable for the present study since, although the expected loadings fell within Boyd design's maximal loading parameters, the present study requires that high power outputs be maintained for several minutes. This was well beyond what was reported to be applied to this pedal (5 minutes at 180W, then 2 minutes at 250 W). This could potentially lead to failure of some of the less robust elements such as the 'crank hanger' (see Figure 4-7).

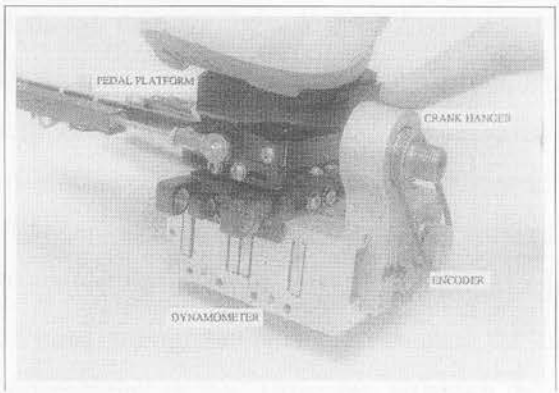

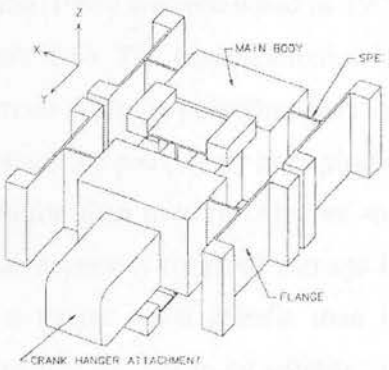

Figure 4-7: Pedal design and schematic of the interior of the pedal dynamometer design of Boyd *et al.* (1996) showing six of the shear plane elements (SPEs). The four SPEs to either side (as shown) supported and measured F_z forces, the SPE on top, F_y and the two below (one shown, the other is similarly orientated and translated in the negative *y* direction) F_x.

The design presented by Perrel *et al.* (1998) is also likely to be unsuitable for the present study since it was designed for clinical use and only used to measure power outputs of 28-70 W with cadences of 20 to 60 rev.min^{-1}. The scant reporting of the design indicated that it used strain-gauges on a double cantilever design, but was reliant upon cinematographical recordings for crank and pedal angles. However, although the frame rates for these were low (50 fps), the subjects were stroke patients and their self-selected cadences were 20 to 60 rev.min^{-1}, so this was likely to have been sufficient.

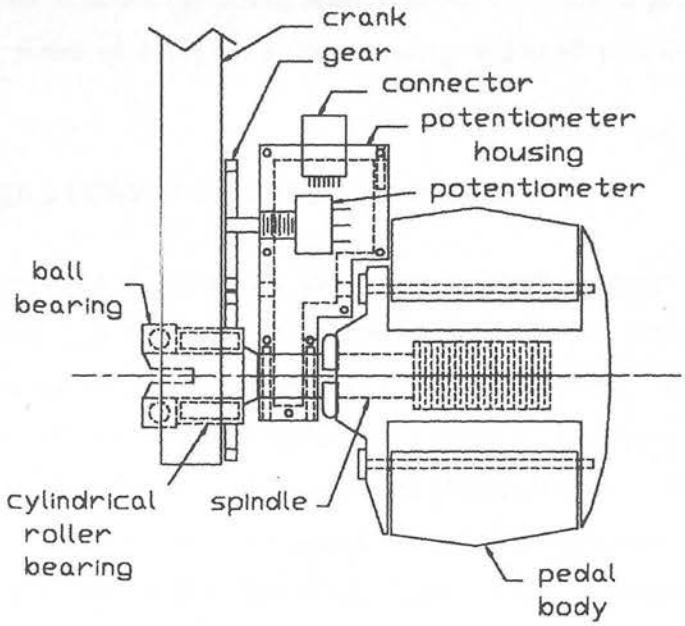

Figure 4-8: Schematic representation of the pedal of Rowe *et al.* (1998)

A design very similar to that of Álvarez and Vinyolas (1996) was presented in 1998 (Rowe *et al.*, 1998) intended for off-road use (Figure 4-8). The modifications with respect to that of Álvarez and Vinyolas involved moving both the potentiometers for measuring crank and pedal angle to an assembly between the pedal body and spindle. This served to locate them in a less vulnerable position than used by Álvarez and Vinyolas' (at the outer edge of the pedal) which was necessary to avoid damage in off-road riding, but also necessitated the use of a longer pedal spindle than in conventional pedals. However, although the effect of this has yet to be empirically determined in cycling, research has shown effects of 'Q-angle' (i.e. that between the tibial tubercle, the middle of the patella and anterior superior iliac spine) on running kinematics (Hamill *et al.*, 1999; Heiderscheit *et al.*, 2000). Since altering the medial/lateral position of the feet may alter this angle, it is suggested that effects may occur. The bearing design was also improved upon that of Álvarez and Vinyolas by the use of both ball and cylindrical roller bearings. However, although this went some way to addressing the questions over the designs' robustness, Rowe *et al.* stated that the maximum dynamic load rating for the bearings were 3700 N and 5930 N for the ball and cylindrical roller bearings respectively but that the maximum load anticipated would be 8000 N. The pedal was calibrated using the apparatus of Hull and Davis (1981) and accuracy checks revealed errors to be 1.9% for F_x and 0.7% for F_y and hysteresis to be <1.1% of full scale. Sample data showed peak F_z forces of ~300N and F_x forces of 120N for a subject riding at 250 W with a cadence of 90 rev.min^{-1}.

4.2: Designs using piezoelectric elements

When a force is applied to a piezoelectric device an electrical charge appears on the faces of the piezoelectric element. This charge is proportional to both the magnitude and direction of the applied force and it is this phenomenon that allows them to be used within force measuring transducers. Unlike strain-gauges, piezoelectric transducers are active devices, i.e. they produce charge. However, '*because charge can leak away through imperfect insulation,* [they] *... are unsuitable for measuring steady force*' (Noltingk, 1996). Thus since, when applied to pedals, '*not all load components have a zero average so extended warm-up periods will cause the*

dynamometer to drift. The capacitance must then be reset to zero load, between warm up and data collection' (Boyd *et al.*, 1996). This also makes them unsuitable for extended periods of data collection so this type of instrumentation should only be used in studies where brief periods of pedalling can be preceded by zero resetting of the piezoelectric charge with the pedal unloaded.

The elements to which the transducers are mounted are also required to be flat and rigid. Indeed, a lack of rigidity can lead to moments of force being applied to the sensor which, beyond certain limits can damage the transducer. Additionally, in order for them to be able to measure both compression and tensile loads and for shear forces to be transferred to them through static friction, they also must be pre-loaded. Thus a pedal dynamometer built using piezoelectric transducers must be capable of providing sufficient rigidity and withstanding the pre-loading in addition to their loading in use. This creates potential design issues in applications such as pedals where the dynamometer weight is of concern. Conversely, piezoelectric devices are less temperature sensitive than strain gauges, have high stiffness, resulting in very high resonant frequencies and possess very large measuring ranges. Additionally, they possess inherently low cross-sensitivity and require less frequent calibration checks than strain gauges. However, although some investigators using piezoelectric transducers in instrumented pedals have relied upon the manufacture's calibration and accuracy checks, this is inappropriate if accurate data are to be assured since the transducers are sensitive to pre-loading and out of plane mounting. Calibration and accuracy should therefore be confirmed by investigators with the transducers *in-situ.*

The first system to be presented designed around the use of piezoelectric devices was that of Ericson *et al.* (1984a). This used a tri-axial transducer (Kistler 9251A) to measure the applied forces with continuous data collection by a UV recorder. Angles were calculated from cinematographical recordings, which, at 60 fps, limited the researchers to being able to resolve these to approximately 6° of the crank cycle at the cadence selected (60 rev.min^{-1}). Although the technical information on the design of the pedals was limited, it is apparent that the transducers were mounted above the standard pedal platform. This would act to substantially raise the pedal platform height which is known to affect the mechanics of pedalling (Hull and Gonzalez,

1990). It was also not indicated if this was countered by raising the height of the opposite, non-instrumented, pedal or if the additional mass of the instrumented pedal was counterbalanced on the other side. Further, although the authors reported that the error of the force transducers themselves was less than 0.3% for the three orthogonal forces (Ericson, 1986), it was not reported whether any verification of this was undertaken with the transducer *in-situ*. Ericsons' group used the pedal to record data from subject riding at up to 240 W with cadences ranging from 40 to 120 rev.min^{-1}, however, only joint moments were reported in all of the papers (Bratt and Ericson, 1985; Ericson *et al.*, 1986; Ericson *et al.*, 1985a; Ericson *et al.*, 1985b) so the forces exerted on the pedal are unknown.

In 1990, Broker and Gregor reported a design based around dual piezoelectric transducers which was thus able to measure not only the components of the uni-axial loads and moments about the pedal axis but also the point of force application (Figure 4-9). The pedal used an inverted L-shaped block with the pedal spindle mounted through the vertical of the 'L', and the force transducers to the upper side of the base. This ensured that, with the pedal top plate mounted on top of the transducers, the pedal platform height was the same as for conventional pedals. Details of the calibration procedures were not given but the authors reported that the full scale accuracy was ± 5% and that the crank and pedal angles were measured with continuous turn potentiometers with an accuracy of ± 2%. However, as already discussed, piezoelectric transducers require rigid mounting, and it is unclear if this requirement is sufficiently met by Broker and Gregor's design since the L-shaped block was only supported by the pedal spindle on one side. The use of the 'L' shaped block, also increases the lateral distance between the pedal surface and, the crank arm, thus altering the angle between the hip joints and pedal surfaces and therefore feet with the potential implications already mentioned.

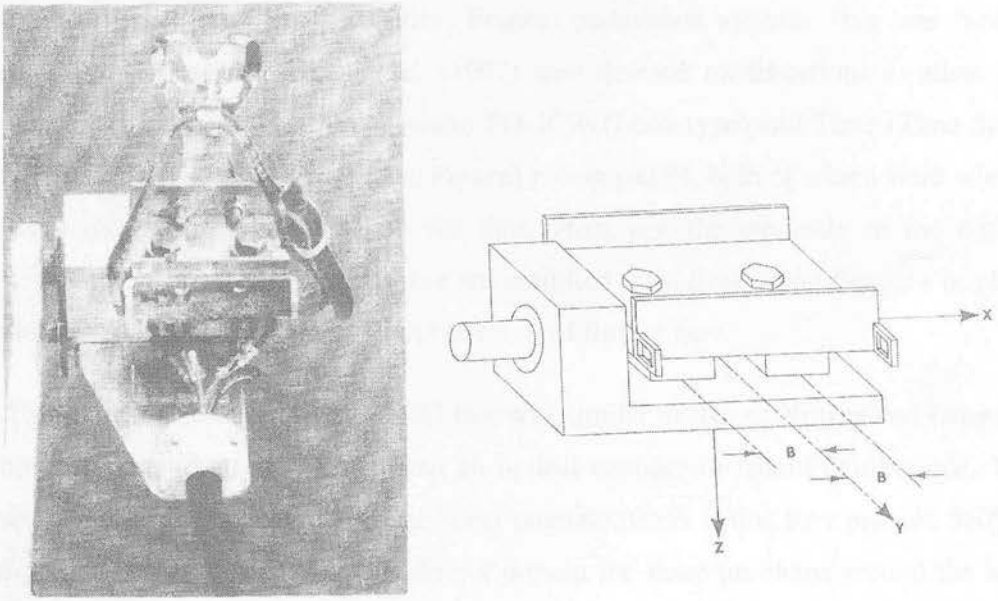

Figure 4-9: Pedal dynamometer and schematic of Broker and Gregor (1990)

One of Broker and Gregor's findings from their application of the pedal is also relevant in pedal design considerations. For the exemplar data, from a subject riding at 300 W with a cadence of 90 rpm, they reported that the centre of pressure (CoP) varied considerably during the crank cycle (2.5 cm medial-lateral, 2cm anterior-posterior). CoP is normally assumed to be at the centre of the pedal surface, and as the authors note '*this excursion can have a significant effect on the calculated pedal moment*'. Therefore, a pedal design that is not capable of measuring this variation may not be suitable for developing accurate inverse dynamic solutions. However, Broker and Gregor's pedal only possessed two force transducers and so, although it was capable of measuring M_z, the calculation of M_x and M_y was based upon the assumption that free moments (i.e. moments not due to eccentric loads) were not present about the x or y axes. However, the authors noted that some subjects using cleated cycling shoes were in fact able to apply free moments about the x-axis resulting in the CoP being erroneously calculated as being outside of the pedal. These assumptions may therefore not be valid.

Modifications of Broker and Gregor's original design were subsequently made in order to make them compatible with 'clipless' shoe/pedals systems that have now been almost universally adopted by cyclists. Firstly, Gregor *et al.* (1991) presented design modification that made the pedals compatible with the popular Look (Look

Cycle International, Nevers, Cedex, France) pedal/shoe system. This was further expanded upon by Wheeler *et al.* (1992) who devised modifications to allow the pedals to be compatible with Shimano PD-1056 (Look type) and Time (Time Sport International, Varennes-Vauzelles, France) racing pedals, both of which were widely used amongst racing cyclists at the time. However, the elements of the design pertinent to the instrumentation were not modified from Broker and Gregor's original design and so these papers will not be reviewed further here.

A design was used by Black (1994) that was similar to that of Broker and Gregor's but was advanced upon it by using an optical encoder to record crank angle. The advantage of optical encoders over linear potentiometers is that they provide 360° of digital electrical output and thus do not present the same problems around the zero crossing. However, since only 1 pedal was instrumented the problems of bilateral asymmetries already mentioned may be compounded by possible fatigue adaptive responses in alterations in this symmetry. A further major criticism of the use of this pedal for Black's study was the duration of the data collection (mean 13.04 minutes) which could introduce substantial errors due to zero drift because of the properties of piezoelectric transducers previously discussed.

The pedal design presented by Coleman and Hale (1998) was intended for the measurement of pedal forces during sprint cycling and thus had to withstand high loadings (maximum F_{eff} of 880 N). The pedals were therefore substantial, with masses of 1.480 kg per pedal (Coleman, 1994). The pedals were calibrated both by the suspension of known masses over relatively low loads (F_x and F_y, 200 N, F_z 300 N), and with a force and displacement measuring instrument over larger ranges (F_x and F_y, 0-2000 N, F_z ±2000 N) (Coleman, 1994). High load/output correlations for both calibration slopes were given (r^2 0.999953 low load, r^2 0.999983 high load) and mean crosstalk values of up 1.07% but no accuracy check was reported (Coleman, 1994). The pedal platform height (27 mm) was also substantially higher relative to conventional pedals which, as previously noted, could affect pedalling mechanics.

4.3: Other designs

Whilst the vast majority of the designs in recent times have used either strain-gauges or piezoelectric devices, there have been a few that have adopted other technologies. These will be discussed in this section along with papers where the reporting of the pedal design has been sparse but that may have something to add to an understanding of pedal design.

The design presented by Dal Monte *et al.* (1973) used pedals with two perpendicularly mounted '*potentio-metric linear tension transducers*'. The nature of these devices was unclear and no description was given although they appear to be some type of slide potentiometer. The outputs from the transducers were displayed on a cathode ray oscilloscope, from which screen images were recorded with a Polaroid camera. The display of the oscilloscope was calibrated to give a known relationship between '*tension*' (presumably force) and signal amplitude. These data were combined with cinematic recordings of crank and pedal positions to calculate forces relative to the crank. Synchronisation of the two data sources was achieved by an oscillating pantograph which activated a micro-switch, suspending the oscilloscope display at '*dynamic dead centre*'. Again, details of this were not given so how synchronisation points were determined in the film data was unclear, as were the accuracy of the activation by the pantograph or the temporal resolution achieved for the oscilloscope. Various combinations of sitting and standing pedalling trials were used whilst riding on the flat or an incline with maximum power outputs of 2400 $Kg.m.min^{-1}$ (392 W) and cadences ranging from 60 (on a slope) to 120 $rev.min^{-1}$ (on the flat). Validation procedures were not reported for the pedals and so the magnitude of errors is unknown. The value of this paper is thus limited by the scant details provided and misuse of technical terminology, it is however of note as the first study to apply instrumentation to both pedals.

A novel approach has recently been presented by Mornieux *et al.* (2006). They separated the cranks from an ergometer and rigidly attached these to a force plate, whilst the remainder of the ergometer was secured so that it would not make contact with the force plate but would still retain the ergometers original configuration.

Additionally, the friction force applied by the tension of the ergometer's belt was also recorded with a strain-gauge. The 3 orthogonal force components applied to each pedal were then calculated from the forces and moments obtained from the force plate, the force exerted by the chain (from the force applied by the tension belt and flywheel inertia) and the locations of the pedals relative to the plate. Static evaluations of the force applied to the pedals were carried out by manual application and measurement with a second strain gauge and inclinometer. However, this was conducted over a smaller range (F_x 100-160 N, F_y 60-65 N, F_z 220-300 N) than was observed for some of the peak forces in the exemplar data presented (300 W at 90 rev.min^{-1}: F_x 160 N, F_y 70 N, F_z 450 N). This evaluation method may also be flawed in that, as the investigators themselves noted, '*it was impossible to accurately maintain the direction of the force applied by the investigator during calibration*'. Despite this however, they obtained errors of 2.60% for F_x, 3.98% for F_y and 3.06% for F_z which is comparable to some of the instrumented pedal systems previously reviewed. The authors also indicate that it may be possible to increase the accuracy of the method by accounting for pedal moments.

Various other papers have made use of instrumented pedals, but the design of the pedals has been of secondary importance to the research question and so little detail has been reported on the pedals design, calibration and validation. For example, the pedal of Cavanagh and Nordeen (1976) was initially only reported as an abstract so provided minimal details of the design. Subsequent papers (Lafortune and Cavanagh, 1980, 1983; Lafortune *et al.*, 1983) focused on application and so add little to the information on the pedal design.

Similarly, Miller and Seireg (1977) only reported that the pedal was capable of measuring normal and tangential forces but no detail of instrumentation or calibration was given. However, it was the first design to use potentiometers to measure pedal and crank angles.

Sanderson's (1986) paper focused on the use of instrumented pedals in the provision of real-time feedback. Thus, although substantial detail of software design was reported, information on the pedals used was scant, other than that both pedals were instrumented and that pedal and crank angles were directly measured.

Patterson and Moreno (1990) reported a design using strain-gauges capable of measuring F_x and F_z forces. They stated that errors were <2% and cross-effects <1.5% but details of the design or testing of the pedals were not given. However, although they report results for subjects riding at 200 W with cadences ranging from 50 to 120 rev.min^{-1}, they noted that they were unable to record the forces associated with the same power output at 40 rev.min^{-1}. Although F_x and F_y and were measured they were not reported, however, F_r forces peaked around 400 N which was well below the figures expected for the present study making the design unsuitable.

Takaishi *et al.* (1998) reported only that the pedal that they used was instrumented with strain-gauges and sampled at 1 kHz. However, it is apparent that the design was only capable of measuring the forces normal to the pedal surface and so was incapable of effectively measuring the propulsive forces produced by the subjects.

4.4: Discussion of designs

Researchers have made use of load measurement technologies to produce a wide variety of pedal designs capable of measuring loadings ranging from the relatively low force associated with clinical populations (e.g. (Ericson *et al.*, 1984b) to the large forces produced by international level sprint cyclists (Coleman and Hale, 1998). These have ranged from simple designs capable of measuring only total applied forces (Brooke *et al.*, 1981) to complex ones capable of measuring all 6 force components (Boyd *et al.*, 1996; Broker and Gregor, 1990; Hull and Davis, 1981). However, pedal designs appears to have reached its apogee since none of new design presented since the mid 1990's have represented a paradigm shift on those that have gone before. Additionally, it should be noted that some researchers have failed to report key information on their designs such as the calibration procedures, accuracy, hysteresis and cross sensitivity. For strain gauge designs, important information on gauge placement has also often been omitted and pre-loadings not given for piezoelectric devices. Whilst in some cases, this may be attributed to the principal research focus being on the pedals design, but in some cases this has been apparent in papers specifically intended to report the equipments design. Failure to adequately

report such details stifles subsequent researcher's attempts to assess the designs and may hinder progress in this area.

An examination of the existing designs reveals them to be unsuitable for the present study for a variety of reasons. Firstly, since the current study requires data to be collected continuously for over 20 minutes, those based around the use of piezoelectric transducers cannot be adopted because of the drift characteristics of such devices. Also, those that are not capable of resolving propulsive force into its orthogonal components are inappropriate since this severely curtails the usefulness of the information that can be gathered with regard to fatigue adaptations. Conversely, whilst adaptation to moments and F_y may occur with fatigue, it is the adaptations that serve to continue the required task with progressing fatigue that is of interest in the present study. Therefore, the designs capable of measuring all 6 force components create more complexity, especially with regard to their calibration than is required to answer the research questions. Many of the remaining designs must be eliminated for consideration since the expected magnitude and duration of loading in the current work exceeds that for which they were designed or because they were not designed to be compatible with the now almost ubiquitous 'clipless' pedal/cleat systems. Hence it was deemed that a new design would need to be produced to meet the specific demands of the current research.

However, there is much in the literature to inform this design. Most simply, the evidence of asymmetry demonstrates that the instrumentation must be applied to both pedals. They must also be able measure both pedal and crank angles and be as geometric similar to riders' own pedals as possible, especially with regard to the pedal platform height and medial/lateral spacing. Further, since the duration of the protocol necessitates the use of strain-gauges, the development of calibration apparatus and procedures that can allow for accurate calibration over the desired range and the measurement of cross-effects will be important.

Thus the current research presents specific design requirements that necessitate the development of new equipment. The design and testing of which is presented in the following chapter.

Chapter 5: Instrumentation of pedal for force measurement, design and static testing

5.1: Introduction

The various challenges and requirements that are presented by any attempt to construct instrumented pedals are apparent from the review of previous literature. However, there are also additional considerations that are particular to the present research. Principally, these relate to the requirement to collect data continuously over extended periods of time combined with power outputs higher than in most of the previous studies examining steady state riding. Of the few studies to have used similarly high power outputs, Black (1994) showed peak F_z forces of 394 ± 80 N at a cadence of 90 rev.min^{-1} for subjects riding at 80% of the maximal power achieved in a ramp test. Similarly, Álvarez and Vinyolas (1996) showed peak F_z forces of 0.74 times body weight (545 N) and peak F_x forces of ~140 N for a subject riding at 390 W. However, in Álvarez and Vinyolas' study, the cadence was lower than those that are expected in the present study (65 rev.min^{-1}) so pedal forces are therefore also expected to be lower. Thus, although data are not available on the pedal forces to be expected with the protocol used for the present research, it is not unreasonable to extrapolate from Black and Álvarez and Vinyolas' data since force production patterns are likely to be similar in pattern, although scaled in magnitude. It can therefore be stated that, in order to be able to successfully design pedals able to provide answers to the primary research questions, the following criteria must be met;

- Both pedals must be instrumented.
- The pedals must be capable of measuring forces normal to the pedal forces in the range of -300 to 700 N and fore-aft forces in the range of ± 150 N.
- Pedal forces must be measured with full scale accuracy of ± 5%, i.e. within -15 to 35 N for normal forces and ± 7.5 N for fore-aft forces at full-scale deflection.

- The pedals must provide an interface that is compatible with the subjects' shoe/ pedal systems.
- The geometry of the pedal/cleat interface must be as close as possible to a conventional pedal.
- The pedals must be capable of providing reliable output during up to 25 minutes of continuous riding.
- The pedals must produce data in a form convenient for computer analysis.

5.2: Method

5.2.1: Design of pedals

To meet these criteria, a design based around an inverted T-beam was developed, with a hollow section through the horizontal section of the T across both axes so that all forces applied to the pedal would be transmitted to the crank via four thin elements (see Figure 5-1). Bonded to the outer surface of these sections were 8 strain-gauges, wired into two fully heat-compensated Wheatstone bridges. The bridge for the vertical forces was made using 2-element paired gauges (see Figure 5-3). Bolted to the inverted T-section was a top-plate that provided an interface compatible with Look (Look Cycle International, Nevers, Cedex, France) type shoe

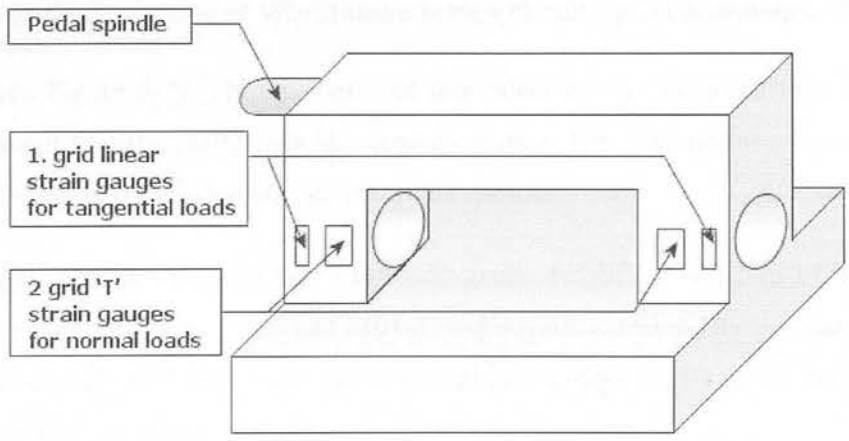

Figure 5-1: Schematic representation of lower inverted 'T' section of force pedal; pedal interface removed. Note, strain gauge placements are identical on opposite side (not to scale).

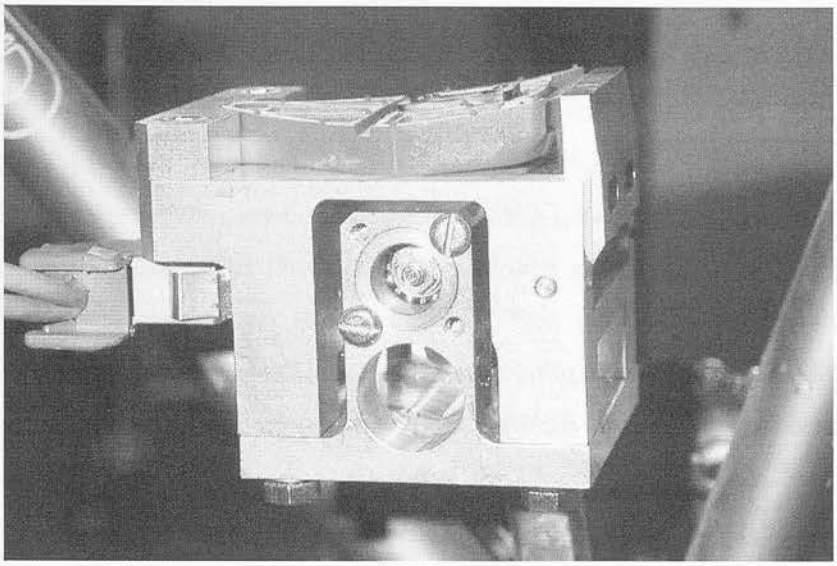

Figure 5-2: Instrumented pedal with angle measurement pick-up removed

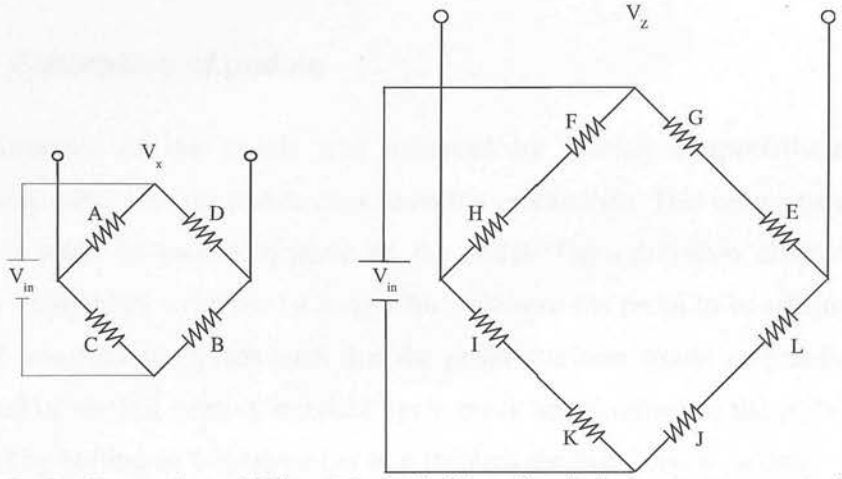

Figure 5-3: Configuration of Wheatstone bridge circuit for measurement of vertical and horizontal forces

cleats (see Figure 5-2). The geometry of this interface was identical to a standard pedal except that the platform was raised by 6 mm. This was necessary to provide clearance between the top-plate and the pedal spindle.

The bridge circuits were connected to strain-gauge amplifiers (RS 846-171) and all data were collected through a CED 1401 (Cambridge Electronic Design, Cambridge, England) capable of 12-bit analogue to digital conversion with a computer running Spike 2 (CED), sampling at 1 kHz.

5.2.2: Design of pedal and crank angle measurement apparatus

Pedal angle was measured by a continuous turn potentiometer (RS 2508975946) mounted on a bracket on the side of the pedal, with the shaft attached to the pedal axle. Crank position was obtained via two meshing identical 80T plastic gears (RS 745-387), one bonded to the inside of the crank arm and the other to the shaft of a Smart Position Sensor (SPS) (RS 601-1045). This gave an output similar to a standard continuous turn potentiometer but gave complete 360° of electrical travel. This was mounted to an aluminium bracket attached to one of the beams of the ergometer (SRM, Jülich, Germany) such that, by adjusting its position on the beam, it could be closely meshed with the other gear. For the final study (see Chapter 8), this was mounted to the tube of the bicycle frame. However, the setup was otherwise identical.

5.2.3: Calibration of pedals

The calibration of the pedals was achieved by placing a specially designed 'calibration cleat' into the pedals cleat retention mechanism. This cleat was designed so that it could be locked in place on the pedal. The calibration cleat was then securely clamped in a custom built rig which allowed the pedal to be orientated and adjusted using screw threads such that the pedal platform would be parallel to the horizontal or vertical axes. A standard cycle crank arm attached to the pedal spindle extended by bolting an additional bar to it through the distal end of which a threaded rod was bolted in place such that it was perpendicular to the crank arm. The threaded rod was loaded with half the highest load to be used for the calibration and the alignment of the pedal was checked with a spirit level. The pre-loading was done so that any distortion of the rig under load would average around zero over the loading range. The pre-load was then removed and a series of 5 kg masses were placed onto the threaded rod vertically aligned with the centre of the pedal with data being collected as the pedal was taken through 3 loading and unloading cycles in the positive and negative x and z directions (See Figure 5-4). In the z-axis a total of 736 N was used in the positive direction and 343 N in the negative direction. In the x-axis, 196 N were used in both the positive and negative directions. These ranges

were at least 10% greater than the values observed in pilot work and are coherent with the observed force ranges in relevant literature (Álvarez and Vinyolas, 1996; Black, 1994; Sanderson and Black, 2003).

Mean values were taken over three seconds for each load for each of the three loading and unloading cycles and the mean zero loading values subtracted. Linear regressions were then calculated between applied load and voltage output and regression slopes used to generate a calibration matrix of direct and cross-effects (see Equation 5-1). Linearity was determined as the maximum deviation in output from linear as a percentage of full scale deflection (FSD) (Bartlett, 1997 pp. 211). Similarly, hysteresis was calculated as the maximum difference in voltage output for the same force between loading and unloading as a percentage of FSD (Bartlett, 1997 pp. 212) and cross effect voltage outputs were calculated as a percentage of direct effect voltages.

$$\begin{Bmatrix} F_x \\ F_z \end{Bmatrix} = \begin{bmatrix} C_{11} & C_{12} \\ C_{21} & C_{22} \end{bmatrix} \begin{Bmatrix} V_x \\ V_z \end{Bmatrix} \qquad \text{Equation 5-1}$$

In order to assess the reliability of the calibration slopes over time four repeated calibrations were conducted over a four week period. These used 6 loads for both F_x and F_z (F_z ± 300N, F_x ± 150N) and thus did not cover the full calibration range.

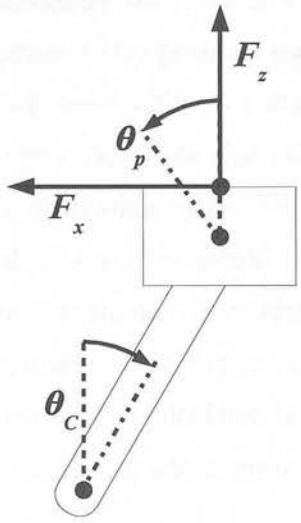

Figure 5-4: Definition of foot-load reactive load components and crank (θ_c) and pedal (θ_p) angles (crank rotating in a clockwise direction)

However, the previous calibration had shown the response to be linear across the range thus 6 points would be sufficient to produce representative calibration coefficients. Typical errors (TE) and intra-class correlation coefficients (ICCs) were calculated to compare the calibration coefficients from the repeat partial calibrations with those obtained from the full-calibration.

To verify the accuracy of the apparent forces, the pedals were statically loaded with known masses up to the same loads used for the calibrations and maximum errors calculated between the apparent force and the known applied load.

5.2.4: Validation of angle measurements

The manufacturers claimed linearities for the potentiometers and SPS were ± 2.0% ± 1% respectively. To verify these figures, the SPS was connected to the regulated supply to be used for the subsequent studies (Heathkit IP-2718) and securely mounted to a bench with the plastic gear attached. A fixed marker was then set up so that it was in close proximity to the outer edge of the gear. Each of the gear's teeth were then aligned in turn to the marker and the voltage across the SPS measured with a digital voltmeter (i.e. every 4.5°). The same procedure was followed for the potentiometers which were removed from the pedals and the gear attached. Linear regression slopes were then calculated for voltage output against angle and linearity calculated as the maximum deviation from linear expressed as a percentage of maximum output. The potentiometers also posses a region of distortion in electrical output around the zero crossing point (20° ±3°) that must be filled with linear interpolation. To minimise the potential error that this could introduce into pedal angles measurements and thus calculation of the forces relative to the crank, the potentiometers were positioned so that this would occur where forces would be lowest, i.e. TDC. To verify the magnitude of potential errors associated with this, data were used from a pedalling trial in which the zero crossing point was not aligned with crank TDC. Percentage errors were calculated between the data from the area where the distortion would normally occur and a linear interpolation of this region.

5.3: Results

The calibration matrices derived for the left (Equation 5-2) and right (Equation 5-3) pedals show cross effects to be around 3% for F_z loading and around 5% for F_x. Linearity was below 6% (see Figure 5-5) and hysteresis below 2% in all cases (Table 5-1). The mean ICCs for the coefficients obtained for the full and repeat calibrations were 0.998 (0.996 to 0.999), mean TE 0.022 N.v^{-1} (min: 0.017, max: 0.030)

$$\begin{Bmatrix} F_x \\ F_z \end{Bmatrix} = \begin{bmatrix} 1.238 & -0.060 \\ -0.012 & 0.403 \end{bmatrix} \begin{Bmatrix} V_x \\ V_z \end{Bmatrix}$$

Equation 5-2: Left pedal

$$\begin{Bmatrix} F_x \\ F_z \end{Bmatrix} = \begin{bmatrix} 1.088 & -0.069 \\ -0.011 & 0.358 \end{bmatrix} \begin{Bmatrix} V_x \\ V_z \end{Bmatrix}$$

Equation 5-3 Right pedal

Table 5-1: Absolute and percentage errors in full scale deflection (FSD), linearity, hysteresis and cross-effects measured for the instrumented pedals

5.3.1:	Left F_x	Left F_z	Right F_x	Right F_z
ABS error (N)	9.4	31.4	2.5	31.7
% error	6.2	4.5	1.7	4.5
Linearity (%FSD)	4.8	3.6	2.4	5.9
Hysteresis (% FSD)	0.4	1.3	1.7	1.6
Cross-talk (%)	4.8	3.0	6.3	3.1

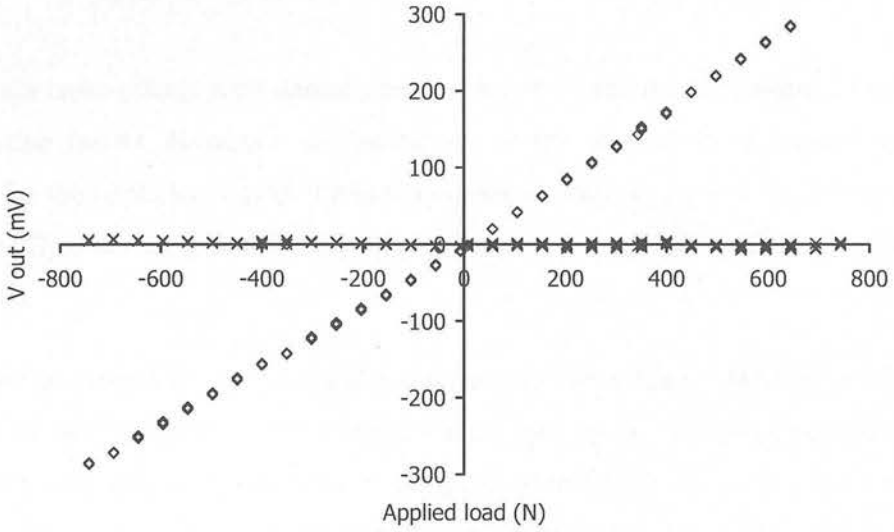

Figure 5-5: Exemplar calibration plot for left F_y showing direct (diamonds) and cross (crosses) outputs against applied load

5.3.2: Test of SPS and potentiometer

In all cases, the linearity of the potentiometers and SPS exceeded the manufacturers claimed linearity (absolute maximum error from a linear slope: left potentiometer: 1.33%, right potentiometer: 0.96%, SPS 1.45%). The errors associated with linear interpolation of the distortion region were found to be <0.8%.

5.4: Discussion

It was stated in the design criteria that these pedals must be capable of measuring F_z forces in the range of -300 to 700N and F_x force of ± 150N. The testing described has shown them to be capable of accurately measuring force over this range. Although their accuracy falls short of those reported by some of the previous researchers (Álvarez and Vinyolas, ; Boyd *et al.*, 1996; Hull and Davis, 1981; Newmiller *et al.*, ; Patterson and Moreno), in most cases (Boyd *et al.*, 1996; Hull and Davis, 1981; Newmiller *et al.*) this was achieved with the elaborate calibration equipment and procedures of Hull and Davis (Hull and Davis, 1981). However, the accuracy of the current design is comparable to that of some others (Broker and Gregor, 1990; Brooke *et al.*, 1981) and, with the exception of the left F_x forces meet the criteria laid out as being necessary to be able to detect the magnitude of changes observed in previous comparable work (Black, 1994; Black *et al.*, 1993b; Sanderson and Black, 2003).

Although cross-effects were demonstrated, these were small and accounted for in the calibration matrix. However, the limitations of the calibration equipment did not allow for the application of multiple simultaneous loads as used by Hull and Davis (1981). Thus the magnitude of any effects from such out of plane loading cannot be assessed.

The design criteria of replicating the geometry of the subjects' normal pedals was met with the exception of the slight (6 mm) increase in the height of the pedal platform with respect to the axis of the pedal spindle. Whilst Hull and Gonzalez (1990) have indicated that joint moments are altered by changes in pedal platform

height, this was for much large deviations (40 mm). This is therefore felt to be an acceptable compromise.

The apparatus for measurement of crank and pedal angles has also been demonstrated to be capable of accurate and valid measurement of these parameters. Although the potentiometers do not provide a full 360° of electrical rotation, the error resulting from interpolation is small (≤2.8°) and, if the area where this occurs is placed around crank TDC, since pedal forces in this are low, any errors in forces calculated relative to the crank will be very small.

The design therefore meets the design criteria specified sufficiently to support the use of the equipment for the collection of the kinetic data for the final study. The only standard that remains to be verified is the ability of the equipment to provide valid and reliable data during prolonged (>21 minutes), dynamic loading. However, this will be assessed in the next chapter.

Chapter 6: Comparison of power output obtained from SRM power measuring crankset to that from instrumented pedals

6.1: Introduction

In developing instrumented pedals, previous researchers have relied upon static measurements and inter-study comparisons to verify the equipment's suitability for their intended use. The reliability and validity of the designs under dynamic loading has therefore not been assessed. The present study seeks to redress this in the present chapter by conducting a dynamic validation against a criterion measure (SRM Power Measuring Crankset, Schoberer Rad Meβtechnik, Germany) under the conditions in which the equipment is intended to be used. The study will thus serve to both establish the equipments suitability for the intended research and confirm that the protocol would ensure that subjects would maintain the intensity required for the final study for an average of around 4.5 minutes.

The validity of the criterion measure has been previously assessed by previous research. The power output measured by these instrumented cranks have been shown to be valid against power obtained from a Monark ergometer that has been driven by normal pedalling (Martin *et al.*, 1998), arm cranking (Balmer *et al.*, 2004) or a motorised treadmill (Jones and Passfield, 1998). They have also been validated against a dynamic calibration rig (CALRIG) (Gardner *et al.*, 2004; Lawton *et al.*, 1999).

6.2: Method

Eight participants (7 male, 1 female, age 36.2 ± 6.4 years, height 1.77 ± 0.07 m, body mass 67.7 ± 7.6 kg) currently competing in an endurance cycling discipline undertook two tests on an SRM ergometer separated by at least 2 days. The first was a maximal ramp test using protocols based on those of the British Cycling World Class programmes, i.e. a ramp rate of 20 $W.min^{-1}$ for male subjects and $15W.min^{-1}$ for female subjects with the power being increased in 5 W steps every 15 s (male) or 20 s (female) (British Cycling, 2003). Starting powers were set according to the

subject's body mass and the racing category in which they currently compete* These are shown in Table 6-1 (male) and Table 6-2 (female). The ergometer was set up to replicate the subject's normal riding position as closely as possible and power data from the SRM ergometer were sampled at 2 Hz. Whilst a higher sample rate would have been preferable to allow for the effects of intra-cycle power fluctuations, this was the highest rate available with the SRM system. The tests were stopped when the subjects voluntarily terminated the test or cadence showed a sustained marked decline for more than 30 seconds. From this test, the subject's maximal minute power (MMP) was calculated as the highest one minute mean power.

Table 6-1: Starting powers for male subjects in ramp test: Ramp rate = 20 W.min $^{-1}$

Body mass (kg)	3/4 Cat. Licence	E/1/2 Cat. licence
<50	120	140
50-59	140	160
60-69	160	180
70-79	180	200
80+	200	220

Table 6-2: Starting powers for female subjects in ramp test: Ramp rate = 15 W.min^{-1}

Body mass (kg)	3/4 Cat. licence	E/1/2 Cat. licence
<45	80	95
45-49	95	110
50-54	110	125
55-59	125	140
60-64	140	155
65+	155	170

For the 'fatigue' trial, the ergometer was set up as before, but with the saddle and handlebar height being raised by 6mm to allow for the difference in pedal platform height between the instrumented and standard pedals. Subjects rode the first 7 minutes at 50% of their MMP, before the power was then increased to 95% MMP over 4 minutes in 4 or 5 W steps. The slight variation in ramp rate was required because power could only be set in 1 W increments on the ergometer, so these were rounded to the nearest integer. The subjects were then asked to sustain this for as

* This is the system adopted by British Cycling to classify competition standard. These categories range from Elite (E) through first (1) to fourth (4) in descending order. Promotion and demotion between categories is determined by placings in races gained in the current and previous year.

long as possible. The test was terminated under the same conditions as for the ramp test.

The 95% MMP power output was selected to elicit failure in around 4 to 5 minutes from reaching the power output (Hettinga *et al.*, 2006). This provided a duration that would create a balance between providing a sufficient duration to allow changes over time to be observed, whilst also producing a relatively rapid deterioration in the subjects' ability to maintain the required power output and so increase the chance of technique changes also being rapid and therefore more identifiable between the time windows. It was also selected to provide a 'real-world' relevance to the findings by coinciding with the duration of a common cycling discipline (4000 metre individual pursuit). The lower fatigue power output was chosen to be around the lowest power output that the subjects would be likely to regularly train at[†] and therefore have well developed techniques appropriate to. From this, the duration of the initial ramp section was determined by pilot work as the highest ramp rate that could be achieved between the two without eliciting premature fatigue in the subsequent steady state section. Minimisation of the ramp duration was required so that the majority of the fatigue effects would occur during the steady state section rather than the ramp. This then dictated the length of the initial section as the only work to have examined the stability of cycling techniques (Sarre *et al.*, 2005) reported that, at least kinetic parameters, are stable after a ten minute 'warm-up' and again, minimum times were sort to minimise fatigue effects.

During this test, the ergometer was also fitted with the instrumented pedals described in Chapter 5 with force and crank and pedal angle data being collected through a CED 1401 (Cambridge Electronic Design, Cambridge, England) sampling at 500 Hz. All data from the pedals (force and angular data) were then filtered at 6 Hz using a finite impulse response filter to attenuate electrical noise. This filter cut-off frequency was selected by residual analysis (Winter, 1990 pp. 41-43). No filtering was applied to the data from the SRM ergometer as the data were already averaged over 0.5 seconds (highest available sample rate) by the equipment and so additional

[†] This equates to the midpoint of 'zone 2' in the British Cycling zoned training system adopted by the majority of riders in endurance disciplines in the UK.

smoothing was deemed unnecessary. Zero offsets were taken by setting the cranks vertically with the right crank at TDC and the pedals horizontally with no loading with alignments checked with a spirit level. Recordings were then taken for several seconds with the process repeated twice pre and twice post test. For the force data, the mean of the two pre and two post test values were taken to give separate pre and post zero offsets whilst the mean of all four values was used for the angle zero positions.

6.3: Data analysis

The power output from the pedals (P_p) was calculated by custom written programs (more details of these and full listings are provided in Appendix 1). The first of these (FP_process, see Appendix I) converted the recorded voltage data to angles and forces. For the angle data, zero offsets were subtracted, and the channel scaled to 0 to 360 degrees. For the pedal angle data, the areas around the potentiometer zero crossing points were also filled by linear interpolation. For the force channels, zero offsets were subtracted allowing for any zero drift during the course of the trial and the data multiplied by the values in the calibration matrix including removal of cross-effects (see Chapter 5). The second program (FP_power, see Appendix 1) applied the filtering to the data, and calculated the power for each pedal as;

$$P = F_{eff} \ell_c \omega_c \qquad \text{Equation 6-1}$$

Where P is power, F_{eff} is effective force, ℓ_c is crank length and ω_c is the angular velocity of the crank and;

$$F_{eff} = F_x Sin\theta_p + F_y Cos\theta_p \qquad \text{Equation 6-2}$$

Where, θ_p is pedal angle and;

$$\omega_c = \frac{\Delta\theta_c}{\Delta t} \qquad \text{Equation 6-3}$$

Where θ_c is crank angle and t is time.

The final program (FP_export, see Appendix 1) calculated means for each data channel over five second time windows and exported them for further analysis. Mean total power was calculated by simple addition of the powers from the two pedals ($\overline{P}_p$) and mean five second power output were also calculated for the SRM cranks ($\overline{P}_s$). Although it would have been preferable to compare the two data sets cycle by cycle, this was not possible because of the technical limitations of the SRM system. Five second means were therefore used as a balance between maximising resolution and avoiding errors in slight differences in the start and end points of partial crank cycles within the time windows.

Linear regressions, typical errors (TE, i.e. the within-subject standard deviations) and intra-class correlation coefficients (ICCs) were calculated between the two sources of power measurement for each subject and for all trials. ICCs were calculated as (Hopkins, 2006);

$$ICC = 1 - TE^2 / (Var_p + Var_s) / 2) \qquad \text{Equation 6-4}$$

Where Var_p and Var_s are the variances for the pedal and SRM data sets respectively.

6.4: Results

Participants achieved a mean MMP of 358 W ± 39 W and were thus required to maintain 340 W ± 37 W at the 95% MMP level. The mean duration from reaching this power output to test termination was 267 s ± 95s (min: 130 s max: 384 s).

Comparison of the data recorded by both devices across all trials showed that the trends of power production were closely matched (see Figure 6-1 and Figure 6-2) throughout the trials. The relationship was also shown to be linear and close to unity over the measured range although an offset was present ($\overline{P}_p = 1.04\,\overline{P}_s + 13.45$) with a mean difference of 9 % (23 W). Typical errors were 18.4 W with an ICC of 0.967 (see Figure 6-3 and Figure 6-4).

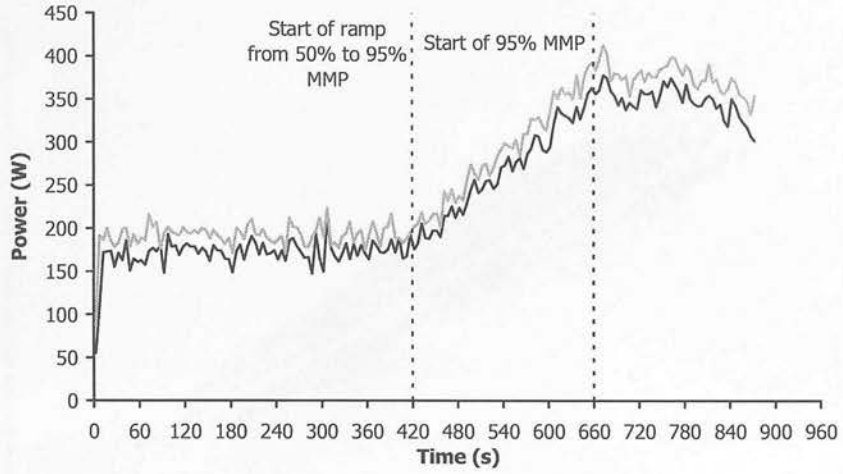

Figure 6-1: Exemplar power output from trial where $\overline{P}_p$ < $\overline{P}_s$ as measured by both the instrumented pedals (black line) and SRM cranks (grey line) during the course of a fatigue trial

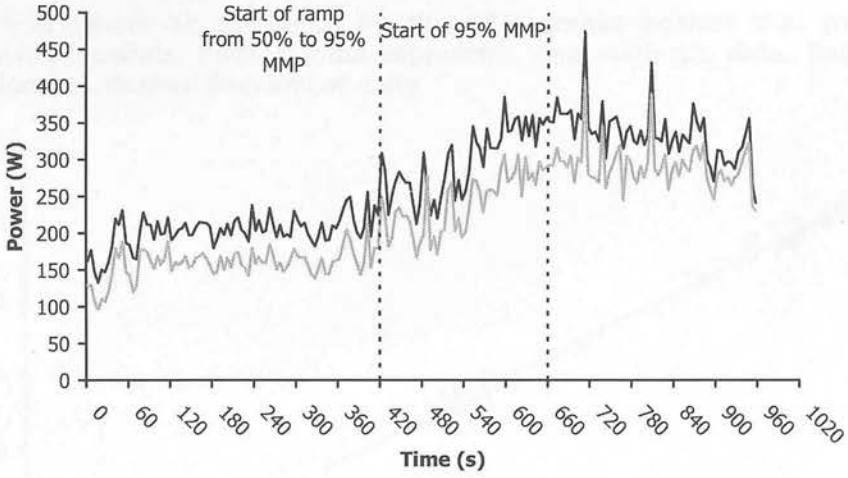

Figure 6-2: Exemplar power output from trial where $\overline{P}_p$ > $\overline{P}_s$ as measured by both the instrumented pedals (black line) and SRM cranks (grey line) during the course of a fatigue trial

Within the individual trials, the relationship was again shown to be linear and close to unity, with a consistent offset ($\overline{P}_p$: 1.02 $\overline{P}_s$ + 18.34 (SD of slope: 0.05, SD of offset: 21.56). However, typical errors were shown to be substantially lower (TE 7 W; 3 W to 10 W and ICCs higher 0.988 ± 0.008; 0.977 to 0.998 compared with the across trial comparisons.

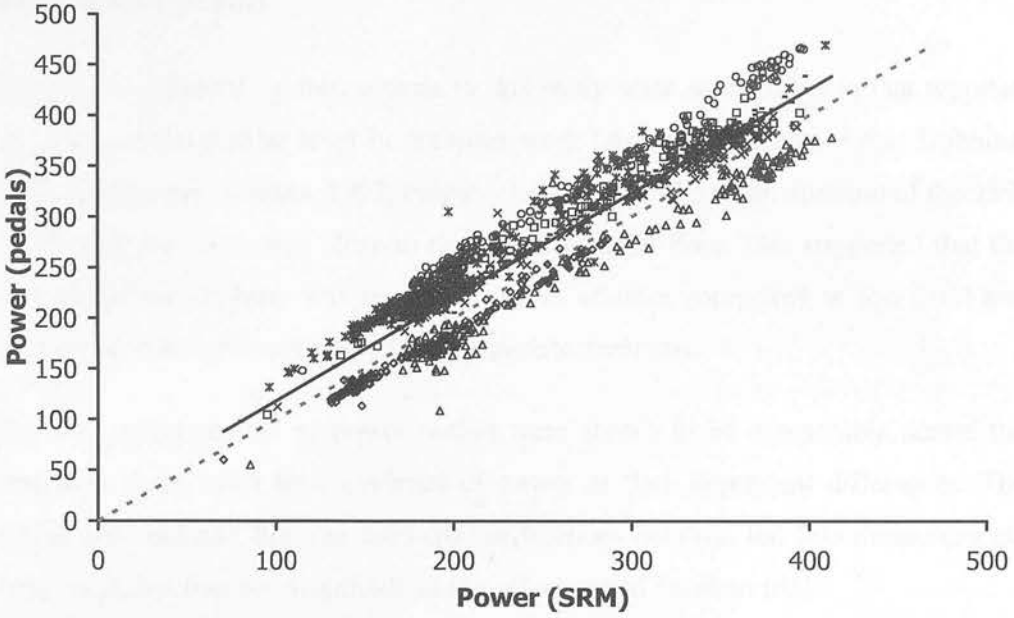

Figure 6-3: Power as measured by the SRM cranks against that from the instrumented pedals. Each symbol represents one subject's data. Solid line: regression line, dashed line: line of unity

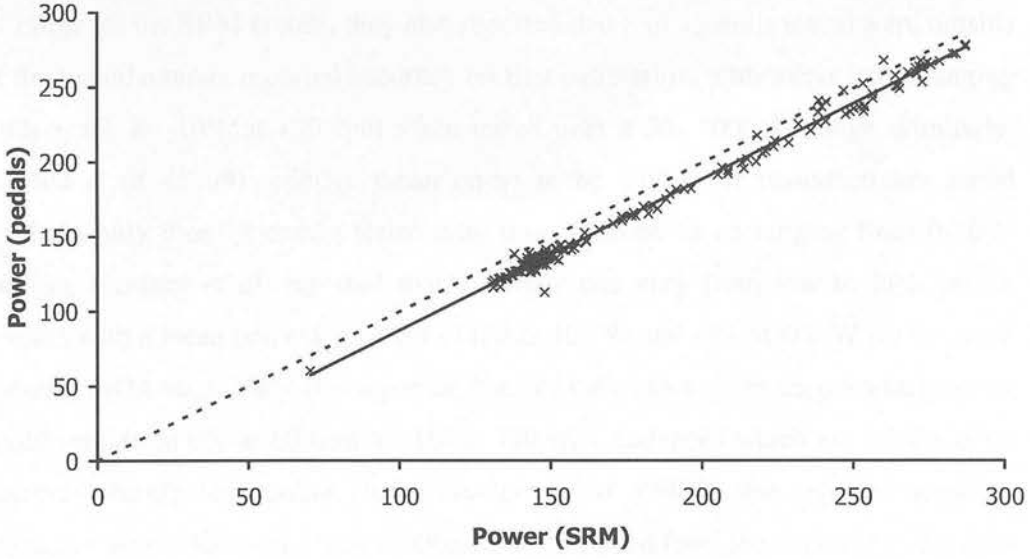

Figure 6-4: Exemplar power output as measured by both SRM cranks against that from the instrumented pedals during the course of a fatigue trial

6.5: Discussion

The MMPs achieved by the subjects in this study were comparable to that reported for athletes of a similar level in previous work (Arts and Kuipers, 1994; Dobbins, 1996; Hawley and Noakes, 1992; Palmer *et al.*, 1994). The mean duration of the 95% MMP level was also very close to the intended target time. This suggested that the standard of the subjects was representative of athletes competing at this level and indicates that the protocol will elicit appropriate durations.

The two measurements of power output were shown to be comparable across the measured range, with little evidence of power or time dependent differences. The results also indicate that the intra-trial differences between the two measurements were small, but that the magnitude of the offset varied between trials.

The assumption in the current study is that the SRM cranks provide a criterion measure since their reliability and validity has been previously established. However, although Gardner *et al.* (2004), reported mean error scores of 2 ± 5% over a 50-1000 W range for the SRM cranks, they also reported that 8 of 19 units tested were outside of the manufacturers reported accuracy on first calibration, with mean errors ranging from + 1% to -10% at 100 rpm when tested over a 50- 1000 W range. Similarly, Lawton *et al.* (1999) reported mean errors to be within the manufacturers stated levels in only 9 or 19 cranks tested with measurement errors ranging from 0-10%. Further, Gardner *et al.* reported that accuracy can vary from low to high power outputs with a mean percentage error of 0% at 100 W and -3% at 800 W for the most accurate SRM used. They also reported that, for the same unit, mean percentage error could vary from 0% at 60 rpm to -1% at 120 rpm, cadences which are within those observed during the current study. Gardner *et al.* (2004) also reported apparent hysteresis when fluctuating power outputs were applied from the dynamic calibration device in some units, although the magnitude of this apparent affect and whether it occurred in all of the SRM units was not detailed. Gardner *et al.* also reported mean errors to be altered by changes in ambient temperature. However, since all testing for the current study was undertaken within a laboratory setting, temperature variation was low (22.1° ± 1.5 °) and so this effect is unlikely to be substantial.

Balmer *et al.* (2004) also reported that significant differences were apparent between the power outputs from the Monark ergometer and SRM system depending upon the time period over which means were taken. When 5 second averages were used, the mean difference between the power outputs obtained from the SRM unit and the Wingate (corrected) was -16%, whilst with 1s averages, this was -27%.

Additionally, there is a potential additional source of error in the power outputs derived from the SRMs. These systems derive ω_c from the times between single pulses obtained each crank cycle. ω_c is therefore assumed to be constant within the crank cycle. However, data from the pedal system shows substantial intra-cycle variations typically of the order of 10-15 rev.min^{-1}. This is likely to lead to both substantial under and overestimation of power output within the crank cycle by the SRM system, especially since maximas and minimas in ω_c and F_{eff} are likely to be coincidental. To verify this, 5 second mean power was calculated from a small sample (~1x10^5 data points, i.e. ~200 s) of the pedal data both using the mean ω_c (i.e. assuming constant ω_c) and using the recorded ω_c. This indicated that power was overestimated by 0.2% when ω_c was assumed constant. These data were taken when ω_c variation was low and so may underestimate the error.

Possible sources of errors in the data from the pedals included those examined in the previous chapter, i.e. the limitations in linearity, hysteresis and cross-talk of the force data and linearity and interpolation in the angle data as well as temporal errors, although the latter were likely to be negligible. Whilst the contribution that each of these may have made to the total error was unclear, most of these were likely to produce largely systematic errors. The more random sources (linearity) appear to have made a smaller contribution to the total error. This is advantageous for the present research since the within and between trial comparisons would be more affected by random than systematic error sources.

It is thus apparent that although differences between the two sources of power output exist, these may, at least partially, be attributable to errors from the SRM system rather than the pedals. It is therefore suggested that both the validity and inter and intra-trial reliability of the data obtained from the pedal system is sufficient to support its use for the subsequent study.

Chapter 7: Error reduction in kinematic data

7.1: Introduction

In addition to the technical challenges associated with the measurement of kinetic changes with fatigue that have been the subjects of the previous chapters, the current research also aims to investigate kinematic changes. This also presents potential methodological issues. Although, as discussed in Chapter 2, there is a body of work on kinematic changes with fatigue across all sports, there is a paucity of such research specific to cycling. Of the few papers that do exist, Amoroso et al (1993a) showed peak hip extension to be greater (1.5°) in a fatigued condition than a 'non-fatigued'. Black et al. (1993b) also showed kinematic changes, at the start and end of exercise intended to increase fatigue. However, this was during an incremental protocol and so any fatigue affects cannot be separated from those resulting from changes in power output. A later paper by the same group (Sanderson and Black, 2003) recognised this deficit and compared low (30% maximal minute power (MMP)) and high (80% MMP) fatigue trials. They showed changes in thigh and shank angle (thigh: 24.5°, 22.2°; shank: -46.8, -48.1°, initial and final minutes respectively) between the initial and final minutes of the high-fatigue protocol. However, comparisons to changes shown for the low fatigue trial are not given and so some of these changes may be attributable to affects other than fatigue.

Thus, the information that is available on kinematic changes with fatigue in cycling is limited and in some cases flawed. However, it does indicate that the changes that can be expected in angular kinematic data are small in magnitude (~ 2°). However, the current research not only seeks to tackle some of the limitations of the previous works, but also to take the investigation further by not only comparing start and end points, but by attempting to elucidate the process of change. However, we remain indigent of knowledge regarding the time course of such changes and so the methodology must be developed with certain assumptions about the nature of these changes.

If these changes are assumed to be linear progressions (which would give the smallest changes per unit time across the whole trial), then their magnitude will be proportional to the inverse of the number of time windows that the fatiguing protocol is to be divided into. In the present research, it is intended to analyse the kinematic data of the high-fatigue section of the protocol in four equal time windows. Thus, if changes are of similar magnitudes to those reported in the earlier research, then changes in the dependent variables of the order of 2°/4, i.e. 0.5° must be identifiable. These changes are of the same order of magnitude as the errors shown by Smith et al. (1997) for angles calculated from dynamic kinematic video data. Thus, the successful identification of these small effects will be dependent upon the effective minimisation of errors.

Sources of error in kinematic data result from a number of factors related to the equipment, the operator and the nature of the task itself. Equipment introduced errors include; movement of the camera, distortion due to the cameras' optical system, precision limits in the digitisation process, errors in measurement and temporal alignment of spatial parameters. Also, there ara errors produced by the operator or resulting from the nature of the action such as misalignment of the camera, perspective error due to either the subject or the calibration object being out of the photographic plane and operator errors of judgement and parallax in locating joint axes of rotation. In addition to these are those errors resulting from the movement of markers in relation to the joint axis of rotation, either through skin movement or axial rotation of the segment (Wood, 1982). Finally, there are potential errors resulting from inaccuracies in the measurement of the calibration object which Allard *et al.* identified as '*probably the most important and most often neglected' error source*' (1995 pp. 35).

This chapter therefore presents two approaches that attempt to counter some of these potential error sources. Firstly, a new methodology for correcting the calibration co-ordinates entered into the reconstruction algorithms from their u, v pixel co-ordinates as displayed on the video images. It was hypothesised that this would reduce errors resulting from misalignment of the calibration object to the vertical and horizontal reference axes with respect to the optical axes of the camera. Further that it would

also attenuate the effects of distortion due to the optical system of the camera and reduce the sensitivity to errors in the measurement of the calibration object. Secondly, a feature in the video analysis software to be used in the final study (Ariel Performance Analysis System (APAS)) was examined. This feature offers the capability to automatically track high contrast markers in a video sequence once their initial positions are identified by the operator. Since this therefore may remove an element of operator error in the digitisation process, it may have the potential to reduce the overall error compared to the manual digitisation of markers. Although other researchers have investigated the magnitude of errors associated with this (Klein and DeHaven, 1995; Lindsay, 1996; Smith *et al.*, 1997; Wilson *et al.*, 1997) and other similar (Lindsay, 1996) automated video analysis systems, this has been in relation to three-dimensional analysis. Since the present research will only be using two-dimensional analysis, these findings cannot be assumed to be applicable. Most of these previous studies also reported errors based on smoothed data thus introducing a confounding variable. Therefore, further investigation is required if such methods are to be employed in the present research.

7.2: Method

7.2.1: Correction of calibration points by their *u*, *v* pixel co-ordinates

If each pair of adjacent points on the calibration objects are considered as representing either end of the hypotenuse of a triangle with its side and base formed by the vertical and horizontal, then two similar triangles can be drawn. One, measured in pixels, of the points as they appear on the video image (Figure 7-1) and one, measured in real-world units (metres) of the same points on the actual calibration object (Figure 7-2).

Looking first at the triangle based on the points as displayed in the video image (see Figure 7-1); if u_i, v_i and u_j, v_j are the pixel co-ordinates of the two adjacent points on the calibration object then the length of the two sides (ℓ_u and ℓ_v) can be found as;

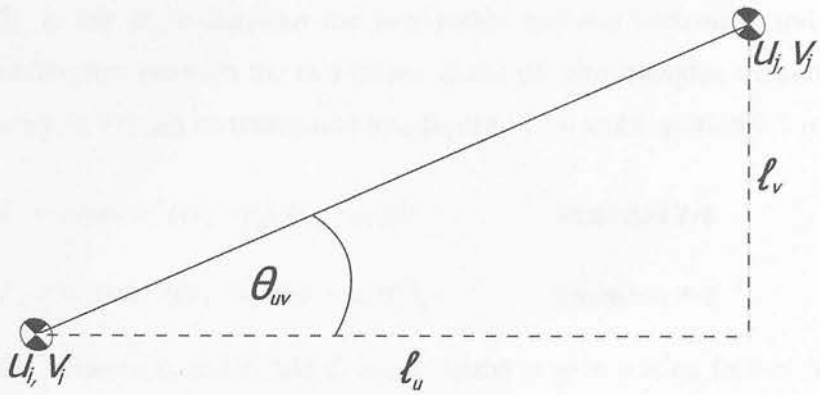

Figure 7-1: Adjacent calibration points as represented on the video image in pixel values

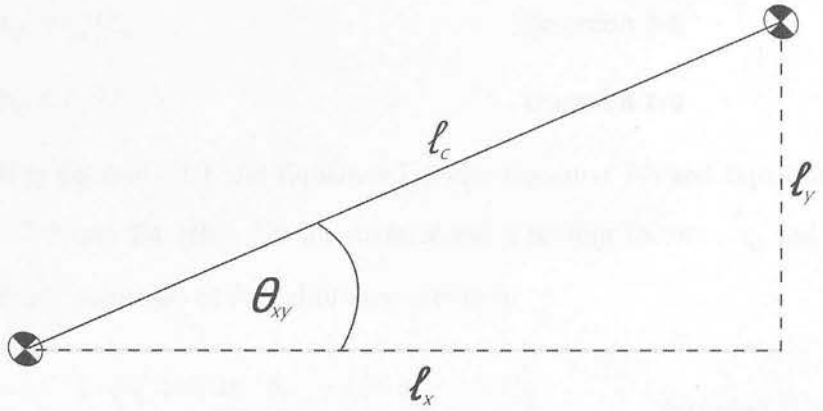

Figure 7-2: Adjacent calibration points on the actual calibration object

$$\ell_u = u_j - u_i \qquad \textbf{Equation 7-1}$$

$$\ell_v = v_j - v_i \qquad \textbf{Equation 7-2}$$

From this, the angle between the image of the calibration points and the horizontal (θ_{uv}) can be found as;

$$\theta_{uv} = \tan^{-1}((v_j - v_i)/(u_j - u_i)) \qquad \textbf{Equation 7-3}$$

For the points on the actual calibration objects (see Figure 7-2), the horizontal (x) and vertical (y) distances between them can be found as;

$$\ell_x = \cos\theta_{xy} \cdot \ell_c \qquad \textbf{Equation 7-4}$$

$$\ell_y = \sin\theta_{xy} \cdot \ell_c \qquad \textbf{Equation 7-5}$$

where θ_{xy} is the angle between the two points and the horizontal and ℓ_c is the measured distance between the two points. Since the two triangles are similar, $\theta_{xy} = \theta_{uv}$ so Equation 7-3 can be transposed into Equation 7-4 and Equation 7-5 to give;

$$\ell_x = \cos(\tan^{-1}((v_j - v_i)/(u_j - u_i)))\ell_c \qquad \textbf{Equation 7-6}$$

$$\ell_y = \sin(\tan^{-1}((v_j - v_i)/(u_j - u_i)))\ell_c \qquad \textbf{Equation 7-7}$$

and a ratio between ℓ_x and ℓ_u and ℓ_y and ℓ_v found to give scaling factors (x_{sf} and y_{sf}) as;

$$x_{sf} = \ell_x / \ell_u \qquad \textbf{Equation 7-8}$$

$$y_{sf} = \ell_y / \ell_v \qquad \textbf{Equation 7-9}$$

Substituting Equation 7-1 and Equation 7-6 into Equation 7-8 and Equation 7-2 and Equation 7-7 into Equation 7-9 the mean x and y scaling factors ($\overline{x_{sf}}$ and $\overline{y_{sf}}$) can then be found across all of the calibration points as;

$$\overline{x_{sf}} = \frac{1}{N_x}\sum_{1}^{N_x}\left(\frac{\cos\left(\tan^{-1}((v_j - v_i)/(u_j - u_i))\ell\right)}{(u_j - u_i)}\right) \qquad \textbf{Equation 7-10}$$

$$\overline{y_{sf}} = \frac{1}{N_y}\sum_{1}^{N_y}\left(\frac{\sin\left(\tan^{-1}((v_j - v_i)/(u_j - u_i))\ell\right)}{(u_j - u_i)}\right) \qquad \textbf{Equation 7-11}$$

Where N_x and N_y are the number of calibration points on the horizontal and vertical scaling objects respectively. Both objects are not used in each case as the means could be distorted by small measurement errors where the length along the axis is low, i.e. for y scaling with the horizontal object and vice versa. Using separate x and y factors renders the scaling factors insensitive to differences between horizontal and vertical scaling of the image.

To correct for any discrepancies between the 'true' vertical and that as it appears in the video image, the u, v co-ordinates of two points (u_1, v_1 and u_2, v_2) on a known 'true' vertical are used to calculate the angle between apparent and 'true' vertical (θ_v) (Figure 7-3) as;

$$\theta_v = \tan^{-1}(u_1 - u_2)/(v_1 - v_2) \qquad \textbf{Equation 7-12}$$

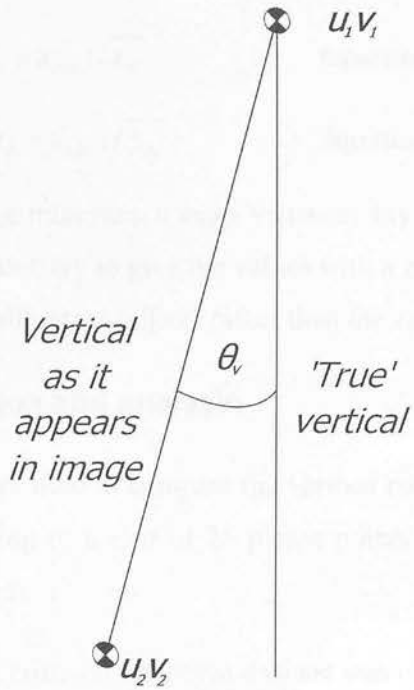

Figure 7-3: Angle between 'true' vertical and that as it appears in the video image

The u and v error between the 'true' and apparent vertical in the video can then be calculated as;

$$e_u = \sin\theta_v(v_p - v_0) \qquad \textbf{Equation 7-13}$$

$$e_v = \sin\theta_v(u_p - u_0) \qquad \textbf{Equation 7-14}$$

Where e_u and e_v are the u and v errors respectively, u_p and v_p and u_0 and v_0 are the u and v co-ordinates of the calibration point and the image zero point respectively. However, since u_0 and v_0 are both 0, these can be eliminated from the equations, and corrected u and v co-ordinates (u_c, v_c) of the calibration points corrected to 'true' vertical can then be found by subtracting the errors (e_u, Equation 7-13 and e_v, Equation 7-14) from the co-ordinates of each point as;

$$u_c = u_p - \sin\theta_v (v_p - v_0)$$ **Equation 7-15**

$$v_c = v_p - \sin\theta_v (u_p - u_0)$$ **Equation 7-16**

From which, the corrected x and y co-ordinates of each calibration point (x_p and y_p) can be found using the previously calculated scaling factors (Equation 7-10 and Equation 7-11) as;

$$x_p = (u_p - \sin\theta_v v_p - u_{\min}) / \overline{x_{sf}}$$ **Equation 7-17**

$$y_p = (v_p - \sin\theta_v u_p - v_{\min}) / \overline{y_{sf}}$$ **Equation 7-18**

Where u_{min} and v_{min} are the minimum u and v values of any of the points. Subtraction of these values is only necessary to give the values with a zero minimum point as the bottom left point of the calibration objects rather than the zero point of the screen.

7.2.2: Data acquisition and analysis

Two video sequences were used to compare the various methodological approaches; a static sequence consisting of a grid of 25 planar points and a dynamic sequence using a swinging pendulum.

For the static sequence, a criterion reference data set was obtained by marking a 5x5 grid onto the surface of a digitizer tablet (TDS LC series II, TDS Nuomonics, Blackburn, England) with the grid lines spaced at 0.25 m for the horizontal and 0.225 m for the vertical, i.e. 1 m x 0.9 m. Whilst it would have been preferable to use a 1 m x 1 m area, i.e. that to be calibrated in the final study, this was greater than the area that could be digitised on the tablet. At each of the 25 intersections, adhesive dots of the same type as those to be used for identifying landmarks on the subjects in the final study (black circles with a 19 mm diameter) were attached. The tablet was then connected to a PC microcomputer (Viglen Genie) running Hyper-terminal (Hilgraeve, Michigan, USA) and the centre of each of the points adhered to the tablet digitized 30 times, with the mean value for each point taken as the criterion value. Since digitisation errors are likely to be random, the errors should be normally distributed and therefore, by central limit theorem, the means should reflect the 'true' value (assuming no systematic error) (Wood, 1982 pp. 314).

For the dynamic sequence, an inverted 'T' shaped pendulum was used with eight markers of the same type as those used for the grid adhered to it (see Figure 7-4). Point 1 was attached over the centre of rotation and all other points were set relative to this. The position of each of the points was measured with a steel rule (Rabone Chesterman RS 539-362) to the nearest 0.5 mm (Table 7-4) and was set to give two sets of nominal angles. The first of these were measured between points on the pendulum, i.e. relative to the internal reference frame on the pendulum itself (RA). These were the angles between the following points; 6-1-5, 6-1-7 (nominally 15°), 6-2-4, 6-2-8 (nominally 30°), 6-3-4 and 6-3-8 (nominally 45°). The second set were the angles to the vertical (VA) formed by points 1-3, 2-6, 4-7 and 5-8. RA was intended to provide an indication of the errors associated with angles measured with an internal reference in the final study, i.e. joint angles, whilst VA would represent segment angles.

Table 7-1: Location of points on inverted 'T' pendulum. Points on arm of pendulum are measured relative to the centre of rotation (point 1) whilst points on the cross-bar of the 'T' are measured relative to the point at the intersection of the two bars (point 6)

Point	Distance to 1 (mm)
2	245.5
3	539.0
6	939.5
Point	**Distance to 6 (mm)**
4	401.0
5	252.5
7	250.0
8	400.5

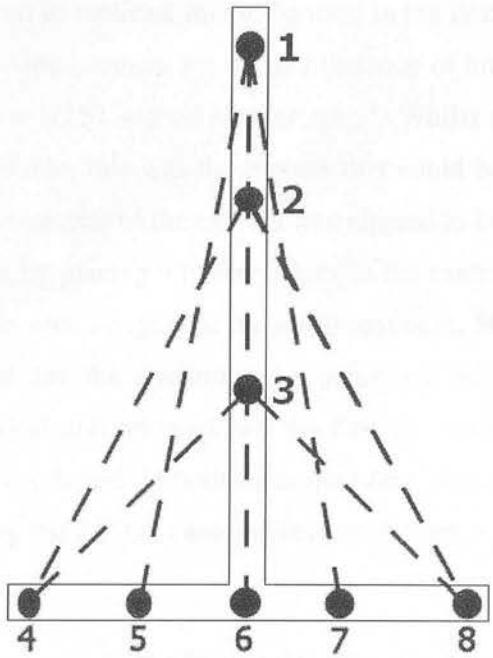

Figure 7-4: Schematic representation of inverted 'T' pendulum

A criterion measurement of the angle of the pendulum arm to the vertical was obtained using two meshing brass spur gears (Meccano, Nikko UK Ltd, Hertfordshire). The first of these, a 57 teeth gear, was attached to the pivot of the pendulum and the second, a 19 tooth gear, to the shaft of a Smart Position Sensor

(SPS) (RS 601-1045) which had a linearity of <1% (procedures to verify this were detailed in Chapter 5). Since, the gearing gave a 3:1 ratio of rotation of the SPS to that of the pendulum, this element of non-linearity in the measurement of the angle to the vertical was also proportionately reduced. The data were collected through a CED 1401 (Cambridge Electronic Design, Cambridge, England) capable of 12-bit analogue to digital conversion with a PC microcomputer (HP Compaq NX9005) running Spike 2 (CED), sampling at 100 Hz. This was twice the frame rate of the camera and thus allowed the two data sources to be synchronised to <1/50 second. Synchronisation was achieved by the use of a manual trigger, which created a square-wave signal on a second channel of the CED 1401, and simultaneous lit a bulb visible in the field of view of the camera. The position of the pendulum when freely hanging was taken as zero degrees to the vertical and the angles calculated from the SPS data normalised to this.

For both sequence, video recording was set up to replicate that to be used in the final study, i.e. using a Canon MVX100i digital video camera set up at a distance of 8m from the object, recording at 50 Hz using a 1/250 second shutter speed. Whilst a higher shutter speed would have been preferable, this was the highest that could be achieved with the available lighting. The optical axis of the camera was aligned to be orthogonal to the tablet surface or pendulum by placing a planar mirror in the centre of the object and aligning the camera with its own image. For the static sequence, 50 frames were captured and digitised whilst for the dynamic, the pendulum was positioned at approximately 45° to the vertical and released and the first complete swing plus 10 frames either side (108 frames) selected. In both cases the same frames were digitised both manually (MD) and using the APAS's automatic marker tracking facility (AD).

The calibration frame used was also that to be used in the final study. This consisted of two square section tubes, each 1 m in length, joined to be perpendicular (87.8°) to each other. These were marked off in high-contrast 200 mm bands, thus giving five vertical and five horizontal calibration points in addition to the common point at the object's union. For the dynamic sequence, since the pendulum would swing horizontally beyond this region, a longer horizontal calibration object (1800 mm)

was used with the same markings, thus giving an additional four horizontal calibration points. For the grid sequence, these were positioned in front of the tablet so that the connection of the orthogonal tubes was just below and to the left of the bottom left point of the grid. In the case of the dynamic sequence, they were aligned to be parallel to the base of the inverted-'T' with the midpoint of the horizontal object aligned with the vertical arm of the pendulum. In order to assess the efficacy of the correction method in reducing errors resulting from misalignment of the calibration objects relative to their assumed orientation, two calibration sequences were used in both cases. The first of these represented an 'ideal situation', where the frame was aligned to 'true' horizontal and vertical. The second one aimed to represent the small errors in alignment that may go un-corrected if visual inspection is relied upon. To achieve this, the calibration frame was rotated slightly during the recording process and then the frames where it was at zero degrees (0C) and 2.5° (2.5C) to the horizontal were identified from the ends of the object's pixel coordinates with these frames subsequently being used for the two calibrations. 2.5° was selected as being the smallest deviation from 'true' that was readily apparent with visual inspection.

For both the static and dynamic sequences the mean root mean square (RMS) errors were compared using a Three Way repeated measures ANOVA (digitisation (MD/AD) x correction (C/UC) x calibration (0C/2.5C)). For the static sequence separate ANOVAs were calculated for x and y values and for x and y together whilst for the dynamic trial, separate ANOVAs were calculated for the angles between points on the pendulum and for those relative to the vertical. Additionally, the RMS errors were calculated as percentages of the calibrated area (1 m x 0.9 m) for the static grid and percentages of the criterion angles for the dynamic sequence. In all cases, no filtering or smoothing was used.

7.3: Results

7.3.1: Static sequence

The results of the Three Way ANOVAs for the static sequence are summarised in Figure 7-2 with full results given in Appendix 2. The mean RMS error across all conditions was 3.77 mm ± 3.54 (as proportion of digitised area, 0.40% ± 0.38%) (see Table 7-4). These errors were significantly lower for AD than MD both across axes and for x and y separately. However, the magnitudes of the actual differences were insubstantial, (-0.1 mm, -3%). This may be accounted for by the fact that the within group variation was very small, thus increasing the sensitivity to between group differences. The calibration correction method was also shown to significantly reduce the mean RMS errors in all cases. However, compared to the differences resulting from the two digitisation methods, the reductions in errors with the use of the correction method were more substantial. Across all conditions the magnitude of mean RMS errors were reduced by 3.6 mm (-64%) with the effect being more pronounced for x (-4.0 mm, -73%) than y (-3.2 mm, -56%). This discrepancy between x and y may be attributable to perspective errors in the image, which is supported by differences in the x and y scaling factors (x: 0.199, y: 0.149 for both calibrations). However, although the main effect of the calibration sequence used was significant in all cases, the interactions between the use of the correction method and the calibration were only significant in the case of the y values. There were

Table 7-2 Summary of the results of Three Way ANOVAs for digitising method (digit), with and without the use of the correction method (correct) and the calibration sequence used (calib) for the static grid. Results are given for all points and as *x* and *y* separately. Shading indicates significance at p<0.05.

	x & *y*		*x*		*y*	
	F	*p*	*F*	*p*	*F*	*p*
calib	4.474	0.040	4.772	0.039	36.078	<0.001
digit	19.101	<0.001	9.675	0.005	9.279	0.006
correct	110.984	<0.001	96.897	<0.001	34.278	<0.001
calib x digit	0.082	0.776	6.341	0.019	4.415	0.046
calib x correct	2.001	0.163	3.804	0.063	16.872	<0.001
digit x correct	12.601	<0.001	14.461	<0.001	2.639	0.117
calib x digit x correct	<0.01	0.976	1.934	0.177	1.989	0.171

however, significant interactions between the calibration used and the digitisation method for both x and y, although not across the two. With the exception of y, significant interactions were also shown between the digitisation method and the use of the calibration correction methods. However, in no cases were the three-way interactions found to be significant.

7.3.2: Dynamic sequence

The results of the Three Way ANOVAs for the dynamic trial are summarised in Table 7-4 with full results given in Appendix 2. Mean RMS errors were found to be substantially smaller for relative angles (RA) (0.44°) than those to the vertical (VA) (2.23°). Looking firstly at the effects of the digitisation method, this was only found to significantly affect the magnitude of mean RMS errors for VA. However, this effect was an increase in the errors (+0.64°, +40%) (see Table 7-5). The use of the correction method was also shown to produce significant main effects in both RA and VA. However, in the case of VA, mean RMS error was higher with the use of the correction method, although in both cases, the actual effect was small (RA: -0.03°, -6.3%; VA: +0.02°, +0.9%). Further, although the mean differences attributable to which calibration sequence used was greater in the case of VA (1.2°, 74%) than RA (0.07°, 17%), the effect was only shown to be significant for RA. In both cases, however, there were significant interactions between the calibration sequence used and the effects of the correction method. However, these interactions

Table 7-3: Summary of the results of Three-Way ANOVAs for digitising method (digit), with and without the use of the correction method (correct), the calibration sequence used (calib) for the dynamic sequence. Relative angles (RA), angles to the vertical (VA). Shading indicates significance at $p<0.05$.

	RA		*VA*	
	F	*p*	*F*	*p*
calib	46.065	0.001	5.027	0.111
digit	1.378	0.293	1,238.969	<0.001
correct	50.409	<0.001	197.922	<0.001
calib x digit	50.007	<0.001	684.169	<0.001
calib x correct	43.085	0.001	65.166	0.004
digit x correct	39.810	0.001	717.920	<0.001
calib x digit x correct	41.050	0.001	598.620	<0.001

were complex. For the RA, the use of the correction method reduced mean RMS errors for both of the calibration sequences (0C: -0.04°, -9%; 2.5C: -0.09°, -17%), whilst, for VA, the correction method succeeded in reducing mean RMS errors for 2.5C (-0.31°, -10%), but increased them for 0C (+0.35°, +12%). The significant interactions between the digitisation method and the use of the corrections were also complex. For RA, the mean RMS errors associated with both MD and AD were lower with the corrections than without (MD: -0.08°, -17%; AD: -0.04°, -8%) whilst for VA mean RMS errors were reduced by the corrections for MD (-0.41°, -19%), but increased for AD (+0.46°, +21%). The significant interactions between digitisation method and calibration sequence however, were less equivocal with MD consistently producing smaller mean RMS errors than AD with the exception of for RA 0C, although this difference was very small (0.02°). Unlike for the static sequence however, the complicated patterns of the results were reflected in strongly significant three-way interactions.

Table 7-4: Absolute and relative errors (mean ± SD) across all points and as x and y separately for automatic (A) and manual (M) digitising, with (C) and without (UC) the use of the correction method for the 'true' (0C) and misaligned (2.5C) calibration for the static grid.

A/M	C/UC	0C/2.5C	All		*x*		*y*	
			ABS (mm)	*x / y (%)*	ABS (mm)	*x / y (%)*	ABS (mm)	*x / y (%)*
A	C	0C	1.68 ± 0.65	0.18 ± 0.07	1.49 ± 0.45	0.15 ± 0.04	1.87 ± 0.77	0.21 ± 0.09
A	C	2.5C	2.13 ± 1.37	0.23 ± 0.16	1.26 ± 0.21	0.13 ± 0.02	3.00 ± 1.48	0.33 ± 0.16
A	C	All	1.91 ± 1.09	0.2 ± 0.12	1.38 ± 0.36	0.14 ± 0.04	2.44 ± 1.30	0.27 ± 0.14
A	UC	0C	4.66 ± 3.75	0.48 ± 0.37	6.58 ± 4.21	0.66 ± 0.42	2.73 ± 1.81	0.3 ± 0.2
A	UC	2.5C	6.37 ± 4.60	0.68 ± 0.51	4.23 ± 2.69	0.42 ± 0.27	8.52 ± 5.13	0.95 ± 0.57
A	UC	All	5.52 ± 4.26	0.58 ± 0.46	5.40 ± 3.69	0.54 ± 0.37	5.63 ± 4.80	0.63 ± 0.53
A	All	0C	3.17 ± 3.07	0.33 ± 0.31	4.03 ± 3.92	0.4 ± 0.39	2.30 ± 1.44	0.26 ± 0.16
A	All	2.5C	4.25 ± 3.99	0.46 ± 0.44	2.75 ± 2.41	0.27 ± 0.24	5.76 ± 4.66	0.64 ± 0.52
A	All	All	3.71 ± 3.59	0.39 ± 0.38	3.39 ± 3.30	0.34 ± 0.33	4.03 ± 3.85	0.45 ± 0.43
M	C	0C	1.84 ± 0.58	0.2 ± 0.07	1.63 ± 0.40	0.16 ± 0.04	2.05 ± 0.65	0.23 ± 0.07
M	C	2.5C	2.30 ± 1.29	0.25 ± 0.15	1.46 ± 0.22	0.15 ± 0.02	3.14 ± 1.37	0.35 ± 0.15
M	C	All	2.07 ± 1.02	0.22 ± 0.12	1.54 ± 0.33	0.15 ± 0.03	2.60 ± 1.20	0.29 ± 0.13
M	UC	0C	4.71 ± 3.63	0.49 ± 0.36	6.52 ± 4.16	0.65 ± 0.42	2.90 ± 1.68	0.32 ± 0.19
M	UC	2.5C	6.44 ± 4.50	0.69 ± 0.5	4.36 ± 2.60	0.44 ± 0.26	8.52 ± 5.06	0.95 ± 0.56
M	UC	All	5.58 ± 4.16	0.59 ± 0.45	5.44 ± 3.60	0.54 ± 0.36	5.71 ± 4.69	0.63 ± 0.52
M	All	0C	3.28 ± 2.96	0.34 ± 0.3	4.08 ± 3.83	0.41 ± 0.38	2.48 ± 1.34	0.28 ± 0.15
M	All	2.5C	4.37 ± 3.90	0.47 ± 0.43	2.91 ± 2.34	0.29 ± 0.23	5.83 ± 4.57	0.65 ± 0.51
M	All	All	3.83 ± 3.50	0.41 ± 0.38	3.49 ± 3.21	0.35 ± 0.32	4.16 ± 3.75	0.46 ± 0.42
All	All	0C	3.22 ± 3.01	0.34 ± 0.3	4.06 ± 3.86	0.41 ± 0.39	2.39 ± 1.39	0.27 ± 0.15
All	All	2.5C	4.31 ± 3.94	0.46 ± 0.44	2.83 ± 2.37	0.28 ± 0.24	5.80 ± 4.59	0.64 ± 0.51
All	C	0C	1.76 ± 0.62	0.19 ± 0.07	1.56 ± 0.42	0.16 ± 0.04	1.96 ± 0.72	0.22 ± 0.08
All	C	2.5C	2.22 ± 1.33	0.24 ± 0.15	1.36 ± 0.24	0.14 ± 0.02	3.07 ± 1.42	0.34 ± 0.16
All	UC	0C	4.69 ± 3.67	0.48 ± 0.36	6.55 ± 4.14	0.66 ± 0.41	2.82 ± 1.73	0.31 ± 0.19
All	UC	2.5C	6.41 ± 4.53	0.69 ± 0.51	4.30 ± 2.62	0.43 ± 0.26	8.52 ± 5.04	0.95 ± 0.56
All	C	All	1.99 ± 1.06	0.21 ± 0.12	1.46 ± 0.36	0.15 ± 0.04	2.52 ± 1.25	0.28 ± 0.14
All	UC	All	5.55 ± 4.20	0.59 ± 0.45	5.42 ± 3.63	0.54 ± 0.36	5.67 ± 4.72	0.63 ± 0.52
All	All	All	3.77 ± 3.54	0.40 ± 0.38	3.44 ± 3.25	0.34 ± 0.32	4.09 ± 3.79	0.45 ± 0.42

Table 7-5: Absolute and relative errors (mean ± SD) for relative angles and angles to vertical for automatic (A) and manual (M) digitising, with (C) and without (UC) the use of the correction method for the 'true' (0C) and misaligned (2.5C) calibration for the pendulum.

A / M	C / UC	0C / 2.5C	Relative angles (RA)		Angles to vertical (VA)	
			ABS (deg)	Error/ angle (%)	ABS (deg)	Error/ angle (%)
A	C	0C	0.39 ± 0.20	1.27 ± 0.14	1.81 ± 0.19	10.25 ± 1.73
A	C	2.5C	0.48 ± 0.22	1.6 ± 0.13	3.55 ± 0.34	18.85 ± 2.2
A	C	All	0.44 ± 0.21	1.43 ± 0.21	2.68 ± 0.97	14.55 ± 4.95
A	UC	0C	0.43 ± 0.21	1.42 ± 0.13	1.45 ± 0.12	8.34 ± 1.92
A	UC	2.5C	0.52 ± 0.24	1.74 ± 0.13	2.99 ± 0.36	16.2 ± 2.46
A	UC	All	0.48 ± 0.22	1.58 ± 0.21	2.22 ± 0.86	12.27 ± 4.67
A	All	0C	0.41 ± 0.20	1.35 ± 0.15	1.63 ± 0.24	9.29 ± 1.98
A	All	2.5C	0.50 ± 0.22	1.67 ± 0.15	3.27 ± 0.44	17.52 ± 2.58
A	All	All	0.46 ± 0.21	1.51 ± 0.22	2.45 ± 0.92	13.41 ± 4.8
M	C	0C	0.40 ± 0.20	1.3 ± 0.15	1.80 ± 0.21	10.03 ± 1.68
M	C	2.5C	0.38 ± 0.19	1.25 ± 0.13	1.79 ± 0.23	10.01 ± 1.74
M	C	All	0.39 ± 0.18	1.27 ± 0.14	1.80 ± 0.20	10.02 ± 1.58
M	UC	0C	0.43 ± 0.20	1.43 ± 0.12	1.45 ± 0.14	7.9 ± 1.52
M	UC	2.5C	0.52 ± 0.22	1.73 ± 0.09	2.97 ± 0.39	16.45 ± 2.25
M	UC	All	0.47 ± 0.21	1.58 ± 0.19	2.21 ± 0.86	12.18 ± 4.9
M	All	0C	0.41 ± 0.19	1.36 ± 0.15	1.62 ± 0.25	8.97 ± 1.87
M	All	2.5C	0.45 ± 0.21	1.49 ± 0.28	2.38 ± 0.70	13.23 ± 3.92
M	All	All	0.43 ± 0.20	1.43 ± 0.22	2.00 ± 0.64	11.1 ± 3.69
All	All	0C	0.41 ± 0.19	1.36 ± 0.15	1.63 ± 0.24	9.13 ± 1.87
All	All	2.5C	0.48 ± 0.21	1.58 ± 0.23	2.83 ± 0.73	15.38 ± 3.9
All	C	0C	0.39 ± 0.19	1.28 ± 0.14	1.80 ± 0.18	10.14 ± 1.58
All	C	2.5C	0.43 ± 0.20	1.42 ± 0.22	2.67 ± 0.98	14.43 ± 5.07
All	UC	0C	0.43 ± 0.20	1.43 ± 0.12	1.45 ± 0.12	8.12 ± 1.62
All	UC	2.5C	0.52 ± 0.22	1.74 ± 0.11	2.98 ± 0.35	16.32 ± 2.19
All	C	All	0.39 ± 0.18	1.27 ± 0.13	2.24 ± 0.81	12.28 ± 4.25
All	UC	All	0.48 ± 0.21	1.58 ± 0.19	2.22 ± 0.83	12.22 ± 4.63
All	All	All	0.44 ± 0.20	1.47 ± 0.22	2.23 ± 0.81	12.25 ± 4.37

7.4: Discussion

The errors found in the static sequence are comparable to those reported in previous literature for two-dimensional analysis. Kerwin (1994) reported RMS errors for x of between 2.1 and 2.5 mm (0.2%) and for y of between 0.38 and 0.42 mm (0.4%) depending on the cameras used, whilst Shapiro *et al.* (1987) reported absolute mean errors of 0.8%. However, absolute errors are always lower than RMS values. The magnitude of the errors are also similar to those obtained from three-dimensional analysis such as those found by Angulo and Dapena (1992) who reported RMS errors of 0.3%. Similar mean errors have also been reported (Kennedy *et al.* (1989) 0.3%; Klien and DeHaven (1995) x: 4.4 mm (0.2%), y: 3.9 mm (0.6%), z: 2.3 mm (0.2%)). However, mean values will underestimate the true errors as they tend to deviate about the mean thus positive and negative errors will tend to cancel each other out.

Examining first the case for the use of AD, this did show small but significant reductions in mean errors in the static trial and for RA in the dynamic sequence. Conversely, the overall errors in VA were higher for AD than MD but showed complex interactions with the effects of calibration frame alignment and the use of the corrections method. These findings do not support those of the only paper to compare the two digitisation methods to date (Wilson *et al.*, 1998) who showed errors in calculated relative angles to be greater with automated digitising than for manual using the APAS system. It thus appears that AD does not offer the potential to substantially reduce the magnitude of errors in comparison to MD. However, it may be of some benefit in error reduction for the data of most importance in the present study, i.e. relative angles. Whilst angles to the vertical (segment angles) will be considered in the final study, since relative angles (joint angles) are the most functionally relevant in terms of neuromuscular co-ordination, it is the accuracy of establishing these that will be of greatest importance. It is plausible that some of the errors in VA may be attributable to the criterion measurement, the Smart Position Sensor. Although the linearity of the actual device has been verified, the changes in angular velocity of the pendulum may have created temporal and angular misalignments between the rotation of the pendulum and that of the SPS, resulting in systematic errors in the criterion measure. Thus, although the case for using AD to

reduce errors was not supported, it can speed up the digitisation process and achieve this without increasing errors in the key variables of interest. It may also reduce errors in the digitisation of points that remain quasi-static, so it will be used, where possible, for the final study. It should be further noted that automated digitisation of sequences will be checked visually and corrected manually in the final study which was not the case for these data.

The case for the use of the correction method was however, more strongly supported. Errors in identifying the positioning of points in space were substantially reduced and there were consistent reductions in the magnitude of errors for relative angles. Whilst there were increases found in the errors of angles relative to the vertical, these increases were small, averaging <0.02° (i.e. below probable measurement error) with a maximum error of 0.6°. Therefore, even in the worst case, these were only marginally above the expected non-linearity of the criterion measure and may be at least partly attributable to errors in the criterion measure itself. Therefore, the correction method will be adopted for the analysis of kinematic data in the final study.

Chapter 8: Time course of kinetic and kinematic changes with fatigue

8.1: Introduction

Although research exists to indicate that technique changes occur during exercise that is likely to lead to increasing fatigue, very little of this has focused specifically upon cycling. Of the work that has examined this sport, (Amoroso *et al.*, 1993a, b; Black *et al.*, 1994; Sanderson and Black, 2003), the analyses have been restricted to comparisons of start and end points and so the manner in which the changes occur over time is unknown. The physiological and/or psychological phenomena that cause the underlying fatigue process to occur are also not well understood. However, the various models that have been proposed generally indicate progressive changes that lead to the development of fatigue rather than bipolar states of 'fatigued' and 'non-fatigued' as often referred to in the biomechanics literature. It is suggested that fatigue related technique changes could be of three types. Firstly, those that precede any measurable physiological manifestation of fatigue and thus serve to attempt to mediate the occurrence of the deleterious effects before they occur. This would support the presence of feed-forward mechanisms, as proposed by the complex systems model of fatigue. Secondly, changes that occur as the physiological effects start to manifest themselves in the form of deteriorations in physiological functions. Finally, those that occur with the ultimate inability of the body to maintain a coherent technique that immediately precedes task failure.

Thus although the deleterious effects of fatigue are well known to athletes, there is much that remains to be understood by workers in this field. By examining the time course of both performance decrements and biomechanical changes, the current research therefore seeks to further illuminate this area and enhance our understanding of the interrelationship between the deleterious effects of fatigue and the technique changes that occur with it.

8.2: Methodology

Nine male subjects (age 36.1 ± 5.6 years, height 1.80 ± 0.06 m, body mass 73.2 ± 5.9 Kg) currently competing in an endurance cycling discipline undertook the same maximal ramp and 'high-fatigue' (HF) tests as those used in Chapter 4. In addition, subjects also completed a 'low-fatigue' (LF) protocol (see Figure 8-1). The first section of this was identical to that used for HF, i.e. 7 minutes at 50% MMP (SS1) followed by a 4 minute ramp to 95% MMP (R1). However, on reaching 95%, the required power output was reduced back to 50% MMP over two minutes (R2) and this was maintained for a further 8 minutes (SS2). The gradual reduction in power output was required due to the large ergometer flywheel which required a prolonged period to decelerate following the reduction in power output. However, even if an instantaneous change in power output had have been possible, this would have resulted in a greater perturbation of the subjects' techniques. Therefore, the benefits of the more rapid power output change would be offset by the increased period required for the subjects' techniques to become stable again. The order in which the subjects undertook LF and HF protocol was randomised to eliminate familiarisation effects. All trials were conducted using a cycle fitted with SRM Power Measuring Crankset mounted on a Kingcycle Tester (EDS Portaprompt Ltd, UK). This provided real-time feedback to the subjects on their power output relative to the prescribed protocol, but, unlike the SRM ergometer used in Chapter 6, did not constrain them to it. This thus allowed measurements of performance decrements relative to the prescribed power outputs. The cycle was also fitted with a Look Ergostem (Look Cycle International, Nevers, Cedex, France) which allowed the configurations of the subjects' own positions to be replicated as in Chapter 6.

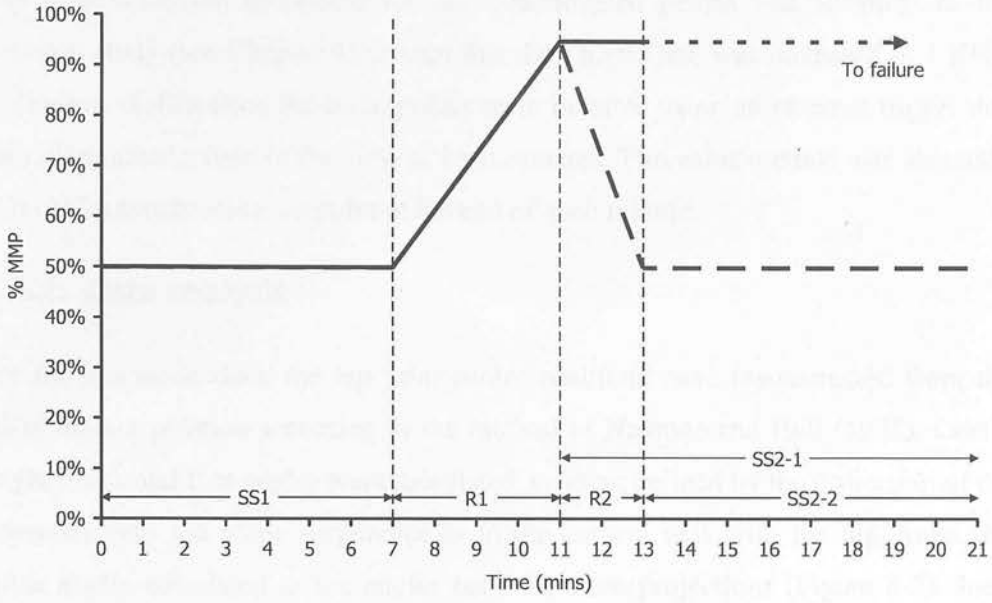

Figure 8-1: Protocol for low (dashed line) and high (solid line) fatigue trials

8.2.1: Data collection

During the HF and LF trials, video and force data were collected throughout the trial. Video data were obtained with two Canon MVX100i digital video cameras recording at 50 Hz using a 1/250s shutter speed. These were positioned either side of the subject with their optical axes perpendicular to the plane of crank rotation, at a distance of 8m. Markers were placed over the anterior superior iliac spine (ASIS), greater trochanter, lateral epicondyle, lateral malleolus and head of the fifth metatarsal head. Five crank cycles from the final 10 s of each minute of the ramp and at 25%, 50%, 75% and 87.5% of time to fatigue together with the entire final 5% of time to fatigue were subsequently digitised using the Aerial Performance Analysis System (Ariel Dynamics, CA, USA). Data were then smoothed with cubic splines with smoothing parameters established using average standard errors derived from repeat digitisation of a sequence (Wood, 1982). Cubic splines were selected as they have been shown to produce more accurate first order derivatives in kinematic data than digital filters (Bartlett, 1997; Challis and Kerwin, 1988). Quintic splines were not deemed to be necessary as higher order derivatives were not to be examined (Kerwin and Challis, 1989).

The data collection procedure for the instrumented pedals was identical to the previous study (see Chapter 4), except that the sample rate was increased to 1 KHz. Collection of data from the force pedals were initiated using an external trigger that also illuminated a light in the view of both cameras. This same method was also used to record a synchronisation pulse at the end of each minute.

8.2.2: Data analysis

For the kinematic data, the hip joint centre positions were reconstructed from the ASIS marker position according to the method of Neptune and Hull (1995). Crank, thigh, shank and foot angles were calculated as being defined by the projection of the segments onto the plane perpendicular to the camera axis with the hip, knee and ankle angles calculated as the angles between these projections (Figure 8-2). Joint angular velocities were also calculated using finite differences. The mean maximum flexion and extension angles for the thigh, shank and foot segments and hip, knee and ankle joints were calculated for each of the digitised sequences together with the mean crank angles at which they occurred. The mean joint angular velocities were also calculated for the three joints.

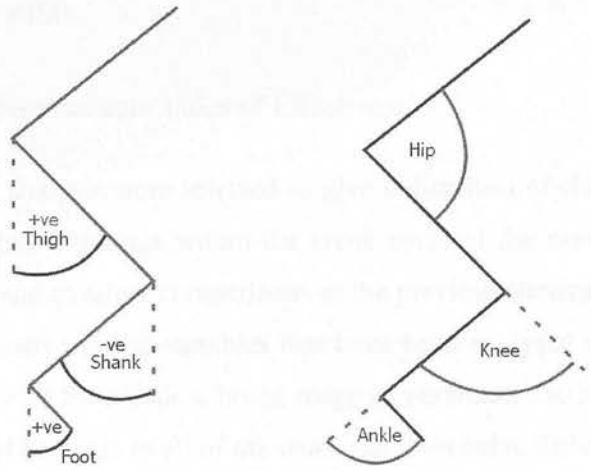

Figure 8-2: Angle conventions for segment and joint angles

The data obtained from the instrumented pedals were processed as in Chapter 4, however, the effective (F_{eff}) and ineffective (F_{ineff}) force components (i.e. those acting in a plane parallel to the crank rotation normal and parallel to the crank arm respectively), the resultant force (F_r), work and Instantaneous Index of Effectiveness were also calculated according to the following formulæ;

$$F_{eff} = F_z Sin\theta_p + F_x Cos\theta_p \qquad \text{Equation 8-1}$$

$$F_{ineff} = F_x Sin\theta_p + F_z Cos\theta_p \qquad \text{Equation 8-2}$$

Where F_x is the force parallel to the pedal surface in the plane normal to the pedal spindle and F_z is the force normal to the pedal surface and θ_p is the pedal angle.

$$F_r = \left(F_{eff}{}^2 + F_{ineff}{}^2\right)^{1/2} \qquad \text{Equation 8-3}$$

Where F_r is resultant force.

$$w = P\Delta t \qquad \text{Equation 8-4}$$

Where w is work, P is power and t is time

$$IIE = \frac{F_{eff}}{F_r} \times 100 \qquad \text{Equation 8-5}$$

Where IIE is the Instantaneous Index of Effectiveness.

The variables for analysis were selected to give indications of changes in either the magnitudes or relative timings within the crank cycle of the movement patterns or force application and to allow comparisons to the previous literature. Since the work in this area is limited and the variables that have been analysed in each study have varied, it was decided to include a broad range of parameters so that, at least partial comparisons could be made to all of the work that does exist. This included variables where significant fatigue effects have not been previously shown, since the methodological limitations or lack of time course analysis within the previous studies may have caused important changes to have been missed. In addition, three sets of variables were included that have not been previously analysed that were deemed to be potentially relevant, specifically, the joint angular velocities of the relevant joints,

the relative timing of the segmental displacement parameters and mean power. The former was included as it would be more sensitive to changes in the movement patterns than angular displacement alone and the latter as an indication of bilateral differences in the performance measure. The relative timing of segmental angular displacement was included in addition to that of the joint angles, which have been previously reported (Amoroso *et al.*, 1993a), as the two could change independently of each other.

All of the data were then divided into 1 minute time windows for the 50% MMP steady-state and ramp. For SS2, two sets of analyses were conducted. The first of these (SS2-2) was conducted on both the LF and HF data. For the force pedal data, this divided the time from where steady state was achieved after the ramp to 95% MMP in both protocols, i.e. after the 2 minute ramp down used in LF, i.e. 13 minutes to time of failure in HF (see Figure 8-1) into 10 equal time windows. For the kinematic data, these analyses were conducted on all of the digitised periods after the period of ramp down in LF. Since the time from the end of R1 to failure was greater than 4 minute for all subjects, this meant that the last four sections (50%, 75%, 87.5% and 95%) could be used in all cases. The second of these (SS2-1) examined the whole of the period at 95% MMP in HF. Since this period contained the 2 minute ramp down in LF, the changing power output did not allow meaningful comparisons between the two and so only HF was examined. For the force pedal data, to ensure that there was no loss of temporal resolution compared to SS2-2, the shortest time window from any subject in SS2-2 (13 seconds) was used to determine the number of time windows to be used (19). For the kinematic data, all five sections were used.

Within these, from the kinematic data, mean and peak angular displacements and velocities were calculated together with the position of peaks within the crank cycle. From the force pedal data a custom written program (FP_export see Appendix 1) was used to calculate, total, positive and negative work together with the crank angle (θ_c) at which positive work started and ended. For positive and negative work, these were calculated by identifying zero work threshold crossing points and then integrating the work between these points and the crank zero crossing points. Also, peak resultant, effective and ineffective forces were calculated together with the crank angle at

which they occurred. Within the same time windows, mean power and crank angular velocity ω_c were calculated across the whole crank cycle. Mean and standard deviations for crank angles were calculated in all cases using circular statistics (see Batschelet, 1981 p. 10; Fisher, 1993 p. 33) as;

$$x_{mean} = \frac{1}{n}\sum_{i=1}^{n}\cos\theta_i \qquad \text{Equation 8-6}$$

And

$$y_{mean} = \frac{1}{n}\sum_{i=1}^{n}\sin\theta_i \qquad \text{Equation 8-7}$$

If $xmean \geq 0$

$$\theta_{mean} = \tan^{-1}\left(\frac{y_{mean}}{x_{mean}}\right) \qquad \text{Equation 8-8}$$

If $xmean < 0$

$$\theta_{mean} = \tan^{-1}\left(\frac{y_{mean}}{x_{mean}}\right) + \Pi \qquad \text{Equation 8-9}$$

$$\theta_{SD} = (2(1-(x_{mean}{}^2 + y_{mean}{}^2)^{1/2}))^{1/2} \qquad \text{Equation 8-10}$$

8.2.3: Statistical analysis

Comparisons of the HF and LF trials were made using Two-Way repeated measure ANOVAs (trial x time). These were conducted on the data from the final minute of the initial steady state (SS1) and ramp sections together and on the final section of the trials where both the high and low fatigue trials were in a steady state (SS2-2). Where significant interactions were identified between trial and time in the latter, these were investigated with separate One-Way ANOVAs between LF and HF at each time window according to the method of Howell (1992 p. 449). The entire second steady state was similarly analysed for the HF trial (i.e. SS2-1) using a One-Way ANOVA. Where significant time effects were shown, *post hoc* analyses were conducted. These were calculated both with Bonferroni corrections and using least

significant differences (LSD) (i.e. no correction for familywise error). Both methods were used since the LSD method may increase the chances of type I errors but may reveal trends hidden by the very conservative Bonferroni method with the relatively low statistical power associated with limited subject numbers.

Additionally, in order to allow the identification of performance decrement and the time course of its occurrence, One-Way ANOVAs were also conducted on the mean net power data obtained from the SRM Power Measuring Crankset during the final steady state section of the high fatigue trial. These were conducted using averaging across the same time windows as used for both sets of force pedal data for the final state section of the high fatigue trial used for the other data (i.e. SS2-1: 19 for whole steady state, SS2-2: 10 windows from the end of R2). This thus provided time aligned comparisons for both the data normalised to time to failure from the start of the final steady state (SS2-1 for force pedal data and kinematic data) and that normalised to the final common steady state section, i.e. SS2-2 force pedal data. In all cases α was set at 0.05 with *p*-value corrections made for violations of assumptions of sphericity according to (Vincent, 1995 pp. 175).

In the case of the joint angular displacement and velocity data, these were found to be skewed and kurtotic. This was remedied prior to analysis by removing one subject's data that were extreme outliers (calculation of the ANOVAs on the variables where significant effects were shown did show any change in the pattern of results where this subject was included) the in all cases and log transforming the angular displacement and ranking the velocity data according to the methods of Hopkins (2006). This was not necessary in the case of any of the kinetic data.

8.3: Results

8.3.1: Maximal ramp test

Participants achieved a mean MMP of 341.8 W ± 34.2 W and were thus required to maintain 324.7 W ± 32.5 W at the 95% MMP level and 170.9 W ± 17.1 W at the 50% MMP level. The mean duration for SS2-1 in the high-fatigue trials was 309 s ± 31s (min: 244 s max: 352 s).

Figure 8-3 illustrates the mean power as recorded by the SRM Power Measuring Crankset alongside the power as prescribed by the protocol. During the initial steady state phase of both trials (SS1) the mean recorded power consistently exceeded the prescribed power (low fatigue: 5.6% ±1.4, high fatigue 5.7% ±1.4). During the course of the ramp up to 95% MMP (R1) the offset between the recorded and prescribed power declined such that the mean recorded power fell below the prescribed power by the top of the ramp in both trials (first 30 seconds: low fatigue: 8.4% ±2.7, high fatigue: 12.0% ±6.4%, last 30 seconds: low fatigue: -3.4% ±3.8, high fatigue: -0.9% ±3.4%). In the case of the low fatigue trial, mean recorded power dropped below the prescribed level during the decreasing power ramp (R2) though the discrepancy decreased during the ramp (first 30 seconds: -8.9% ±7.2, last 30 seconds -5.2% ±7.9) and recorded power exceeded prescribed for the remainder of the analysed portion of the trial (SS2-2) (4.1% ±5.9). For the high fatigue trial, mean power fell below the prescribed level throughout the final steady state section of the trial (SS2-1) with a trend for this to fall further towards the point of failure (first 10% of time to failure: -3.0% ±3.3, final 10%: -6.5% ±5.1).

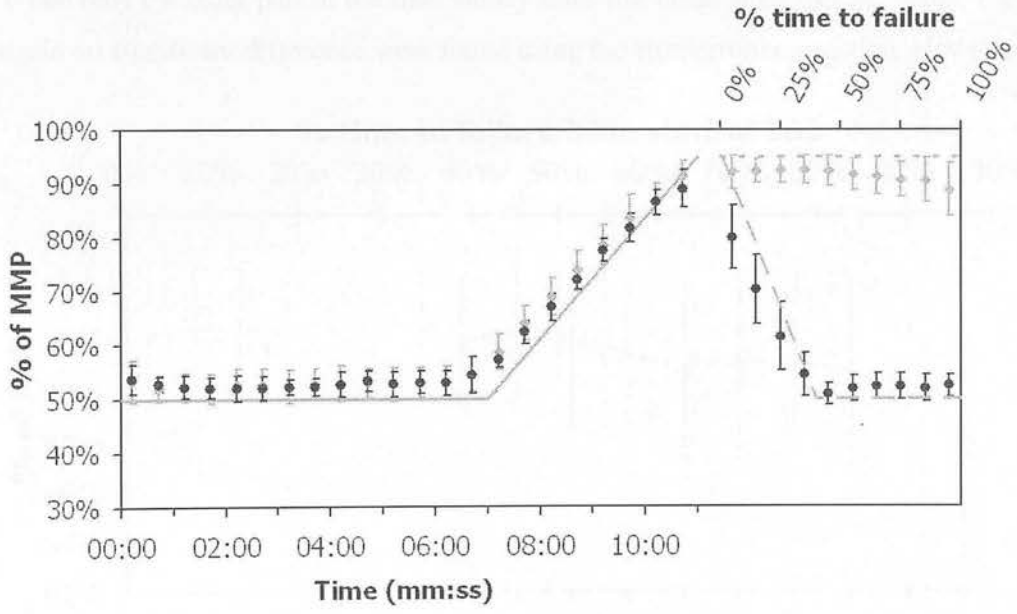

Figure 8-3: Mean (SD) power as recorded by the SRM Power Measuring Crankset as a percentage of subject's maximal minute power during the low (black circles) and high (grey diamonds) fatigue trials. Means are calculated as 30 second averages for the first 11 minutes (SS1 & R1: lower abscissa) and as 10% time to failure increments for the latter part of the trial (SS2-1: upper abscissa)

Statistical analyses of these data showed significant time effects in the final steady state section of the high fatigue trials, both when the entire section was considered (SS2-1: F= 5.716, p= 0.005, η_p^2 = 0.417) and only the portion where steady state was also achieved in the low fatigue trial (SS2-2: F= 5.866, p= 0.006, η_p^2 = 0.423) (full results are given in Appendix 4), although the size of these effects may be regarded as moderate (Table 1 1). *Post hoc* analyses of SS2-1 using the Bonferroni method failed to shown any significant effects, however, without this, significant differences were found between the final 5% of the trial and all other sections (Table 1 3). An area of significant differences was also bounded by 31% and 71%, i.e. there were consistent effects between the times either side of these two points, but little within. An examination of the trends of the changes (Figure 8-4) indicated that the power output prior to the first of these was relatively constant whilst greater fluctuations were apparent after it. The latter also occurred around the point where the progressive decline in mean power output towards failure began. Concentrations of significant effects also appeared around 45% and 61% of time to failure which coincided with peaks in mean power output during an otherwise downward trend. When only the latter part of the final steady state was considered (SS2-2: Table 1 2), again no significant difference were found using the Bonferroni correction. However,

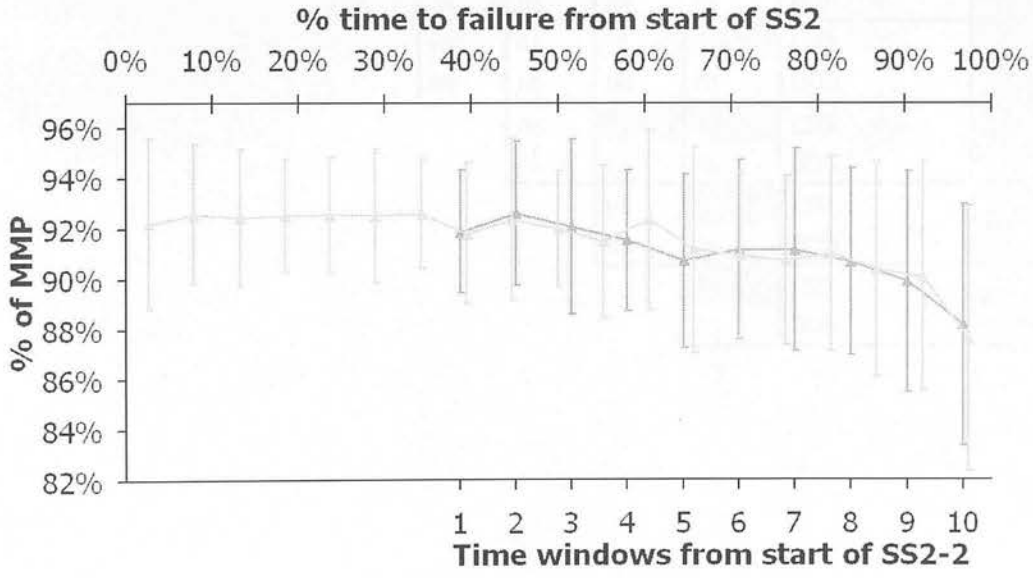

Figure 8-4: Group mean (±SD) net power from the SRM Power Measuring Crankset (light grey: SS2-1: 19 windows of % time to failure from the start of SS2, dark grey: SS2-2: 10 windows from start of common steady state to failure)

without this, effects were shown between the final time window and all preceding ones as well as between 2 and 3 and many of the following ones. Whilst the differences in starting points do not allow the two to be exactly time matched, this would be around 45% of time to failure from the start of the high fatigue steady state.

Table 8-1: Cohen's standards for interpreting effect sizes (Cohen, 1988)

Effect Size	Cohen's Standard
0.8	Large
0.5	Moderate
0.2	Small

Table 8-2: Summary of pairwise comparisons of mean net power from SRM power cranks in SS2-2 with (BON) and without (LSD: least significant difference) Bonferroni correction (*: $p < 0.05$, **: $p < 0.01$, ns: $p \geq 0.05$)

2	3	4	5	6	7	8	9	10	←Time window ↓	
ns	ns	ns	ns	ns	ns	ns	ns	*	LSD	1
ns	ns	ns	ns	ns	ns	ns	ns	ns	BON	
	ns	ns	*	*	*	**	**	**	LSD	2
	ns	ns	ns	ns	ns	ns	ns	ns	BON	
		ns	ns	ns	ns	*	*	**	LSD	3
		ns	ns	ns	ns	ns	ns	ns	BON	
			ns	ns	ns	ns	ns	*	LSD	4
			ns	ns	ns	ns	ns	ns	BON	
				ns	ns	ns	ns	*	LSD	5
				ns	ns	ns	ns	ns	BON	
					ns	ns	**	**	LSD	6
					ns	ns	ns	ns	BON	
						ns	*	**	LSD	7
						ns	ns	ns	BON	
							ns	*	LSD	8
							ns	ns	BON	
								*	LSD	9
								ns	BON	

Table 8-3: Summary of pairwise comparisons of mean net power from SRM power cranks in SS2-1 with (BON) and without (LSD: least significant difference) Bonferroni correction (*: $p < 0.05$, **: $p < 0.01$, ns: $p \geq 0.05$, %TTF: % time to failure)

8%	13%	18%	24%	29%	34%	39%	45%	50%	55%	61%	66%	71%	76%	82%	87%	92%	97%	←% TTF	↓
ns	ns	ns	ns	ns	ns	ns	ns	ns	ns	ns	ns	ns	ns	ns	ns	ns	**	LSD	3%
ns	ns	ns	ns	ns	ns	ns	ns	ns	ns	ns	ns	ns	ns	ns	ns	ns	ns	BON	
	ns	ns	ns	ns	ns	ns	ns	ns	ns	ns	ns	*	**	ns	*	*	**	LSD	8%
	ns	ns	ns	ns	ns	ns	ns	ns	ns	ns	ns	ns	ns	ns	ns	ns	ns	BON	
		ns	ns	ns	ns	ns	ns	ns	ns	ns	ns	**	*	ns	ns	*	**	LSD	13%
		ns	ns	ns	ns	ns	ns	ns	ns	ns	ns	ns	ns	ns	ns	ns	ns	BON	
			ns	ns	ns	*	ns	*	ns	ns	ns	**	*	ns	ns	*	**	LSD	18%
			ns	ns	ns	ns	ns	ns	ns	ns	ns	ns	ns	ns	ns	ns	ns	BON	
				ns	ns	ns	ns	ns	ns	ns	ns	**	*	ns	ns	*	**	LSD	24%
				ns	ns	ns	ns	ns	ns	ns	ns	ns	ns	ns	ns	ns	ns	BON	
					ns	ns	ns	ns	ns	ns	ns	**	*	*	*	*	**	LSD	29%
					ns	ns	ns	ns	ns	ns	ns	ns	ns	ns	ns	ns	ns	BON	
						*	ns	*	*	ns	ns	**	**	ns	*	*	**	LSD	34%
						ns	ns	ns	ns	ns	ns	ns	ns	ns	ns	ns	ns	BON	
							ns	ns	ns	ns	ns	ns	ns	ns	ns	ns	*	LSD	39%
							ns	ns	ns	ns	ns	ns	ns	ns	ns	ns	ns	BON	
								ns	*	ns	*	**	*	*	**	*	**	LSD	45%
								ns	ns	ns	ns	ns	ns	ns	ns	ns	ns	BON	
									ns	ns	ns	*	ns	ns	ns	ns	*	LSD	50%
									ns	ns	ns	ns	ns	ns	ns	ns	ns	BON	
										ns	ns	ns	ns	ns	ns	ns	*	LSD	55%
										ns	ns	ns	ns	ns	ns	ns	ns	BON	
											*	*	*	**	**	**	**	LSD	61%
											ns	ns	ns	ns	ns	ns	ns	BON	
												ns	ns	ns	ns	*	**	LSD	66%
												ns	ns	ns	ns	ns	ns	BON	
													ns	ns	ns	ns	*	LSD	71%
													ns	ns	ns	ns	ns	BON	
														ns	ns	ns	**	LSD	76%
														ns	ns	ns	ns	BON	
															ns	ns	*	LSD	82%
															ns	ns	ns	BON	
																ns	**	LSD	87%
																ns	ns	BON	
																	*	LSD	92%
																	ns	BON	

8.3.2: Segmental angular displacement

8.3.2.1: Trial effects

The statistical analyses of the segmental angular displacement data are summarised in Table 1 4 for the thigh, Table 1 5 for the shank and Table 8-6 for the foot (full results are given in Appendix 3 and figures for all variables in Appendix 4). During the final minute of the initial steady state and ramp (SS1, 7 + R1), no significant trial effects were found. While in the case of the final steady state portion of the trial (SS2-2), moderate (Table 1 1) significant trial effects were only shown minimum thigh angles for the left leg.

Table 8-4: Summary of results of Two-Way ANOVA on thigh segment angular displacement data (SS1, 7: final minute of initial steady state, R1: ramp from 50% MMP to 95% MMP, SS2-2: final section of trials where power output was again constant, Int: interaction, shading indicates significance at $p < 0.05$)

			Min		θc Min		Max		θc Max	
			L	R	L	R	L	R	L	R
SS1,7 + R1	Trial	F	2.157	0.034	3.372	0.955	0.062	1.144	0.335	0.364
		p	0.185	0.859	0.109	0.373	0.811	0.326	0.581	0.568
		η_p^2	0.236	0.006	0.325	0.160	0.009	0.160	0.046	0.057
	Time	F	5.562	10.621	0.120	1.301	27.666	4.626	4.459	0.662
		p	0.028	0.012	0.974	0.303	<0.001	0.030	0.067	0.624
		η_p^2	0.443	0.639	0.017	0.207	0.798	0.435	0.389	0.099
	Int	F	2.557	0.223	0.717	0.144	0.148	0.297	0.907	2.584
		p	0.061	0.923	0.587	0.963	0.962	0.877	0.473	0.063
		η_p^2	0.268	0.036	0.093	0.028	0.021	0.047	0.115	0.301
SS2-2	Trial	F	7.663	4.465	0.460	0.673	1.619	1.956	2.252	1.067
		p	0.028	0.079	0.519	0.443	0.244	0.211	0.177	0.342
		η_p^2	0.523	0.427	0.062	0.101	0.188	0.246	0.243	0.151
	Time	F	0.606	0.655	1.215	0.356	0.140	0.814	1.380	1.373
		p	0.619	0.590	0.329	0.785	0.935	0.503	0.276	0.283
		η_p^2	0.080	0.098	0.148	0.056	0.020	0.119	0.165	0.186
	Int	F	0.319	1.686	1.001	1.958	0.737	0.739	0.151	3.082
		p	0.812	0.206	0.412	0.156	0.542	0.543	0.928	0.054
		η_p^2	0.044	0.219	0.125	0.246	0.095	0.110	0.021	0.339

8.3.2.2: Time effects

Significant time main effects were shown in the initial common portions (SS1, 7 + R1) of the two trials for both minimum and maximum thigh angles (both left and right), minimum left shank angle, maximum right shank angle and the crank angle at which maximum right shank angle occurred. Time main effects were also shown in the foot angular displacement for both minimum angle (left and right), the crank angle at which both the minimum and maximum left angles occurred and the right maximum value. However, in the latter portions of the two trials where power outputs were constant, the only significant time effect shown was for the maximum angle of right foot angular displacement. In all cases the effect sizes were medium with the exceptions of the maximum thigh and the minimum shank and crank angles of minimum foot displacement for the left leg, where effects were large.

Table 8-5: Summary of results of Two-Way ANOVA on shank segment angular displacement data (SS1, 7: final minute of initial steady state, R1: ramp from 50% MMP to 95% MMP, SS2-2: final section of trials where power output was again constant, Int: interaction, shading indicates significance at P < 0.05)

			Min		θc Min		Max		θc Max	
			L	R	L	R	L	R	L	R
SS1,7 + R1	Trial	F	0.987	0.817	1.918	0.558	1.986	0.029	0.415	0.160
		p	0.353	0.401	0.209	0.483	0.202	0.871	0.540	0.703
		η_p^2	0.124	0.120	0.215	0.085	0.221	0.005	0.056	0.026
	Time	F	21.329	1.265	0.522	1.163	2.402	6.969	9.219	3.144
		p	<0.001	0.311	0.720	0.352	0.074	0.019	0.002	0.090
		η_p^2	0.753	0.174	0.069	0.162	0.255	0.537	0.568	0.344
	Int	F	0.960	0.338	1.683	0.967	0.127	0.652	1.255	1.059
		p	0.445	0.850	0.182	0.444	0.971	0.631	0.311	0.398
		η_p^2	0.121	0.053	0.194	0.139	0.018	0.098	0.152	0.150
SS2-2	Trial	F	0.725	2.135	0.512	0.043	1.630	3.399	0.012	3.074
		p	0.423	0.194	0.497	0.843	0.242	0.115	0.915	0.130
		η_p^2	0.094	0.262	0.068	0.007	0.189	0.362	0.002	0.339
	Time	F	0.308	2.019	1.013	0.857	0.669	2.168	0.463	1.203
		p	0.819	0.147	0.407	0.481	0.581	0.127	0.711	0.337
		η_p^2	0.042	0.252	0.126	0.125	0.087	0.265	0.062	0.167
	Int	F	2.131	3.015	2.085	0.497	2.484	4.386	0.671	0.212
		p	0.127	0.057	0.133	0.689	0.089	0.065	0.579	0.887
		η_p^2	0.233	0.334	0.230	0.076	0.262	0.422	0.087	0.034

8.3.2.3: Time and trial interaction effects

For either section of the trials, the only significant time and trial interaction shown was for the crank angle at which the maximum right foot angular displacement occurred in the final steady state section of the trials (SS2-2) (Figure 8-5) where a moderate effect was shown. *Post hoc* analysis (see Table 1 7) of the crank angle at which the maximum right foot angular displacement occurred showed no significant differences between trials when examined at each time window. However, significant time effects were shown across time for the high fatigue trial. This may be explained by the fact that whilst a trend for maximum foot angle to occur progressively later in the crank cycle appeared, the similar trend for the low fatigue trial was interrupted by a marked shift to earlier in the cycle in the low fatigue trial at between 75 and 87.5% time to failure. Thus whilst the trends with time differed between the trials, the separation between the two was limited.

Table 8-6: Summary of results of Two-Way ANOVA on foot segment angular displacement data (SS1, 7: final minute of initial steady state, R1: ramp from 50% MMP to 95% MMP, SS2-2: final section of trials where power output was again constant, Int: interaction, shading indicates significance at P < 0.05)

			Min		θc Min		Max		θc Max	
			L	R	L	R	L	R	L	R
SS1,7 + R1	Trial	F	0.174	2.959	0.001	0.394	0.178	0.012	0.354	0.891
		p	0.689	0.136	0.978	0.553	0.686	0.915	0.570	0.382
		η_p^2	0.024	0.330	<0.001	0.062	0.025	0.002	0.048	0.129
	Time	F	11.135	4.520	56.633	0.383	0.140	6.164	6.187	0.412
		p	0.007	0.035	<0.001	0.819	0.966	0.012	0.018	0.798
		η_p^2	0.614	0.430	0.890	0.060	0.020	0.507	0.469	0.064
	Int	F	1.242	0.336	0.299	0.611	1.806	0.569	0.099	0.300
		p	0.316	0.851	0.876	0.659	0.156	0.687	0.982	0.875
		η_p^2	0.151	0.053	0.041	0.092	0.205	0.087	0.014	0.048
SS2-2	Trial	F	1.193	0.086	1.233	0.172	0.013	0.116	0.290	0.520
		p	0.311	0.779	0.303	0.692	0.914	0.745	0.607	0.498
		η_p^2	0.146	0.014	0.150	0.028	0.002	0.019	0.040	0.080
	Time	F	1.188	1.759	0.930	1.105	2.756	3.248	0.367	0.412
		p	0.338	0.191	0.444	0.373	0.068	0.046	0.777	0.747
		η_p^2	0.145	0.227	0.117	0.156	0.282	0.351	0.050	0.064
	Int	F	1.490	2.124	0.554	0.829	3.009	3.052	1.474	5.348
		p	0.246	0.133	0.651	0.495	0.053	0.055	0.250	0.023
		η_p^2	0.175	0.261	0.073	0.121	0.301	0.337	0.174	0.471

Table 8-7: Summary of post-hoc analyses of crank angle at maximum right foot angle data

	Between trial comparison at each time window				Within trial across time	
	50%	75%	87.5%	95%	Low	High
F	<0.01	0.094	0.927	0.912	0.669	5.904
P	0.949	0.768	0.368	0.371	0.582	0.017
η_p^2	0.001	0.013	0.117	0.115	0.100	0.458

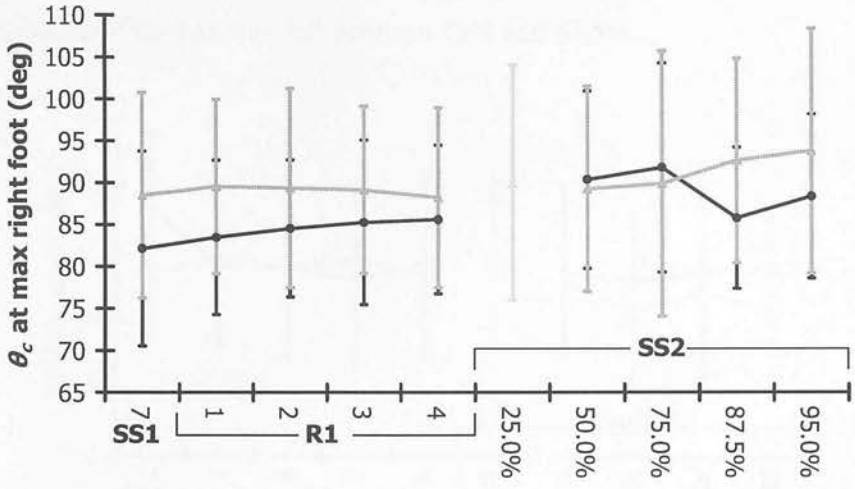

Figure 8-5: Group mean (±SD) crank angle (θ_c) at which maximum right foot angle occurred. (black diamonds: low fatigue trial, grey triangles: high fatigue trial, lighter grey 25% in SS)

8.3.2.4: Time effects in high-fatigue trial

Results of the One-Way ANOVAs on the data from all of the time windows in the final steady state section of the high fatigue (SS2-1) are summarised in Table 8-6 with complete results given in Appendix 3. The only variables to reach significance were those of minimum and maximum foot angles (both left (Figure 8-6 and Figure 8-8) and right (Figure 8-7 and Figure 8-9) However, although moderate effect sizes were found for the minimum angles, those for the maximums were small. For both left and right feet, the trends across the trial were for decrease for both minimum and maximum angles. For the maximum angles, this represented a reversal of the trends in the earlier part of the trials whilst apparent trends for decreasing angles were observed for the minimum angles, at least in the case of the right. For the left foot, there were temporary reversals of the trends towards decreasing angles with minimum foot angles increasing around 87.5% of time to failure. Pairwise comparisons of these results showed that, for the left minimum foot angle (

Table 8-8), no differences were apparent when the Bonferroni method was used, but that without it (i.e. least significant difference) the relationships between the 25% window and all other were significant, but that no others were. For the right side (Table 1 8), the only comparison shown to be significant with the use of the Bonferroni method was that between the 25% and 50% windows. In the absence of the correction, comparisons between the first and all subsequent windows were again shown to be significant as was that between 75% and 87.5%.

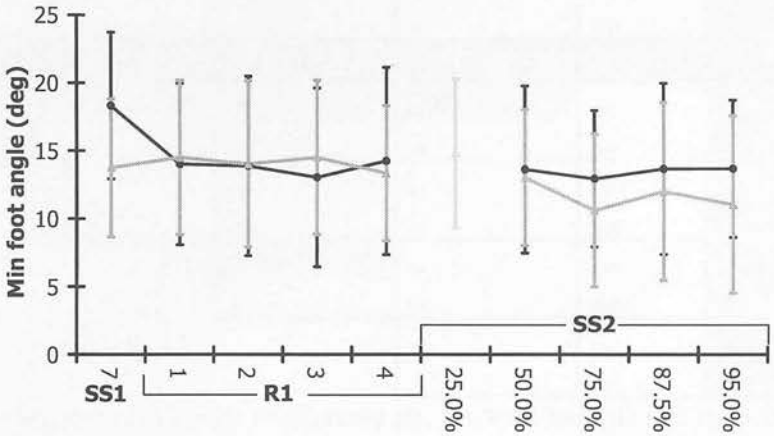

Figure 8-6: Group mean (±SD) left minimum foot angle (black diamonds: low fatigue trial, grey triangles: high fatigue trial, lighter grey 25% in SS2-1 in high fatigue; SS1 & R1: minutes, SS2: % time to failure)

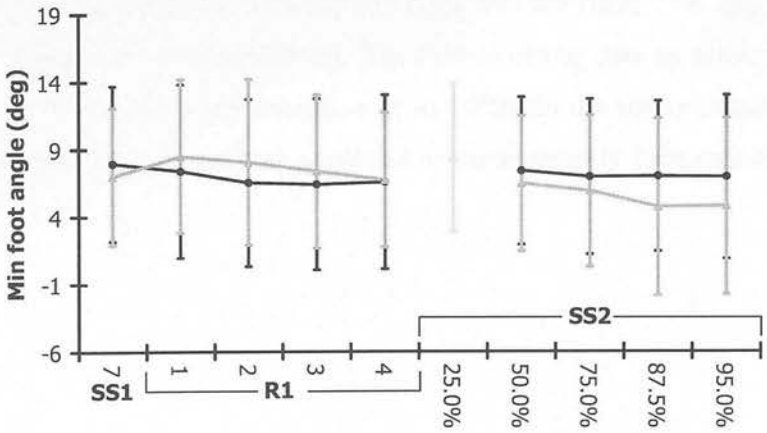

Figure 8-7: Group mean (±SD) right minimum foot angle (black diamonds: low fatigue trial, grey triangles: high fatigue trial, lighter grey 25% in SS2-1 in high fatigue; SS1 & R1: minutes, SS2: % time to failure)

Table 8-8: Summary of pairwise comparisons of minimum foot displacement data with (Bon) and without (LSD) Bonferroni corrections. Percentages are % time to failure (*: $p < 0.05$, **: $p < 0.01$, ns: $p \geq 0.05$)

50%	75%	87.5%	100%	←% Time to failure ↓	
*	*	*	*	LSD	25%
ns	ns	ns	ns	Bon	
	ns	ns	ns	LSD	50%
	ns	ns	ns	Bon	
		ns	ns	LSD	75%
		ns	ns	Bon	
	Left		ns	LSD	87.5%
			ns	Bon	

50%	75%	87.5%	100%	←% Time to failure ↓	
**	*	**	*	LSD	25%
*	ns	ns	ns	Bon	
	ns	ns	ns	LSD	50%
	ns	ns	ns	Bon	
		*	ns	LSD	75%
		ns	ns	Bon	
	Right		ns	LSD	87.5%
			ns	Bon	

For the maximum foot angular displacements, for both the left and right legs (Table 19), significant differences were again only found without the use of the Bonferroni method. These were between 25% and 75%, 25% and 100%, 50% and 75% and 50% and 100% were significant for both left and right. For the right, 75% and 100% and 87.5% and 100% were also significant. The failure of the data to show significant differences at 87.5% (with the exception of to 100% on the right) despite the time points either side doing so may be attributed to the temporary increases observed at this point.

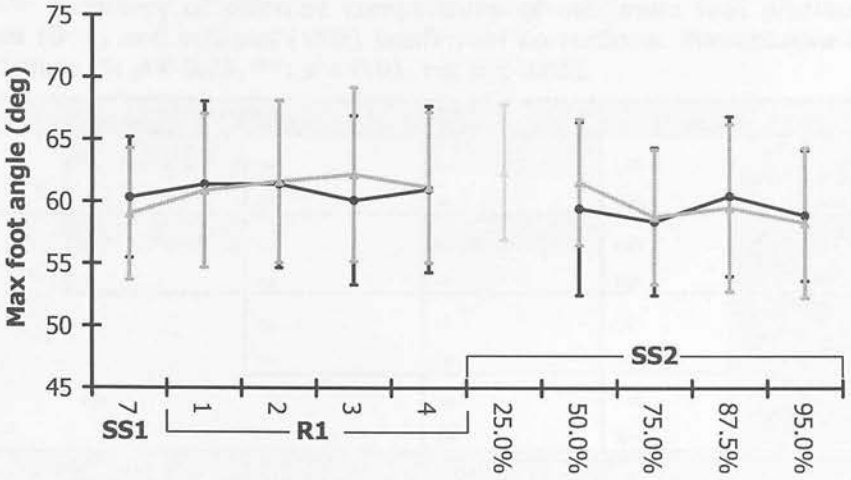

Figure 8-8: Group mean (±SD) left maximum foot angle (black diamonds: low fatigue trial, grey triangles: high fatigue trial, lighter grey 25% in SS2-1 in high fatigue; SS1 & R1: minutes, SS2: % time to failure)

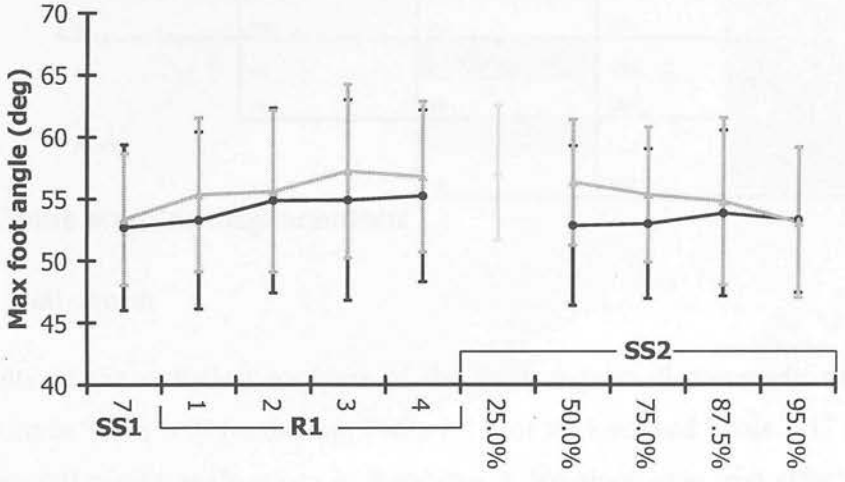

Figure 8-9: Group mean (±SD) right maximum foot angles (black diamonds: low fatigue trial, grey triangles: high fatigue trial, lighter grey 25% in SS2-1 in high fatigue; SS1 & R1: minutes, SS2: % time to failure)

Table 8-9: Summary of pairwise comparisons of maximum foot displacement data with (Bon) and without (LSD) Bonferroni corrections. Percentages are % time to failure (*: $p < 0.05$, **: $p < 0.01$, ns: $p \geq 0.05$)

50%	75%	87.5%	100%	←% Time to failure ↓	
ns ns	* ns	ns ns	* ns	LSD Bon	25%
	* ns	ns ns	** ns	LSD Bon	50%
		ns ns	ns ns	LSD Bon	75%
	Left		ns ns	LSD Bon	87.5%

50%	75%	87.5%	100%	←% Time to failure ↓	
ns ns	* ns	ns ns	** ns	LSD Bon	25%
	* ns	ns ns	** ns	LSD Bon	50%
		ns ns	* ns	LSD Bon	75%
	Right		* ns	LSD Bon	87.5%

8.3.3: Joint angular displacement

8.3.3.1: Trial effects

The results of the statistical analyses of the joint angular displacement data are summarised in Table 1 10 for the hip, Table 1 11 for the knee and Table 1 12 for the ankle with full results again given in Appendix 3. No significant trial effects were found in the initial common parts of the two trials (SS1, 7 + R1). However, during the final steady state (SS2-2) portion of the trial, effects were shown for both the right peak ankle plantar and dorsiflexion as well as the crank angle at which maximum knee flexion occurred. In all cases, effects sizes were moderate. In all cases, effect sizes were moderate with the exception of maximum left knee flexion angles and the crank angles at maximum ankle dorsiflexion angle in the initial phase of the trial where effect sizes were large.

Table 8-10: Summary of results of Two-Way ANOVA on hip joint angular displacement data (SS1, 7: final minute of initial steady state, R1: ramp from 50% MMP to 95% MMP, SS2-2: final section of trials where power output was again constant, Int: interaction, ext: extension, flex: flexion, shading indicates significance at $P < 0.05$).

			Max flex		θc Max flex		Max ext.		θc Max ext.	
			L	R	L	R	L	R	L	R
SS1,7 + R1	Trial	F	0.397	0.129	0.908	0.364	0.628	0.510	1.784	0.509
		P	0.549	0.732	0.372	0.568	0.454	0.502	0.223	0.502
		η_p^2	0.054	0.021	0.115	0.057	0.082	0.078	0.203	0.078
	Time	F	10.488	2.104	12.386	0.662	1.486	2.240	0.926	1.186
		P	0.013	0.112	0.009	0.624	0.233	0.095	0.463	0.342
		η_p^2	0.600	0.260	0.639	0.099	0.175	0.272	0.117	0.165
	Int	F	0.359	1.158	0.416	2.584	1.184	1.604	0.685	0.181
		P	0.835	0.354	0.795	0.063	0.339	0.206	0.609	0.946
		η_p^2	0.049	0.162	0.056	0.301	0.145	0.211	0.089	0.029
SS2-2	Trial	F	0.008	0.822	2.402	0.860	0.096	0.921	0.455	0.658
		P	0.932	0.399	0.165	0.390	0.766	0.374	0.522	0.448
		η_p^2	0.001	0.121	0.255	0.125	0.014	0.133	0.061	0.099
	Time	F	0.832	0.334	1.438	1.046	0.721	0.400	1.242	0.350
		P	0.491	0.801	0.260	0.396	0.551	0.755	0.320	0.790
		η_p^2	0.106	0.053	0.170	0.148	0.093	0.062	0.151	0.055
	Int	F	0.676	0.835	0.008	3.072	0.895	1.032	1.266	1.961
		P	0.577	0.492	0.999	0.054	0.460	0.402	0.312	0.156
		η_p^2	0.088	0.122	0.001	0.339	0.113	0.147	0.153	0.246

8.3.3.2: Time effects

In the initial common portions (SS1, 7 + R1) of the two trials, significant time main effects were shown for the left peak hip flexion and the crank angle at which this occurred. The left maximum knee flexion and the crank angle at maximum knee extension were also shown to possess significant time main effects, whilst for the right, this was only shown for maximum extension. Significant time main effects were also shown for right maximum ankle plantar-flexion and the crank angle at right peak dorsiflexion. However, no significant time main effects were found for the second steady state part of the trials (SS2-2).

Table 8-11: Summary of results of Two-Way ANOVA on knee joint angular displacement data (SS1, 7: final minute of initial steady state, R1: ramp from 50% MMP to 95% MMP, SS2-2: final section of trials where power output was again constant, Int: interaction, ext: extension, flex: flexion, shading indicates significance at $P < 0.05$)

			Max flex		θc Max flex		Max ext.		θc Max ext.	
			L	R	L	R	L	R	L	R
SS1,7 + R1	Trial	F	0.378	1.138	0.064	0.315	2.669	0.166	0.346	0.163
		P	0.558	0.327	0.808	0.595	0.146	0.698	0.575	0.700
		η_p^2	0.051	0.159	0.009	0.050	0.276	0.027	0.047	0.026
	Time	F	28.989	1.785	2.456	1.501	3.291	11.705	3.960	0.685
		P	<0.001	0.165	0.069	0.233	0.095	0.008	0.041	0.609
		η_p^2	0.805	0.229	0.260	0.200	0.320	0.661	0.361	0.102
	Int	F	0.333	1.221	0.474	0.840	1.327	0.335	1.296	0.384
		P	0.853	0.328	0.755	0.513	0.284	0.852	0.296	0.818
		η_p^2	0.045	0.169	0.063	0.123	0.159	0.053	0.156	0.060
SS2-2	Trial	F	0.034	0.692	5.882	1.339	0.018	0.198	0.525	1.623
		P	0.858	0.437	0.046	0.291	0.896	0.672	0.492	0.250
		η_p^2	0.005	0.103	0.457	0.182	0.003	0.032	0.070	0.213
	Time	F	0.650	1.273	0.743	0.082	2.544	2.081	0.611	0.239
		P	0.592	0.314	0.539	0.969	0.084	0.139	0.615	0.868
		η_p^2	0.085	0.175	0.096	0.014	0.267	0.257	0.080	0.038
	Int	F	0.774	1.506	2.111	1.945	1.679	2.225	1.748	2.295
		P	0.522	0.247	0.129	0.159	0.202	0.120	0.188	0.112
		η_p^2	0.100	0.201	0.232	0.245	0.193	0.270	0.200	0.277

8.3.3.3: Time and trial interaction effects

No significant time and trial interactions were shown in any joint angular displacement angle throughout the trials.

Table 8-12: Summary of results of Two-Way ANOVA on ankle joint angular displacement data (SS1, 7: final minute of initial steady state, R1: ramp from 50% MMP to 95% MMP, SS2-2: final section of trials where power output was again constant, Int: interaction, plant: plantar-flexion, dorsi: dorsiflexion, shading indicates significance at $P < 0.05$).

			Max plant		θc Max plant		Max dorsi		θc Max dorsi	
			L	R	L	R	L	R	L	R
SS1,7 + R1	Trial	F	0.030	5.178	1.691	0.233	0.003	1.282	0.017	1.160
		p	0.867	0.063	0.235	0.647	0.961	0.301	0.899	0.323
		η_p^2	0.004	0.463	0.195	0.037	<0.001	0.176	0.002	0.162
	Time	F	1.440	2.883	1.435	1.759	1.468	1.200	2.902	21.483
		p	0.247	0.044	0.248	0.170	0.238	0.336	0.053	<0.001
		η_p^2	0.171	0.325	0.170	0.227	0.173	0.167	0.293	0.782
	Int	F	2.663	0.595	1.173	0.308	1.702	1.146	0.381	1.066
		p	0.053	0.670	0.344	0.870	0.178	0.359	0.821	0.395
		η_p^2	0.276	0.090	0.143	0.049	0.196	0.160	0.052	0.151
SS2-2	Trial	F	1.550	11.426	0.208	1.020	0.886	7.983	3.536	3.026
		p	0.253	0.015	0.662	0.352	0.378	0.030	0.102	0.133
		η_p^2	0.181	0.656	0.029	0.145	0.112	0.571	0.336	0.335
	Time	F	0.481	0.803	0.434	1.069	0.938	0.458	0.277	2.303
		p	0.699	0.509	0.731	0.387	0.440	0.715	0.842	0.112
		η_p^2	0.064	0.118	0.058	0.151	0.118	0.071	0.038	0.277
	Int	F	1.137	0.696	0.273	0.870	1.346	0.963	0.762	1.838
		p	0.357	0.567	0.844	0.475	0.286	0.432	0.528	0.176
		η_p^2	0.140	0.104	0.038	0.127	0.161	0.138	0.098	0.235

8.3.3.4: Time effects in high-fatigue trial

Results of the One-Way ANOVAs on the data from all of the time windows in the high fatigue trial are summarised in Table 8-13 with complete results given in Appendix 3. Only two variables reached significance, the maximum left knee extension angle (Figure 8-11) and the crank angle at which the maximum right hip flexion was recorded (Figure 8-10), although for the latter, the effect size was very small. In the case of the latter, the trend was for maximum extension to occur progressively later in the trial from 50% of time to failure onwards. The maximum knee extension angle was also shown to increase throughout the trial although the rate of increase was minimal between 75% and 87.5% of time to failure. For both variables, pairwise comparisons (maximum left knee extension: Table 1 15 , crank angle at which the maximum right hip extension: Table 1 14) using Bonferroni

corrections showed no significant results. However, significant differences were observed without corrections between the final time window (100%) and all others with the exception of the penultimate one (87.5%) for both variables.

Table 8-13: Summary of One-Way ANOVAs on the complete final steady state section (SS2-1) of the high fatigue trial for joint angular displacements.

		Min*		θc Min*		Max*		θc Max*	
		L	R	L	R	L	R	L	R
Hip	F	0.127	0.095	0.787	3.797	0.287	0.057	0.582	0.984
	p	0.972	0.983	0.543	0.038	0.884	0.994	0.678	0.432
	η_p^2	0.018	0.013	0.039	0.008	0.101	0.352	0.077	0.123
Knee	F	4.945	3.881	0.438	0.773	0.362	1.970	2.427	0.427
	p	0.042	0.077	0.833	0.552	0.833	0.127	0.071	0.788
	η_p^2	0.414	0.357	0.049	0.22	0.059	0.099	0.257	0.057
Ankle	F	3.059	1.410	1.122	2.199	2.558	1.542	3.155	1.912
	p	0.071	0.257	0.366	0.095	0.061	0.217	0.054	0.136
	η_p^2	0.304	0.168	0.268	0.181	0.138	0.239	0.311	0.215

Joint	**Hip**	**Knee**	**Ankle**
Min*	Flexion	Extension	Dorsiflexion
Max*	Extension	Flexion	Plantar-flexion

Table 8-14: Summary of pairwise comparisons of crank angle at maximum right hip flexion with (Bon) and without (LSD) Bonferroni corrections (*: $p < 0.05$, **: $p < 0.01$, ns: $p \geq 0.05$)

50%	75%	87.5%	100%	←% Time to failure ↓	
ns	ns	ns	*	LSD	25%
ns	ns	ns	ns	Bon	
	ns	ns	*	LSD	50%
	ns	ns	ns	Bon	
		ns	*	LSD	75%
		ns	ns	Bon	
			ns	LSD	87.5%
			ns	Bon	

Table 8-15: Summary of pairwise comparisons of maximum left knee extension angle with (Bon) and without (LSD) Bonferroni corrections (*: $p < 0.05$, **: $p < 0.01$, ns: $p \geq 0.05$)

50%	75%	87.5%	100%	←% Time to failure ↓	
ns ns	ns ns	ns ns	* ns	LSD Bon	25%
	ns ns	ns ns	* ns	LSD Bon	50%
		ns ns	* ns	LSD Bon	75%
			ns ns	LSD Bon	87.5%

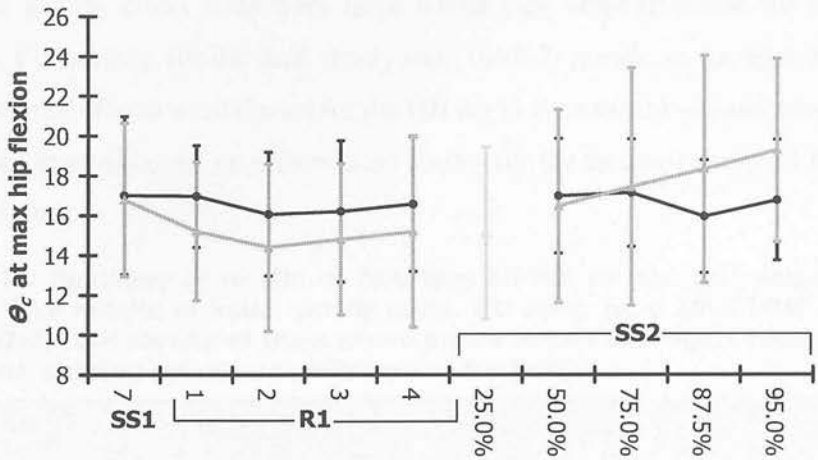

Figure 8-10: Group mean (±SD) crank angle (θ_c) at which maximum right hip flexion angles occurred (black diamonds: low fatigue trial, grey triangles: high fatigue trial, lighter grey 25% in SS2-1 in high fatigue; SS1 & R1: minutes, SS2: % time to failure)

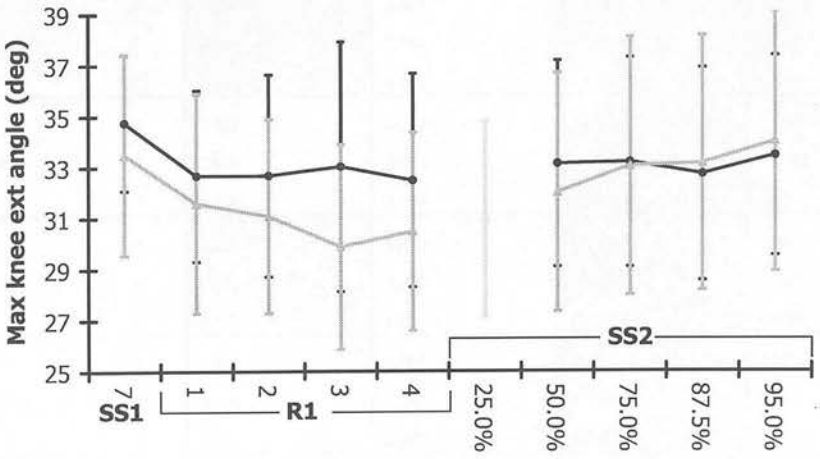

Figure 8-11: Group mean (±SD) maximum left knee extension angle. (black diamonds: low fatigue trial, grey triangles: high fatigue trial, lighter grey 25% in SS2-1 in high fatigue; SS1 & R1: minutes, SS2: % time to failure)

8.3.4: Joint velocity

8.3.4.1: Trial effects

The results of the statistical analyses of the joint velocity data are summarised in Table 1 16 for the hip, Table 1 17 for the knee and Table 1 18 for the ankle with full results given in Appendix 3. In the initial common parts of the two trials (SS1, 7 + R1), significant trial effects were found in the minimum velocities only in the case of left knee. However, significant effects were shown in the maximum velocities for the right ankle and all of the left joint velocities. In the case of the right maximum hip and ankle angles, effect sizes were large whilst they were moderate for the other variables. Conversely, for the final steady state (SS2-2) portion of the trial, moderate significant trial effects were shown for the left leg in both maximum and minimum at the hip and knee although no effects were shown for the ankle or at any of the joints of the right leg.

Table 8-16: Summary of results of Two-Way ANOVA on hip joint velocity data (SS1, 7: final minute of initial steady state, R1: ramp from 50% MMP to 95% MMP, SS2-2: final section of trials where power output was again constant, Int: interaction, shading indicates significance at $P < 0.05$).

			Min		Max	
			L	R	L	R
SS1,7 + R1	Trial	F	1.262	1.372	54.293	0.110
		P	0.298	0.286	<0.001	0.751
		η_p^2	0.153	0.186	0.886	0.018
	Time	F	10.189	2.629	13.290	13.737
		P	0.002	0.059	0.004	<0.001
		η_p^2	0.593	0.305	0.655	0.696
	Int	F	0.212	1.369	22.361	13.679
		P	0.930	0.274	<0.001	<0.001
		η_p^2	0.029	0.186	0.762	0.695
SS2-2	Trial	F	8.811	0.370	9.519	0.125
		P	0.021	0.565	0.018	0.735
		η_p^2	0.557	0.058	0.576	0.020
	Time	F	1.977	1.382	4.970	1.036
		P	0.148	0.280	0.017	0.400
		η_p^2	0.220	0.187	0.415	0.147
	Int	F	1.848	0.256	4.868	0.749
		P	0.170	0.856	0.020	0.537
		η_p^2	0.209	0.041	0.410	0.111

8.3.4.2: Time effects

Significant time main effects were also shown for all maximum joint velocities in the initial common portions (SS1, 7 + R1) of the two trials, as well as for the minimum velocities of the left hip and right knee. In the case of the maximum left knee angle and ankle angles effect sizes were shown to be large, whilst they were moderate in the remaining variables. Conversely, the only variables to show significant time main effects in the second steady state part of the trials were left minimum knee velocity and left maximum hip velocities where effect sizes were moderate.

Table 8-17: Summary of results of Two-Way ANOVA on knee joint velocity data (SS1, 7: final minute of initial steady state, R1: ramp from 50% MMP to 95% MMP, SS2-2: final section of trials where power output was again constant, Int: interaction, shading indicates significance at $P < 0.05$).

			Min		Max	
			L	R	L	R
SS1,7 + R1	Trial	F	13.016	0.151	11.495	2.053
		p	0.009	0.711	0.012	0.202
		η_p^2	0.650	0.025	0.622	0.255
	Time	F	3.776	6.571	31.460	8.408
		p	0.067	0.014	<0.001	0.008
		η_p^2	0.350	0.523	0.818	0.584
	Int	F	9.128	14.091	27.041	19.662
		p	0.006	0.001	<0.001	<0.001
		η_p^2	0.566	0.701	0.794	0.766
SS2-2	Trial	F	11.919	1.075	11.352	0.729
		p	0.011	0.340	0.012	0.426
		η_p^2	0.630	0.152	0.619	0.108
	Time	F	7.634	1.516	3.078	0.841
		p	0.011	0.244	0.082	0.489
		η_p^2	0.522	0.202	0.305	0.123
	Int	F	4.130	0.516	1.520	0.423
		p	0.043	0.677	0.239	0.739
		η_p^2	0.371	0.079	0.178	0.066

8.3.4.3: Time and trial interaction effects

Significant time and trial interactions were shown for all joints, for both minimum and maximum velocities in the initial section of the trials (SS1, 7 + R1) with the exception of the minimum hip velocity which was not significant for either left or

right. The effect sizes were shown to be moderate with the exception of the maximum velocities for the left hip and knee and right ankle. For the second steady state section (SS2-2) however, the time/ trial interactions were only found to be significant in the case of maximum left hip (Figure 8-12) and minimum left knee velocities (Figure 8-13) where effect sizes were moderate. The only trends for both of these appeared to be a slight convergence of the two trials towards the end. *Post hoc* analyses of these data showed that, for both variables, significant differences were only apparent across time in the high fatigue trial and that significant trial differences existed at each time window with the exception of the last (95%) (minimum left knee: Table 1 20, maximum left hip: Table 1 19).

Table 8-18: Summary of results of Two-Way ANOVA on ankle joint velocity data (SS1, 7: final minute of initial steady state, R1: ramp from 50% MMP to 95% MMP, SS2-2: final section of trials where power output was again constant, Int: interaction, shading indicates significance at $P < 0.05$).

			Min		Max	
			L	R	L	R
SS1,7 + R1	Trial	F	5.524	1.228	28.206	11.739
		P	0.051	0.310	0.001	0.014
		η_p^2	0.441	0.170	0.801	0.662
	Time	F	3.449	3.021	19.830	21.519
		P	0.082	0.089	0.001	<0.001
		η_p^2	0.330	0.335	0.739	0.782
	Int	F	10.983	8.252	15.827	20.495
		P	0.003	0.005	<0.001	<0.001
		η_p^2	0.611	0.579	0.693	0.774
SS2-2	Trial	F	0.120	0.059	3.864	1.109
		P	0.740	0.816	0.090	0.333
		η_p^2	0.017	0.010	0.356	0.156
	Time	F	2.499	1.610	0.205	0.172
		P	0.087	0.222	0.891	0.914
		η_p^2	0.263	0.212	0.029	0.028
	Int	F	1.233	0.069	1.177	0.510
		P	0.323	0.976	0.342	0.680
		η_p^2	0.150	0.011	0.144	0.078

Table 8-19: Summary of post-hoc analyses of maximum left hip velocity data

	Between trial comparison at each time window				Within trial across time	
	50%	75%	87.5%	95%	Low	High
F	8.414	12.067	6.847	3.952	0.912	8.213
P	0.023	0.010	0.035	0.087	0.452	0.003
η_p^2	0.546	0.633	0.494	0.361	0.115	0.540

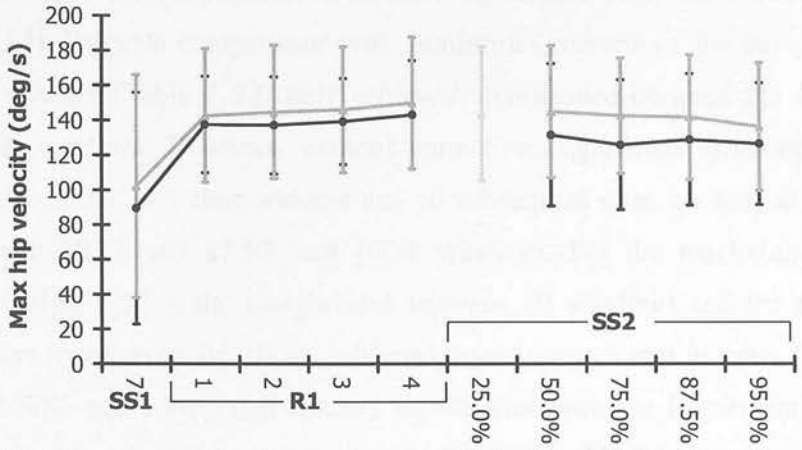

Figure 8-12: Group mean (±SD) maximum left hip velocity. (black diamonds: low fatigue trial, grey triangles: high fatigue trial, lighter grey 25% in SS2-1 in high fatigue; SS1 & R1: minutes, SS2: % time to failure)

Table 8-20: Summary of post-hoc analyses of minimum left knee velocity data

	Between trial comparison at each time window				Within trial across time	
	50%	75%	87.5%	95%	Low	High
F	11.919	9.37	10.08	2.721	2.195	8.811
P	0.011	0.018	0.016	0.143	0.119	0.002
η_p^2	0.630	0.572	0.590	0.280	0.239	0.557

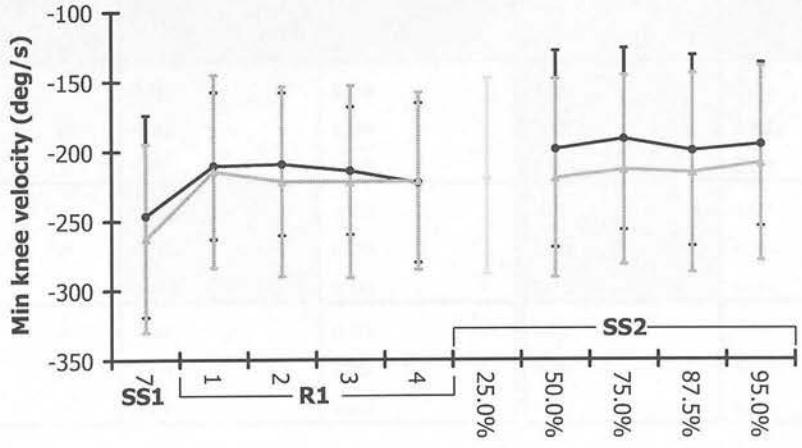

Figure 8-13: Group mean (±SD) minimum left knee velocity. (black diamonds: low fatigue trial, grey triangles: high fatigue trial, lighter grey 25% in SS2-1 in high fatigue; SS1 & R1: minutes, SS2: % time to failure)

8.3.5: Time effects in high-fatigue trial

Results of the One-Way ANOVA on the complete final section of the high fatigue trial (SS2-1) (Table 8-21) showed significant moderate effects for the left minimum knee (Figure 8-13) velocity and left maximum hip (Figure 8-12) and knee velocities (Figure 8-14). Pairwise comparisons with Bonferroni corrections for the minimum left knee velocity (Table 1 23) only achieved significance between the 50% and 100% time windows. However, without correction, significant differences were shown between the 50% time window and all subsequent ones, as well as between the 25% and 100% and 87.5% and 100% windows. For the maximum left hip velocity ((Table 1 22), the comparisons between all windows and the final one (100%) were found to be significant without corrections and two of these (25% and 100% and 50% and 100%) still reached significance with the Bonferroni method. However, for the maximum left knee velocity (Table 8-24), no pairing showed significant differences when the corrections were applied although all of the windows, with the exception of 75%, revealed significant differences to the final (100%) window without.

Table 8-21: Summary of One-Way ANOVAs on the complete final steady state section (SS2-1) of the high fatigue trial for joint velocities

		Min		Max	
		L	R	L	R
Hip	F	2.352	0.739	7.008	0.688
	P	0.078	0.573	<0.001	0.606
	η_p^2	0.252	0.095	0.500	0.090
Knee	F	5.319	1.095	3.972	1.648
	P	0.012	0.378	0.020	0.190
	η_p^2	0.432	0.135	0.362	0.191
Ankle	F	0.865	0.313	1.325	0.440
	P	0.497	0.866	0.285	0.778
	η_p^2	0.110	0.050	0.159	0.059

Table 8-22: Summary of pairwise comparisons of maximum left hip velocity data for final steady state section of high fatigue trial (SS2-1) with (Bon) and without (LSD) Bonferroni corrections (*: $p < 0.05$, **: $p < 0.01$, ns: $p \geq 0.05$)

50%	75%	87.5%	100%	←% Time to failure ↓	
ns ns	ns ns	ns ns	** *	LSD Bon	25%
	ns ns	ns ns	** *	LSD Bon	50%
		ns ns	** ns	LSD Bon	75%
			* ns	LSD Bon	87.5%

Table 8-23: Summary of pairwise comparisons of minimum left knee velocity data for final steady state section of high fatigue trial (SS2-1) with (Bon) and without (LSD) Bonferroni corrections (*: $p < 0.05$, **: $p < 0.01$, ns: $p \geq 0.05$)

50%	75%	87.5%	100%	←% Time to failure ↓	
ns ns	ns ns	ns ns	* ns	LSD Bon	25%
	* ns	** ns	** *	LSD Bon	50%
		ns ns	ns ns	LSD Bon	75%
			* ns	LSD Bon	87.5%

Table 8-24: Summary of pairwise comparisons of maximum left knee velocity data for final steady state section of high fatigue trial (SS2-1) with (Bon) and without (LSD) Bonferroni corrections (*: $p < 0.05$, **: $p < 0.01$, ns: $p \geq 0.05$)

50%	75%	87.5%	100%	←% Time to failure ↓	
ns ns	ns ns	ns ns	* ns	LSD Bon	25%
	ns ns	ns ns	* ns	LSD Bon	50%
		ns ns	ns ns	LSD Bon	75%
			* ns	LSD Bon	87.5%

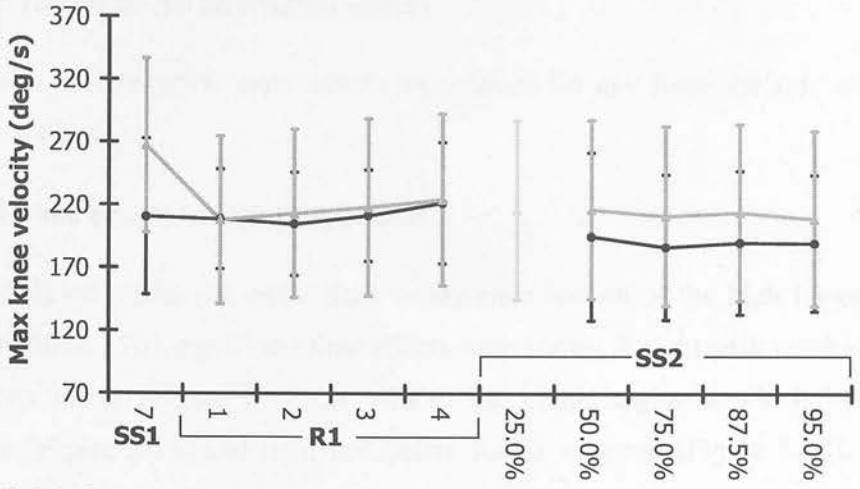

Figure 8-14: Group mean (±SD) maximum left knee velocity. (black diamonds: low fatigue trial, grey triangles: high fatigue trial, lighter grey 25% in SS2-1 in high fatigue; SS1 & R1: minutes, SS2: % time to failure)

8.3.6: Effective, ineffective and resultant forces

8.3.6.1: Trial effects

None of the resultant (Table 8-25), effective or ineffective (Table 1 27) force parameters showed significant trial effects for the initial phase of the trial (SS1, 7 +R1). However, in the latter part of the trial (SS2-2), significant effects were obtained for the magnitudes of peak resultant, effective and ineffective forces for both pedals as well as the crank angle at which right peak ineffective force was achieved. In the case of the resultant and effective forces, the effect sizes were large whilst those for the magnitudes and relative timings of the ineffective forces were moderate.

8.3.6.2: Time effects

In the initial phase of the two trials (SS1,7 + R1), significant time main effects were found for all of the force magnitudes as well as the crank angle at which peak ineffective forces occurred for both sides. Again, for the resultant and effective forces, the effect sizes were large whilst those for the magnitudes and relative timings of the ineffective forces were moderate. Conversely, for the final section (SS2-2), only right peak resultant and ineffective forces and the crank angle at which left peak ineffective forces occurred achieved significance with moderate effect sizes in all cases.

8.3.6.3: Time and trial interaction effects

No significant interaction main effects were found for any force variable in either part of the trials.

8.3.6.4: Time effects in high-fatigue trial

When analysed across the entire final steady state section of the high fatigue trial (SS2-1) (Table 1 26), significant time effects were shown in right peak resultant and ineffective forces (Figure 8-17) as well as the crank angles at which left peak effective (Figure 8-16) and right ineffective forces occurred (Figure 8-18). Effect sizes were moderate in all cases. The trends for the right peak resultant and ineffective forces throughout the entire trial were to increase steadily until the final segment where they dropped markedly. Peak ineffective force was also shown to occur later in the crank cycle with the rate of this shift increasing slightly after around 50% of time to failure, with a decrease in the standard deviation of the angles preceding this. There was also a shift towards the peak occurring later in the cycle at the final segment. Conversely, the crank angle at which left peak effective force occurred remained relatively constant for the first 50% of the section but then occurred progressively later in the cycle for the remainder of the trial. This trend was however, interrupted by a marked shift towards an earlier peak around 71% of time to failure. *Post hoc* analyses of these results showed no significant pairwise comparisons for any of the variables when Bonferroni corrections were used. Without these, a pattern of significant results was apparent for the crank angle at which left peak effective force was recorded (Table 1 29) between the windows covering the first 55% of the trial and the final 24%. Similar, trends emerged for the crank angle at which right peak ineffective force occurred (Table 1 31) between the first 45% and final 39% of the trial. Significant effects were also shown for the final time window compared to almost all of the rest of the trial. Conversely, for the right peak resultant (Table 1 28) and ineffective forces (Table 1 30), no clear trends were apparent, although in both cases none of the comparisons achieved significance for the final window despite many of those for the previous windows doing so.

Figure 8-15: Group mean (±SD) right peak resultant force (F_r), (black diamonds: low fatigue trial, grey triangles: high fatigue trial, lower abscissa: SS1 & R1: minutes, SS2-1: % time to failure in high fatigue trial (lighter grey), upper abscissa: SS2-2: time windows)

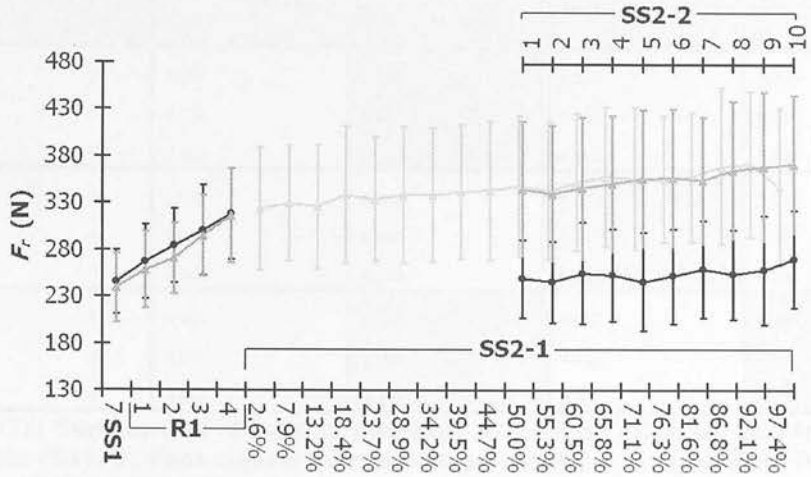

Table 8-25: Summary of results of Two-Way ANOVA on peak resultant force data (SS1, 7: final minute of initial steady state, R1: ramp from 50% MMP to 95% MMP, SS2-2: final section of trials where power output was again constant, Int: interaction, shading indicates significance at P < 0.05)

			Fr		*θC Fr*	
			L	R	L	R
SS1,7 + R1	Trial	*F*	0.165	0.927	0.746	3.717
		P	0.696	0.364	0.413	0.090
		η_p^2	0.020	0.104	0.085	0.317
	Time	*F*	62.804	26.885	0.927	1.325
		P	<0.001	<0.001	0.461	0.282
		η_p^2	0.887	0.771	0.104	0.142
	Int	*F*	0.823	0.305	1.035	0.643
		P	0.520	0.872	0.404	0.636
		η_p^2	0.093	0.037	0.115	0.074
SS2-2	Trial	*F*	21.420	28.147	1.614	0.085
		P	0.002	<0.001	0.240	0.778
		η_p^2	0.728	0.779	0.168	0.011
	Time	*F*	2.398	6.655	1.083	1.113
		P	0.075	0.003	0.386	0.365
		η_p^2	0.231	0.454	0.119	0.122
	Int	*F*	1.245	1.452	0.733	1.382
		P	0.282	0.183	0.677	0.212
		η_p^2	0.135	0.154	0.084	0.147

Table 8-26: Summary of One-Way ANOVAs on the complete final steady state section (SS2-1) of the high fatigue trial for resultant, effective and ineffective forces

		Peak		θc peak	
		L	R	L	R
Fr	*F*	1.501	4.400	1.784	2.495
	P	0.098	0.017	0.200	0.138
	η_p^2	0.158	0.355	0.182	0.238
Feff	*F*	0.697	0.982	5.078	2.033
	P	0.810	0.484	0.011	0.182
	η_p^2	0.080	0.109	0.388	0.203
Fineff	*F*	0.469	6.651	2.807	5.204
	P	0.967	0.005	0.080	0.009
	η_p^2	0.055	0.454	0.260	0.394

Table 8-27: Summary of results of Two-Way ANOVA on effective and ineffective force data (SS1, 7: final minute of initial steady state, R1: ramp from 50% MMP to 95% MMP, SS2-2: final section of trials where power output was again constant, Int: interaction, shading indicates significance at P < 0.05)

			Feff		θc *Feff*		*Fineff*		θc *Fineff*	
			L	R	L	R	L	R	L	R
SS1,7 + R1	Trial	*F*	0.246	0.459	0.179	1.121	0.014	0.576	<0.01	0.371
		P	0.633	0.517	0.683	0.321	0.908	0.470	0.995	0.559
		η_p^2	0.030	0.054	0.022	0.123	0.002	0.067	<0.001	0.044
	Time	*F*	104.138	65.120	0.732	2.890	16.236	12.454	8.188	8.288
		P	<0.001	<0.001	0.577	0.061	<0.001	0.002	0.006	0.005
		η_p^2	0.929	0.891	0.084	0.265	0.670	0.609	0.506	0.509
	Int	*F*	1.393	1.230	1.164	1.573	0.853	0.191	0.453	0.315
		P	0.259	0.318	0.345	0.205	0.503	0.942	0.770	0.866
		η_p^2	0.148	0.133	0.127	0.164	0.096	0.023	0.054	0.038
SS2-2	Trial	*F*	40.978	61.706	0.004	0.193	15.127	12.214	4.691	6.851
		P	<0.001	<0.001	0.952	0.672	0.005	0.008	0.062	0.031
		η_p^2	0.837	0.885	<0.001	0.024	0.654	0.604	0.370	0.461
	Time	*F*	1.647	1.296	1.839	1.054	0.892	2.930	3.896	2.948
		P	0.118	0.254	0.076	0.407	0.537	0.027	0.024	0.059
		η_p^2	0.171	0.139	0.187	0.116	0.100	0.268	0.327	0.269
	Int	*F*	1.676	1.379	2.684	2.848	0.421	2.054	0.856	2.160
		P	0.111	0.214	0.102	0.105	0.920	0.095	0.568	0.065
		η_p^2	0.173	0.147	0.251	0.263	0.050	0.204	0.097	0.213

Table 8-28: *p*-values for post-hoc pair-wise comparisons of peak resultant force at the right pedal with (BON) and without (LSD: least significant difference) Bonferroni correction (*: $p < 0.05$, **: $p < 0.01$, ns: $p \geq 0.05$, %TTF: % time to failure)

8%	13%	18%	24%	29%	34%	39%	45%	50%	55%	61%	66%	71%	76%	82%	87%	92%	97%	←% TTF →	
ns	ns	ns	*	*	ns	*	**	*	ns	*	**	**	**	**	**	**	ns	LSD	3%
ns	ns	ns	ns	ns	ns	ns	ns	ns	ns	ns	ns	ns	ns	ns	ns	ns	ns	BON	
	ns	ns	ns	ns	ns	*	*	*	ns	*	**	**	**	**	**	**	ns	LSD	8%
	ns	ns	ns	ns	ns	ns	ns	ns	ns	ns	ns	ns	ns	ns	ns	ns	ns	BON	
		ns	ns	*	*	**	**	**	*	**	**	**	**	**	**	**	ns	LSD	13%
		ns	ns	ns	ns	ns	ns	ns	ns	ns	ns	ns	ns	ns	ns	ns	ns	BON	
			ns	ns	ns	ns	ns	ns	ns	*	*	*	ns	*	**	**	ns	LSD	18%
			ns	ns	ns	ns	ns	ns	ns	ns	ns	ns	ns	ns	ns	ns	ns	BON	
				ns	ns	*	*	*	ns	**	**	**	**	**	*	**	ns	LSD	24%
				ns	ns	ns	ns	ns	ns	ns	ns	ns	ns	ns	ns	ns	ns	BON	
					ns	ns	ns	ns	ns	*	*	*	ns	*	**	**	ns	LSD	29%
					ns	ns	ns	ns	ns	ns	ns	ns	ns	ns	ns	ns	ns	BON	
						ns	ns	**	ns	*	*	*	**	**	*	*	ns	LSD	34%
						ns	ns	ns	ns	ns	ns	ns	ns	ns	ns	ns	ns	BON	
							ns	ns	ns	ns	*	ns	*	*	*	*	ns	LSD	39%
							ns	ns	ns	ns	ns	ns	ns	ns	ns	ns	ns	BON	
								ns	ns	ns	*	ns	ns	ns	*	*	ns	LSD	45%
								ns	ns	ns	ns	ns	ns	ns	ns	ns	ns	BON	
									ns	ns	ns	ns	ns	ns	ns	*	ns	LSD	50%
									ns	ns	ns	ns	ns	ns	ns	ns	ns	BON	
										ns	ns	ns	*	*	ns	*	ns	LSD	55%
										ns	ns	ns	ns	ns	ns	ns	ns	BON	
											ns	ns	ns	ns	*	*	ns	LSD	61%
											ns	ns	ns	ns	ns	ns	ns	BON	
												ns	ns	ns	ns	ns	ns	LSD	66%
												ns	ns	ns	ns	ns	ns	BON	
													ns	ns	ns	ns	ns	LSD	71%
													ns	ns	ns	ns	ns	BON	
														ns	ns	ns	ns	LSD	76%
														ns	ns	ns	ns	BON	
															ns	ns	ns	LSD	82%
															ns	ns	ns	BON	
																ns	ns	LSD	87%
																ns	ns	BON	
																	ns	LSD	92%
																	ns	BON	

Table 8-29: *p*-values for post-hoc pair-wise comparisons of left crank angle at peak effective force with (BON) and without (LSD: least significant difference) Bonferroni correction (*: $p < 0.05$, **: $p < 0.01$, ns: $p \geq 0.05$, %TTF: % time to failure)

8%	13%	18%	24%	29%	34%	39%	45%	50%	55%	61%	66%	71%	76%	82%	87%	92%	97%	←% TTF →	
ns	ns	ns	ns	ns	ns	ns	ns	ns	ns	ns	ns	ns	ns	ns	*	**	*	LSD	3%
ns	ns	ns	ns	ns	ns	ns	ns	ns	ns	ns	ns	ns	ns	ns	ns	ns	ns	BON	
	ns	ns	ns	ns	ns	ns	ns	ns	ns	ns	ns	ns	ns	*	*	*	*	LSD	8%
	ns	ns	ns	ns	ns	ns	ns	ns	ns	ns	ns	ns	ns	ns	ns	ns	ns	BON	
		ns	ns	ns	ns	ns	ns	ns	ns	ns	ns	ns	ns	ns	ns	*	*	LSD	13%
		ns	ns	ns	ns	ns	ns	ns	ns	ns	ns	ns	ns	ns	ns	ns	ns	BON	
			ns	ns	ns	ns	ns	ns	ns	*	ns	ns	*	*	**	**	*	LSD	18%
			ns	ns	ns	ns	ns	ns	ns	ns	ns	ns	ns	ns	ns	ns	ns	BON	
				ns	ns	ns	ns	ns	ns	ns	ns	ns	ns	ns	*	*	*	LSD	24%
				ns	ns	ns	ns	ns	ns	ns	ns	ns	ns	ns	ns	ns	ns	BON	
					ns	ns	ns	ns	ns	ns	ns	ns	ns	ns	*	*	*	LSD	29%
					ns	ns	ns	ns	ns	ns	ns	ns	ns	ns	ns	ns	ns	BON	
						ns	ns	ns	ns	ns	ns	ns	*	ns	*	*	*	LSD	34%
						ns	ns	ns	ns	ns	ns	ns	ns	ns	ns	ns	ns	BON	
							ns	ns	ns	ns	ns	ns	*	*	**	*	*	LSD	39%
							ns	ns	ns	ns	ns	ns	ns	ns	ns	ns	ns	BON	
								ns	ns	ns	ns	ns	*	ns	*	*	*	LSD	45%
								ns	ns	ns	ns	ns	ns	ns	ns	ns	ns	BON	
									ns	ns	ns	ns	ns	ns	*	*	*	LSD	50%
									ns	ns	ns	ns	ns	ns	ns	ns	ns	BON	
										ns	ns	ns	*	ns	*	*	ns	LSD	55%
										ns	ns	ns	ns	ns	ns	ns	ns	BON	
											ns	ns	ns	ns	ns	ns	ns	LSD	61%
											ns	ns	ns	ns	ns	ns	ns	BON	
												ns	ns	ns	ns	ns	ns	LSD	66%
												ns	ns	ns	ns	ns	ns	BON	
													*	ns	*	*	ns	LSD	71%
													ns	ns	ns	ns	ns	BON	
														ns	ns	ns	ns	LSD	76%
														ns	ns	ns	ns	BON	
															ns	ns	ns	LSD	82%
															ns	ns	ns	BON	
																ns	ns	LSD	87%
																ns	ns	BON	
																	ns	LSD	92%
																	ns	BON	

Table 8-30: *p*-values for post-hoc pair-wise comparisons of right peak ineffective force with (BON) and without (LSD: least significant difference) Bonferroni correction (*: $p < 0.05$, **: $p < 0.01$, ns: $p \geq 0.05$, %TTF: % time to failure)

8%	13%	18%	24%	29%	34%	39%	45%	50%	55%	61%	66%	71%	76%	82%	87%	92%	97%	←% TTF →	
ns	ns	ns	ns	*	*	*	**	**	*	**	**	**	**	**	**	**	ns	LSD	3%
ns	ns	ns	ns	ns	ns	ns	ns	ns	ns	ns	ns	ns	ns	ns	ns	ns	ns	BON	
	ns	ns	ns	ns	*	**	*	*	*	**	**	**	**	**	**	**	ns	LSD	8%
	ns	ns	ns	ns	ns	ns	ns	ns	ns	ns	ns	ns	ns	ns	ns	ns	ns	BON	
		ns	ns	*	*	*	**	**	*	**	**	**	**	**	**	**	ns	LSD	13%
		ns	ns	ns	ns	ns	ns	ns	ns	ns	ns	ns	ns	ns	ns	ns	ns	BON	
			ns	ns	ns	ns	ns	ns	ns	*	*	*	*	*	**	**	ns	LSD	18%
			ns	ns	ns	ns	ns	ns	ns	ns	ns	ns	ns	ns	ns	ns	ns	BON	
				ns	*	*	*	*	*	*	**	*	**	**	**	**	ns	LSD	24%
				ns	ns	ns	ns	ns	ns	ns	ns	ns	ns	ns	ns	ns	ns	BON	
					ns	ns	ns	*	ns	*	*	*	*	*	*	**	ns	LSD	29%
					ns	ns	ns	ns	ns	ns	ns	ns	ns	ns	ns	ns	ns	BON	
						ns	ns	ns	ns	ns	*	ns	*	*	*	**	ns	LSD	34%
						ns	ns	ns	ns	ns	ns	ns	ns	ns	ns	ns	ns	BON	
							ns	ns	ns	*	**	*	**	**	**	**	ns	LSD	39%
							ns	ns	ns	ns	ns	ns	ns	ns	ns	ns	ns	BON	
								ns	ns	ns	*	ns	*	*	**	**	ns	LSD	45%
								ns	ns	ns	ns	ns	ns	ns	ns	ns	ns	BON	
									ns	ns	ns	ns	ns	ns	*	*	ns	LSD	50%
									ns	ns	ns	ns	ns	ns	ns	ns	ns	BON	
										ns	ns	ns	*	*	*	*	ns	LSD	55%
										ns	ns	ns	ns	ns	ns	ns	ns	BON	
											ns	*	ns	*	*	*	ns	LSD	61%
											ns	ns	ns	ns	ns	ns	ns	BON	
												ns	ns	ns	*	*	ns	LSD	66%
												ns	ns	ns	ns	ns	ns	BON	
													ns	*	*	ns	ns	LSD	71%
													ns	ns	ns	ns	ns	BON	
														*	*	ns	ns	LSD	76%
														ns	ns	ns	ns	BON	
															ns	ns	ns	LSD	82%
															ns	ns	ns	BON	
																ns	ns	LSD	87%
																ns	ns	BON	
																	ns	LSD	92%
																	ns	BON	

Table 8-31: *p*-values for post-hoc pair-wise comparisons of crank angle at right peak ineffective force with and without (least significant difference) Bonferroni correction (*: $p < 0.05$, **: $p < 0.01$, ns: $p \geq 0.05$, %TTF: % time to failure)

8%	13%	18%	24%	29%	34%	39%	45%	50%	55%	61%	66%	71%	76%	82%	87%	92%	97%	←% TTF →	
ns	ns	ns	ns	ns	ns	ns	ns	ns	ns	*	ns	ns	*	*	*	ns	**	LSD	3%
ns	ns	ns	ns	ns	ns	ns	ns	ns	ns	ns	ns	ns	ns	ns	ns	ns	ns	BON	
	ns	ns	ns	ns	ns	ns	ns	ns	ns	*	ns	ns	ns	*	*	ns	**	LSD	8%
	ns	ns	ns	ns	ns	ns	ns	ns	ns	ns	ns	ns	ns	ns	ns	ns	ns	BON	
		ns	ns	ns	ns	ns	ns	ns	ns	ns	ns	ns	ns	ns	ns	ns	**	LSD	13%
		ns	ns	ns	ns	ns	ns	ns	ns	ns	ns	ns	ns	ns	ns	ns	ns	BON	
			ns	ns	ns	ns	ns	ns	ns	*	ns	ns	ns	*	ns	ns	**	LSD	18%
			ns	ns	ns	ns	ns	ns	ns	ns	ns	ns	ns	ns	ns	ns	ns	BON	
				ns	*	ns	ns	ns	ns	**	*	ns	*	*	*	*	**	LSD	24%
				ns	ns	ns	ns	ns	ns	ns	ns	ns	ns	ns	ns	ns	ns	BON	
					ns	ns	ns	ns	*	**	*	ns	*	*	*	*	**	LSD	29%
					ns	ns	ns	ns	ns	ns	ns	ns	ns	ns	ns	ns	ns	BON	
						ns	ns	ns	ns	ns	ns	ns	ns	ns	ns	ns	**	LSD	34%
						ns	ns	ns	ns	ns	ns	ns	ns	ns	ns	ns	ns	BON	
							ns	ns	ns	**	*	ns	*	*	*	*	**	LSD	39%
							ns	ns	ns	ns	ns	ns	ns	ns	ns	ns	ns	BON	
								ns	ns	ns	ns	ns	*	*	ns	**	LSD	45%	
								ns	ns	ns	ns	ns	ns	ns	ns	ns	ns	BON	
									ns	ns	ns	ns	ns	ns	ns	ns	**	LSD	50%
									ns	ns	ns	ns	ns	ns	ns	ns	ns	BON	
										ns	ns	ns	ns	ns	ns	ns	*	LSD	55%
										ns	ns	ns	ns	ns	ns	ns	ns	BON	
											ns	ns	ns	ns	ns	ns	*	LSD	61%
											ns	ns	ns	ns	ns	ns	ns	BON	
												ns	ns	ns	*	ns	*	LSD	66%
												ns	ns	ns	ns	ns	ns	BON	
													ns	ns	*	ns	*	LSD	71%
													ns	ns	ns	ns	ns	BON	
														ns	ns	ns	*	LSD	76%
														ns	ns	ns	ns	BON	
															ns	ns	ns	LSD	82%
															ns	ns	ns	BON	
																ns	ns	LSD	87%
																ns	ns	BON	
																	ns	LSD	92%
																	ns	BON	

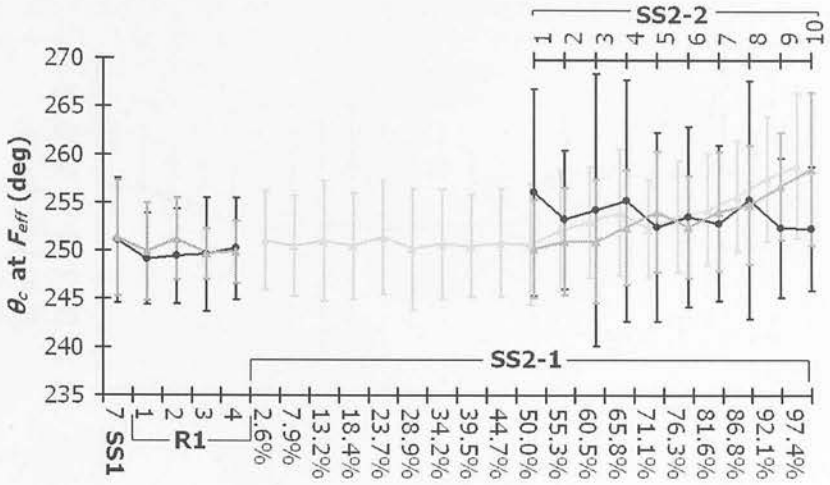

Figure 8-16: Group mean (±SD) crank angles (θ_c) at left peak effective force (F_{eff}) force (black diamonds: low fatigue trial, grey triangles: high fatigue trial, lower abscissa: SS1 & R1: minutes, SS2-1: % time to failure in high fatigue trial (lighter grey), upper abscissa: SS2-2: time windows)

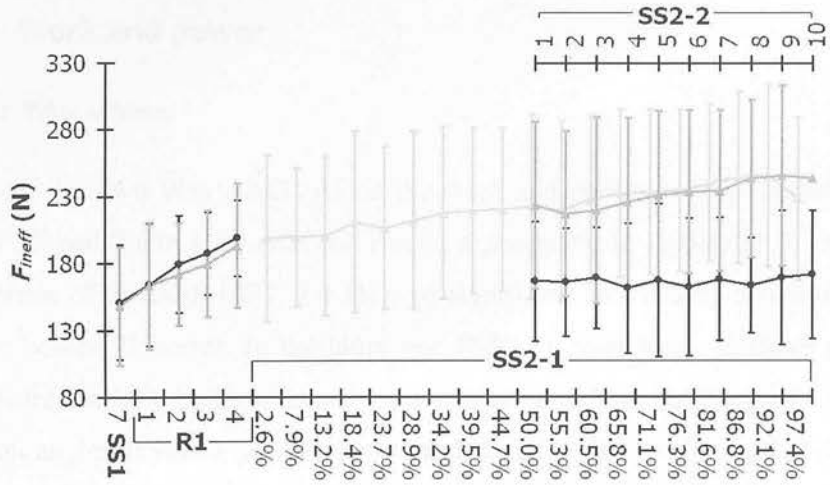

Figure 8-17: Group mean (±SD) right peak ineffective force (F_{ineff}) force (black diamonds: low fatigue trial, grey triangles: high fatigue trial, lower abscissa: SS1 & R1: minutes, SS2-1: % time to failure in high fatigue trial (lighter grey), upper abscissa: SS2-2: time windows)

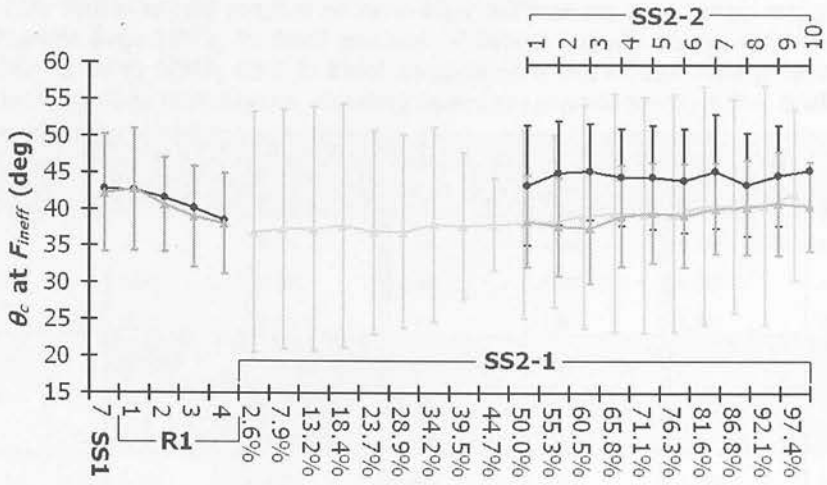

Figure 8-18: Group mean (±SD) crank angles (θ_c) at right peak ineffective force (F_{ineff}) force (black diamonds: low fatigue trial, grey triangles: high fatigue trial, lower abscissa: SS1 & R1: minutes, SS2-1: % time to failure in high fatigue trial (lighter grey), upper abscissa: SS2-2: time windows)

8.3.7: Work and power

8.3.7.1: Trial effects

Results of the Two-Way ANOVAs on the work and power data are summarised in Table 1 32 and Table 1 33 with full results again given in Appendix 3. During the initial phase of the trials (SS1, 7 + R1), no significant trial effects were observed in work or power. However, in the latter part (SS2-2), total work, positive work and power were found to be significant for both sides as well as right negative work and the crank angles at which positive work started and ended on the right pedal. In the case of total and right negative work and power effect sizes were large while they were moderate for the other variables.

8.3.7.2: Time effects

All of the work and power related variables were shown to possess significant time main effects in the initial part of the trial with the exception of the crank angle at which left positive work started with the effect sizes being large for total work and power. Conversely, in the case of the final part of the trial (SS2-2), the only variable to show significant time main effects was the crank angle at which positive work ended on the left pedal, where effect sizes were moderate.

Table 8-32: Summary of results of Two-Way ANOVA on sum total, negative and positive work data (SS1, 7: final minute of initial steady state, R1: ramp from 50% MMP to 95% MMP, SS2-2: final section of trials where power output was again constant, Int: interaction, shading indicates significance at P < 0.05)

			Total work		Positive work		Negative work	
			L	R	L	R	L	R
SS1,7 + R1	Trial	F	0.933	0.138	2.551	4.560	0.306	1.120
		p	0.362	0.720	0.149	0.065	0.595	0.321
		η_p^2	0.104	0.017	0.242	0.363	0.037	0.123
	Time	F	216.601	177.081	5.585	17.662	4.175	10.039
		p	<0.001	<0.001	0.035	0.001	0.029	0.002
		η_p^2	0.964	0.957	0.411	0.688	0.343	0.557
	Int	F	1.144	0.361	1.011	2.837	1.765	0.181
		p	0.354	0.835	0.417	0.070	0.160	0.947
		η_p^2	0.125	0.043	0.112	0.262	0.181	0.022
SS2-2	Trial	F	144.007	179.247	15.203	16.152	0.003	7.912
		p	<0.001	<0.001	0.005	0.004	0.961	0.023
		η_p^2	0.947	0.957	0.655	0.669	<0.001	0.497
	Time	F	1.302	1.492	1.021	0.670	0.917	1.006
		p	0.251	0.168	0.432	0.733	0.515	0.443
		η_p^2	0.140	0.157	0.113	0.077	0.103	0.112
	Int	F	0.419	1.946	0.777	0.535	1.503	0.697
		p	0.921	0.059	0.638	0.844	0.163	0.710
		η_p^2	0.050	0.196	0.089	0.063	0.158	0.080

8.3.7.3: Time and trial interaction effects

The only significant time and trial interaction effect shown anywhere in the trials was that of the crank angle at which positive work started on the left pedal in SS2-2 (Figure 8-19) where a moderate effect was shown. Examination of the trends of the data showed a clear trend towards positive work starting earlier in the first 50% of the trial where a marked reversal of this trend occurred. This tendency for positive work to start later in the crank cycle continued throughout the trial but at a lower rate after 71% of time to failure. *Post hoc* analyses (Table 1 34) showed significant time effects within each trial for both left and right pedals but that between trial differences were only apparent in the second time window.

Table 8-33: Summary of results of Two-Way ANOVA on the crank angles at which positive work started and ended and power data (SS1, 7: final minute of initial steady state, R1: ramp from 50% MMP to 95% MMP, SS2-2: final section of trials where power output was again constant, Int: interaction, shading indicates significance at P < 0.05)

			θc start +ve work		θc end +ve work		Power	
			L	R	L	R	L	R
SS1,7 + R1	Trial	F	0.048	0.356	1.976	1.720	0.897	0.113
		p	0.833	0.567	0.197	0.226	0.371	0.746
		η_p^2	0.006	0.043	0.198	0.177	0.101	0.014
	Time	F	3.390	16.577	5.614	9.498	94.375	94.610
		p	0.069	<0.001	0.031	0.007	<0.001	<0.001
		η_p^2	0.298	0.674	0.412	0.543	0.922	0.922
	Int	F	0.641	1.468	1.596	0.812	1.016	0.693
		p	0.637	0.235	0.199	0.527	0.414	0.602
		η_p^2	0.074	0.155	0.166	0.092	0.113	0.080
SS2-2	Trial	F	1.281	6.579	0.440	10.413	169.775	148.891
		p	0.290	0.033	0.526	0.012	<0.001	<0.001
		η_p^2	0.138	0.451	0.052	0.566	0.955	0.949
	Time	F	2.606	1.164	3.098	1.325	1.218	1.752
		p	0.051	0.331	0.034	0.239	0.298	0.093
		η_p^2	0.246	0.127	0.279	0.142	0.132	0.180
	Int	F	4.864	1.410	0.898	1.091	1.681	1.668
		p	0.012	0.200	0.532	0.380	0.109	0.113
		η_p^2	0.378	0.150	0.101	0.120	0.174	0.173

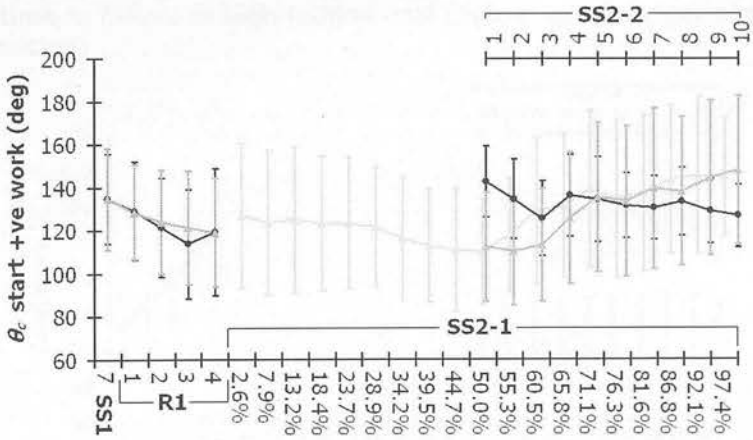

Figure 8-19: Group mean (±SD) crank angles (θ_c) at which positive work started on the left pedal (black diamonds: low fatigue trial, grey triangles: high fatigue trial, lower abscissa: SS1 & R1: minutes, SS2-1: % time to failure in high fatigue trial (lighter grey), upper abscissa: SS2-2: time windows)

Table 8-34: Summary of post-hoc analyses of crank angle where positive work started for the left leg (TW: Time window)

Within trial by time

	Low	High
F	2.611	4.100
P	0.019	0.030
η_p^2	0.246	0.339

Between trial

TW	*1*	*2*	*3*	*4*	*5*	*6*	*7*	*8*	*9*	*10*
F	4.795	5.732	2.921	2.861	1.038	0.615	0.339	0.536	0.065	<0.01
P	0.06	0.044	0.126	0.129	0.338	0.455	0.576	0.485	0.806	0.982
η_p^2	0.375	0.417	0.267	0.263	0.115	0.071	0.041	0.063	0.008	<0.001

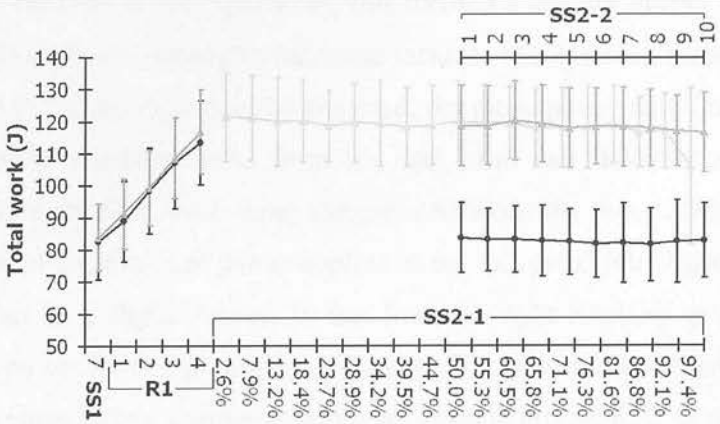

Figure 8-20: Group mean (±SD) sum work on the left pedal (black diamonds: low fatigue trial, grey triangles: high fatigue trial, lower abscissa: SS1 & R1: minutes, SS2-1: % time to failure in high fatigue trial (lighter grey), upper abscissa: SS2-2: time windows)

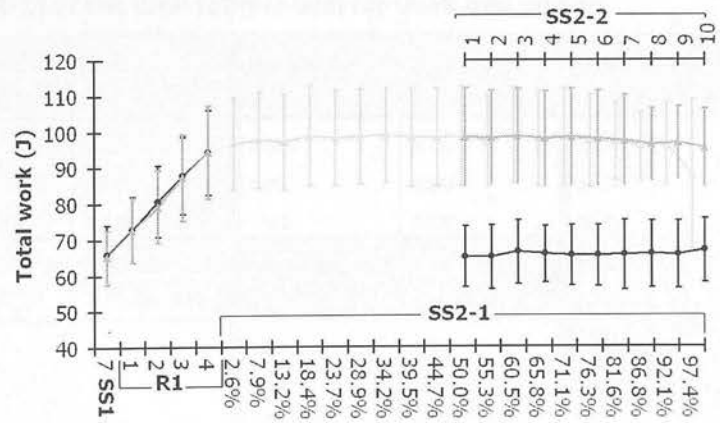

Figure 8-21: Group mean (±SD) sum work on the right pedal (black diamonds: low fatigue trial, grey triangles: high fatigue trial, lower abscissa: SS1 & R1: minutes, SS2-1: % time to failure in high fatigue trial (lighter grey), upper abscissa: SS2-2: time windows)

8.3.8: Time effects in high-fatigue trial

Analysis of the entire final steady state section of the high fatigue trial (SS2-1) (Table 1 35), shows significant time effects in total work (left: Figure 8-20, right: Figure 8-21) and power for both pedals (left: Figure 8-22, right: Figure 8-23) and for the crank angle at which positive work started at the left pedal (Figure 8-19). In all cases, effect sizes were moderate. In addition to the changes already discussed in the crank angle at which positive work started on the left pedal, trends were also apparent in the other variables. Both left and right total work showed progressive declines in the latter half of the trial with marked drops in the final segment. However, in the case of the right work, this increased slightly during the first 50% whilst the left declined, although a moderate increase was apparent between 39% and 50% of time to failure. As would be expected, the mean power data from the pedals followed similar trends to those from the data from the SRM Power Measuring Crankset, although there were some variances between the two pedals. For around the first 24% of the trial, the power applied at the left pedal fell slightly. However, this was offset by a slight increase in that from the right resulting in the relatively constant net power for this phase. Subsequent to this, power at both pedals remained relatively constant before starting a downward trend at around 82% of time to failure and dropping markedly in the final 5%.

Table 8-35: Summary of One-Way ANOVAs on the complete final steady state section (SS2-1) of the high fatigue trial for work and power

	Total work		**Positive work**		**Negative work**	
	L	R	L	R	L	R
F	3.045	4.23	0.756	1.175	0.835	1.584
P	0.046	0.033	0.747	0.289	0.656	0.071
η_p^2	0.276	0.346	0.086	0.128	0.095	0.165
	Start positive work		**End positive work**		**Power**	
	L	R	L	R	L	R
F	2.995	0.898	1.291	0.202	3.745	3.783
P	0.047	0.582	0.567	0.918	0.027	0.037
η_p^2	0.272	0.101	0.139	0.066	0.319	0.321

Although no significant differences were found with the use of the Bonferroni method for the *post hoc* analyses, without it, multiple significant differences between

the final time window and those preceding it were shown for the right total work (Table 1 37), although no clear trends emerged for the left (Table 1 36). For the crank angle at which positive work started on the left pedal (Table 1 38), concentrations of significant differences occurred around 34% to 39% of time to failure and the latter half of the trial and around 50% of time to failure and the final 23% of the trial. For power, the majority of significant differences occurred relative to the final 3% of the trial (left: Table 1 39, right: Table 1 40).

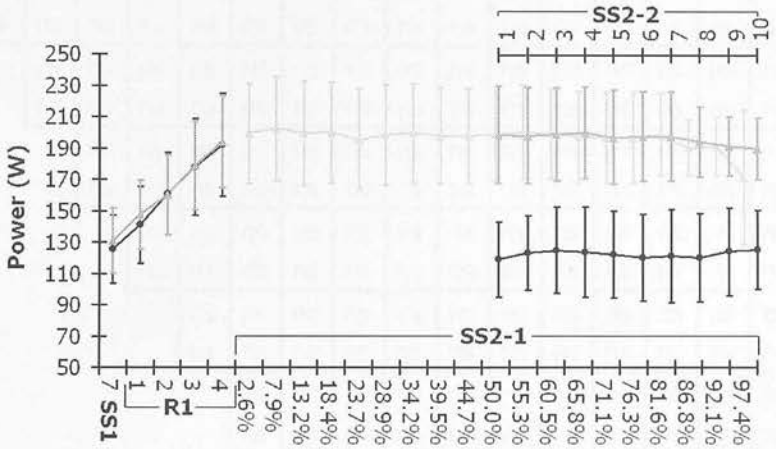

Figure 8-22: Group mean (±SD) mean power on the left pedal (black diamonds: low fatigue trial, grey triangles: high fatigue trial, lower abscissa: SS1 & R1: minutes, SS2-1: % time to failure in high fatigue trial (lighter grey), upper abscissa: SS2-2: time windows)

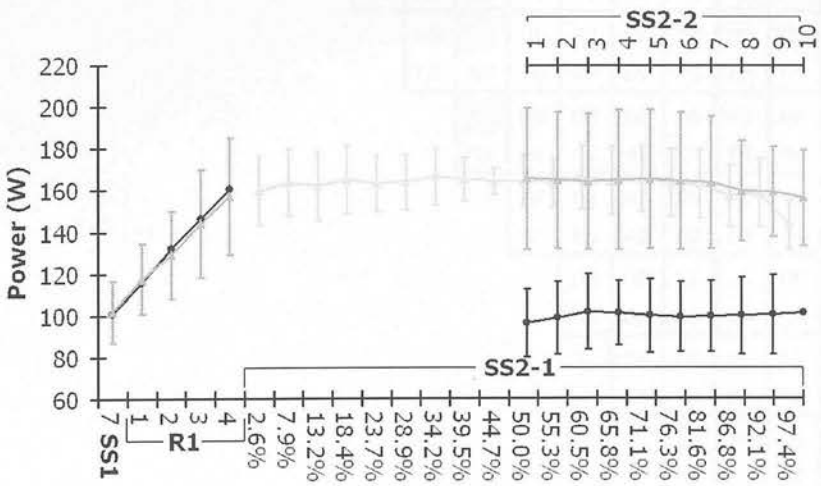

Figure 8-23: Group mean (±SD) mean power on the right pedal (black diamonds: low fatigue trial, grey triangles: high fatigue trial, lower abscissa: SS1 & R1: minutes, SS2-1: % time to failure in high fatigue trial (lighter grey), upper abscissa: SS2-2: time windows)

Table 8-36: p-values for post-hoc pair-wise comparisons of total work on the left pedal with and without (least significant difference) Bonferroni correction (*: $p < 0.05$, **: $p < 0.01$, ns: $p \geq 0.05$, %TTF: % time to failure)

8%	13%	18%	24%	29%	34%	39%	45%	50%	55%	61%	66%	71%	76%	82%	87%	92%	97%	←% TTF →	
ns	ns	ns	ns	ns	ns	ns	ns	ns	ns	ns	ns	ns	ns	ns	ns	ns	ns	LSD	3%
ns	ns	ns	ns	ns	ns	ns	ns	ns	ns	ns	ns	ns	ns	ns	ns	ns	ns	BON	
	ns	ns	ns	ns	ns	*	ns	ns	ns	ns	ns	ns	ns	ns	ns	ns	*	LSD	8%
	ns	ns	ns	ns	ns	ns	ns	ns	ns	ns	ns	ns	ns	ns	ns	ns	ns	BON	
		ns	ns	ns	ns	ns	ns	ns	ns	ns	ns	ns	ns	ns	ns	ns	ns	LSD	13%
		ns	ns	ns	ns	ns	ns	ns	ns	ns	ns	ns	ns	ns	ns	ns	ns	BON	
			ns	ns	ns	ns	ns	ns	ns	ns	ns	ns	ns	ns	ns	ns	ns	LSD	18%
			ns	ns	ns	ns	ns	ns	ns	ns	ns	ns	ns	ns	ns	ns	ns	BON	
				ns	ns	ns	ns	ns	ns	ns	ns	ns	ns	ns	ns	ns	ns	LSD	24%
				ns	ns	ns	ns	ns	ns	ns	ns	ns	ns	ns	ns	ns	ns	BON	
					ns	ns	ns	ns	ns	ns	ns	ns	ns	ns	ns	ns	ns	LSD	29%
					ns	ns	ns	ns	ns	ns	ns	ns	ns	ns	ns	ns	ns	BON	
						ns	ns	ns	ns	ns	ns	ns	ns	ns	ns	ns	ns	LSD	34%
						ns	ns	ns	ns	ns	ns	ns	ns	ns	ns	ns	ns	BON	
							ns	ns	ns	ns	ns	ns	ns	ns	ns	ns	ns	LSD	39%
							ns	ns	ns	ns	ns	ns	ns	ns	ns	ns	ns	BON	
								ns	ns	ns	ns	ns	ns	ns	ns	ns	ns	LSD	45%
								ns	ns	ns	ns	ns	ns	ns	ns	ns	ns	BON	
									ns	ns	ns	ns	ns	ns	ns	ns	*	LSD	50%
									ns	ns	ns	ns	ns	ns	ns	ns	ns	BON	
										ns	*	ns	ns	ns	ns	ns	ns	LSD	55%
										ns	ns	ns	ns	ns	ns	ns	ns	BON	
											*	ns	ns	ns	ns	ns	ns	LSD	61%
											ns	ns	ns	ns	ns	ns	ns	BON	
												ns	ns	ns	ns	ns	ns	LSD	66%
												ns	ns	ns	ns	ns	ns	BON	
													ns	ns	ns	ns	ns	LSD	71%
													ns	ns	ns	ns	ns	BON	
														ns	ns	ns	ns	LSD	76%
														ns	ns	ns	ns	BON	
															**	*	ns	LSD	82%
															ns	ns	ns	BON	
																ns	ns	LSD	87%
																ns	ns	BON	
																	ns	LSD	92%
																	ns	BON	

Table 8-37: p-values for post-hoc pair-wise comparisons of total work on the right pedal with and without (least significant difference) Bonferroni correction (*: $p < 0.05$, **: $p < 0.01$, ns: $p \geq 0.05$, %TTF: % time to failure)

8%	13%	18%	24%	29%	34%	39%	45%	50%	55%	61%	66%	71%	76%	82%	87%	92%	97%	←% TTF →	
ns	ns	*	ns	ns	*	ns	ns	ns	ns	*	ns	ns	ns	ns	ns	ns	ns	LSD	3%
ns	ns	ns	ns	ns	ns	ns	ns	ns	ns	ns	ns	ns	ns	ns	ns	ns	ns	BON	
	ns	ns	ns	ns	ns	ns	ns	ns	ns	ns	ns	ns	ns	ns	ns	ns	*	LSD	8%
	ns	ns	ns	ns	ns	ns	ns	ns	ns	ns	ns	ns	ns	ns	ns	ns	ns	BON	
		**	ns	ns	**	ns	ns	*	ns	ns	ns	ns	ns	ns	ns	ns	ns	LSD	13%
		ns	ns	ns	ns	ns	ns	ns	ns	ns	ns	ns	ns	ns	ns	ns	ns	BON	
			ns	ns	ns	ns	ns	ns	ns	ns	ns	ns	ns	ns	ns	ns	*	LSD	18%
			ns	ns	ns	ns	ns	ns	ns	ns	ns	ns	ns	ns	ns	ns	ns	BON	
				ns	ns	ns	ns	ns	ns	ns	ns	ns	ns	ns	ns	ns	*	LSD	24%
				ns	ns	ns	ns	ns	ns	ns	ns	ns	ns	ns	ns	ns	ns	BON	
					ns	ns	ns	ns	ns	ns	ns	ns	**	ns	ns	ns	*	LSD	29%
					ns	ns	ns	ns	ns	ns	ns	ns	ns	ns	ns	ns	ns	BON	
						ns	ns	ns	ns	ns	ns	ns	*	ns	ns	*	*	LSD	34%
						ns	ns	ns	ns	ns	ns	ns	ns	ns	ns	ns	ns	BON	
							ns	ns	ns	ns	ns	ns	ns	ns	ns	ns	*	LSD	39%
							ns	ns	ns	ns	ns	ns	ns	ns	ns	ns	ns	BON	
								ns	ns	ns	ns	ns	ns	ns	ns	ns	*	LSD	45%
								ns	ns	ns	ns	ns	ns	ns	ns	ns	ns	BON	
									ns	ns	ns	ns	ns	ns	ns	ns	*	LSD	50%
									ns	ns	ns	ns	ns	ns	ns	ns	ns	BON	
										ns	ns	ns	ns	ns	ns	ns	ns	LSD	55%
										ns	ns	ns	ns	ns	ns	ns	ns	BON	
											ns	ns	ns	ns	ns	ns	*	LSD	61%
											ns	ns	ns	ns	ns	ns	ns	BON	
												ns	ns	ns	ns	ns	ns	LSD	66%
												ns	ns	ns	ns	ns	ns	BON	
													ns	ns	ns	ns	*	LSD	71%
													ns	ns	ns	ns	ns	BON	
														ns	ns	ns	ns	LSD	76%
														ns	ns	ns	ns	BON	
															ns	ns	ns	LSD	82%
															ns	ns	ns	BON	
																ns	ns	LSD	87%
																ns	ns	BON	
																	ns	LSD	92%
																	ns	BON	

Table 8-38: p-values for post-hoc pair-wise comparisons of the crank angle at which positive work started on the left pedal with and without (least significant difference) Bonferroni correction (*: $p < 0.05$, **: $p < 0.01$, ns: $p \geq 0.05$, %TTF: % time to failure)

8%	13%	18%	24%	29%	34%	39%	45%	50%	55%	61%	66%	71%	76%	82%	87%	92%	97%	←% TTF→	
ns	ns	ns	ns	ns	ns	ns	ns	ns	ns	ns	ns	ns	ns	ns	ns	ns	ns	LSD	3%
ns	ns	ns	ns	ns	ns	ns	ns	ns	ns	ns	ns	ns	ns	ns	ns	ns	ns	BON	
	ns	ns	ns	ns	ns	ns	ns	ns	ns	*	*	ns	ns	ns	ns	ns	ns	LSD	8%
	ns	ns	ns	ns	ns	ns	ns	ns	ns	ns	ns	ns	ns	ns	ns	ns	ns	BON	
		ns	ns	ns	ns	ns	ns	ns	ns	ns	ns	ns	ns	ns	ns	ns	ns	LSD	13%
		ns	ns	ns	ns	ns	ns	ns	ns	ns	ns	ns	ns	ns	ns	ns	ns	BON	
			ns	ns	ns	ns	ns	ns	ns	ns	*	ns	ns	ns	ns	ns	ns	LSD	18%
			ns	ns	ns	ns	ns	ns	ns	ns	ns	ns	ns	ns	ns	ns	ns	BON	
				ns	*	*	ns	ns	ns	ns	*	ns	ns	ns	ns	ns	ns	LSD	24%
				ns	ns	ns	ns	ns	ns	ns	ns	ns	ns	ns	ns	ns	ns	BON	
					ns	*	ns	ns	ns	ns	ns	ns	ns	ns	ns	ns	ns	LSD	29%
					ns	ns	ns	ns	ns	ns	ns	ns	ns	ns	ns	ns	ns	BON	
						ns	ns	ns	ns	*	**	*	ns	ns	*	*	*	LSD	34%
						ns	ns	ns	ns	ns	ns	ns	ns	ns	ns	ns	ns	BON	
							ns	ns	ns	*	**	*	*	*	**	*	*	LSD	39%
							ns	ns	ns	ns	ns	ns	ns	ns	ns	ns	ns	BON	
								ns	ns	ns	ns	ns	ns	ns	ns	ns	*	LSD	45%
								ns	ns	ns	ns	ns	ns	ns	ns	ns	ns	BON	
									ns	ns	ns	ns	ns	ns	*	*	*	LSD	50%
									ns	ns	ns	ns	ns	ns	ns	ns	ns	BON	
										ns	ns	ns	ns	ns	ns	ns	*	LSD	55%
										ns	ns	ns	ns	ns	ns	ns	ns	BON	
											ns	ns	ns	ns	ns	ns	ns	LSD	61%
											ns	ns	ns	ns	ns	ns	ns	BON	
												ns	ns	ns	ns	ns	ns	LSD	66%
												ns	ns	ns	ns	ns	ns	BON	
													ns	ns	ns	ns	ns	LSD	71%
													ns	ns	ns	ns	ns	BON	
														ns	ns	ns	ns	LSD	76%
														ns	ns	ns	ns	BON	
															ns	ns	ns	LSD	82%
															ns	ns	ns	BON	
																ns	ns	LSD	87%
																ns	ns	BON	
																	ns	LSD	92%
																	ns	BON	

Table 8-39: p-values for post-hoc pair-wise comparisons of mean power at the left pedal with and without (least significant difference) Bonferroni correction (*: $p < 0.05$, **: $p < 0.01$, ns: $p \geq 0.05$, %TTF: % time to failure)

8%	13%	18%	24%	29%	34%	39%	45%	50%	55%	61%	66%	71%	76%	82%	87%	92%	97%	←% TTF→	
*	ns	ns	ns	ns	ns	ns	ns	ns	ns	ns	ns	ns	ns	ns	ns	ns	*	LSD	3%
ns	ns	ns	ns	ns	ns	ns	ns	ns	ns	ns	ns	ns	ns	ns	ns	ns	ns	BON	
	ns	ns	*	ns	ns	ns	ns	ns	ns	ns	ns	ns	ns	ns	ns	ns	*	LSD	8%
	ns	ns	ns	ns	ns	ns	ns	ns	ns	ns	ns	ns	ns	ns	ns	ns	ns	BON	
		ns	*	ns	ns	ns	ns	ns	ns	ns	ns	ns	ns	ns	ns	ns	*	LSD	13%
		ns	ns	ns	ns	ns	ns	ns	ns	ns	ns	ns	ns	ns	ns	ns	ns	BON	
			*	ns	ns	ns	ns	ns	ns	ns	ns	ns	ns	ns	ns	ns	*	LSD	18%
			ns	ns	ns	ns	ns	ns	ns	ns	ns	ns	ns	ns	ns	ns	ns	BON	
				ns	*	ns	ns	ns	ns	ns	ns	ns	ns	ns	ns	ns	ns	LSD	24%
				ns	ns	ns	ns	ns	ns	ns	ns	ns	ns	ns	ns	ns	ns	BON	
					ns	ns	ns	ns	ns	ns	ns	ns	ns	ns	ns	ns	*	LSD	29%
					ns	ns	ns	ns	ns	ns	ns	ns	ns	ns	ns	ns	ns	BON	
						ns	ns	ns	ns	ns	ns	ns	ns	ns	ns	ns	*	LSD	34%
						ns	ns	ns	ns	ns	ns	ns	ns	ns	ns	ns	ns	BON	
							ns	ns	ns	ns	ns	ns	ns	ns	ns	ns	*	LSD	39%
							ns	ns	ns	ns	ns	ns	ns	ns	ns	ns	ns	BON	
								ns	ns	ns	ns	ns	ns	ns	ns	ns	*	LSD	45%
								ns	ns	ns	ns	ns	ns	ns	ns	ns	ns	BON	
									ns	ns	ns	ns	ns	ns	ns	ns	*	LSD	50%
									ns	ns	ns	ns	ns	ns	ns	ns	ns	BON	
										ns	**	*	ns	ns	ns	ns	*	LSD	55%
										ns	ns	ns	ns	ns	ns	ns	ns	BON	
											ns	ns	ns	ns	ns	ns	*	LSD	61%
											ns	ns	ns	ns	ns	ns	ns	BON	
												ns	ns	ns	ns	ns	*	LSD	66%
												ns	ns	ns	ns	ns	ns	BON	
													ns	ns	ns	ns	*	LSD	71%
													ns	ns	ns	ns	ns	BON	
														ns	ns	ns	*	LSD	76%
														ns	ns	ns	ns	BON	
															ns	ns	*	LSD	82%
															ns	ns	ns	BON	
																ns	ns	LSD	87%
																ns	ns	BON	
																	ns	LSD	92%
																	ns	BON	

Table 8-40: p-values for post-hoc pair-wise comparisons of mean power at the right pedal with and without (least significant difference) Bonferroni correction (*: $p < 0.05$, **: $p < 0.01$, ns: $p \geq 0.05$, %TTF: % time to failure)

8%	13%	18%	24%	29%	34%	39%	45%	50%	55%	61%	66%	71%	76%	82%	87%	92%	97%	←% TTF →	
*	ns	*	ns	ns	*	ns	ns	ns	ns	*	*	**	ns	ns	ns	ns	ns	LSD	3%
ns	ns	ns	ns	ns	ns	ns	ns	ns	ns	ns	ns	ns	ns	ns	ns	ns	ns	BON	
	ns	ns	ns	ns	ns	ns	ns	ns	ns	ns	ns	ns	ns	ns	ns	ns	*	LSD	8%
	ns	ns	ns	ns	ns	ns	ns	ns	ns	ns	ns	ns	ns	ns	ns	ns	ns	BON	
		*	ns	ns	*	ns	ns	*	ns	ns	ns	ns	ns	ns	ns	ns	ns	LSD	13%
		ns	ns	ns	ns	ns	ns	ns	ns	ns	ns	ns	ns	ns	ns	ns	ns	BON	
			ns	ns	ns	ns	ns	ns	ns	ns	ns	ns	ns	ns	ns	ns	*	LSD	18%
			ns	ns	ns	ns	ns	ns	ns	ns	ns	ns	ns	ns	ns	ns	ns	BON	
				ns	*	ns	ns	ns	ns	ns	ns	ns	ns	ns	ns	ns	*	LSD	24%
				ns	ns	ns	ns	ns	ns	ns	ns	ns	ns	ns	ns	ns	ns	BON	
					ns	ns	ns	ns	ns	ns	ns	ns	ns	ns	ns	ns	*	LSD	29%
					ns	ns	ns	ns	ns	ns	ns	ns	ns	ns	ns	ns	ns	BON	
						ns	ns	ns	*	ns	ns	ns	**	ns	ns	ns	*	LSD	34%
						ns	ns	ns	ns	ns	ns	ns	ns	ns	ns	ns	ns	BON	
							ns	ns	ns	ns	ns	ns	ns	ns	ns	ns	*	LSD	39%
							ns	ns	ns	ns	ns	ns	ns	ns	ns	ns	ns	BON	
								ns	ns	ns	ns	ns	ns	ns	ns	ns	*	LSD	45%
								ns	ns	ns	ns	ns	ns	ns	ns	ns	ns	BON	
									ns	ns	ns	ns	ns	ns	ns	ns	*	LSD	50%
									ns	ns	ns	ns	ns	ns	ns	ns	ns	BON	
										ns	ns	ns	ns	ns	ns	ns	*	LSD	55%
										ns	ns	ns	ns	ns	ns	ns	ns	BON	
											ns	ns	ns	ns	ns	ns	*	LSD	61%
											ns	ns	ns	ns	ns	ns	ns	BON	
												ns	ns	ns	ns	ns	*	LSD	66%
												ns	ns	ns	ns	ns	ns	BON	
													*	ns	ns	ns	*	LSD	71%
													ns	ns	ns	ns	ns	BON	
														ns	ns	ns	*	LSD	76%
														ns	ns	ns	ns	BON	
															ns	ns	*	LSD	82%
															ns	ns	ns	BON	
																ns	ns	LSD	87%
																ns	ns	BON	
																	ns	LSD	92%
																	ns	BON	

8.3.9: Instantaneous index of effectiveness and crank velocity

8.3.9.1: Trial effects

Trial effects were only apparent in the right Instantaneous Index of Effectiveness (IIE) and crank velocity in the latter part of the trial (SS2-2) (Table 8-41) although the effect size was large in both cases.

8.3.9.2: Time effects

All three variables showed significant time effects in the initial phase of the two trials (SS1, 7 +R1) as did IIE for both right and left pedals in the latter part with moderate effect sizes in all cases.

8.3.9.3: Time and trial interaction effects

No time and trial interactions were found to be significant in SS1, 7 +R1, however, those for IIE for both pedals were in the final section (left: Figure 8-24, right: Figure 8-25) although the effect sizes were only moderate. Examination of the graphs revealed clear downward trends throughout this section of the high fatigue trials for both the left and right pedals. This trend increased in the case of the right pedal around window 7, although any such change was less apparent for the left. Highly pronounced trends were also shown in the low fatigue trial with rapid increases occurring at both pedals for the first three time windows followed by a marked drop in the index at the fourth. Beyond this however, the trends were opposite for the two pedals with the left having increased for the remainder of the trial whilst the right decreased. *Post hoc* analyses of these interactions (Table 1 42) showed significant time effects in both the low and high fatigue trials for both pedals. Analyses between trials indicate significant trial effects at time windows 1, 2 and 4 in the case of the left pedal and for all windows with the exception of 3 for the right.

Table 8-41: Summary of results of Two-Way ANOVA on Instantaneous Index of Effectiveness (IIE) and crank velocity (CV) (SS1, 7: final minute of initial steady state, R1: ramp from 50% MMP to 95% MMP, SS2-2: final section of trials where power output was again constant, Int: interaction, shading indicates significance at P < 0.05)

			IIE		CV
			L	R	
SS1,7 + R1	Trial	F	0.165	1.287	0.007
		P	0.695	0.289	0.933
		η_p^2	0.020	0.139	<0.001
	Time	F	9.214	15.485	18.608
		P	0.010	<0.001	<0.001
		η_p^2	0.535	0.659	0.699
	Int	F	2.318	0.732	1.423
		P	0.123	0.577	0.249
		η_p^2	0.225	0.084	0.151
SS2-2	Trial	F	4.344	25.805	32.639
		P	0.071	<0.001	<0.001
		η_p^2	0.352	0.763	0.803
	Time	F	2.215	4.139	1.023
		P	0.047	0.011	0.430
		η_p^2	0.217	0.341	0.113
	Int	F	3.813	2.457	2.261
		P	0.021	0.027	0.121
		η_p^2	0.323	0.235	0.220

Table 8-42: Summary of post-hoc analyses of Instantaneous Index of Effectiveness (IIE) at the right and left pedals (TW: time winidow)

Within trial by time

	Left		Right	
	Low	High	Low	High
F	2.373	3.365	2.637	4.495
P	0.027	0.046	0.018	0.008
η_p^2	0.229	0.296	0.248	0.360

Between trial

TW		1	2	3	4	5	6	7	8	9	10
L	F	31.306	16.576	2.506	5.698	1.605	1.345	1.442	1.860	0.021	0.032
	P	<0.001	0.004	0.152	0.044	0.241	0.280	0.264	0.210	0.889	0.863
	η_p^2	0.796	0.674	0.239	0.416	0.167	0.144	0.153	0.189	0.003	0.004
R	F	54.199	27.130	4.936	10.693	11.790	23.216	14.759	13.857	20.990	10.575
	P	<0.001	<0.001	0.057	0.011	0.009	0.001	0.005	0.006	0.002	0.012
	η_p^2	0.871	0.772	0.382	0.572	0.596	0.744	0.648	0.634	0.724	0.569

8.3.10: Time effects in high-fatigue trial

Significant time effects were shown across the entire final steady state section of the high fatigue trial (SS2-1) (Table 1 43) only in the case of right Instantaneous Index of Effectiveness (Figure 8-25) where the effect size was moderate. In addition to the downward trend already discussed in the latter part of the high fatigue trial, a trend for the index to increase for around the first 34% of the section was also shown, although with a decrease around 18%. The increase rate of decline previously observed around window 7 in SS2-2 was also shown around 82% of time to failure, which would be approximately concurrent. Similar trends were also observed for the left pedal although these did not achieve significance in this part of the analysis (see Appendix 4). Pairwise comparisons of these results (Table 1 44) indicated that the significant effects largely occurred around the final two time windows with significant effects being shown in some cases even with the use of the Bonferroni corrections. Groups of significant effects also appeared between around 34% and 39% of time to failure and the final third of the trial.

Table 8-43: Summary of One-Way ANOVAs on the complete final steady state section (SS2-1) of the high fatigue trial for Instantaneous Index of Effectiveness (IIE) and crank velocity (CV)

	IIE		CV
	L	R	
F	1.623	3.472	1.486
P	0.062	0.022	0.103
η_p^2	0.169	0.303	0.157

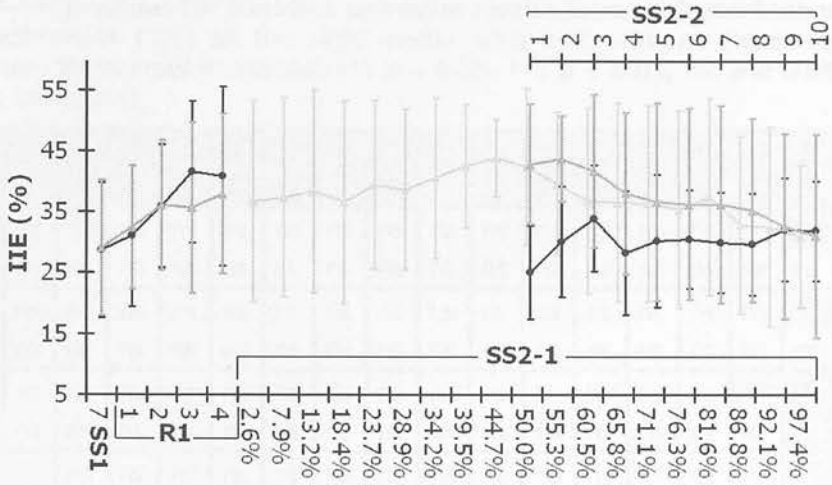

Figure 8-24: Group mean (±SD) left Instantaneous Index of Effectiveness (IIE). (black diamonds: low fatigue trial, grey triangles: high fatigue trial, lower abscissa: SS1 & R1: minutes, SS2-1: % time to failure in high fatigue trial (lighter grey), upper abscissa: SS2-2: time windows)

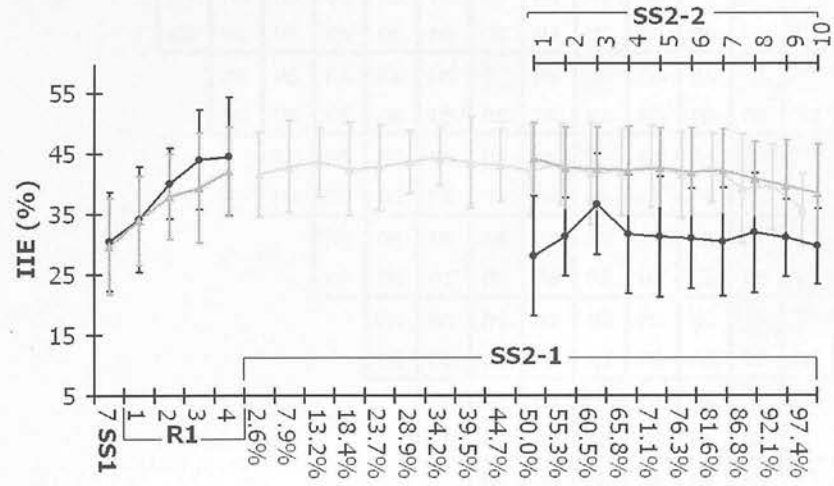

Figure 8-25: Group mean (±SD) right Instantaneous Index of Effectiveness (IIE). (black diamonds: low fatigue trial, grey triangles: high fatigue trial, lower abscissa: SS1 & R1: minutes, SS2-1: % time to failure in high fatigue trial (lighter grey), upper abscissa: SS2-2: time windows)

Table 8-44: p-values for post-hoc pair-wise comparisons of Instantaneous Index of Effectiveness (IIE) at the right pedal with and without (least significant difference) Bonferroni correction (*: $p < 0.05$, **: $p < 0.01$, ns: $p \geq 0.05$, %TTF: % time to failure)

8%	13%	18%	24%	29%	34%	39%	45%	50%	55%	61%	66%	71%	76%	82%	87%	92%	97%	←% TTF	↓
ns	ns	ns	*	ns	ns	ns	ns	ns	ns	ns	ns	ns	ns	ns	ns	ns	*	LSD	3%
ns	ns	ns	ns	ns	ns	ns	ns	ns	ns	ns	ns	ns	ns	ns	ns	ns	ns	BON	
	ns	ns	ns	ns	ns	ns	ns	ns	ns	ns	ns	ns	ns	ns	ns	ns	**	LSD	8%
	ns	ns	ns	ns	ns	ns	ns	ns	ns	ns	ns	ns	ns	ns	ns	ns	ns	BON	
		ns	ns	ns	ns	ns	ns	ns	ns	ns	ns	ns	ns	ns	ns	**	**	LSD	13%
		ns	ns	ns	ns	ns	ns	ns	ns	ns	ns	ns	ns	ns	ns	ns	*	BON	
			ns	ns	ns	ns	ns	ns	ns	ns	ns	ns	ns	ns	ns	ns	**	LSD	18%
			ns	ns	ns	ns	ns	ns	ns	ns	ns	ns	ns	ns	ns	ns	ns	BON	
				ns	ns	ns	ns	ns	ns	ns	ns	ns	ns	ns	ns	ns	*	LSD	24%
				ns	ns	ns	ns	ns	ns	ns	ns	ns	ns	ns	ns	ns	ns	BON	
					ns	ns	ns	ns	ns	ns	ns	ns	ns	ns	ns	**	**	LSD	29%
					ns	ns	ns	ns	ns	ns	ns	ns	ns	ns	ns	ns	*	BON	
						ns	ns	ns	ns	ns	*	ns	*	ns	ns	**	**	LSD	34%
						ns	ns	ns	ns	ns	ns	ns	ns	ns	ns	ns	ns	BON	
							ns	ns	ns	ns	ns	ns	*	ns	ns	*	**	LSD	39%
							ns	ns	ns	ns	ns	ns	ns	ns	ns	ns	ns	BON	
								ns	ns	ns	ns	ns	ns	ns	ns	**	**	LSD	45%
								ns	ns	ns	ns	ns	ns	ns	ns	ns	*	BON	
									ns	ns	ns	ns	ns	ns	ns	*	**	LSD	50%
									ns	ns	ns	ns	ns	ns	ns	ns	ns	BON	
										ns	ns	ns	*	ns	ns	*	**	LSD	55%
										ns	ns	ns	ns	ns	ns	ns	ns	BON	
											ns	ns	ns	ns	ns	ns	**	LSD	61%
											ns	ns	ns	ns	ns	ns	ns	BON	
												ns	ns	ns	ns	*	**	LSD	66%
												ns	ns	ns	ns	ns	ns	BON	
													ns	ns	ns	**	**	LSD	71%
													ns	ns	ns	ns	ns	BON	
														ns	ns	ns	**	LSD	76%
														ns	ns	ns	ns	BON	
															ns	*	**	LSD	82%
															ns	ns	ns	BON	
																ns	ns	LSD	87%
																ns	ns	BON	
																	*	LSD	92%
																	ns	BON	

8.4: Discussion

As with the data for the earlier study (Chapter 6), the maximal minute powers (MMP) achieved by the subjects in this study were comparable to that reported for athletes of a similar level in previous work (Arts and Kuipers, 1994; Dobbins, 1996; Hawley and Noakes, 1992; Palmer *et al.*, 1994). The mean duration of the 95% MMP level in the high-fatigue trial (SS2-1) was also of similar duration to the previous data. The slight increase in mean duration in the current study compared to that in the previous chapter may be attributable to the different ergometers used. Unlike the SRM ergometer used in the previous study, the Kingcycle used in the present one did not constrain power output and thus allowed the power outputs maintained to fall slightly below the prescribed levels. Therefore, although the prescribed power outputs in the protocols were identical, subjects were thus exercising at slightly lower intensities in the latter stages of the current study.

8.4.1: Time course of changes in SRM power data

In order to elucidate the time-course of fatigue related changes and give an indication of possible causality, it is necessary to investigate the presence and time-course of any performance decrement. If the mean power outputs recorded by the SRM Power Measuring Crankset are assumed to be valid and linear across the measured range (see Chapter 6), then the differences between prescribed and recorded power outputs must be taken as indicative of the subjects' modulating their power output to factors in addition to the task requirements themselves. The fact that, in both trials, recorded mean power output consistently exceeded prescribed at the 50% MMP level whilst falling below it at the 95% MMP level, may suggest that, at the lower power output, which was well within the subjects capabilities for the prescribed duration, subjects used the prescribed level as a 'floor' to their efforts, whilst when they were required to ride at close to their physiological limits at the 95% MMP level, the prescription level was treated as a 'ceiling'. Since, even at the 95% MMP level, subjects were still riding at sub-maximal power outputs, this suggests that modification in subjects' behaviours pre-empted the manifestation of the deleterious effects of fatigue. However, whilst the subjects managed to maintain their power outputs with relative

constancy for approximately the first third of the final section of the trial, albeit at a circumscribed level, beyond this point, it is apparent that even this could not be maintained. This abatement did not appear to be a simple progressive decline, but rather to have occurred in four stages. The first was marked by constant power output being maintained, but at a level below that prescribed. The second, starting at around one third of the time to task failure, exhibited both a progressive decline in the maintained power output and an increase in the fluctuations of the mean. The third, beginning around two thirds of time to task failure, was indicated by an increasing rate of decline together with reduced deviations in the mean. The final brief covered the last few seconds of the trial where power output dropped rapidly immediately before task failure. Such a staged response would also fit with the perceptions of the trial as reported by several of the subjects who stated that the first sixty to ninety seconds after achieving the 95% level (around 30% of time to task failure) was perceived as being very difficult. They also stated that, during this period, they doubted that they would be able to maintain the power output for the expected duration. However, after this time, the task was perceived as being more manageable up to around three minutes (approximately 60% of time to task failure). Beyond this, the subjects reported that a great deal of mental effort was required to maintain the power output. It therefore appears that both the maintained power outputs and the subjective assessment of the task passed through a series of stages that occurred with similar time courses. It is hence suggested that, if staged responses were apparent in both of these, then similar demarcations in the biomechanical responses may be expected. Any physiological basis for this non-linearity is unclear, indeed the location of the fatigue mechanisms are disputed with some authors arguing that the decline in power output in this type of effort is mediated by central mechanisms, (Ansley *et al.*, 2004; Bangsbo *et al.*, 1992; Noakes, 1998), whilst other suggest that the limitations are peripheral (Hettinga *et al.*, 2006). However, there is support for non-linearity from investigations of the effects of fatigue on myoelectric signals (Ikegawa *et al.*, 2000; Nieman and Takala, 1996; Webber *et al.*, 1995) although the applicability of these results to the present study cannot be assumed as isometric contractions were used in these studies.

8.4.2: Initial common phases of trials (SS1,7 and R1)

8.4.2.1: Trial effects

The fact that no trial effects were shown for any of the segmental or joint angular displacement or kinetic variables for the initial stages of the two trials suggests that these variables were reliable between trials. Indeed, since the initial phases included the entire power output ranges used in the study, this suggests reliability of the parameters across the tested ranges. However, it may also be that differences were obscured by measurement error, for example, in the kinematic variables, that resulting from motion blur due to the shutter speed used (1/250s). Since, these effects would be greatest for those markers with the highest linear velocity, the associated segment angles would also be most affected (i.e. the foot, up to ~5°). However, since this segment was also least constrained by the task, the greatest scope for technique modifications would also be present here thus reducing the obscuring effects of measurement error. The differences that did occur in some of the joint velocity parameters (maximum left hip, knee and ankle velocity, maximum right ankle velocity and minimum left knee velocity) could be taken as indicative of lower inter-trial reliability in these variables. However, it could also be explicable by anticipatory effects since, although the power outputs were the same in this section of both trials, the subjects were aware that the tasks in the subsequent part of the trials would differ. If it is argued that adaptations could occur to fatigue before its deleterious physiological effects become apparent, then this could also be extended to suggest that differences in such effects could occur depending on whether the subjects were anticipating the start of a high or low fatigue protocol. However, research has yet to be conducted to establish whether such anticipatory effects occur in technique. The support for this from within the current study is also mixed. Whilst the fact that all of those variables to have shown significant trial effects, also showed significant trial and time interactions may suggest anticipatory effects, such effects would also be expected within the kinetic parameters, which was not the case.

8.4.2.2: Time effects

Since this phase of the trials included progressive changes in the prescribed power output, changes in the kinetic parameters related to increasing power output (magnitudes of peak effective and resultant forces, sum total and positive work and mean power) were expected. This was indeed the case. However, the magnitudes of both the peak ineffective forces and sum negative work also showed significant increases over time. This may be due to these parameters changing simply because the total forces being applied were increasing rather than alterations in their relative magnitude. The absence of significant time effects in the crank angle at which peak effective and resultant forces occurred concurs with some of the previous literature (Soden and Adeyefa, 1979) suggesting that, whilst the magnitudes of the propulsive forces changed with power output, the pattern of their application did not. However, peak ineffective forces did occur significantly earlier in the crank cycle suggesting non-propulsive elements may have been altered. Positive work also started earlier and finished later in the crank cycle suggesting that the work was being done over a larger range as power output increased. The increases in the Index of Effectiveness observed with increased power output have also been found by previous researchers (Black *et al.*, 1993; Davis and Hull, 1981).

Contrary to the pattern of the time effects shown in the kinetic data, there were many magnitude changes in the segmental angular displacement variables, but relatively few changes in relative timings. However, this was less apparent in the joint angular displacement parameters. This apparent contradiction between some of the significant segmental angular displacement effects not being reflected in similar changes in their connecting joints may be explicable by the fact that the peaks of each do not necessarily occur concurrently. The differences between the two may indicate that maintaining joint angles was of more importance in the body's co-ordination strategies in achieving the task than the alignment of the limbs to external reference planes. Verification of these findings with reference to the existing body of literature is problematic since, there is little research into kinematic changes with power. However, of the work that does exist, the findings of Black *et al.* (1993) were not supported by the current work since Black *et al.* found that the ankle became

more dorsiflexed with increased power output whilst the only significant change in the current study was for increased maximum plantar-flexion angles of the right ankle in the current work. Within the joint velocity data, there appeared to be a consistent trend for increasing peak joint velocities across all joints which may be expected since there was also a concomitant increase in crank velocity. It thus appears that, although subjects were instructed to try to maintain a constant cadence, one of their primary strategies for achieving (and maintaining in the high fatigue trial) the higher power outputs, was to increase their cadence. This would support the suggestion by Sargeant and Greig (1988) that the selection of higher cadences may be a strategy for minimising peripheral fatigue. The simultaneous changes in cadence and power make causal attribution of the observed effects problematic. However, increases in the magnitude of peak forces (Kautz *et al.*, 1991; Soden and Adeyefa, 1979) and Index of Efficiency (Black *et al.*, 1993) have been shown with increasing power, i.e. paralleling the changes observed in this section of the current study, whilst opposing trends have been shown with increasing cadence (Black *et al.*, 1993; Sargeant and Greig, 1988). This thus suggests that power had the dominant effect, at least in some of the kinetic variables. However, positive and negative work have been reported to be increased both by higher power outputs (Black, 1994) and higher cadences (Sarre *et al.*, 2005) so the similar changes observed in the current study cannot be conclusively attributed to either. The cause of the effects in the kinematic data also cannot be verified since the effects of cadence and power on these parameters has yet to be investigated.

8.4.2.3: Trial and time interactions

The only variables to have shown significant time and trial interactions were those of the joint velocities. Since no such effect was shown for cadence, this suggests that other factors may be involved in explaining the velocity changes. As has already been discussed, this could simply be indicative of limited reliability in the data. However, if feed-forward mechanisms do exist, these could be regarded as a fatigue related response even though they pre-empt the start of the task that would be expected to necessitate them, although if this were the case, similar effects would again have been expected in some of the kinetic parameters.

8.4.3: Final phase of trials (SS2)

8.4.3.1: Trial effects

In the discussion of the time effects in the initial phase of the two trials, the observed changes were attributed primarily to changes in power output. It would therefore be expected that very similar trial effects would be observed in the latter part of the trial where there were marked differences in the prescribed power outputs. In the case of the kinetic parameters this was indeed the case, with almost every variable that demonstrated significant time effects in the initial phase, also showing significant trial effects in the final section. However, since significant trial effects were also shown in cadence, the issues of attribution to cadence or power previously discussed are also applicable. Conversely, for the kinematic variables there was little concurrence between the initial time and final trial effects. Indeed, relatively few variables showed significant trial effects in the latter part of the trial. There a number of possible explanations for this. Firstly, it may indicate that the time effects in the kinematic data in the earlier stage were a result of changes over time irrespective of power, i.e. they indicate that a stable technique, at least in the kinematic parameters had not been achieved. Secondly, it may be that the effects are attributable to increasing power, rather than to differences in power *per se*. Finally, it may be that the effort required to maintain the higher power output may have enforced constraints on the subjects' techniques thus eliminating the opportunity for such responses. However, whilst Sarre *et al.* (2005) have shown kinetic parameters (sum net positive and negative work and crank angle of peak net torque) to be stable for an hour after a 10 minute warm up, no research has yet examined the time required for pedalling kinematics to become stable or the possibility of the other suggested explanations.

8.4.3.2: Time effects

In the kinematic data, time effects were observed for left maximum hip and minimum knee velocities, although the only angular displacement parameter to show time effects was right maximum foot angle. As previously discussed the time course of kinematic changes has yet to be established, but these data would suggest that

changes could still be occurring after around sixteen minutes of continuous exercise independently of high levels of fatigue. However, in the case of the joint velocity parameters, given that these were both also shown to possess significant time/ trial interactions, the time effects may be, at least partly due to these. It should also be noted that, since fatigue has been defined as a progressive process that occurs prior to any performance decrement, fatigue would also have been occurring in the low fatigue trial, albeit at a lower rate. This therefore could still offer a potential explanation. However, the time effects could also suggest, either periods of adaptation resulting from perturbation of the technique caused by the prior ramp sections or 'warm-up' effects. Since the low fatigue trials were continued for ten minutes after achieving the final steady state, it seems unlikely that these effects can be attributed to alterations in anticipation of the end of the trial.

With regard to the kinetic data, time effects were observed in the magnitude of peak resultant and ineffective forces on the right pedal as well as the crank angles at which peak ineffective force occurred and positive work ended on the left pedal, as well as in the Index of Effectiveness at both pedals. Again, the only work to have investigated the time course of kinetic changes independent of fatigue is that of Sarre *et al.* (2005), who did not include these variables. With the exception of Index of Effectiveness, none of these variables also showed significant interactions and so the suggestion that time effects could be partly attributable to fatigue effects cannot be supported and they must therefore be dependent upon the other factors previously discussed.

8.4.3.3: Trial and time interactions and time effects in high fatigue trial.

The time/trial interaction effects in this part of the trials may be taken as being indicative of fatigue related changes, although, since no measurement of fatigue was taken, other time and intensity related changes cannot be discounted as potential explanations. This could include differences in 'warm-up' effects at the different power outputs or periods of acclimatisation to altered task requirements. Therefore, no causal relationship can be inferred between the biomechanical changes observed and fatigue. It is argued however, that, the occurrence of performance decrement and, ultimately, task failure can be taken as evidence of the presence of fatigue, so

the changes observed can therefore be defined as *occurring with*, if not necessarily *caused by*, fatigue.

Few variables achieved significant time/trial interactions in the final part of the two trials (crank angle at maximum right foot angle, maximum left hip and minimum knee velocities, the crank angle at which positive work started on the left pedal and the Instantaneous Index of Effectiveness at both pedals). Comparison of these findings to the existing research is limited by the sparsity of work in this area. However, the research that does exist shows only limited agreement. Examining firstly the segmental angular displacements, the changes in minimum thigh and shank angles observed by Sanderson and Black (2003) were not found in the current study, although divergent trends are apparent in the minimum shank angles between the two trials. The changes in minimum and maximum foot angles over time found in the complete final steady state section of the high fatigue trials (SS2-1) were not however, observed by Sanderson and Black (2003). The relative timings of the segment angles within the crank cycle have not previously been reported, so the effects shown at the right foot cannot be readily compared. Even comparisons to research on other activities are not possible since the majority of these have been conducted on tasks where the timing of the task co-ordination must be made relative to the point of impact (running and jumping). Therefore, relative timing comparisons may well not be valid since no such constraint occurs in cycling. The only study to have examined an unconstrained task (O'Donovan and Anderson, 2000) (rowing) did not examine relative timings and so comparisons are not possible. Joint angle changes with fatigue in cycling have also only been reported in a single study (Amoroso *et al.*, 1993a). These researchers showed effects in maximum hip flexion and extension angles and ankle plantar and dorsiflexion angles, none of which were observed in the current study. However, although not significant, divergent trends can again be observed in the two trials of the present study for both the hip angle parameters, at least for the right leg. The changes in left maximum knee extension in the high fatigue trial (SS2-1) do not however concur with the findings of Amoroso *et al.* (1993a). Additionally, the joint velocity changes observed in the present work cannot be compared to the previous literature investigating cycling since none of the prior studies have included these parameters. However, no significant effects on

velocity changes were reported by the only study to include these parameters in the investigation of fatigue (Williams *et al.*, 1991), but since this focused on running comparisons may not be appropriate.

Sanderson and Black (2003) reported that effective forces increased with fatigue which was again not found. However, the findings of the current study may gain support from those of Sarre *et al.(2005)* which showed no change in peak net torque, although this was for a prolonged trial, but not one to failure and therefore fatigue effects cannot be assumed. However, Delextrat *et al.* (2005) also showed that such changes only occurred in the non-dominant leg, although this was using a non-specific prior fatigue task (swimming). Sanderson and Black (2003) also did not observe changes in peak resultant or ineffective forces or the crank angles at which peak effective force was recorded such as those observed in the final steady section of the high fatigue trial (SS2-1). Nor did Delextrat *et al.* (2005) show changes in the crank angle at peak torque. The other parameter to show significant time effects in the latter part of the high fatigue trial (crank angle at peak ineffective force) was not measured by Sanderson and Black (2003) or the other previous works and so cannot be compared. The absence of changes in sum positive or negative work found in the current work do also concur with previous literature (Sanderson and Black, 2003; Sarre *et al.*, 2005), However, the changes in total work with time in the high fatigue trial (SS2-1) were not reported by either of these works and so cannot be compared. Conversely, although the crank angles at which positive work starts and ends have not previously been reported, Sanderson and Black (2003) did state that no differences were found in the crank angle at which positive impulse started which would be expected to be similar, although affected by intra-cycle crank velocity variations. This therefore does not support the findings of the current study. Finally, the observed changes in the Index of Effectiveness do not concur with Sanderson and Black (2003) who did not find significant effects.

Whilst there appears to be only limited agreement with the current and previous research this is perhaps unsurprising given the lack of research in this area. Thus comparisons to single studies that have used varying protocols may well yield inconclusive of incomparable results. It should also be noted that the findings of

Amoroso *et al.* (1993a) were based on intra-trial comparisons and therefore other time-related effects cannot be discounted. Further, since the previous studies using protocols designed to elicit fatigue only examined start and end points, this would not allow for initial technique stabilisation and may not identify changes that occurred within the trials. This may have been the case for the Index of Effectiveness since the post-hoc analysis showed significant inter-trial comparisons only up to the first four time windows for the left pedal (Sanderson and Black (2003) only examined one side). Indeed for several of the variables where significant time/trial interactions were shown in the current study, the direction of changes over time inverted during the course of the final section of the trials (SS2) (crank angle at the start of positive work and Instantaneous Index of Effectiveness). Therefore, whilst substantial changes occurred within the trials, the start and end points were similar. Conversely, since the inter-trial comparisons in the final steady state section of the two trials (SS2-2) did not include the initial two minutes of the high-fatigue section of the trial, it is highly plausible that the changes observed in the other studies occurred within this time and so were not detected in the current work.

8.4.4: Time course of changes

The current study showed that, not only the decline in performance started long before ultimate task failure, but that there were apparent stages in this process. Such turning points in responses were also apparent in some of the kinetic variables (Instantaneous Index of Effectiveness and the crank angles at the start of positive work and at peak effective force). However, these were less evidenced in the other kinetic parameters. In the case of the Index of Effectiveness, the first of these appeared to have occurred around one third of time to task failure for both pedals, with a second around 82%, although the existence of the second was unclear on the right. The first of these therefore coincide with the timing of those observed in the net mean power, whilst the second is less clear and occurs later. As for the relative timing variables, the turning point of both of these appeared to have been around half way to task failure, i.e. around the midpoint of the second stage in the net power data. Whether any such trends were apparent in the kinematic data is less easily

established since the limited temporal resolution did not allow changes in trend directions to be discriminated from fluctuations in the variables.

8.5: Conclusions

The purpose of this study was to examine the time course of kinetic and kinematic changes in the pedalling technique of cyclists' with fatigue by examining the effects of manipulating the major factors that would determine its occurrence, i.e. time and power output. Interaction effects were shown between these two independent variables suggesting fatigue related changes for several parameters, although either power or other time related factors were shown to be possible explanations for some of these and so they cannot be conclusively attributed to fatigue. However, in the case of the crank angles at which maximum right foot angle occurred and left positive work started no confounding effects were shown and thus suggesting that these changes can be defined as occurring with fatigue. This may indicate that the major adaptations with fatigue relate not to changes in the magnitude of the forces of the movement patterns but to the relative timing of these within the crank cycle. The examination of the time-course of observed changes also indicated that the pattern of these within the trial may have led previous investigators to erroneously discount fatigue related effects in some parameters. It is also noted that the inclusion of a non-constant power output section in the low fatigue trial may have led to separating fatigue related effects from those that were solely time related being problematic in this section of the trials. It has also been speculated that changes occurring in the power output that the subjects were able to maintain as well, as some of the kinetic parameters measured, occurred in discrete stages, although the evidence of temporal alignment of the two was limited. It was also apparent that joint velocities may have been sensitive to fatigue and effects may even have occurred prior to the start of the high fatigue section of the protocol. This study has therefore evidenced the existence of not only fatigue related technique changes, but variable time courses of these, although further work is required to clarify and verify these observations.

Chapter 9: General discussion and conclusions

9.1: Overview of findings

The initial section of this thesis reported the stages of technical development that have been undertaken to attempt to address the primary research questions. The instrumented pedals that have been developed were shown to provide valid and reliable measurements of the forces applied to the pedals parallel to the crank rotation as well as the angular positions of the pedals and cranks. This, together with the custom written programs has allowed the measurement of the necessary parameters throughout the fatigue trials. Additionally, the methodological approaches to the kinematic data analysis have shown the potential to reduce the errors in the data collected in the final major study. The findings of this indicate that modifications occurred with fatigue in both kinetic and kinematic parameters as well as in the manner in which the subjects controlled their performance of the task. It was shown that performance management strategies were adopted in the manner in which power output was regulated relative to the prescribed levels. This was the case even in the initial low fatiguing section of the protocol, although whether the subjects strove to keep down to the 'floor' of the lower intensity effort or up to the 'ceiling' of a high intensity one differed. This may suggest that conscious control is required by riders to maintain a lower intensity effort and that, without continuing feedback, the tendency would be for them to exceed this. It also raises the question of at what point the opposing strategies change. It is speculated that technique changes could even occur depending on which strategy was being adopted and so may not only be power output dependent but could change with fatigue as a moderate intensity effort became increasingly difficult to sustain. Beyond these strategies, evidence was shown of staged responses in the ability of the subjects to maintain the prescribed performance criteria. It may be that these stages are reflective of the extent to which the body is able to manage the task so that the initial phase represents positive adaptations to modulate the initial effects of fatigue, the second as coping with these effects before the final stages of disintegration of co-ordination and ultimate task failure.

Within the biomechanical responses, the kinematic variables, showed only limited evidence of fatigue related changes in the displacement variables with the exception of the foot. This suggests that movement patterns are relatively robust with fatigue, both in terms of the angular ranges covered by the limbs and the timing of these relative to the crank cycle. It would be expected that changes would be more likely to occur at the foot since the movements patterns of other segments are largely constrained by the nature of the task. However, the joint velocity findings may indicate that changes do occur but may be too subtle to be detected by displacement parameters alone and so higher order derivatives may be useful. The changes in the joint and segment angles appeared to be simple gradual changes. Whilst this still may be indicative of fatigue responses, the type of phased response that have been proposed to exist in some of the other variables do not appear to occur. It is speculated that these type of changes may have occurred in some of the relative timing and joint velocity variables but that the temporal resolution was insufficient to detect it.

The kinetic data offered little evidence that the changes with fatigue occurred in the magnitude of the forces since the effects shown in force peaks, power total power could well be attributable to the decline in mean net power. The effects in the timings relative to the crank cycle and Instantaneous Index of Effectiveness could not however be explained by this. It is also in these parameters that the clearest evidence of discrete staged responses were apparent. This therefore suggests that the primary modifications of technique with fatigue occurs in relatively subtle changes to the application of force within the crank cycle and that these, together with the decline in power output, were phased as fatigue progresses, although the evidence of temporal alignment of the two was limited. The nature of some of these changes also suggested that previous investigators may have erroneously discounted fatigue related effects in them by limiting their analyses to start and end points.

9.2: Implications of the findings

Previous research has shown changes in co-ordination in response to chronic alterations to the nature of a task, for example through injury (Berchuck *et al.*, 1990; Lewek *et al.*, 2002; Rudolph *et al.*, 1998) or strength training (Carroll *et al.*, 2001) as well as acute changes with altered external task characteristics such as gradient. (Caldwell *et al.*, 1999; Caldwell *et al.*, 1998; Li and Caldwell, 2000) or crank inertial load (Fregly *et al.*, 1996; Hansen *et al.*, 2002; Hansen and Sjoggard, 2000). However, the current work also suggests that acute changes similarly occur where the alterations are entirely within the performer. Since, even for chronic conditions, periods of adaptation are required to modify techniques to accommodate these effects, it is likely that regular exposure to the conditions associated with the acute changes would be required for situation specific techniques to be developed. However, whilst the need for specificity of technique development in response to externally dictated task characteristics is well recognised, the advice given to coaches to date has often been that work on developing techniques should stop when fatigue causes 'deteriorations' in technique (for example, Sharp, 1992 p. 87). However, the current work indicates that more work is required to investigate whether athletes competing in sports where the maintenance of effective techniques under conditions of high fatigue are required, should avoid attempting to develop their techniques when fatigue becomes apparent or actively seek to train techniques in and specific to, these conditions. These investigations would also need to examine whether, if stages of fatigue do occur, that athletes in such sports may benefit from developing a package of variations on certain techniques that are adapted to suit the different levels of fatigue.

If, as the current work suggests, elements of technique changed with fatigue in a non-linear manner, then this could have implications for injury potential beyond cycling and indeed even sport. For example, if an operative conducting manual tasks reaches a critical fatigue threshold and continues the task, then their technique could rapidly alter, potentially increasing injury risk, even though their ability to undertake the task had not yet been diminished.

9.3: Limitations and future directions

There are various limitations apparent in the present work, some related to the technical properties of the work, some emanating from the exploratory nature of the work necessitated by the paucity of the antecedent research and others arising from the various assumptions that have been made. For example, both kinetic and kinematic data sources have been assumed to be planar and to occur in a plane parallel to the crank rotation. However, previous research has shown this not to be the case, although the movements and forces outside of this plane are small and so this was likely to have been an acceptable compromise. The technical limitations of the pedals also did not allow the measurement of centre of pressure. Without this, accurate inverse dynamic solutions could not be calculated (Broker and Gregor, 1990) which may have yielded additional useful information. In particular, it limited the assessment of efficiency that could be made, which may be expected to alter with fatigue. Whilst the Index of Effectiveness was included, as was discussed in Chapter 3, the work of Kautz and Hull (1993) and Fregly and Zajac (1996) have shown that this does not allow for the contribution of non-muscular components of the pedal forces and therefore, whilst it may be useful in indicating changes in the patterns of force application, it cannot be regarded as a valid measure of technique efficiency. Additionally, although kinetic data collection was continuous, kinematic was based upon time windows. This means that the two data types are not directly comparable since one represented an average over a period of time, whilst the other represents a 'snap-shot' that was assumed to be representative of that time window. This also created issues of at what point in the window the 'snap-shot' was taken when both power output (in the case of the ramp phases) and fatigue were varying over time. The reliance on time windows also placed restrictions on the resolution at which time related changes could be examined and it was apparent that this may have obfuscated the observation of the time course of changes in the kinematic data. Thus the ideal situation would have been to use continuous data collection for all parameters throughout the trial. However, although this challenge has been successfully addressed for the kinetic parameters in this research, this approach would present substantial practical technical challenges if it were to be applied to the kinematic

data. Therefore, whilst this may be advisable for subsequent investigations, the limitations are deemed acceptable for the present study which represents a first foray into this area.

There are also numerous areas that could be affected by fatigue that were not examined in the current work. For example, whilst this investigation has shown effects in discrete or summary parameters (peaks, sums and means) it is plausible that other changes could have occurred within the cycle that would not have been apparent in these measures. Indeed, the changes shown in relative timings of some of the parameters suggests that more complex intra-cycle effects may well have occurred. This is an area that has yet to receive adequate investigation in cycling. The current work also did not allow for the examination of inter-individual differences which has been noted in some of the previous work focusing on running (Adrian and Kreighbaum, 1973; Brüeggemann and Arndt, 1994; Chapman and Medhurst, 1981; Darras and Burden, 1994; Siler and Martin, 1991) as well as that of Black (1994) which examined cycling. Additionally, although bilateral measurements were taken of all of the parameters, the issue of asymmetry was not specifically addressed. This previous authors have reported in pedal forces in other contexts (Briggs *et al.*, 1987; Sargeant and Davies, 1977; Smak *et al.*, 1999; Wheeler *et al.*, 1992, 1995) and the bilateral differences in many of the observed effects in the current study may suggest could have altered with fatigue. Further, variability was not examined, nor did the current work attempt to examine co-ordination *per-se*, i.e. from a motor control perspective and there is clearly much that could be derived from the data using such approaches. It is suggested that the application of analysis techniques from this discipline (e.g. the analysis of continuous relative phase) may provide the tools to identify the possible more subtle intra-cycle changes previously mentioned. More information could also be usefully be gained by the integration of other techniques such as electromyography (EMG), which may give an indication of the changes occurring within the actuators of the system as it responds to the task. Techniques also exist that may also allow EMG to be used as a tool to measure the process of fatigue (De Luca, 1984; Webber *et al.*, 1995). Clearly, if the time course of biomechanical changes could be related to that of the underlying physiological phenomenon occurring around the muscles producing the action, this could be highly

illuminating. Whilst all of the above omissions may be regarded as limitations of the present work, no single work can expect to address every aspect of a research area and so future work may be needed to examine these elements. Even with this circumscription of the areas of investigation the multiple dependent variables included in this study created statistical issues, in that it increased the probability that at least some of the observed effects would actually be statistical aberrations and so increased the probability of type I errors. The decision to include variables not shown to display effects with fatigue in previous studies was validated by finding effects that have not been previously reported. Specifically those that occurred within the trials that would not necessarily be evidenced in analysis restricted to an examination limited to trial start and end points as previously conducted (i.e. Index of Effectiveness and the crank angles at the start of positive work and peak effective force) and those that had not been previously investigated (i.e. joint velocities). However, it could be argued that the statistical effects of conducting analyses on multiple parameters should have been allowed for by grouping related variables and using MANOVA techniques. However, since the power of MANOVAs are dependent upon both the correlations between the dependent variables and the effect sizes (Field 2000) this would have been problematic since neither could be known *a priori*. It is however, suggested that the findings of the current study be used to guide the selection of variables and analysis methods for subsequent studies in this area.

The decision to include non-constant elements in the low fatigue protocol also represented a degree of compromise. The inclusion of the ramp up to 95% MMP and therefore ramp back down to 50% MMP rendered not only useful comparisons between the two trials impossible for the duration of this period, it also did not allow the time normalisation of the subsequent data relative to the rest of this part of the trial. However, its omission would also have presented a number of issues. Firstly, it would not have allowed comparisons across power outputs between the two trials and therefore inter-trial reliability across the measured power ranges could not be assessed. Secondly, it would have increased the likelihood of physiological differences between the two trials (especially warm-up effects) and excluded the possible effects of perturbation of technique by the ramp from one trial, thus introducing potential confounding variables. It would therefore clearly have been

preferable to retain the ramp up to 95% MMP in both trial but to have switched back between the two power outputs in a shorter period of time in the low fatigue. However, the technical limitations of the ergometer (Kingcycle) did not allow this as the flywheel required an extended period to decelerate. However, even if these technical limitations were removed, the rapid change in power output could have perturbed the subjects' techniques thus requiring a period of adjustment before a stable technique was again established. This could potentially have been as long as the duration of the ramp and so would not have eliminated this problem. A possible partial solution to this would have been to increase the power output required in the low fatigue trial thus reducing the range of power that the subjects would have needed to cross. However, this would have reduced the difference in the expected fatigue levels between the two trials and thus potentially obfuscated differences in the technique responses. Therefore, whilst the protocol used in the current work may be problematic, an ideal solution does not exist.

A further issue in the design of the protocol for this study was that two independent variables (time and power output) were manipulated simultaneously in order to attempt to produce a third that was the one of interest to the research, i.e. fatigue. Although this complicated the interpretation of the data, it was necessary as the physiological mechanisms of fatigue are dependent upon both of these parameters. This could perhaps be addressed by examining technique changes over time in the moderate intensity segments of an intermittent protocol, using repeated bouts of higher intensity effort. Thus if the duration of these higher intensity efforts were varied, the progressive development of fatigue could regulated whilst still allowing assessment of technique at the same power output and duration and whilst still including peturbations to technique by changing power output in all trials. However, the issues regarding the time required for technique to stabilise after such power changes previously mentioned would need to be investigated and allowed for in the design of the protocol.

As well as the limitations highlighted in the current work, it has also illuminated other areas that are yet to be adequately explored by research. For example, more work is needed to investigate the time-course of technique changes under various

constant conditions. Most biomechanics research relies upon a limited number of repetitions of a task, generally taken with little prior activity and more examination is required of the prerequisites for establishing both stable and ecologically representative techniques. More research is also needed to investigate the effects of various other competition related factors (e.g. stress or tactical considerations) on technique. Other areas highlighted that are not specific to the investigation of fatigue include clarifying what differences exist in the responses to various task attributes comparing trials where these are fixed, but different to those where they are changing across the same ranges. For example, the differences in the kinematic variables observed in the current research during the initial ramp increase in power output compared to when the power outputs were different but constant in the two trials.

Specifically within cycling, more work is required to clarify what constitutes 'optimal' technique and what factors affect this, including fatigue. Leading on from this, there is still very little work on the efficacy of using the feedback provided by technologies such as the instrumented pedals in intervention strategies in modifying riders' techniques. Whilst there are anecdotal reports of the benefits of such interventions (Armstrong and Carmichael, p. 136; Cavanagh and Sanderson, 1989 pp. 114-115), there is little research work published to support this (Sanderson, 1986, 1987; Sanderson and Cavanagh, 1990).

9.4: Conclusions

Technical developments have been described that have allowed the demonstration of changes over time in both kinetic and kinematic parameters. Within these, the clearest evidence of fatigue related modifications in movement patterns was shown to be in the joint velocities of the active limbs, whilst in the kinetic parameters the primary changes appear to be related to the patterns of force application rather than in their magnitude. The kinetic data together with changes in the performance measure (power output) also suggest that some of these changes occur in stages rather than as linear progressions. However, more work is required to clarify the relationship between the two and further investigate the kinematic responses.

References

Abbiss CR and Laursen PB. (2005) Models to Explain Fatigue During Prolonged Endurance Cycling. *Sports Medicine* 35: 865-898.

Adrian M and Kreighbaum E. (1973) Mechanics of Distance Running During Competition. *Medicine and Sports, Biomechanics III*, edited by Watrtenweiler J, Rome. S. Karger, Basel, 354-358.

Allard P, Blanchi J-P and Aïssaoui R. (1995) Bases of Three-Dimensional Reconstruction. In: *Three-Dimensional Analysis of Human Movement*, edited by Blanchi J-P, Stokes IAF, Blanchi J-P. Champaign, Illinois: Human Kinetics, 19-40.

Álvarez G and Vinyolas J. (1996) A New Bicycle Pedal Design for On-Road Measurement of Cycling Forces. *Journal of Applied Biomechanics* 12: 130-142.

Amoroso A, Sanderson DJ and Hennig EM. (1993a) Kinematic and Kinetic Changes in Cycling Resulting from Fatigue. *Abstracts of the International Society of Biomechanics XIVth congress*, Paris, 94-95.

Amoroso A, Sanderson DJ and Hennig EM. (1993b) Kinematic and Kinetic Changes in Cycling During an Exhaustive Steady-State Ride. *Proceedings of the 17th annual Congress of the American Society of Biomechanics*, Iowa City, Iowa, 157-157.

Anderson R. (2002) *An Ipsative-Based Biofeedback System to Improve Rowing Performance* (PhD). Limerick: University of Limerick.

Angulo RM and Dapena J. (1992) Comparison of Film and Video Techniques for Estimating Three-Dimensional Coordinates within a Large Field. *International Journal of Sport Biomechanics* 8: 145-151.

Ansley L, Schabort EJ, St. Clair Gibson A, Lambert MI and Noakes TD. (2004) Neural Regulation of Pacing Strategies in 4 Km Time Trials. *Medicine and Science in Sports and Exercise* 38: 1819-1825.

Armstrong L and Carmichael C. (2006) *The Lance Armstrong Performance Program.* Emmaus, PA: Rodale.

Arts FJP and Kuipers H. (1994) The Relation between Power Output, Oxygen Uptake and Heart Rate in Male Athletes. *International Journal of Sports Medicine* 15: 228-231.

Balmer J, Bird SR, Davison RCR, Doherty M and Smith PM. (2004) Mechanically Braked Wingate Powers: Agreement between SRM, Corrected and Conventional Methods of Measurement. *Journal of Sport Sciences* 22: 661-667.

Bangsbo J, Graham T, Kiens B and Saltin B. (1992) Elevated Muscle Glycogen and Anaerobic Energy Production During Exhaustive Exercise in Man. *Journal of Physiology* 451: 205-227.

Bartlett R. (1997) *Introduction to Sports Biomechanics.* London: E and FN Spon.

Bates BT and Haven BH. (1974) Effects of Fatigue on the Mechanical Characteristics of Highly Skilled Female Runners. In: *International Series on Sport Sciences, Biomechanics IV*, edited by Morehouse CA. London: Macmillan Press, 121-125.

Bates BT, Osternig LR and James SL. (1977) Fatigue Effects in Running. *Journal of Motor Behaviour* 9: 203-207.

Batschelet E. (1981) *Circular Statistics in Biology.* London: Academic Press.

Berchuck M, Andriacchi TP, Bach BR and Reider B. (1990) Gait Adaptations by Patients Who Have a Deficient Anterior Cruciate Ligament. *Journal of Bone and Joint Surgery. American Volume* 72: 871-877.

Bertucci W, Grappe F, Girard A, Betik A and Rouillon JD. (2005) Effects on the Crank Torque Profile When Chaining Pedalling Cadence in Level and Uphill Road Cycling. *Journal of biomechanics* 38: 1003-1010.

Black AH. (1994) *The Effect of Steady Rate Exercise on the Pattern of Force Production of the Lower Limbs in Cycling* (MSc): University of British Columbia.

Black AH, Sanderson DJ and Hennig EM. (1993a) Effectiveness of Force Application in Cycling. *Journal of Biomechanics* 26: 317.

Black AH, Sanderson DJ and Hennig EM. (1993b) Kinematic and Kinetic Changes During an Incremental Exercise Test on a Bicycle Ergometer. *Abstracts of the International Society of Biomechanics, XIVth Congress*, Paris, 186-187.

Black AH, Sanderson DJ and Hennig EM. (1994) Kinematic and Kinetic Changes During an Incremental Exercise Test on a Bicycle Ergometer. *Journal of Biomechanics* 27: 656.

Boyd TF, Hull ML and Wooten D. (1996) An Improved Six-Load Component Pedal Dynamometer for Cycling. *Journal of Biomechanics* 29: 1105-1110.

Bratt Å and Ericson MO. (1985) Biomechanical Model for Calculation of Joint Loads During Ergometer Cycling. In: *Technical reports from Department of Mechanics, Royal Institute of Technology, Stockholm and Kinesiological Research Group, Department of Physical Medicine*. Stockholm, Sweden: Karolinska Institute, 1-36.

Bremble and Brown. (1985) The Design of an Instrumented Bicycle Pedal. *Communication to Sports Biomechanics Study Group*, Leeds.

Briggs DW, Foulke J, Woolley C, and Fedel FJ. (1987) Measurement of Competitive Cycling Performance Using an on-Board Computer. *Personal Communication*, M. Ypsilanti, Michigan, 9.

British-Cycling. (2006) *Road Race Event Classification System* (Website): http://www.britishcycling.org.uk/web/site/BC/roa/road_event_classification.asp, Accessed on: 21st September 2006

BritishCycling. (2003) *British Cycling World Class Laboratory Procedures Manual*: http://www.britishcycling.org.uk/gb_cycling_team/2003/contents.shtml, Accessed on: 28th June 2003

Broker JP and Gregor RJ. (1990) A Dual Piezoelectric Element Force Pedal for Kinetic Analysis of Sport. *International Journal of Sport Biomechanics* 6: 394-403.

Broker JP and Gregor RJ. (1994) Mechanical Energy Management in Cycling: Source Relations and Energy Expenditure. *Medicine and Science in Sports and Exercise* 26: 64-74.

Broker JP, Gregor RJ and Schmidt RA. (1993) Extrinsic Feedback and the Learning of Kinetic Patterns in Cycling. *Journal of Applied Biomechanics* 9: 111-113.

Brooke JD, Hoare J, Rosenrot P and Triggs R. (1981) Computerised System for Measurement of Forces Exerted within Each Pedal Revolution During Cycling. *Physiology and Behaviour* 26: 139-143.

Browning RC, Gregor RJ and Broker JP. (1992) Lower Extremity Kinetics in Elite Cyclists in Aerodynamic Positions. *Medicine and Science in Sports and Exercise* 24: 186.

Browning RC, Gregor RJ, Broker JP and Whitting WC. (1988) Effect of Seat Height Changes on Joint Forces and Moment Patterns in Experienced Cyclists. *12 th annual meeting of the American Society of Biomechanics*, Urbana, Illinois, 871.

Brüeggemann GP and Arndt A. (1994) Fatigue and Lower Extremity Function. *Proceedings of the eighth biennial conference and symposium of the Canadian Society for Biomechanics*, Alberta, Calgary, 316-317.

Caldwell GE, Hagberg JM, McCole SD and Li L. (1999) Lower Extremity Joint Movements During Uphill Cycling. *Journal of Applied Biomechanics* 15: 166-181.

Caldwell GE, Li L, McCole SD and Hagberg JM. (1998) Pedal and Crank Kinetics in Uphill Cycling. *Journal of Applied Biomechanics* 14: 245-259.

Carroll TJ, Riek S and Carson RG. (2001) Neural Adaptation to Resistance Training. Implications for Movement Control. *Sports Medicine* 31: 829-840.

Cavanagh PR and Nordeen KS. (1976) Biomechanical Studies of Cycling: Instrumentation and Application. *Medicine and Science in Sports and Exercise* 8: 61-62.

Cavanagh PR and Sanderson DJ. (1989) The Biomechanics of Cycling: Studies of the Pedalling Mechanics of Elite Pursuit Riders. In: *Science of Cycling*, edited by Burke ER. Champaign, Ill: Human Kinetics, 92-121.

Challis JH and Kerwin DG. (1988) Optimal Filtering and Differentiation of Biomechanical Data Using Cross-Validated Splines. *Journal of Sport Sciences* 6: 152.

Chalmers GF. (1992) Materials, Construction and Performance Characteristics. In: *Strain Gauge Technology* (2nd ed.), edited by Window AL. London, England: Elsevier Applied Science, 1.

Chapman AE. (1982) Hierarchy of Changes Induced by Fatigue in Sprinting. *Canadian Journal of Applied Sport Science* 7: 116-122.

Chapman AE and Medhurst CW. (1981) Cyclographic Identification of Fatigue in Sprinting. *Journal of Human Movement Studies* 7: 255-272.

Chappell JD, Herman DC, Knight BS, Kirkendall DT, Garrett WE and Yu B. (2005) Effect of Fatigue on Knee Kinetics and Kinematics in Stop-Jump Tasks. *American Journal of Sports Medicine* 33: 1022-1029.

Christina KA, White SC. and Gilchrist LA. (2001) Effects of Localized Muscle Fatigue on Vertical Ground Reaction Forces and Ankle Joint Motion During Running. *Human Movement Science* 20: 257-276.

Cohen, J. (1988). *Statistical Power Analysis for the Behavioral Sciences* (2nd ed.). Hillsdale, NJ: Lawrence Earlbaum Associates.

Coleman SGS. (1994) *The Measurement of Maximal Power Output During Short-Term Cycle Ergometry* (PhD Thesis). Loughborough, UK: Loughborough University of Technology.

Coleman SGS and Hale T. (1998) The Use of Force Pedals for Analysis of Cycling Sprint Performance. *Biomechanics in Sports XVI*, edited by Vieten M, Konstanz, Germany, 138-141.

Coyle EF, Feltner ME, Kautz SA, Hamilton MT, Montain SJ, Baylor AM, Abraham LD and Petrek GW. (1991) Physiological and Biomechanical Factors Associated with Elite Endurance Cycling Performance. *Medicine and Science in Sports and Exercise* 23: 93-107.

Crowninshield RD and Brand RA. (1981) A Physiologically Based Criterion of Muscle Force Prediction in Locomotion. *Journal of Biomechanics* 14: 793-801.

Dal Monte A, Manoni A and Fucci S. (1973) Biomechanical Study of Competitive Cycling. *Medicine and Sport* 8: 434-439.

Darras NG and Burden AM. (1994) The Effects of Fatigue on the Lower Limb Kinematics of Treadmill Running at 90% VO2max. *Proceedings of the Biomechanics section of The British Association of Sport and Exercise Sciences*, 25-25.

Davids K, Glazier P, Araújo D and Bartlett R. (2003) Movement Systems as Dynamical Systems: The Functional Role of Variability and Its Implications for Sports Medicine. *Sports Medicine* 33: 245-260.

Davis RR and Hull ML. (1981) Measurement of Pedal Loading in Bicycling: II. Analysis and Results. *Journal of Biomechanics* 14: 857-872.

De Luca CJ. (1984) Myoelectrical Manifestation of Localized Muscular Fatigue. *CRC critical reviews in biomedical engineering* 11: 251-279.

Delextrat A, Tricot V, Bernard T, Vercruyssen F, Hausswirth C and Brisswalter J. (2005) Modification of Cycling Biomechanics During a Swim-to-Cycle Trial. *Journal of Applied Biomechanics* 21: 297-308.

Despires M. (1974) An Electromyographic Study of Competitive Road Cycling Conditions Simulated on a Treadmill. In: *International Series on Sport Sciences, Volume 1, Biomechanics IV*, edited by Morehouse CA. London: Macmillan Press, 349-355.

Dobbins T. (1996) Prediction of Cycling Time-Trial Performance Using Maximal Laboratory Measures. *Journal of Sport Sciences* 14: 74.

Edwards RHT. (1983) Biochemical Bases of Fatigue in Exercise Performance: Catastrophe Theory of Muscular Fatigue. In: *Biochemistry of Exercise*, edited by Knuttgen, H.G. Champaign, Ill: Human Kinetics, 3-28.

Elliot BC and Ackland T. (1981) Biomechanical Effects of Fatigue on 10,000 Meter Running Technique. *Research Quarterly for Exercise and Sport* 52: 160-166.

Elliott BC and Ackland T. (1981) Biomechanical Effects of Fatigue on 10,000 Meter Running Technique. *Research Quarterly for Exercise and Sport* 52: 160-166.

Elliott BC and Roberts AD. (1980) A Biomechanical Evaluation of the Role of Fatigue in Middle-Distance Running. *Canadian Journal of Applied Sport Science* 5: 203-207.

Enoka RM and Stuart DG. (1985) The Contribution of Neuroscience to Exercise Studies. *Federation Proceedings*, 2279-2285.

Ericson MO. (1986) On the Biomechanics of Cycling: A Study of Joint and Muscle Load During Exercise on the Bicycle Ergometer. *Scandinavian Journal of Rehabilitation Medicine*: 4-43.

Ericson MO, Bratt Å, Nisell R, Németh G and Ekholm J. (1986) Load Moments About the Hip and Knee Joints During Ergometer Cycling. *Scandinavian Journal of Rehabilitation Medicine* 18: 165-172.

Ericson MO, Ekholm J, Svensson O and Nisell R. (1984a) Load on Ankle Joint Structures During Ergometer Cycling. *Foot and Ankle* 6: 135-142.

Ericson MO, Ekholm J, Svensson O and Nisell R. (1985a) The Forces of Ankle Joint Structures During Ergometer Cycling. *Foot and Ankle* 6: 135-42.

Ericson MO, Nisell R, Arborelius UP and Ekholm J. (1985b) Muscular Activity During Ergometer Cycling. *Scandinavian Journal of Rehabilitation Medicine* 17: 53-61.

Ericson MO, Nisell R and Ekholm J. (1984b) Varus and Valgus Loads on the Knee Joint During Ergometer Cycling. *Scandinavian Journal of Sport Science* 6: 39-45.

Evans SA, Ng K and McDowell S. (1994) The Effect of Fatigue on Lower Limb Kinematics in Female Distance Runners. *Research Quarterly* 65: A-17.

Fecteau AJ and Smith GA. (1992) Frontal Plane Knee Kinematics During Stationary Cycling with Clipless Pedals. *Medicine and Science in Sports and Exercise* 24: S186.

Field A. (2000) *Discovering Statistics Using SPSS for Windows*. London, UK: Sage.

Fisher NI. (1993) *Statistical Analysis of Circular Data*. Cambridge: Cambridge University Press.

Fregly BJ and Zajac FE. (1996) A State-Space Analysis of Mechanical Energy Generation, Absorption and Transfer During Pedalling. *Journal of Biomechanics* 29: 81-90.

Fregly BJ, Zajac FE and Dairaghi CA. (1996) Crank Inertial Load Has Little Effect on Steady-State Pedalling Co-Ordination. *Journal of Biomechanics* 29: 1559-1567.

Gardner AS, Stephens S, Martin DT, Lawton E, Lee H and Jenkins D. (2004) Accuracy of SRM and Power Tap Power Monitoring Systems for Bicycling. *Medicine and Science in Sports and Exercise* 36: 1252-1258.

Gerlach KE, White SC, Burton HW, Dorn JM, Leddy JJ and Horvath PJ. (2005) Kinetic Changes with Fatigue and Relationship to Injury in Female Runners. *Medicine and Science in Sports and Exercise* 37: 657-663.

Gonzalez HK and Hull ML. (1989) Multivariate Optimization of Cycling Biomechanics. *Journal of Biomechanics* 22: 1151-1161.

Gonzalez-Alonso J, Teller C, Anderson SL, Jensen FB, Hyldig T and Nielsen B. (1999) Influence of Body Temperature on the Development of Fatigue During Prolonged Exercise in the Heat. *Journal of Applied Physiology* 86: 1032-1039.

Gregersen CS and Hull ML. (2003) Non-Driving Intersegmental Knee Moments in Cycling Computed Using a Model That Includes Three-Dimensional Kinematics of the Shank/Foot and the Effect of Simplifying Assumptions. *Journal of Biomechanics* 36: 803-813.

Gregor RJ, Broker JP and Ryan MM. (1991) The Biomechanics of Cycling. *Exercise and Sport Science Reviews* 19: 127-169.

Gregor RJ, Cavanagh PR and LaFortune M. (1985) Knee Flexor Moments During Propulsion in Cycling- a Creative Solution to Lombard's Paradox. *Journal of Biomechanics* 18: 307-316.

Hamill J, van Emmerik RE, Heiderscheit BC and Li L. (1999) A Dynamical Systems Approach to Lower Extremity Running Injuries. *Clinical Biomechanics* 14: 297-308.

Hamley EJ and Thomas V. (1976) Physiological and Postural Factors in the Calibration of the Bicycle Ergometer. *Journal of Physiology* 19: 55p-57p.

Hampson DB, Gibson ASC, Lambert MI and Noakes TD. (2001) The Influence of Sensory Cues on the Perception of Exertion During Exercise and Central Regulation of Exercise Performance. *Sports Medicine* 31: 935-952.

Hansen EA, Jørgensen LV, Jensen K, Fregly BJ and Sjøgaard G. (2002) Crank Inertial Load Affects Freely Chosen Pedal Rate During Cycling. *Journal of Biomechanics* 35: 277-285.

Hansen EA and Sjøggard G. (2000) Freely Chosen Pedalling Rate Is Affected by Crank Inertial Load. In: *5th Annual Conference of the European College of Sport Science*, edited by Komulainen J. Jyväskylä, Finland, 308.

Harman E, Knuttgen HG and Frykman P. (1987) Automated Data Collection and Processing for a Cycle Ergometer. *Journal of Applied Physiology* 62: 831-836.

Hawley JA and Noakes TD. (1992) Peak Power Output Predicts Maximal Oxygen Uptake and Performance Time in Trained Cyclists. *European Journal of Applied Physiology* 65: 79-83.

Hay JG. (1993) *The Biomechanics of Sports Technique*. New Jersey: Prentice Hall.

Heiderscheit BC, Hamill J and Caldwell GE. (2000) Influence of Q-angle on Lower-Extremity Running Kinematics. *Journal of Orthopaedic and Sports Physical Therapy* 30: 271-8.

Hettinga FJ, De Koning JJ, Broersen FT, Van Geffen P and Foster C. (2006) Pacing Strategy and the Occurrence of Fatigue in 4000-M Cycling Time Trials. *Medicine & Science in Sports & Exercise August* 38: 1484-1491.

Hoes JJ, Binkhorst RA, Smeekes-Kuyl AE and Vissers AC. (1968) Measurement of Forces Exerted on Pedal and Crank During Work on a Cycle Ergometer at Different Workloads. *Internationale Zeitschrift for Angeuandte Physiologie, Einschliesslich Arbeitsphysiolgie* 26: 33-42.

Hopkins W. (2006) *Reliability from Consecutive Pairs of Trials (Excel Spreadsheet). In: A New View of Statistics. Sportsci.Org: Internet Society for Sport Science* (Web): sportsci.org/resource/stats/xrely.xls, Accessed on: 25/07/06 2006

Houtz SA and Fischer FJ. (1959) An Analysis of Muscle Action and Joint Excursions During Exercise on a Stationary Bicycle. *Journal of joint and bone surgery (American)* 41: 123-131.

Howell DC. (1992) *Statistical Methods for Psychology.* Belmont, California: Duxubury.

Hull ML and Davis RR. (1981) Measurement of Pedal Loading in Bicycling: I. Instrumentation. *Journal of Biomechanics* 14: 843-856.

Hull ML and Gonzalez HK. (1988) Bivariate Optimization of Pedalling Rate and Crank Length in Cycling. *Journal of Biomechanics* 21: 839-849.

Hull ML and Gonzalez HK. (1990) The Effect of Pedal Platform Height on Cycling Biomechanics. *International Journal of Sport Biomechanics* 6: 1-17.

Hull ML and Jorge M. (1985) A Method for Biomechanical Analysis of Bicycle Pedalling. *Journal of Biomechanics* 18: 631-644.

Hunter SK, Duchateau J and Enoka RM. (2004) Muscle Fatigue and the Mechanisms of Task Failure. *Exercise and Sport Science Reviews* 32: 44-49.

Ikegawa S, Shinohara M, Fukunaga T, Zbilut JP and Webber CL, Jr. (2000) Nonlinear Time-Course of Lumbar Muscle Fatigue Using Recurrence Quantifications. *Biological Cybernetics* 82: 373-82.

Inbar O, Dotan R, Trousil T and Dvir Z. (1983) The Effect of Bicycle Crank-Length Variations Upon Power Performance. *Ergonomics* 26: 1139-1146.

Jobson S, Nevill A, Palmer G, Jeukendrup A, Doherty M and Atkinson G. (2006) The Ecological Validity of Laboratory Cycling: Does Body Size Explain the Difference between Laboratory- and Field-Based Cycling Performance? *Journal of Sports Sciences*: 1-7.

Johnston RB, 3rd, Howard ME, Cawley PW and Losse GM. (1998) Effect of Lower Extremity Muscular Fatigue on Motor Control Performance. *Medicine & Science in Sports & Exercise* 30: 1703-7.

Jones SM and Passfield L. (1998) The Dynamic Calibration of Bicycle Power Measuring Cranks. In: *The Engineering of Sport*, edited by Haake SJ. Oxford: Blackwell science, 265-275.

Kaneko M and Yamazaki T. (1978) Internal Mechanical Work Due to Velocity Changes in Working on a Bicycle Ergometer. *Biomechanics VI-A*, edited by Jorgensen K, Baltimore, MD. University Park Press, 86-92.

Kautz SA, Feltner ME, Coyle EF and Baylor AM. (1991) The Pedalling Technique of Elite Endurance Cyclists: Changes with Increasing Workload at Constant Cadence. *International Journal of Sport Biomechanics* 7: 29-53.

Kautz SA and Hull ML. (1991) The Relationship between Mechanical Energy Expenditure and Internal Work During Cycling. *Advances in Bioengineering. ASME* 27: 57-60.

Kautz SA and Hull ML. (1993) Theoretical Basis for Interpreting the Force Applied to the Pedal in Cycling. *Journal of Biomechanics* 26: 155-165.

Kautz SA and Hull ML. (1995) Dynamic Optimization Analysis for Equipment Setup Problems in Endurance Cycling. *Journal of Biomechanics* 28: 1391-1401.

Kennedy PW, Wright DL and Smith GA. (1989) Comparison of Film and Video Techniques for Three-Dimensional DLT Reproduction. *International Journal of Sport Biomechanics* 5: 457-460.

Kerwin DG. (1994) Video and Cinefilm Digitisation Accuracy. *Proceedings of the Biomechanics section of The British Association of Sport and Exercise Sciences*, 21-24.

Kerwin DG and Challis JH. (1989) Correspondence: The Selection of Filtering and Differentiating Techniques for Biomechanical Data. *Journal of Sport Sciences* 7: 175-177.

Klein PJ and DeHaven JJ. (1995) Accuracy of Three-Dimensional Linear and Angular Estimates Obtained with the Ariel Performance Analysis System. *Archives of Physical Medicine and Rehabilitation* 76: 183-189.

Knutzen KM and Schot PK. (1987) The Influence of Foot Position on Knee Joint Kinematics During Cycling. *Biomechanics X-A*, edited by Jonsson B, Champaign, Illinois. Human Kinetics Publishers, 599-603.

Lafortune MA and Cavanagh PR. (1980) Force Effectiveness During Cycling. *Medicine and Science in Sports* 12: 95.

Lafortune MA and Cavanagh PR. (1983) Effectiveness and Efficiency During Bicycle Riding. *Biomechanics VII- A and B, Proceedings of the 8th International Congress of Biomechanics*, edited by Kobayashi K, Nagoya, Japan. Human Kinetics, 928-936.

Lafortune MA, Cavanagh PR, Valiant GA and Burke ER. (1983) A Study of the Riding Mechanics of Elite Cyclists. *Medicine and Science in Sports and Exercise* 15: 113.

Lawton EW, Martin DT and Lee H. (1999) Validation of SRM Power Cranks Using Dynamic Calibration. *5th International Olympic Committee Congress on Sport Sciences*, Sydney, 199.

Lewek M, Rudolph K, Axe M and Snyder-Mackler L. (2002) The Effect of Insufficient Quadriceps Strength on Gait after Anterior Cruciate Ligament Reconstruction. *Clinical Biomechanics* 17: 56-63.

Li L and Caldwell G. (2000) Task Specific Coordination of Leg Muscles During Cycling. *Proceedings of the XVIII International Symposium on Biomechanics in Sport*, Hong Kong. The Chinese University of Hong Kong, 215-222.

Lindsay MR. (1996) A Comparison of Automatic and Manual Data Collection Systems. *Proceedings of the Biomechanics Section of the British Association of Sport and Exercise Sciences*, edited by Watkins J, Loughborough University, 6-8.

Mann RV, Sprague P, Coley P and Schultz C. (1980) Kinetic Patterns of Human Locomotion- Walking, Jogging, Running and Sprinting. *Medicine and Science in Sports and Exercise* 12: 92.

Marsh AP, Martin PE and Sanderson DJ. (2000) Is a Joint Moment-Based Cost Function Associated with Preferred Cycling Cadence? *Journal of Biomechanics* 33: 173-180.

Martin JC, Miliken DL, Cobb JE, McFadden KL and Coggan AR. (1998) Validation of a Mathematical Model for Road Cycling Power. *Journal of Applied Biomechanics* 14: 276-291.

Maughan R and Gleeson M. (2004) *The Biochemical Basis of Sports Performance.* Oxford, UK: Oxford University Press.

McArdle WD, Katch FL and Katch VL. (1996) *Exercise Physiology, Energy Nutrition and Human Performance.* Baltimore, USA: Williams and Wilkins.

Miller N and Seireg A. (1977) Effect of Load, Speed and Activity History on the EMG Signal from Intact Human Muscle. *Journal of Bioengineering* 1: 147.

Mohr M, Krustrup P and Bangsbo J. (2005) Fatigue in Soccer: A Brief Review. *Journal of Sport Sciences* 23: 593-599.

Mornieux G, Zameziati K, Mutter E, Bonnefoy R and Belli A. (2006) A Cycle Ergometer Mounted on a Standard Force Platform for Three-Dimensional Pedal Forces Measurement During Cycling. *Journal of Biomechanics* 39: 1296-1303.

Morris C. (1992) Academic Press Dictionary of Science and Technology. San Diego, California: Academic Press.

Neptune RR and Herzog W. (2000) Adaptation of Muscle Coordination to Altered Task Mechanics During Steady-State Cycling. *Journal of Biomechanics* 33: 165-172.

Neptune RR and Hull ML. (1995) Accuracy Assessment of Methods for Determining Hip Movement in Seated Cycling. *Journal of Biomechanics* 28: 423-437.

Neptune RR and Hull ML. (1996) Methods for Determining Hip Movement in Seated Cycling and Their Effect on Kinematics and Kinetics. *Journal of Applied Biomechanics* 12: 493-507.

Neptune RR, Kautz SA and Zajac FE. (2000) Muscle Contributions to Specific Biomechanical Functions Do Not Change in Forward Versus Backward Pedalling. *Journal of Biomechanics* 33: 155-164.

Newmiller J, Hull ML and Zajac FE. (1988) A Mechanically Decoupled Two Force Component Bicycle Pedal Dynamometer. *Journal of Biomechanics* 21: 375-386.

Nieman H and Takala EP. (1996) Evidence of Deterministic Chaos in the Myoelectric Signal. *Electromyography and Clinical Neurophysiology* 36: 49-58.

Noakes TD. (1998) Maximal Oxygen Uptake: "Classical" Versus "Contemporary" Viewpoints: A Rebuttal. *Medicine and Science in Sports and Exercise* 30: 1381-1398.

Noakes TD. (2000) Physiological Models to Understand Exercise Fatigue and the Adaptations That Predict or Enhance Athletic Performance. *Scandinavian Journal of Medicine and Science in Sports* 10: 123-145.

Noltingk BE. (1996) Measurement of Strain. In: *Instrumentation Reference Book* (2nd ed.), edited by Noltingk BE. Oxford, England: Butterworth-Heinmann, 4.67-4.108.

Nordeen KS and Cavanagh PR. (1976) Simulation of Lower Limb Kinematics During Cycling. In: *Biomechanics V-B*, edited by Komi PV. Baltimore, Maryland: University Park Press, 26-33.

Nummela A, Rusko H and Mero A. (1994) EMG Activities and Ground Reaction Forces During Fatigued and Non-Fatigues Sprinting. *Medicine and Science in Sports and Exercise* 26: 605-609.

Nyland JA, Caborn DNM, Shapiro R and Johnson DL. (1999) Crossover Cutting During Hamstring Fatigue Produces Transverse Plane Knee Control Deficits. *Journal of Athletic Training* 34: 137-143.

O'Donovan G and Anderson R. (2000) Does Fatigue Alter Kinematics of the Rowing Stroke over the Racing Distance? *5th Annual conference of the European College of Sport Science*, edited by Komulainen J, Jyväskylä, Finland, 541.

Palmer GS, Dennis SC, Noakes TD and Hawley JA. (1996) Assessment of the Reproducibility of Performance Testing on an Air-Braked Cycle Ergometer. *International Journal of Sports Medicine* 17: 293-298.

Palmer GS, Hawley JA, Dennis SC and Noakes TD. (1994) Heart Rate Response During a 4-d Cycle Stage Race. *Medicine and Science in Sports and Exercise* 26: 1278-1283.

Patterson RP and Moreno MI. (1990) Bicycle Pedalling Force as a Function of Cadence and Power Output. *Medicine and Science in Sports and Exercise* 22: 512-526.

Perell KL, Gregor RJ and Scremin EAM. (1998) Lower Limb Cycling Mechanics in Subjects with Unilateral Cerebrovascular Accidents. *Journal of Applied Biomechanics* 14: 158-179.

Pierson-Carey CD, Brown DA and Dairaghi CA. (1997) Changes in Resultant Pedal Reaction Forces Due to Ankle Immobilization During Pedalling. *Journal of Applied Biomechanics* 13: 334-346.

Pope J. (1979) *British Society of Strain Measurement Reference Book*. Newcastle, England: British Society of Strain Measurement.

Price D and Donne B. (1997) Effect of Variation in Seat Tube Angle at Different Seat Heights on Submaximal Cycling Performance in Man. *Journal of Sport Sciences* 15: 395-402.

Prilutsky BI, Gregor RJ, Albrecht AM and Ryan MM. (1997) Two Cycling Techniques, One Strategy of Muscle Co-Ordination? *Abstracts of the American Society of Biomechanics Meeting*, South Carolina, 62

Rodacki ALF, Fowler NE and Bennet SJ. (2001) Vertical Jump Coordination: Fatigue Effects. *Medicine and Science in Sports and Exercise* 33: 105-116.

Rowe T, Hull ML and Wang EL. (1998) A Pedal Dynamometer for Off-Road Bicycling. *Journal of Biomechanical Engineering* 120: 160-4.

Rudolph K, Eastlack ME, Axe M and Snyder-Mackler L. (1998) Movement Patterns after Anterior Cruciate Ligament Injury: A Comparison of Patients Who Compensate Well for the Injury and Those That Require Operative Stabilization. *Journal of Electromyography and Kinesiology* 8: 349-362.

Rugg SG and Gregor RJ. (1987) The Effect of Seat Height on Muscle Lengths, Velocities and Moment Arm Lengths During Cycling. *Journal of Biomechanics* 20: 899.

Sanderson DJ. (1986) An Application of Computer Based Real-Time Data Acquisition and Feedback System. *International Journal of Sports Biomechanics* 2: 210-214.

Sanderson DJ. (1987) *The Use of Augmented Feedback for the Modification of Riding Mechanics of Inexperienced Cyclists.* (PhD): Pennsylvania State University.

Sanderson DJ and Black A. (2003) The Effect of Prolonged Cycling on Pedal Forces. *Journal of Sports Sciences* 21: 191-199.

Sanderson DJ and Cavanagh PR. (1990) Use of Augmented Feedback for the Modification of the Pedalling Mechanics of Cyclists. *Canadian Journal of Sport Sciences* 15: 38-42.

Sargeant AJ and Davies CTM. (1977) Forces Applied to Cranks of a Bicycle Ergometer During One- and Two-Leg Cycling. *Journal of Applied Physiology* 42: 514-518.

Sargeant AJ and Greig C. (1988) Maximal Leg Force and Proportional Utilisation During Cycling. *Biomechanics XI-B*, edited by Van Schenau GJ, Amsterdam. Free University Press, 907-909.

Sarre G, Lepers R and van Hoecke J. (2005) Stability of Pedalling Mechanics During a Prolonged Cycling Exercise Performed at Different Cadences. *Journal of Sport Sciences* 23: 693-701.

Scott R. (1889) *Cycling, Art, Energy and Locomotion.* Philadelphia: J.B. Lippincott Co.

Shapiro R, Blow C and Rash G. (1987) Video Digitizing Analysis System. *International Journal of Sport Biomechanics* 3: 80-86.

Sharp A. (1896) *Bicycles and Tricycles (Re-Published 1989).* Cambridge, MA

Sharp B. (1992) *Acquiring Skill in Sport.* Eastbourne, UK: Sports Dynamics.

Shennum PL and DeVries HA. (1976) The Effect of Saddle Height on Oxygen Consumption During Bicycle Ergometer Work. *Medicine and Science in Sports and Exercise* 8: 119-121.

Siler WL and Martin PE. (1991) Changes in Running Patterns During a Treadmill Run to Volitional Exhaustion: Fast Versus Slow Runners. *International Journal of Sports Biomechanics* 7: 12-28.

Smak W, Neptune RR and Hull ML. (1999) The Influence of Pedalling Rate on Bilateral Asymmetry in Cycling. *Journal of Biomechanics* 32: 899-906.

Smith BK, Wilson DJ, Keegan KG and Thomas TR. (1997) The Effects of Marker Size on the Accuracy of the Ariel Performance Analysis System (APASTM). *Proceedings of the XV International Symposium on Biomechanics in Sports*, edited by Zimmermann WJ, Texas. Texas Woman's University Press, 169-175.

Soden PD and Adeyefa BA. (1979) Forces Applied to a Bicycle During Normal Cycling. *Journal of Biomechanics* 12: 527-541.

Sprague P and Mann RV. (1983) Effects of Muscular Fatigue on the Kinetics of Sprint Running. *Research quarterly for Exercise and Sport* 50: 60-66.

Stone C and Hull ML. (1993) Rider/ Bicycle Interaction Loads During Standing Treadmill Cycling. *Journal of Applied Biomechanics* 9: 202-218.

Takaishi T, Yamamoto T, Ono T, Ito T and Moritani T. (1998) Neuromuscular, Metabolic and Kinetic Adaptations for Skilled Pedalling Performance in Cyclists. *Medicine and Science in Sports and Exercise* 30: 442-449.

Too D and Landwer GE. (2000) The Effect of Pedal Crank Arm Length on Joint Angle and Power Production in Upright Cycle Ergometry. *Journal of Sports Sciences* 18: 153-61.

Ulmer HV. (1996) Concept of an Extracellular Regulation of Muscular Metabolic Rate During Heavy Exercise in Humans by Psychophysiological Feedback. *Experientia* 52: 416-420.

Vilimek M. (2006) The Simulation of Cycling-Optimization of Sport Performance Based on Different Frequency of Pedalling. *Journal of Biomechanics, Abstracts of the 5th World Congress of Biomechanics* 39: S549.

Vincent WJ. (1995) *Statistics in Kinesiology*. Champaign, Illinois: Human Kinetics.

Webber CL, Schmidt MA and Walsh JM. (1995) Influence of Isometric Loading on Biceps EMG Dynamics as Assessed by Linear and Nonlinear Tools. *Journal of Applied Physiology* 78: 814-822.

Wheeler JB, Gregor RJ and Broker JP. (1992) A Dual Piezoelectric Bicycle Pedal with Multiple Shoe/Pedal Interface Compatibility. *International Journal of Sport Biomechanics* 8: 251-258.

Wheeler JB, Gregor RJ and Broker JP. (1995) The Effect of Clipless Pedal Design on Shoe /Pedal Interface Kinetics and Overuse Knee Injuries During Cycling. *Journal of Applied Biomechanics* 11: 119-141.

Williams KR, Snow R and Arguss C. (1991) Changes in Distance Running Kinematics with Fatigue. *International Journal of Sport Biomechanics* 7: 138-162.

Wilson DJ, Smith BK and Gibson JK. (1997) Accuracy of Reconstructed Angular Estimates Obtained with the Ariel Performance Analysis System. *Physical Therapy* 77: 1741-1746.

Wilson DJ, Smith BK, Gibson JK, Choe BK, Gaba BC and Voelz JT. (1998) Accuracy of Digitization Using Automated and Manual Methods. *Proceedings I of the XVI International Society of Biomechanics in Sport symposium*, edited by Vieten MM, Knonstantz, Germany. UVK-Universitätsverlag Konstantz, Germany, 590-592.

Winter DA. (1984) Kinematic and Kinetic Patterns in Human Gait: Variability and Compensating Effects. *Human Movement Science* 3: 51-76.

Winter DA. (1990) *Biomechanics and Motor Control in Human Movement*. New York: Wiley-Interscience.

Wood GA. (1982) Data Smoothing and Differentiation Procedures in Biomechanics. *Exercise and Sport Science Reviews* 10: 308-362.

Yoshihuku Y and Herzog W. (1990) Optimal Design Parameters of the Bicycle-Rider System for Maximal Muscle Power Output. *Journal of Biomechanics* 23: 1069-1079.

Zameziati K, Mornieux G, Rouffet D and Belli A. (2006) Relationship between the Increase of Effectiveness Indexes and the Increase of Muscular Efficiency with Cycling Power. *European Journal of Applied Physiology* 96: 274-281.

Appendices

Appendix 1: Software for analysing data from instrumented pedals.

1.1: Overview of programs

The programming task was accomplished by three separate scripts. The first of these (FP_Process) took the data file as collected with voltage readings for the strain-gauge and positional data and converted these to force and angle data respectively. The second (FP_Power) took this data and converted it from forces relative to the pedal (i.e. F_x and F_z) to those relative to the crank (i.e. F_{eff} and F_{ineff}) as well as calculating other variables of interest (work, power, IIE and α_c). The final program extracted summary data from these variables and output the results to a text file that could be used for further graphical and statistical analysis.

One of the key challenges presented by the nature of the research is the volume of data that must be collected and analysed. In particular, for the kinetic parameters where data were collected at 1 KHz continuously for up to 21 minutes (i.e. ~8.82 x 10^6 data points per trial across the 7 channels). With this volume of data, manual correction of noisy data would therefore clearly be impractical and so the software therefore had to be designed to be robust enough to automatically handle potentially noisy data without introducing errors. Much of this these programs are therefore dedicated to error trapping and error handling.

Within each script, brief explanations are given as comments at the start of each function and procedure as well as at other key points to indicate their action. Notes also indicate which variables are being passed and returned by each function and procedure. For all three scripts, global constant and variable declarations are at the start of the script together with notes as to what the declared parameters are. Similarly, local variables are declared at the start of each procedure and function and comments indicate what variables are being passed and returned. All three scripts are based around calls to the various functions and procedures from a routine which is called 'main' in all three scripts.

1.2: FP_Process

```
'= JK 06/04/04
=====================================================
' Processes data from force pedals and outputs results to a new file
'
' Version info
' ------------
'
' 1.1:
' 1.2:
' 1.3:  Array arithmetic implemented for anglesums and forcesums
' 1.4:
' 1.5:
' 1.6:  Debugging
' 1.7.1: Method for checking slope of angle channels in findcross made more robust
' 1.7.2: Method for handling zero crossings lagging data modified and flat-spots and zero
crossings sorted (use interpolation)
' 1.7.3: Modulus function in anglesums replaced as mod doesn't work properly with
negatives in Spike
'### 1.7.4: Artefacts around zero crossings sorted
' 1.8.1: Cross-effect coefficients added to calculations
' ### 1.8.2: Method for calculating cross-effect coefficients changed
' ### 1.8.3: Modified to allow for opposite negative and positives slopes for cross-effect
coefficients
' ### 1.8.5: Modified to allow for different negative and positives slopes for cross-effect
coefficients
' 1.8.6: Channel naming conventions changed so that channel designation is used to name
channels rather than source channels.
' The previous method created problems if the default channel assignment wasn't used
'
' Still to be done!
' -----------------
"
' Error handing required
' ----------------------
'
' Currently seems to handle errors okay, but not really tried to crash it yet!
'
' Known bugs
' ----------
'
' If there are more than 1 duplicate channels, checkwavs% miss reports
' the number of duplicates (this is a pretty minor bug though).
'
'=====================================================
===========

'=====================================================
===========
' Global constant declarations
'=====================================================
===========
```

```
Const arraymax%:= 3000;  ' Maximum size of array      to read/write blocks of data in
(optimised for shortest run time)
Const ver$ := "1.8.6";' Version of script

'============================================================
===========
'Global variable declarations
'============================================================
===========
Var v1% := 0;                ' Current view number
Var er%;                     ' Used for error codes
Var i%,j%;                   ' Looping variables
Var wavlist%[7];             ' Array to hold list of channels for processing in order: crank, L
pedal, R pedal, LFx, LFy, Rfx, RFy
Var fzpre[4];              ' Array for pre test zero offsets (LFx, LFy, Rfx, Rfy)
Var fzslope[4];            ' Array for slopes of zero offset (LFx, LFy, Rfx, Rfy)
Var fcalib[12];            ' Array for calibration slopes (DLFx, DLFy, DRfx, DRfy, CLFy, CLFx,
CRfy, CRfx (pos then neg))
Var anglezero[3];            ' Array for crank, left pedal and right pedal zero offsets (in that
order)
Var zeros[15000];            ' Array for zero crossing times
Var rwarray[arraymax%][2];' Array for reading/writing data to/from, Fx, Fy

'============================================================
===========
' Main procedures
'============================================================
===========


' ------------------------------------------------------------------
Proc Choosev(times%[]); 'Choose the time view to be used                (Array of time view
handles)
   Var title$;                ' Variable to return view titles to
   Var timetitle$[20];        ' Array for time view titles
   Var dummy%;                        ' Variable to return item selected in dialogue to

   For i% := 1 to times%[0] Do' Fill an array with time view titles
      View(times%[i%]);
      title$ := windowtitle$();
      timetitle$[i%-1]:= title$;  ' (timelist%[0]=No of time views)
   Next
   timetitle$[times%[0]] := "- New file -";        'Add new file option to list
   DlgCreate("Time views already open!",0,0,0,0);
   DlgList(1,"Select time view",timetitle$[],(times%[0]+1));
   er% := DlgShow(dummy%);
   If er% < 1 Then    ' user cancelled
      leaveall();
   EndIf
   If dummy% = times%[0] Then        ' new file selected
      getfile();
   Else
      v1% := times%[dummy%+1]; 'returns selected view as active view (+1 since 0 is No
of views)
   EndIf
```

```
End

' ------------------------------------------------------------------
Proc getfile()
    v1% := FileOpen("",0,1);
    If v1% <= 0 Then
    Message ("No file!");
        leaveall();
    EndIf
End

' ------------------------------------------------------------------
Proc leaveall()       'quits program
    Var lvall%;          ' Quit script?

    lvall% := Query("Quit script?|Quit?");
    If lvall% Then
        halt
    Else
        main();
    EndIf
End

' ------------------------------------------------------------------
Proc checkfile() ' Checks that opened file is appropriate
    Var waves%[1];    ' Dummy array for waveform channels
    Var numwavs%;    ' Number of waveform channels found

    numwavs% := Chanlist(waves%[],8193);      ' fill arary with waveform channel numbers
    If numwavs% < 7 Then
        Message ("Incompatible file!|Only %d waveform channel(s) founds\nProgram requires
7",numwavs%);
        leaveall();
    EndIf
End

' ------------------------------------------------------------------
Func savenew%(); ' Creates a new time view to write processed channels to
    Var abort%;          ' Abort trying to save
    Var msgstring$;' String for using in prompt
    Var filestring$;  ' String for default file name

    filestring$:=FileName$(3)+"_p";
    msgstring$:="Save prcossed data from "+WindowTitle$()+" as...";
    er% := FileSaveAs(filestring$,0,0,msgstring$);          ' Save copy of file.
    If er% <0 Then' File save unsuccesful
        abort% := Query("Could not save file|Abort save?");
        If abort% = 1 Then    ' Yes selected
            er% := Query("Delete new channels?");
            If er% = 1 Then
                binselect();
            EndIf
        leaveall();
        EndIf
    Else
```

```
    EndIf

    Return (er%)    ' Return error code
End

' ---------------------------------------------------------------------
Proc getch()     ' Procedure to identify channels
    Var waves%[32];  ' Dummy array for waveform channels
    Var numwavs%;    ' Number of waverform channels returned

    numwavs% := Chanlist(waves%[],8193);
    For i% := 1 to numwavs% Do                                  ' Get channels with
matching names
        DoCase
            Case ChanTitle$(waves%[i%]) = "crank" Then wavlist%[0] := waves%[i%];
            Case ChanTitle$(waves%[i%]) = "L_pedal" Then wavlist%[1] := waves%[i%];
            Case ChanTitle$(waves%[i%]) = "R_pedal" Then wavlist%[2] := waves%[i%];
            Case ChanTitle$(waves%[i%]) = "L_Fx" Then wavlist%[3] := waves%[i%];
            Case ChanTitle$(waves%[i%]) = "L_Fy" Then wavlist%[4] := waves%[i%];
            Case ChanTitle$(waves%[i%]) = "R_Fx" Then wavlist%[5] := waves%[i%];
            Case ChanTitle$(waves%[i%]) = "R_Fy" Then wavlist%[6] := waves%[i%];
        EndCase
    Next

    DlgCreate("Please identify channels",0,0);     ' Display dailogue to allow user to alter if
needed
    DlgChan(1,"Crank channel",8193);
    DlgChan(2,"Left pedal channel",8193);
    DlgChan(3,"Right pedal channel",8193);
    DlgChan(4,"Left Fx channel",8193);
    DlgChan(5,"Left Fy channel",8193);
    DlgChan(6,"Right Fx channel",8193);
    DlgChan(7,"Right Fy channel",8193);
    er% :=
DlgShow(wavlist%[0],wavlist%[1],wavlist%[2],wavlist%[3],wavlist%[4],wavlist%[5],wavlist
%[6]);
    If er% = 0 Then
        leaveall();
    EndIf

    For i% := 0 to 6 Do             ' Dump channel list to log
        PrintLog("Channel %d = %s\n",wavlist%[i%],ChanTitle$(wavlist%[i%]));
    Next
End

' ---------------------------------------------------------------------
Func checkch%(); 'Check that none of the channels selected are duplicates
    Var k%;          ' Looping variable
    Var n% := 0;           ' Number of duplicates found

    For j% := 0 To 6 Do
        k% := j% + 1;
        While k%<6 Do
            If wavlist%[j%] = wavlist%[k%] Then
            n% += 1;
```

```
            EndIf
            k% += 1;
        Wend
    Next
    If n% >0 Then
        Message("Error!|%d duplicate channels found",n%);
    EndIf
    Return(n%);
End

' ---------------------------------------------------------------------
Func getzerodrift%()  ' Get the 0 offsets, time of 0 offsets, time of start of data collection,
Pedal and crank values at TDC, crank length and Fx, Fy slopes
    Var fzpost[4];              ' Array for post test zero offsets (LFx, LFy, Rfx, Rfy)
    Var Postt%;                 ' Time post test zero offeset values taken (relative to first,
seconds)
    Var startt%;                ' Time test started
    Var maxoffset% := 5000;     ' Magnitude of maximum permissable zero offset (normally
200)

    DlgCreate("Enter Fx and Fy zero offsets",0,0);
    DlgText("Values taken prior to test",1,1);
    DlgReal(1,"Left Fx offset",maxoffset%*-1,maxoffset%,24,2);
    DlgText("mV",37,2);
    DlgReal(2,"Left Fy offset",maxoffset%*-1,maxoffset%,24,3);
    DlgText("mV",37,3);
    DlgReal(3,"Right Fx offset",maxoffset%*-1,maxoffset%,24,4);
    DlgText("mV",37,4);
    DlgReal(4,"Right Fy offset",maxoffset%*-1,maxoffset%,24,5);
    DlgText("mV",37,5);
    DlgText("Values taken after test",1,7);
    DlgReal(5,"Left Fx offset",maxoffset%*-1,maxoffset%,24,8);
    DlgText("mV",37,8);
    DlgReal(6,"Left Fy offset",maxoffset%*-1,maxoffset%,24,9);
    DlgText("mV",37,9);
    DlgReal(7,"Right Fx offset",maxoffset%*-1,maxoffset%,24,10);
    DlgText("mV",37,10);
    DlgReal(8,"Right Fy offset",maxoffset%*-1,maxoffset%,24,11);
    DlgText("mV",37,11);
    DlgInteger(9,"Time post offset taken",1,7200,24,13);
    DlgText("Secs",37,13);
    DlgInteger(10,"Time test started",1,7200,24,14);
    DlgText("Secs",37,14);
    er% :=
DlgShow(fzpre[0],fzpre[1],fzpre[2],fzpre[3],fzpost[0],fzpost[1],fzpost[2],fzpost[3],postt%,st
artt%);
    If er% = 0 Then
        leaveall();
    EndIf
    PrintLog("\nSlopes of pedal drift (mV/min)");
    PrintLog("\nLFx\t\tLFy\t\tRFx\t\tRFy\n");
    For j% := 0 To 3 Do
        Fzslope[j%] := (fzpost[j%]-fzpre[j%])/postt%;
        PrintLog("%.5f\t\t", fzslope[j%]*60);
    Next
```

```
    PrintLog("\n");
    Return(startt%);   ' Return time test started
End

' ------------------------------------------------------------------
Proc getpedaloffs()' Get the pedal and crank offsets and crank length
    DlgCreate("Enter Crank and pedal offsets",0,0);
    DlgReal(1,"Crank zero offset",-5,5,36,1);
    DlgText("volts",49,1);
    DlgReal(2,"Left pedal zero offset",-5,5,36,2);
    DlgText("volts",49,2);
    DlgReal(3,"Right pedal zero offset",-5,5,36,3);
    DlgText("volts",49,3);
    er% := DlgShow(anglezero[0], anglezero[1], anglezero[2]);
    If er% = 0 Then
        leaveall();
    EndIf
End

' ------------------------------------------------------------------
Proc getforcecalib()    ' Get force calibration slopes
    Var max% := 1000000;                ' Maximum acceptable value for slope (5)
    Var l1%, l2%, l3%;            ' Looping variables
    Var text$, lr$, dc$, xy$;     ' strings for text output
    Var gap%:=0;                  ' Create gaps between slopes

    '========================== Default calibration slope values
==========================
    fcalib[0]:= 1.237737672;    ' LFx- Direct
    fcalib[1]:= 0.403355568;    ' LFy
    fcalib[2]:= 1.088467403;    ' RFx
    fcalib[3]:= 0.357709229;    ' RFy

    fcalib[4]:= -0.060134077;   ' LFx- Cross +ve
    fcalib[5]:= 0.00042159;     ' LFy
    fcalib[6]:= -0.06941123;    ' RFx
    fcalib[7]:= -0.011160975;   ' RFy

    fcalib[8]:= 0.001892628;    ' LFx- Cross -ve
    fcalib[9]:= -0.012457137;   ' LFy
    fcalib[10]:= 0.035393491;   ' RFx
    fcalib[11]:= -0.137010883;  ' RFy
    '=========================================================
==================================

    DlgCreate("Enter pedal calibration coefficients",0,0,0);
    For l1%:= 0 to 2 Do   'direct, cross +ve, cross -ve)
        gap%+=1;
        DoCase
            case l1%=0 Then dc$:="direct ";
            case l1%=1 Then dc$:="cross +ve ";
            case l1%=2 Then dc$:="cross -ve ";
        EndCase
        For l2%:=0 to 1 Do ' left and right
            If l2%=0 then
```

```
            lr$:="Left ";
         Else
            lr$:="Right ";
         EndIf
         For l3%:=0 to 1 Do ' x and y
            If l3%=0 Then
               xy$:="Fx ";
            Else
               xy$:="Fy ";
            EndIf
            text$:=lr$+xy$+dc$;
            DlgReal(l1%*4+l2%*2+l3%+1,text$,max%*-
1,max%,19,l1%*4+l2%*2+l3%+1+gap%);
            DlgText("mV/N",32,l1%*4+l2%*2+l3%+1+gap%);
         Next
      Next
   Next
   er% := DlgShow(fcalib[]);
   If er% = 0 Then
      leaveall();
   EndIf
   PrintLog("\nCalibration coefficients\nChannel\t\tDirect\t\tCross+\t\tCross-\n");
   For l1%:=0 to 3 Do
      DoCase
         Case l1%=0 Then  text$:="LFx";
         Case l1%=1 Then  text$:="LFy";
         Case l1%=2 Then  text$:="RFx";
         Case l1%=3 Then  text$:="RFy";
      EndCase

   PrintLog("%s\t\t%#.6f\t%#.6f\t%#.6f\n",text$,fcalib[l1%],fcalib[l1%+4],fcalib[l1%+8])
;
   Next
End

' ---------------------------------------------------------------------
Func findcross%(cmin,cmax)    ' Finds zero crossings and write their times to an array
(Minimum and maximum value in channel)
   Const slopesize% := 1000;   ' Size of array to read slope check data into

   Var zeroev%;                ' Channel for zero crossing events
   Var slopecheck[slopesize%];' Small array to check direction of slope
   Var er%;                    ' Used for error handling
   Var slope;                  ' slope value;
   Var slopetype%;             ' Whether a -ve (2) or +ve slope (3) used in event
extraction
   Var numcross%;                    ' Number of zero crossings in channel
   Var t;                      ' Time of event crossing
   Var readt;                  ' Time block to read
   Var level;                  ' Level to detect threshold crossings at

   zeroev% := MemChan (2);  ' Create event channel
   If zeroev% < 1 Then
      Message("ERROR!|Unable to create memory channels");
      leaveall();
```

```
    EndIf
    ChanTitle$(zeroev%,ChanTitle$(wavlist%[i%])+"_ev");
    readt := (slopesize%-1)*binsize(wavlist%[i%])/2;
    er% := ChanData(wavlist%[i%],slopecheck[],MaxTime(wavlist%[i%])/2-
readt,readt+MaxTime(wavlist%[i%])+readt); 'Read from middle of file to avoid probs if not
pedalling at start/ end
    If er% <1 Then
        Message("ERROR!|Data read error!");
        leaveall();
    EndIf
    For j% := 0 to slopesize% -6 Do
        If ABS((slopecheck[j%+5]-slopecheck[j%])) <0.5 Then ' Don't add zero crossings
            slope += (slopecheck[j%+5]-slopecheck[j%]);
        EndIf
    Next
    If slope >0 Then ' Positive slope
        slopetype% := 3;
        level := cmax-1
    Else
        slopetype% := 2;
        level := cmin+1
    EndIf
    MemImport(zeroev%,wavlist%[i%],0,MaxTime(wavlist%[i%]),slopetype%,0.4,level);
    numcross%:= MemGetItem(zeroev%,0); ' Get number of zero crossings in channel
    For j% := 1 To numcross% Do
        t := MemGetItem(zeroev%,j%);
        If t <0 Then
            Message("ERROR!|Data read error\n\nEvent time read= %g!",t);
            leaveall();
        EndIf
        zeros[j%] := t; ' Fill array with zero crossing times
    Next
    er% := ChanDelete(zeroev%,0);                ' Finished with event channel so get rid of it
(don't ask just do it!)
    If er% <0 Then
        Message("ERROR!|Could not delete event channel %d",zeroev%);
        leaveall();
    EndIf
    Return (numcross%);
End

' ------------------------------------------------------------------
Func getmin(ch%) ' Gets minimum values in angle channels (channel to get value from)
    Var min1 := -5,min2; ' Mimimum values found
    Var stt := 0;        'Start time for finding minimum
    Var endt;            'End time for finding minimum

    For j% := 0 To 2 Do
        endt:= Maxtime(ch%)*(j%+1)/3;
        min2 := (ChanMeasure(ch%,9,stt,endt));
        If min2 > min1 Then min1 := min2; EndIf' Use highest to avoid didgy dodgy data
        stt:=endt;
    Next
    Return (min1)
End
```

```
' ------------------------------------------------------------------
Func getmax(ch%)' Gets maximum values in angle channels (channel to get value from)
   Return(ChanMeasure(ch%,8,0,Maxtime(ch%)));
End

' ------------------------------------------------------------------
Func readwav (ch%,t,el%,xy%)' Read wave data into an array (Channel to read, time to
read from, number of elements to read, index to read into (0,1))
   Var readsize%;     ' Number of data points read in
   Var readt;         ' Time of last data point read in
   Var maxreadtime;        ' The maximum amount of time that can be read into array

   readt:= (el%)*binsize(ch%);          ' Calculate time window that will fit it the array
   If readt+t > MaxTime(ch%) Then     ' Would read from beyond end of file
      readt := MaxTime(ch%)-t;
   EndIf
   readsize% := ChanData(ch%,rwarray[][xy%],t,t+readt);      ' Read in array full
   If readsize% <1 Then
      Message("ERROR!|Data read error!");
      leaveall();
   EndIf
   Return (t+readt);
End

' ------------------------------------------------------------------
Proc writewav(memch%,t,x%,rw%);     ' Write array data to wav channel (Channel to write
to, time to start write from, number of elements to write, index of rwarray to write)
   MemSetItem(memch%,0,t,rwarray[0:x%][rw%]);     ' Write data to memory channel
End

' ------------------------------------------------------------------
Func dupwav%(wChan%) 'Copy waveform to a memory channel
   var mc%;

   If ChanKind(wChan%)<>1 then return 0 endif; 'Not a waveform!
   mc% := MemChan(1,0,BinSize(wChan%));    'Create waveform channel
   If mc% < 1 Then
      Message("ERROR!|Unable to duplicate channels");
      leaveall();
   EndIf
  ChanScale(mc%, ChanScale(wChan%));                              'Copy scale
  ChanOffset(mc%, ChanOffset(wChan%));                          '...and offset...
  ChanUnits$(mc%, ChanUnits$(wChan%));                          '...and units
  ChanTitle$(mc%, ChanTitle$(wavlist%[i%])); '... and title
  MemImport(mc%, wChan%, 0, MaxTime());                         'Copy data
   ChanShow(mc%); ' Show new channel (has to be shown to be able to select it!)
   ChanSelect(mc%,1);                    'Flag new channel for deletion
   Return mc%;  'Return the new channel number
End;

' ------------------------------------------------------------------
Func createwav%(ymin,ymax,unit$)     ' Create wav channel (min and max Y range)
   Var chanmem%;   ' Handle of channel created
```

```
    chanmem% := MemChan(1,0,BinSize(wavlist%[i%]));          ' Create waveform channel
to write to
    If chanmem% < 1 Then
        Message("ERROR!|Unable to create memory channels");
        leaveall();
    EndIf
    ChanUnits$(chanmem%,unit$);
    ChanScale(chanmem%,1000);
    FrontView(v1%);
    YRange(chanmem%,ymin,ymax);
    ChanShow(chanmem%);
    ChanSelect(chanmem%,1); ' Set channel as selected (used for export)
    Return(chanmem%);      ' Handle of channel created
End

' ---------------------------------------------------------------------
Proc fixzeros(ch%,ncross%);     ' Correct dodgy data at zero crossings (Channel to process,
number of zero crossings in channel)
    Const win% := 40;' Size of array to read in
    Var zeroel%;        ' Element of array containing zero crossing
    Var k%;             ' Counting variable
    Var t;            ' Time to start read from
    Var slope1;         ' Slope of line before zero crossing
    Var slope2;         ' Slope of line after zero crossing

    For j% := 0 to ncross%-1 Do
        t:= zeros[j%]-(win%/2)*BinSize(wavlist%[i%]);
        If t<0 Then ' If have zero crossing right at start of file
            t:= 0;
        EndIf
        readwav (wavlist%[i%],t,win%,0);                    ' Call wav read function (channel to
read from, time to read from, read size, rwarray index)
        slope1 := 0;
        slope2 := 0;
        For k%:=0 to 5 Do ' Only use first and last six points
            slope1+=rwarray[k%+1][0]-rwarray[k%][0];
        Next
        slope1 /= 6;
        For k%:=win%-7 to win%-2 Do
            slope2+= (rwarray[k%+1][0]-rwarray[k%][0]);
        Next
        slope2 /= 6;
        slope1 +=slope2;
        slope1/=2;
        For k% := 6 to win%/2 Do          ' Fill array with interpolated data
        '### NOTE this is susceptible to distortion by bad data since extrapolates from a
single point. However, in practice it seems to
        ' be okay since the data is pretty clean
            rwarray[k%][0] := rwarray[k%-1][0]+slope1;
        Next
        For k% := win%-8 to win%/2+1 Step -1 Do
            rwarray[k%][0] := rwarray[k%+1][0]-slope1;
        Next
        For k%:=0 to win%-1 Do
```

```
        If rwarray[k%][0] <-0.5 AND k% >0 Then      ' Take out bad data (k%>0 just so
wouldn't crash if bad data in first array element)
            rwarray[k%][0]:=rwarray[k%-1][0];
        EndIf
    Next
      writewav(wavlist%[i%],t,win%-1,0);
  Next
End
' ------------------------------------------------------------------
'Func modulus(val,div);   ' Calculate modulus of array (value, divisor) [mod function doesn't
work properly with negatives]
'   val:= val-div*round(val/div-0.49999999);
'   Return(val);
'End

' ------------------------------------------------------------------
Proc anglesums(cmin, cmax)' Convert voltages to degrees allowing for offsets (min and max
values in channel)
  Var modsum[arraymax%];   ' Temporary array for doing modulus calc

  ArrSub(rwarray[][0],anglezero[i%]);
  ArrMul(rwarray[][0],(360/(cmax-cmin)));
  If i% = 1 then  ' Left pedal
    ArrAdd(rwarray[][0],180); 'offset left pedal by 180 degrees
  Else
    ArrSubR(rwarray[][0],360);        ' Reverse slopes
  EndIf
  ArrConst(modsum[],rwarray[][0]);  ' Copy rwarray to temp array     }
  ArrDiv(modsum[],360);             ' n-d
      }
  ArrSub(modsum[],0.49999999);              ' int (n-d)
      } just does MOD
  Round(modsum[]);                  ' "    "
  }
  ArrMul(modsum[],360);             ' 360 * int (n-d)                                    }
  ArrSub(rwarray[][0],modsum[]);    ' n - 360 * int (n-d)                          }
End


' ------------------------------------------------------------------
Proc forcesums(ch%,time[]) ' Convert force channels to actual forces     (Channel to
process, time array)
  Var sumsarr[arraymax%];    ' Array to use in sums
  Var temparr[arraymax%][4];' Array for holding channel data
  Var k%;                    ' looping variable

  ' Remove drift and offsets from channels
  For j% := 0 to 1 Do       ' Do for Fx and Fy
    ArrConst(sumsarr[],time[]);
  ' Copy time array onto array to use in sums
    ArrMul(sumsarr[],fzslope[i%-3+j%]);                                              '
Multiply by the drift slope
    ArrSub(rwarray[][j%],fzpre[i%-3+j%]);                                  ' Subtract
the pre-test zero offset
```

```
        ArrSub(rwarray[][j%],sumsarr[]);                                    '
Subtract the drift slope
        ' Fill temporary arrays and divide by calibration coefficients
        For k% := 0 to 1 Do  ' Do for Main and cross effects
            ArrConst(temparr[][j%*2+k%],rwarray[][j%]);                     '
Copy channel data to temp arrays
        Next
    Next
    ' Remove cross effects and divide by calibration slope
    ' NB. Cross effects x,y designation refers to the channel in which the effect appears NOT
the one in which the loading occurs.
    For j% := 0 to 1 Do        ' Do for Fx and Fy
        For k%:= 0 to arraymax%-1 Do
            If temparr[k%][2*j%+1]>0 Then        ' If positive
                temparr[k%][2*j%+1]*=fcalib[i%+2-j%];
            Else
                temparr[k%][2*j%+1]*=fcalib[i%+2-j%+4];
            EndIf
        Next
        ArrAdd(temparr[][j%*2],temparr[][j%*2+1]);              ' Remove cross effects
        If fcalib[i%-3+j%] <>0 Then                                         '
Avoid problems if entered as zero
            ArrDiv(temparr[][j%*2],fcalib[i%-3+j%]);            ' Divide by load calibration
slope
        EndIf
    Next

    ' Add to elements back to rwarray
    ' ########## This can probably be made redundant if only two temporary arrays are
used for the cross effects ######
    For j% := 0 to 1 Do        ' Do for Fx and Fy
        ArrConst(rwarray[][j%],temparr[][j%*2]);                ' Copy in main effects to
array
    Next
End

' ---------------------------------------------------------------------
Func freech%()' Find spare channel
    Var k%;  ' Counting variable
    k% := 1;
    While ChanKind(k%) <> 0 And k% <= 32 Do          ' Look for free channel
        k% += 1;
    Wend
    If k% > 32 Then' No free channels
        Message("ERROR!|No free Channels\nCannot save!");
        leaveall();
    EndIf
    Return(k%);
End

' ---------------------------------------------------------------------
Proc binselect();        ' Bin selected channels
    ChanDelete(-3,0);  ' Delete selected channels
End
```

```
' ------------------------------------------------------------------
Proc toolbarmsg(); ' Put progress info on toolbar
    Var toolbar$;                   ' String for messages for toolbar

    toolbar$ := "Processing " + ChanTitle$(wavlist%[i%]) + " channel";
    ToolbarText(toolbar$);
End

' ------------------------------------------------------------------
Proc cleanchan(tmpch%);    ' Tidy up created channels
    Var f%;  ' Handle of free channel

    f% := freech%();
    er% := MemSave(tmpch%,f%,0);
    If er% <0 Then
        Message("Error!|Could not save memory channel");
        leaveall();
    EndIf
    ChanDelete(tmpch%);
    ChanShow(f%);
    Optimise(f%);
    ChanSelect(f%,1);      ' Flag created channels for deletion
    ExportChanList(0,MaxTime(wavlist%[i%]),f%);         ' Flag channel for export
End

'============================================================
===========
' Main routine
'============================================================
===========

Proc main()
    Var offset;                 ' Zero offset value
    Var currentch%;                 ' Channel number currently processing
    Var tempch%[2];                 ' Temporary memory channels created (Fx, Fy)
    Var lastt;                  ' Last time read in
    Var t;                      ' Time to read from
    Var chmin,chmax;                ' Minimum and maximum values in channel
    Var timelist%[20];          ' Array for list of time views (assumes no more than 20)
    Var titlech$[7];            ' Title of created channel
    Var testst%;                    ' Time test started relative to first calibration
    Var times[arraymax%];       ' Array of time to multiply by in force sums
    Var arrindex%[arraymax%]; ' Array to fill with index of array (used in forcesums)
    Var numcross%;                  ' Number of zero crossings found in channel

    titlech$[0]:="CA_p";        ' Set channel names
    titlech$[1]:="LPA_p";
    titlech$[2]:="RPA_p";
    titlech$[3]:="LFx_p";
    titlech$[4]:="LFy_p";
    titlech$[5]:="RFx_p";
    titlech$[6]:="RFy_p";

    ToolbarText("Running script version " + ver$);
    Viewlist (timelist%[], 1); ' Are there any time views already open
```

```
    If timelist%[0] > 0 Then  'There are some time views
        choosev(timelist%[]);
    Else
        getfile();      ' No time views open go and get one
    EndIf
    View(v1%); ' Set returned view as active
    checkfile();
    ChanSelect(-1,0);  ' Deselect all channels or will delete anything that is selected at
program start
    PrintLog("\n\n=====>> FP_process v%s
<<=====================================>>> %s
<<<=====================================\n\n",ver$,Windowtitle$());
    Repeat
        getch();
        er% := checkch%();
    until er% = 0;
    teststt% := getzerodrift%();
    getpedaloffs();
    getforcecalib();
    ExportChanList();  ' Clear channel export list
    For j% := 0 to arraymax%-1 Do       ' Fill array with index of array (used in forcesums)
        arrindex%[j%] := j%;
    Next
    For i% := 0 to 2 Do    ' Do angle channels
============================================================
====================
        toolbarmsg();
        tempch%[0] := dupwav%(wavlist%[i%]);
        wavlist%[i%] := tempch%[0];     ' Shift flag to duplicate channel
        chmin := getmin(wavlist%[i%]);
        chmax := getmax(wavlist%[i%]);
        numcross% := findcross%(chmin,chmax); ' Find zero crossings
        If i%>0 Then ' Don't bother with crank channel
            fixzeros(wavlist%[i%],numcross%);               ' Check 0 crossing data and correct
    (Channel to process, number of zero crossings)
        EndIf
                '(channel to search, start and end time of array, min and max values in
channel)
                ' ### In theory this shouldn't be neccesary for the crank channel but without it
you do get occasional spikes around
                ' the zero crossing so leave it in there.
        chmin := getmin(wavlist%[i%]);  ' Redo as will have changed
        chmax := getmax(wavlist%[i%]); '          "                          "
    "
        tempch%[0] := createwav%(0,360,"deg");          ' Create waveform channel to write
processed angle data to (min, max y scaling, new units)
'       titlech$ := Left$(ChanTitle$(wavlist%[i%]),7)+"_p"; ' Take first 7 characters of
existing name (max len = 9) and add _p
'       ChanTitle$(tempch%[0],titlech$);
        ChanTitle$(tempch%[0],titlech$[i%]);
        t := 0;    ' Start at time = 0;
        Repeat ;
            lastt := readwav (wavlist%[i%],t,arraymax%-1,0);                ' Call wav read
function (channel to read from, time to read from, read size (full array less one or leaves
gaps), rwarray index)
```

```
            anglesums(chmin,chmax);                ' Do calculations to change voltages to
degrees etc  (min and max values in channel)
            writewav(tempch%[0],t,arraymax%-1,0);        ' Call wav write function (channel to
write to, time to write from, write size (full array), index of rwarry to write)
            t := lastt;
        Until lastt >= MaxTime(wavlist%[i%]); ' Reached end of file
        cleanchan(tempch%[0]);
    Next
    For i% := 3 to 5 Step 2 Do ' Do Force channels
============================================================
====================
        For j% := 0 to 1 Do
            tempch%[j%] := createwav%(-300,1000,"N");' Create waveform channel to write
processed force data to (min, max y scaling, New units)
'           titlech$ := Left$(ChanTitle$(wavlist%[i%+j%]),7)+"_p"; ' Take first 7 characters
of existing name (max len = 9) and add _p
'           ChanTitle$(tempch%[j%],titlech$);
            ChanTitle$(tempch%[j%],titlech$[i%+j%]);
        Next
        ArrConst(times[],arrindex%[]);    ' Set to be equal to arrindex
        ArrMul(times[],BinSize(wavlist%[0])); ' Times by binsize to convert to time ###
Assumes all binsizes are the same
        ArrAdd(times[],teststt%);' Add time of test start
        t := 0;    ' Start at time = 0;
        Repeat ;
            lastt := readwav (wavlist%[i%],t,arraymax%-1,0);      ' Read Fx channel data
(channel to read from, time to read from, read size (full array less one or leaves gaps), Fx)
            readwav (wavlist%[i%+1],t,arraymax%-1,1);             ' Read Fy channel data
(channel to read from, time to read from, read size (full array less one or leaves gaps), Fy)
            ' ### This assumes start and end times are the same for the Fx and Fy Channels
            forcesums(wavlist%[i%],times[]);                ' Do calculations to change voltages
to Newtons  (Channel to process, time array)
            For j% := 0 to 1 Do
                writewav(tempch%[j%],t, arraymax%-1,j%);        ' Call wav write function
(channel to write to, time to write from, write size (full array), index of rwarray to write)
            Next
            ArrAdd(times[],lastt-t);                                ' add t to index array
            t := lastt;
        Until lastt >= MaxTime(wavlist%[i%]); ' Reached end of file
        For j% := 0 to 1 Do
            cleanchan(tempch%[j%]);
        Next
    Next  '
============================================================
=====================================
    er% := 1;
    Repeat
        er% := savenew%();     ' Export Memory channels to new file (returns error code)
    Until  er%=0; ' Keep trying until file save succesful (can escape from file save function)
    binselect();  ' Ditch selected channels
    leaveall();
    main();
End

main();   ' Gets the thing going!!!
```

1.3: FP_Power

```
'= JK 06/04/04
=======================================================
' Take processed data from force pedals and calculate;
' Feff, Fineff, crank vel, power, IIE, Work and Impulse
'
' Version info
' ----------------
'
' 1.0
' 2.0
' 3.0
' 3.1
' 3.2
' 3.3
' 3.4 Implemented array arithmetic in dosums, crankvel and rad
' 4.1 Calculation of work and impulse added
' 4.1.2 #### Calculation of Fr added
'
' Still to be done!
' ----------------
'
' Check calculations
'       Impulse = Fe x time (Not going to use impulse so not going to worry about it!)
'
' Error handing required
' ---------------------
'
' Currently seems to handle errors okay, but not really tried to crash it yet!
'
' Known bugs
' ----------
'
'
' If there are more than 1 duplicate channels, checkwavs% missreports
' the number of duplicates (this is a pretty minor bug though)
'
'=======================================================
==========

'=======================================================
==========
' Global consant declarations
'=======================================================
==========
Const arraymax%:= 4000;       ' Maximum size of array to read/write blocks of data in
   (small is faster)
Const ver$ := "4.1";          ' Version of script
Const rads:= 57.29577951;     ' Conversion factor for degrees to rads

'=======================================================
==========
'Global variable declarations
```

```
'=============================================================
==========
Var v1% := 0;                    ' Current view number
Var er%;                         ' Used for error codes
Var i%,j%;                       ' Looping variables
Var wavlist%[7];                 ' Array to hold list of channels for processing in order: L
pedal, LFx, LFy, R pedal, Rfx, RFy, crank
Var readvals[4][arraymax%];   ' Array for reading data into (PA, Fx, Fy,  CA/CV)
Var writevals[7][arraymax%];  ' Array for reading data into (Feff, Fineff, IIE, power,
Impulse, Work, CV)
Var filtch%[4];               ' Channels to filter (force, CV, cut-off, transition gap)
Var tempch%[13];                 ' Temporary memory channels created [L,R- Feff, Fineff, IIE,
power, Impulse, Work & crank vel]
Var cl;                          ' Crank length (mm)
Var filt%;                       ' Whether channels to be filtered (1) or not (0)

'=============================================================
==========
' Main procedures
'=============================================================
==========


' ---------------------------------------------------------------------
Proc Choosev(times%[]); 'Choose the time view to be used                (Array of time view
handles)
    Var title$;                  ' Variable to return view titles to
    Var timetitle$[20];          ' Array for time view titles
    Var dummy%;                          ' Variable to return item selected in dialogue to

    For i% := 1 to times%[0] Do' Fill an array with time view titles
        View(times%[i%]);
        title$ := windowtitle$();
        timetitle$[i%-1]:= title$;  ' (timelist%[0]=No of time views)
    Next
    timetitle$[times%[0]] := "- New file -";        'Add new file option to list
    DlgCreate("Time views already open!",0,0,0,0);
    DlgText("Select time view",0,1);
    DlgList(1,35,timetitle$[],(times%[0]+1),15,1);
    er% := DlgShow(dummy%);
    If er% < 1 Then    ' user cancelled
        leaveall();
    EndIf
    If dummy% = times%[0] Then        ' new file selected
        getfile();
    Else
        v1% := times%[dummy%+1]; 'returns selected view as active view (+1 since 0 is No
of views)
    EndIf
End

' ---------------------------------------------------------------------
Proc getfile()
    v1% := FileOpen("",0,1);
    If v1% <= 0 Then
```

```
    Message ("No file!");
        leaveall();
    EndIf
End

' ---------------------------------------------------------------------
Proc leaveall()       'quits program
    Var lvall%;          ' Quit script?

    lvall% := Query("Quit script?|Quit?");
    If lvall% Then
        halt
    Else
        main();
    EndIf
End

' ---------------------------------------------------------------------
Proc checkfile() ' Checks that opened file is appropriate
    Var waves%[1];    ' Dummy array for waveform channels
    Var numwavs%;    ' Number of waveform channels found

    numwavs% := Chanlist(waves%[],8193);      ' fill arary with waveform channel numbers
    If numwavs% < 7 Then
        Message ("Incompatible file!|Only %d waveform channel(s) founds\nProgram requires
7",numwavs%);
        leaveall();
    EndIf
End

' ---------------------------------------------------------------------
Func checkbins()   ' Checks that binsize of selected channels are identical
    Var bins; ' Binsize of channels

    bins := BinSize(wavlist%[0]);
    For i% := 1 to 6 Do
        If BinSize(wavlist%[i%]) <> bins Then
            Message("Error!|Binsizes of selected channels are not identical");
            leaveall();
        EndIf
    Next
    Return (bins);
End

' ---------------------------------------------------------------------
Func checklen(bins)   ' Checks that lengths of selected channels are identical (binsize of file)

    Var length;  ' length of channels

    length := MaxTime(wavlist%[0]);
    For i% := 1 to 6 Do
        If MaxTime(wavlist%[i%]) < length - 1/bins Or MaxTime(wavlist%[i%])> length +
1/bins Then '(with 1 bin of each other)
            Message("Error!|Selected channels are not identical in length\n(+/- 1* binsize)");
            leaveall();
```

```
        EndIf
    Next
    Return (length);
End

' ---------------------------------------------------------------------
Func savenew%(); ' Creates a new time view to write processed channels to
    Var abort%;     ' Abort trying to save

    er% := FileSaveAs("",0,0,"Name for new file?");        ' Save copy of file.
    If er% <0 Then' File save unsuccesful
        abort% := Query("Could not save file|Abort save?");
        If abort% = 1 Then    ' Yes selected
            er% := Query("Delete new channels?");
            If er% = 1 Then
                binselect();
            EndIf
        leaveall();
        EndIf
    EndIf
    Return (er%)    ' Return error code
End

' ---------------------------------------------------------------------
Func getch%()      ' Procedure to identify channels
    Var waves%[32];  ' Dummy array for waveform channels
    Var numchans%;       ' Temporary number of channels returned
    Var cvyes% := 1;  ' Whether to export crank velocity or not

    cl := 175;    ' Default crank length
    numchans% := ChanList(waves%[],8193);

    For i% := 1 to numchans% Do                                    ' Get channels with
matching names
        DoCase
            Case ChanTitle$(waves%[i%]) = "LPA_p" Then wavlist%[0] := waves%[i%];
            Case ChanTitle$(waves%[i%]) = "LFx_p" Then wavlist%[1] := waves%[i%];
            Case ChanTitle$(waves%[i%]) = "LFy_p" Then wavlist%[2] := waves%[i%];
            Case ChanTitle$(waves%[i%]) = "RPA_p" Then wavlist%[3] := waves%[i%];
            Case ChanTitle$(waves%[i%]) = "RFx_p" Then wavlist%[4] := waves%[i%];
            Case ChanTitle$(waves%[i%]) = "RFy_p" Then wavlist%[5] := waves%[i%];
            Case ChanTitle$(waves%[i%]) = "CA_p" Then wavlist%[6] := waves%[i%];
        EndCase
    Next
    DlgCreate("Please identify channels",0,0);      ' Display dailogue to allow user to alter if
needed
    DlgChan(1,"Crank channel",8193);
    DlgChan(2,"Left pedal channel",8193);
    DlgChan(3,"Right pedal channel",8193);
    DlgChan(4,"Left Fx channel",8193);
    DlgChan(5,"Left Fy channel",8193);
    DlgChan(6,"Right Fx channel",8193);
    DlgChan(7,"Right Fy channel",8193);
    DlgReal(8,"Crank length",150,190,20,9);
    DlgText("mm",33,9);
```

```
    DlgCheck(9, "Export crank velocity", 2,10);
    er% :=
DlgShow(wavlist%[6],wavlist%[0],wavlist%[3],wavlist%[1],wavlist%[2],wavlist%[4],wavlist
%[5], cl,cvyes%);
    If er% = 0 Then
        leaveall();
    EndIf
    For i% := 0 to 6 Do            ' Dump channel list to log
        PrintLog("Channel %d = %s\n",wavlist%[i%],ChanTitle$(wavlist%[i%]));
    Next
    Return(cvyes%);
End

' ---------------------------------------------------------------------
Func getmin(ch%,maxt)  ' Gets minimum values in angle channels (channel to get value
from, Maxtime in file)

    Return(ChanMeasure(ch%,9,0,maxt));
End

' ---------------------------------------------------------------------
Func getmax(ch%,maxt) ' Gets maximum values in angle channels (channel to get value
from, Maxtime in file)

    Return(ChanMeasure(ch%,8,0,maxt));
End

' ---------------------------------------------------------------------
Func readwav (ch%,t,bins,maxt)          ' Readwave data into an array (Channel to read,
time to read from, binsize of file, Maxtime of file)
    Var readsize%;     ' Number of data points read in
    Var readt;         ' Time of last data point read in
    Var maxreadtime;  ' The maximum amount of time that can be read into array

    readt:= (arraymax%)*bins;            ' Calculate time window that will fit it the array
    If readt+t > maxt Then   ' Would read from beyond end of file
        readt := maxt-t;
    EndIf
    readsize% := ChanData(ch%,readvals[j%][],t,t+readt);       ' Read in data
    If readsize% <1 Then
        Message("ERROR!|Data read error!\nChannel %d",ch%);
        leaveall();
    EndIf
    Return (readsize%);
End

' ---------------------------------------------------------------------
Proc writewav(t,loop%,last%,chloop%); ' Write array data to wav channel (time to start
write from, index of array to write, number of elements to write, channel number to write
to)

    er% := MemSetItem(tempch%[chloop%],0,t,writevals[loop%][0:last%]);      ' Write
data to memory channel
    If er% <0 Then
        Message("ERROR!|Error writing data to \nChannel %d",tempch%[chloop%]);
```

```
        leaveall();
    EndIf

End

' ---------------------------------------------------------------------

Proc createwav(ch%,loop%,bins)          ' Create wav channel (Channel to use as template,
array indez (j%), binsize of file)
    Const scalef := 6553.6;        ' Channel scaling factor (see help)

    Var titlech$,unit$;  ' Title and units of created channel
    Var miny%, maxy%;       ' Minimum and maximum scale of new channel
    Var side$;                 ' Whether left or right side
    Var scale;                 ' Channel scale value

    If i% = 0 Then ' Left
        side$ := "L_";
    Else
        side$ := "R_";
    EndIf
    DoCase
        Case loop% = 0    Then ' Effective forces
            scale := scalef;
            miny% := -200;
            maxy% := 400;
            unit$ := "N";
            titlech$ :=side$ + "Feff";
        Case loop% = 1    Then ' Ineffective forces
            scale := scalef;
            miny% := -200;
            maxy% := 400;
            unit$ := "N";
            titlech$ :=side$ + "Fineff";
        Case loop% = 2    Then ' IIE
            scale := scalef;
            miny% := -200;
            maxy% := 400;
            unit$ := "%";
            titlech$ :=side$ + "IIE";
        Case loop% = 3    Then ' Power
            scale := scalef;
            miny% := -200;
            maxy% := 400;
            unit$ := "W";
            titlech$ :=side$ + "Power";
        Case loop% = 4    Then ' Impulse
            scale := scalef/1000;
            miny% := -0.4;
            maxy% := 0.8;
            unit$ := "Ns";
            titlech$ :=side$ + "Impulse";
        Case loop% = 5    Then ' Work
            scale := scalef/1000;
            miny% := -0.4;
```

```
            maxy% := 0.8;
            unit$ := "j";
            titlech$ :=side$ + "Work";
        Case loop% = 12  Then ' Crank velocity
            scale := scalef;
            miny% := 3;
            maxy% := 21;
            unit$ := "rad/s";
            titlech$ :="CV";

    EndCase
    tempch%[i%*6+loop%] := MemChan(1,0,bins);       ' Create waveform channel to write
to
    If tempch%[i%*4+loop%] < 1 Then

        Message("ERROR!|Unable to create memory channels");
        leaveall();
    EndIf
    ChanUnits$(tempch%[i%*6+loop%],unit$);

    ChanTitle$(tempch%[i%*6+loop%],titlech$);

    ChanScale(tempch%[i%*6+loop%],scale);
    YRange(tempch%[i%*6+loop%],miny%,maxy%);

    ChanShow(tempch%[i%*6+loop%]);

    ChanSelect(tempch%[i%*6+loop%],1);       ' Set channel as selected (used for export)

End

' ---------------------------------------------------------------------
Func checkwavs%(maxt) ' Check that selected channels are appropriate (max length of
channel)
    Var chchk;          ' values in channels to check (min, max)
    Var k%;             ' Looping variable
    Var dup% := 0;    ' Number of duplicates found
    Var range% := 0;  ' Flag if channel data out of range

    For j% := 0 To 5 Do ' Check for duplicate channels and none identical binsizes
        k% := j% + 1;
        While k%<=6 Do
            If wavlist%[j%] = wavlist%[k%] Then ' Duplicate channels
                dup% += 1;
            EndIf

            k% += 1;
        WEnd
    Next
    If dup% >0 Then
        Message("Error!|%d duplicate channels found",dup%);
        Return(dup%);
    EndIf
    For i% := 0 to 6 step 3 Do   ' Check angle magnitudes of channels are appropriate
        chchk := getmax(wavlist%[i%],maxt);
```

```
        If chchk <355 Or chchk > 365 Then
            Message("Error!| Max values in %s channel out of range\n+355 to +365\nMax =
%.2f",ChanTitle$(wavlist%[i%]),chchk);
            range% := 1;
            Return(range%);
        EndIf
        chchk := getmin(wavlist%[i%], maxt);
        If chchk <-5 Or chchk > 5 Then
            Message("Error!|Min values in %s channel out of range\n-5 to +5\nMin =
%.2f",ChanTitle$(wavlist%[i%]),chchk);
        range% := 1;
            Return(range%);
        EndIf
    Next
End

' ---------------------------------------------------------------------
Func freech%() ' Find spare channel
    var k% := 1;

    While ChanKind(k%) <> 0 And k% <= 32 Do          ' Look for free channel
        k% += 1;
    Wend
    If k% > 32 Then' No free channels
        Message("ERROR!|No free Channels\nCannot save!");
        leaveall();
    EndIf
    Return(k%);
End

' ---------------------------------------------------------------------
Proc binselect();       ' Bin selected channels
    ChanDelete(-3,0); ' Delete selected channels
End

' ---------------------------------------------------------------------
Proc crankvel(n%,bins)   ' Calculate crank angular velocity and write this to a memory
channel (array element,binsize of file)
    Var k%:=0; ' Looping variable
    Var cvbuff;  ' Buffer for replacing rougue values (e.g. at zero crossings)

    ArrDiv(readvals[3][],rads);
    ArrDiff(readvals[3][]);
    Repeat
        cvbuff := readvals[3][k%];
        k%+=1;
        If k%>= arraymax% Then ' all data dodgy in array
            Message("ERROR|Bad data error in crank channel");
            leaveall();
        EndIf
    Until cvbuff >-5/rads And cvbuff <5/rads;
    For k% := 0 to arraymax% -1 Do
        If readvals[3][k%] < -5/rads Or readvals[3][k%] > 5/rads Then
            readvals[3][k%] := cvbuff;
        EndIf
```

```
    Next
    ArrDiv(readvals[3][],bins);
    ArrConst(writevals[4][],readvals[3][]);
End

' ------------------------------------------------------------------
Proc dosums(bins) ' calculate effective forces
    Var temp1[arraymax%]; ' Temporary array to use in calculations
    Var temp2[arraymax%]; ' Temporary array to use in calculations

        ' ======================== Feff/ Fineff calculations
============================
        ArrDiv(readvals[0][],rads);                                    ' Combined
    Convert PA to rads
        ArrConst(writevals[0][],readvals[0][]);     ' Combined      Copy PA to Feff array
        Cos(writevals[0][]);                                           ' Combined
    Calcualte cosine of PA in Feff array
        ArrConst(writevals[1][],writevals[0][]);    ' Fineff        Copy Feff array to Fineff
(cosine(rad(PA))
        ArrMul(writevals[0][],readvals[1][]);               ' Feff          Multiply Feff
(cosine(rad(PA))by Fx
        ArrMul(writevals[1][],readvals[2][]);               ' Fineff        Multiply Fineff
(cosine(rad(PA))by Fy
        ArrConst(temp1[],readvals[0][]);                    ' Combined      Copy PA to
temp1
        Sin(temp1[]);                                                  ' Combined
    Calculate Sin of PA
        ArrConst(temp2[],temp1[]);                                             ' Fineff
    Copy temp1 (Sin(rad(PA)) to temp2
        ArrMul(temp1[],readvals[2][]);                      ' Feff          Multiply
temp1 (Sin(rad(PA))by Fy
        ArrMul(temp2[],readvals[1][]);                      ' Fineff        Multiply
temp2 (Sin(rad(PA))by Fx
        ArrAdd(writevals[0][],temp1[]);                     ' Feff          Add temp1
(Fy(Sin(rad(PA))) to writevals[0] (Fx(cosine(rad(PA)))
        ArrAdd(writevals[1][],temp2[]);                     ' Fineff        Add temp2
(Fx(Sin(rad(PA))) to writevals[1] (Fy(cosine(rad(PA)))
        ' ======================== IIE calculations
============================
        ArrConst(writevals[2][],writevals[0][]);
        ArrConst(temp1[],writevals[1][]);
        ArrMul(writevals[2][],writevals[2][]);
        ArrMul(temp1[],temp1[]);
        ArrAdd(temp1[],writevals[2][]);
        sqrt(temp1[]);
        ArrDivR(temp1[],writevals[0][]);
        ArrMul(temp1[],100);
        ArrConst(writevals[2][],temp1[]);
        ' ======================== Power calculations
============================
        ArrConst(writevals[3][],writevals[0][]);
        ArrMul(writevals[3][],cl/1000);
        ArrMul(writevals[3][],readvals[3][]);
        ' ======================== Impulse calculations
============================
```

```
        ArrConst(writevals[4][],writevals[0][]);
        ArrMul(writevals[4][],bins);
        ' ======================== Work calculations
============================
        ArrConst(writevals[5][],writevals[3][]);
        ArrMul(writevals[5][],bins);
End

' ---------------------------------------------------------------------
Proc chanwrite(ch%, freech%,maxt)      ' Write memory channels to permenant channels
(memory channel to save, channel to write to, Maxtime in file)

    ExportChanList(0,maxt,freech%);      ' Flag channel for export
    er% := MemSave(tempch%[ch%],freech%,0);
    If er% <0 Then
        Message("Error!|Could not save memory channel");
        leaveall();
    EndIf
    er% := ChanDelete(tempch%[ch%]);
    If er% <0 Then
        Message("Warning!|Failed to delete channel %d",tempch%[ch%]);
    EndIf
    Optimise(freech%);
    ChanShow(freech%);
    ChanSelect(freech%,1);       ' Flag created channels for deletion
End

' ---------------------------------------------------------------------
Func getfilt()    ' Filter set up

    ArrConst(filtch%[],1); ' set defaults
    filtch%[2] := 6;
    filtch%[3] := 6;
    DlgCreate("Low-pass filter",0,0);
    DlgCheck(1, "Crank velocity",5,1);
    DlgCheck(2, "Force data", 5,2);
    DlgInteger(3,"Cut off frequency",1,50,18,4);
    DlgText("Hz",30,4);
    DlgInteger(4,"Transition gap",1,50,18,5);
    DlgText("Hz",30,5);
    er% := DlgShow(filtch%[1],filtch%[0],filtch%[2],filtch%[3]);
    If er% <1 Then
        Message("Error!|Filtering cancelled");
        leaveall();
    EndIf
End

' ---------------------------------------------------------------------
Func filterch(ch%, maxt) ' Runs a low pass filter on channel (channel to filter, maxtime in
file)

    er% := FiltCreate(0,2,filtch%[3],filtch%[2]);
    If er% <0 Then
        Message("Error!|Could not create filter");
        leaveall();
```

```
    EndIf
    er% := FiltApply(0,0,ch%,0,maxt,1);
    If er% <0 Then
        Message("Error!|Could not apply filter");
        leaveall();
    EndIf
    ChanShow(er%);  ' Channel must be visible to be selected?
    ChanSelect(er%,1); ' Flag created channel for deletion
    ChanTitle$(er%,ChanTitle$(ch%));   ' Copy channel title
    Return (er%); ' Handle of new channel
End

'============================================================
===========
' Main routine
'============================================================
===========

Proc MAIN()
    Var currentch%;       ' Channel number currently processing
    Var lastt;            ' Last time read in
    Var t;                ' Time to read from
    Var timelist%[20]; ' Array for list of time views (assumes no more than 20)
    Var free%;            ' Handle of empty channel
    Var k%;               ' Looping variable
    Var expcv%;           ' Whether (1) or not (0) to export crank velocity channel
    Var chr%;             ' Channel to read/write from/to
    Var cvch%;            ' Handle of crank velocity channel
    Var nread%;           ' Number of data points read
    Var filebins;         ' Binsize of channels in file
    Var filelen;          ' Maxtime of channels in file

    ' ============ file handling bit ================================
    ToolbarText("Running script version " + ver$);
    Viewlist (timelist%[], 1); ' Are there any time views already open
    If timelist%[0] > 0 Then  'There are some time views
        choosev(timelist%[]);
    Else
        getfile();     ' No time views open go and get one
    EndIf
    FrontView(LogHandle());
    View(v1%); ' Set returned view as active
    checkfile();
    ChanSelect(-1,0);  ' Deselect all channels or will delete anything that is selected at
program start
    PrintLog("\n\n=====>> FP_power v%s
<<==================================>>> %s
<<<==================================\n\n",ver$,Windowtitle$());
    Repeat
        expcv% := getch%();
        filebins :=   checkbins();
        filelen := checklen(filebins);
        er% := checkwavs%(filelen);
    until er% = 0;
    PrintLog("Sample rate %.3f Hz\nChannel length %.2f\n",1/filebins,filelen);
```

```
    ExportChanList();  ' Clear channel export list
    ExportChanList(0,filelen,wavlist%[6]);          ' Flag crank channel for export
    getfilt();
    ' ============ crank velocity bit
================================
    i% := 0;
    t := 0;    ' Start at time = 0;
    j% := 3;
    lastt := 0;
    createwav(wavlist%[0],12,filebins); ' Create channel for crank velocity
    Repeat
        chr% := wavlist%[6];     'Crank angle
        nread% := readwav (chr%,t,filebins,filelen);                    ' Call wav read function
(channel to read from, time to read from, binsize of file, Max channel length in file)
        lastt+= nread%*filebins;
        crankvel(k%,filebins);
        writewav(t,4,nread%,12);' Write crank vel data (time to write from, index of array to
write, number of elements, temp channel to write to)
        t := lastt;
    Until lastt >= filelen; ' Reached end of file
    If filtch%[1] = 1 then ' CV channel filtering selected
        ToolbarText("Filtering crank velocity data");
        tempch%[12] := filterch(tempch%[12],filelen);    ' (Handle of channel to filter,
maxtime in file)
    EndIf
    wavlist%[6] := tempch%[12];
    If expcv% = 1 Then   ' CV channel flagged for export
        free% := freech%();
        chanwrite(12,free%,filelen);
        wavlist%[6] := free%;
    EndIf
    ' ============ pedal sums bit ================================
    If filtch%[0] = 1    Then ' Force data filtering selected
        ToolbarText("Filtering force data");
        For i% := 1 to 2 Do    ' Left force data
            wavlist%[i%] := filterch(wavlist%[i%], filelen);
        Next
        For i% := 4 to 5 Do    ' Right force data
            wavlist%[i%] := filterch(wavlist%[i%],filelen);
        Next
    EndIf

    For i% := 0 to 1 Do    ' Once for left pedal once for right
        If i% = 0 Then
            ToolbarText("Processing left pedal data");
        Else
            ToolbarText("Processing right pedal data");
        EndIf
        For j% := 0 To 5 Do   ' 0-Feff, 1-Fineff, 2-IIE, 3-power, 4-Impulse, 5-Power
            createwav(wavlist%[0],j%,filebins);              ' Creates new channels
        Next
        t := 0;    ' Start at time = 0;
        lastt := 0;
        Repeat
            For j% := 0 to 3 Do    ' Fx, Fy, PA, CV
```

```
            If j% >2 Then  ' CV
               chr% := wavlist%[6];   ' Crank velocity
            Else
               chr% := wavlist%[i%*3+j%];
            EndIf
            nread% := readwav (chr%,t,filebins,filelen);                    ' Call wav read
function (channel to read from, time to read from, binsize of file, Max channel length in file)
         Next
         lastt+= nread%*filebins;
            dosums(filebins);  ' Do sums (Binsize of channels)
         For j% := 0 to 5 Do
            chr% := j%+i%*6;' ### was *3
            writewav(t, j%,nread%,chr%);      ' Call wav write function (time to write
from, index of array to write, channel to write to)
         Next
         t := lastt;
      Until lastt >= filelen; ' Reached end of file
   ' ============ Export new channels bit
================================
      For j% := 0 to 5 Do
         free% := freech%();
         chanwrite(i%*6+j%, free%,filelen);
      Next
         ExportChanList(0,filelen,free%);        ' Flag channel for export
   Next
   er% := 1;
   Repeat
      er% := savenew%();     ' Export Memory channels to new file (returns error code)
   Until  er%=0; ' Keep trying until file save succesful (can escape from file save function)
   binselect();  ' Ditch selected channels
   leaveall();
   main();
End

main();  ' Gets the thing going!!!
```

1.4: FP_Extract

```
'=========================================================
====================
' Extracts time window means and SDs of sum, mean or peaks within segments of
' crank cycle, crank position and sum values between thresholds crossings or
' crank position and amplitude of peaks.
'
' Version info
' ------------
'
' 1.0: Get the thing started
' 1.1: Processes all channels succesfully but just exports data to log window
'          and doesn't do time windowing
' 1.2: Export to text file implemented
' 1.3: Time windowing implemented
' 1.4: Debugging
' 1.5: Error handling tightened up (window size is > file length, no crank channel selected)
' 2.0: Error handling introduced to handle noisy data in crank channel that leads to
erroneous event markers
' 3.0: Modified to allow selection of channels for analysis, variable start and end times
' 4.0: Modified to do processing by thresholds and peaks in source channels
' 4.1: Routine added to find max values
' 4.2: Routines added to allow threshold crossing to be found where peaks occur around
crank zero crossing
' 4.3: Debugging plus circular stats added to calculate mean angles (see Batschelet, 1981
and Fisher, 1993)
' 4.3.1: Degugging plus making log window front view so user can keep track of what doing
' 4.3.2: Finding of thresholds for on/off positions modified to allow for double peaks
' 4.3.2: getch modified to allow selection of different groups of channel (FP: peak, mean and
threshold)
'
' Still to be done!
' -----------------
'
' * Should really add a routine to getthreshpos to remove outliers in array which could occur
if
' there are spikes in the crank data though. This is only theoretically a problem though as in
practice
' this doesn't happen.
'
' Checks to be made
' ----------------------
'
'
' Error handing required
' ----------------------
' Error handling in place to handle sum x and y = 1. It works but its ugly programming!
'
' Known bugs
' ----------
'
'=========================================================
===========
```

```
'=============================================================
' Global consant declarations
'=============================================================
Const arraymax%:= 1000;       ' Maximum size of array  to read/write blocks of data in
Const timesize%:= 8000;    ' Maximum number of level crossing times that it can handle
Const ver$ := "4.3.3";    ' Version of script
Const twmax%:= 1000;          ' Maximum number of time windows can handle
Const maxthresh% := 15000;  ' Maximum number of threshold crossings

'=============================================================
'Global variable declarations
'=============================================================
Var v1% := 0;                    ' Current view number
Var er%;                         ' Used for error codes
Var i%,j%;                       ' Looping variables
Var wavlist%[32];                ' Array to hold list of channels for processing (crank angle in
0)
Var readarray[arraymax%];        ' Array for reading data into
var segments%;                          ' Size of crank segments to divide crank cycle into
var timew%;                             ' Size of time windows
Var firstt;                      ' Time of first threshold crossing
Var winedge%[1500][2];           ' Array to fill with indexes of threshold crossings as edge of
time windows and angles at which they occur
Var thresht[36][maxthresh%];  ' Array to hold threshold crossing times (threshold)(time (up
tp approx 35 mins at 120 rpm, 10 degree segments))
Var startt,endt;                 ' Start and end times for analysis
Var thresh,int%;                 ' Threshold analysis parameters (threshold value, include
sums between thresholds)
Var chthresh[32];                ' Array for thrshold values found in channels
Var peakt2;                      ' Time of 2nd peak (used in threshold crossings)

'=============================================================
' Main procedures
'=============================================================


' ------------------------------------------------------------------
Proc Choosev(times%[]);'Choose the time view to be used                (Array of time view
handles)
   Var title$;                   ' Variable to return view titles to
   Var timetitle$[20];           ' Array for time view titles
   Var dummy%;                           ' Variable to return item selected in dialogue to

   For i% := 1 to times%[0] Do' Fill an array with time view titles
      View(times%[i%]);
      title$ := windowtitle$();
      timetitle$[i%-1]:= title$;  ' (timelist%[0]=No of time views)
   Next
```

```
    timetitle$[times%[0]] := "- New file -";        'Add new file option to list
    DlgCreate("Time views already open!",0,0);
    DlgText("Select time view",0,1);
    DlgList(1,35,timetitle$[],(times%[0]+1),15,1);
    er% := DlgShow(dummy%);
    If er% < 1 Then    ' user cancelled
        leaveall();
    EndIf
    If dummy% = times%[0] Then        ' new file selected
        getfile();
    Else
        v1% := times%[dummy%+1]; 'returns selected view as active view (+1 since 0 is No
of views)
    EndIf
End

' ---------------------------------------------------------------------
Proc getfile()
    v1% := FileOpen("",0,1);
    If v1% <= 0 Then
        Message ("No file!");
        leaveall();
    EndIf
End

' ---------------------------------------------------------------------
Proc leaveall()   'quits program
    Var lvall%;          ' Quit script?

    lvall% := Query("Quit script?|Quit?");
    If lvall% Then
        halt
    Else
        main();
    EndIf
End

' ---------------------------------------------------------------------
Func getch%(crank%)        ' Procedure to identify channels (handle of crank angle channel)
    Const maxch%:=32;          ' Maximum number of channels to allow

    Var waves%[maxch%];        ' Dummy array for waveform channels
    Var chsel%[maxch%];        ' Flags for selected channels
    Var chtype%;               ' Type of channels to look for (FP/EMG)
    Var fp%;                   ' Flagged as a force pedal channel

    er%:=    Chanlist(waves%[],8193);
    If er%<1 Then
        Message("Error!|View is not a time view");
        leaveall();
    EndIf
    For i% := 1 to waves%[0] Do          ' Remove crank channel form the list
        If waves%[i%] = crank% Then    ' is crank channel
            ArrConst(waves%[i%:(waves%[0]-i%+1)],waves%[i%+1:waves%[0]-i%+1]);
            waves%[0]-=1;
```

```
    EndIf
  Next
  DlgCreate("Channel type to look for?",0,0,35);          ' Just speeds up tick box checking
  DlgList(1,25,"1: FP- Force|2: FP- Power/ IE/ CV|3: FP: Work|4: EMG|5: Other",5,2,1);
  er% := DlgShow(chtype%);
  If er% = 0 Then
    leaveall();
  EndIf
  If chtype% <5 Then   ' Set default channel flagging
    For i% := 1 to waves%[0] Do
      DoCase
        Case chtype% = 0 Then     ' Force pedal peak channels
          If lcase$(Mid$(ChanTitle$(waves%[i%]),3)) = "feff"
            Or lcase$(Mid$(ChanTitle$(waves%[i%]),3)) = "fineff"
            Or lcase$(Mid$(ChanTitle$(waves%[i%]),3)) = "fr"
          Then
            chsel%[i%]:= 1;
          EndIf
        Case chtype% = 1 Then     ' Force pedal mean channels
          If lcase$(ChanTitle$(waves%[i%])) = "cv"
            Or lcase$(Mid$(ChanTitle$(waves%[i%]),3)) = "iie"
            Or lcase$(Mid$(ChanTitle$(waves%[i%]),3)) = "power"
          Then
            chsel%[i%]:= 1;
          EndIf
      Case chtype% = 2 Then         ' Force pedal threshold channels
        If lcase$(Mid$(ChanTitle$(waves%[i%]),3)) = "work"
        Then
          chsel%[i%]:= 1;
        EndIf
      Case chtype% = 3 Then         ' EMG channels
          If lcase$(Right$(ChanTitle$(waves%[i%]),2)) = "ga"
            Or lcase$(Right$(ChanTitle$(waves%[i%]),2)) = "vm"
            Or lcase$(Right$(ChanTitle$(waves%[i%]),2)) = "rf"
            Or (lcase$(ChanTitle$(waves%[i%]))) = "rta" ' Right only as left has
cross-talk in is filtered channel selected below
            Or lcase$(Right$(ChanTitle$(waves%[i%]),2)) = "st"
            Or lcase$(Right$(ChanTitle$(waves%[i%]),2)) = "bf"
            Or lcase$(ChanTitle$(waves%[i%])) = "filtered"
          Then
            chsel%[i%]:= 1;
          EndIf

      Else
        chsel%[i%]:= 0;
      EndCase
    Next
  EndIf
  DlgCreate("Please select channels for analysis",0,0);
  For i% :=1 to waves%[0] Do
    DlgCheck(i%,ChanTitle$(waves%[i%]),1,i%)
  Next
  er% := DlgShow(chsel%[1:waves%[0]]);
  If er% = 0 Then
    leaveall();
```

```
    EndIf
    j%:=1;
    PrintLog("Channels selected for processing as follows;\n\n");
    For i% :=1 to waves%[0] Do

        If chsel%[i%]= 1 Then
            wavlist%[j%] := waves%[i%];
            PrintLog("%d\t%s\n",wavlist%[j%],ChanTitle$(wavlist%[j%]));
            j%+=1;
        EndIf
    Next
    Return(j%); ' Return number of selected channels
End


' ------------------------------------------------------------------
Func getca%()      ' Procedure to identify crank channel
    Var waves%[32];      ' Dummy array for waveform channels            THIS DUPLICATES
CODE IN CHECKFILE!
    Var numwavs%;           ' Number of waverform channels returned
    Var ca%:=0;                 ' Handle of crank channel

    numwavs% := Chanlist(waves%[],8193);
    For i% := 1 to numwavs% Do                                  ' Get channel with
matching name
        If ChanTitle$(waves%[i%]) = "CA_p" Then
            ca% := waves%[i%];
        EndIf
    Next
    Repeat
        DlgCreate("Please identify crank channel",0,0);     ' Display dialogue to allow user to
alter if needed
        DlgChan(1,"Crank channel",8193);
        er% := DlgShow(ca%);
        If er% = 0 Then
            leaveall();
        EndIf
        If ca% <1 Then
            Message("Error!|No channel selected!");
        EndIf
    Until ca% > 0; ' Crank channel found
    PrintLog("Crank channel: %d\t%s\n",ca%,ChanTitle$(ca%));
    Return (ca%);
End

' ------------------------------------------------------------------
Func gettype%(); ' Choose type of analysis to be conducted (0: by segments of crank cycle,
1: thresholds by whole of crank cycle)
    var t%;  ' Type of analysis selected

    DlgCreate("Analysis Type",0,0);
    DlgText("Type of analysis",0,1);
    DlgList(1,35,"1: Analysis by crank segments|2: Threshold analysis of whole cycle|3: Peak
analysis",3,16,1);
    er% := DlgShow(t%);
```

```
    If er% = 0 Then
        leaveall();
    EndIf
    Return (t%)
End

' ------------------------------------------------------------------
Func getpeakcoeff(peakcoeff);  ' Get % of peak value must fall below to be detected as a
peak (default value)

    DlgCreate("% of peak",0,0);
    DlgText("% of peak to detect threshold at",0,1);
    DlgInteger(1,4,1,100,32,1);
    er% := DlgShow(peakcoeff);
    If er% = 0 Then
        leaveall();
    EndIf
    Return (peakcoeff)
End

' ------------------------------------------------------------------
Proc gettimes(dtw%,dstt,dent); ' Get parameters of analysis to carry out (default values)
    Var mintw;          ' Minimum size of time window available in file

    timew%:=dtw%; startt := dstt; endt := dent;
    Repeat
        DlgCreate("Time parameters",0,0);
        DlgInteger(1,"Size of time windows (s) (5-360)",5,360,0,1);
        DlgReal(2,"Start time (s)",0,MaxTime(),0,3);
        DlgReal(3,"End time (s)",0,MaxTime(),0,4);
        DlgText("Enter 0 to set end time to max time",3,5);
        er% := DlgShow(timew%,startt,endt);
        If er% = 0 Then
            leaveall();
        EndIf
        If endt = 0 Then
            endt := MaxTime();
        EndIf
        If MaxTime()/timew% > twmax% Then
            mintw := 1-((Maxtime()/twmax%)-Round((Maxtime()/twmax%)));      ' Round up
to nearest second
            mintw+=(Maxtime()/twmax%);
            Message("Invalid data entred!|File is too long to process with that time
window\n\nMinimum time window available is %d seconds",mintw);
            er% := 0;
        EndIf
        If startt>endt Then
            Message("Error!|End time must be greater than start time!");
            er% :=0;
        EndIf
        If er% <>0 And startt+timew%>endt Then
            er% := Query("Warning!|Less than one time window between selected
times!\n\nContinue anyway?");
        EndIf
    Until er%<> 0;
```

```
End

' ------------------------------------------------------------------
Func getsegs%(segs%); ' Get size of crank angle segments (Default value)
   Repeat
      DlgCreate("Angle segments",0,0);
      DlgInteger(1,"Size of segments (deg) (10-360)",10,360,0,1);
      er% := DlgShow(segs%);
      If er% = 0 Then
         leaveall();
      EndIf
      If 360 mod segs% > 0 Then
         Message("Invalid data entered!|Size of increments must be a factor of
360\ne.g.1,5,10,15,30");
         er% :=0;
      EndIf
   Until er%<> 0;
   Return(segs%);
End

' ------------------------------------------------------------------
Func checkch%(numch%);  'Check that none of the channels selected are duplicates
(number of waveform channels found)
   Var k%;              ' Looping variable
   Var n% := 0;         ' Number of duplicates found
   Var chmin := 0;' Length of shortest channels

   For j% := 0 To numch%-2 Do
      k% := j% + 1;
      While k%<numch%-1 Do
         If wavlist%[j%] = wavlist%[k%] Then
         n% += 1;
         EndIf
         k% += 1;
      Wend
      If chmin < MaxTime(wavlist%[j%]) Then
         chmin := MaxTime(wavlist%[j%])
      EndIf
   Next
   If chmin < timew% Then ' Is timewindow greater than length of shortest channel?
      Message("Error!|Time window exceeds length of some channels");
      Leaveall();
   EndIf
   If n% >0 Then
      Message("Error!|%d duplicate channels found",n%);
   EndIf
   Return(n%);
End

' ------------------------------------------------------------------
Func setevent(cross,stt,ent,chan%,mode%,cz%,ind%,fill%)      ' Finds threshold crossing
points and fills array with times
   ' (level wave must cross,start and end times, channel to find events in, event mode,
looking for crank zero, index of array
   ' to assign data to, flag for if doing filling)
```

```
    Var er%;                    ' Used for error handling
    Var t;                    ' Time of event crossing
    Var readt;                  ' Time block to read
    Var k%;                     ' Looping variable
    Var itemn%;                 ' Number of items added to channel
    Var tempch%;                ' Temporary event channel for segments threshold crossings
    Var mingap;                 ' Minimum time gap between thresholds
    Var r;                    ' Value to return, either number of events if filling or time of event
if not

    tempch% := MemChan (2); ' Create event channel
    If tempch% < 1 Then
        Message("ERROR!|Unable to create memory channels");
        leaveall();
    EndIf
    If cz% = 1 Then    ' Looking for crank zero crossings
        cross := 180;
        mingap := 0.4 ;' 150 rpm
    Else
        mingap := 0.4*(ind%*segments%/360);  ' Not 0.4 since noise at zero crossing will
lead it to miss subsequent thresholds
    EndIf
    itemn% := MemImport(tempch%,chan%,stt,ent,mode%,mingap,cross);
    If itemn% <0 Or itemn% > maxthresh% Then
            Message("ERROR!|All gone Pete Tong with finding events\n\nFound %d events
between %.3f and %.3f s in channel %d",itemn%,stt,ent,chan%);
        leaveall();
    EndIf
    If fill% = 1 Then
        For k% := 1 to itemn% do          ' Fill array with event times
            thresht[ind%][k%-1] := MemGetItem(tempch%,k%);
            If thresht[ind%][k%-1] <0 Then
                Message("ERROR!|Event data read error\n\nEvent time read= %g!",t);
                leaveall();
            EndIf
        Next
        r := itemn%;
    Else
        DoCase
            Case itemn% = 1 Then
                r :=MemGetItem(tempch%,1);
                peakt2 := r;
            Case itemn% = 2 Then          ' >>>> Reverse these???
                r := MemGetItem(tempch%,2);
                peakt2 := MemGetItem(tempch%,1);
            Else
                r := itemn% * -1;
        EndCase
    EndIf
    er% := ChanDelete(tempch%,0);              ' Finished with event channel so get rid of it
(don't ask just do it!)
    If er% <0 Then
        Message("ERROR!|Could not delete event channel %d",tempch%);
        leaveall();
    EndIf
```

```
    Return(r);
End

' ------------------------------------------------------------------
Func readwav% (chan%,tst,tend)        ' Readwave data into an array (Channel to read,
time to start and end read from)
    Var readsize%;      ' Number of data points read in
    Var readt;          ' Time of last data point read in
    Var temp;           ' Temp buffer variable for sorting times

    If tst > tend Then ' start time is before end time- swap times
        temp:=tst;
        tst:=tend;
        tend:=temp;
    EndIf
    readsize% := ChanData(chan%,readarray[],tst,tend);
    If readsize% <1 Then
        Message("ERROR!|Read size error reading from %s channel!\nTime: %.6f -
%.6f",Chantitle$(chan%),tst,tend);
        leaveall();
    EndIf
    Return (readsize%);
End
' ------------------------------------------------------------------
Func getthresh%();    ' Get information on threshold crossing analysis
    Var threshty%;    ' Type of threshold (0:fixed, 1: % max)

    int% := 1;   ' Default to on
    Repeat
        DlgCreate("Threshold parameters",0,0,42);
        DlgReal(1,"Threshold level",-10000,10000,16,1);
        DlgList(2,10,"1: Fixed|2: % max",2,30,1);
        DlgCheck(3,"Incluse summing between thresholds?",1,3);
        er% := DlgShow(thresh,threshty%,int%);
        If er% = 0 Then
            leaveall();
        EndIf
        If thresh>100 And threshty%=1 Then
            Message("Error!|Threshold cannot exceed 100%%");
            er% :=0;
        EndIf
    Until er%<> 0;
    Return(threshty%);
End

' ------------------------------------------------------------------
Func getsegsums%(); ' Get variables to be returned from segments of crank cycle
    Var csums%;       ' Variables to be return

    DlgCreate("Crank cycle variables",0,0,35);
    DlgList(1,"Return","1: Mean|2: Sum|3: RMS",3,12,1);
    er% := DlgShow(csums%);
    If er% = 0 Then
        leaveall();
    EndIf
```

```
    Return (csums%);
End

' ---------------------------------------------------------------------
Func makeres%(); 'Create text file to write to
    Var rh%;            ' Handle for text file window
    Var temp%[32];      ' Array for any exisitng text files open
    Var k%:=0;          ' Looping variable

    Repeat
        rh% := FileOpen("Comma seperated values (*.csv)|*.csv||",8,1,"File to save data
to");
        If rh% <0 then
            er% := Query("Warning!|Error in opening export file!\n\nRetry?");
            If er% = 0 Then
                leaveall();
            EndIf
        EndIf
    Until rh% >=0;
    Print("%s\n",View(v1%).WindowTitle$());
    View(v1%);      ' Reset time view as active window
    Return (rh%);
End

' ---------------------------------------------------------------------
Func closeres%(rh%,q%); 'Close text file (view to close, whether to query (-1:no)

    er% := View(rh%).FileClose(0,q%);
    If er% > 0 Then
        Message("Error!|Could not close new text file");
    EndIf
End

' ---------------------------------------------------------------------
Func dosums(ch%,t1,t2,vars%); ' reads in data between times and returns mean, sum or
RMS depending on value of vars%
    '(Channel to use, start and end times, type of measurement to use (see chanmeasure))
    Var er%;            ' Used for error codes
    Var val;            ' Value returned (mean/integral)

    val:= ChanMeasure(ch%,vars%,t1,t2,er%);
    If er% = 0 Then
        Message("Error!|ChanMeasure failed to return value between %.2f and %.2f",t1,t2);
        leaveall();
    EndIf
    Return(val);
End

' ---------------------------------------------------------------------
Proc writechhead(rh%,ch%,at%,th);     ' Create header for channel in text file (text file
handle, channel to create header for,
'   type of analysis, threshold)
    Var chan$;              ' Name of channel being processed (used in toolbar text)

    chan$ := ChanTitle$(ch%);
```

```
    ToolBarText("Processing "+chan$+" channel");
    View(rh%);
    Print("\nChannel %d: %s",ch%,View(v1%).ChanTitle$(ch%));
    If at% = 1 Or at% = 3 ThenPrint(",,,Threhsold,%.3f",th);     EndIf
    Print("\nStart t,End t,Trunc,");
    DoCase
    Case at% = 0 Then    ' If doing by crank segment
       For i% := 0 to 360- segments% step segments% Do
          Print("%d to %d,,",i%,i%+segments%);
       Next
       Print("\n,,");
       For i% := 0 to 360- segments% step segments% Do
          Print(",mean,SD");
       Next
    Case at% = 1 Then    ' If doing by thresholds
       Print("Rising to falling,,Falling to rising\n,,");
       For i% := 0 to 1 Do
          Print(",mean,SD");
       Next
    Case at% = 2 Then    ' If doing by peaks
       Print("peak,,Angle of peak\n,,");
       For i% := 0 to 1 Do
          Print(",mean,SD");
       Next
    Case at% = 3 Then ' Threshold crossing angles
       Print("Start angle,,End angle\n,,");
       For i% := 0 to 1 Do
          Print(",mean,SD");
       Next
    Else
       Message("Error!|Incorrect analysis type passed (%d)",at%);
       leaveall();
    EndCase
    Print("\n");
    View(v1%)
End


' ---------------------------------------------------------------------
Func findmaxt();   ' Find maximum threshold crossing time
    Var maxt;        ' Highest threshold crossing time

    For j% := 0 to 35 Do  ' Find first and last threshold crossings
       If thresht[j%][max(thresht[j%][])] > maxt Then
          maxt := thresht[j%][max(thresht[j%][])];
      EndIf
    Next
    Return(maxt);
End

' ---------------------------------------------------------------------
Proc writedata(minsgs%,maxsgs%,rh%,smean[][],sn%[],ang%,at%,t,ch%);      'Write
means and SDs to file (minimum and maximum of segments
    ' in data, text file handle to write to, segment meand and segment n's, if doing angles (1:
yes), (start time of read, channel)
```

```
    ' only used for error messages)
    Var winmean[360];           ' Array for segment means for time window
    Var winsd[360];         ' Array for segment SDs for time window
    Var ind%;                   ' Index of array
    Var k%;                     ' Looping variables
    Var minor := 0.3;           ' Coefficient for accepting peaks as small
    Var pi;
    Var x[maxthresh%];
    Var y[maxthresh%];
    Var meanx,meany;

    pi := 4.0*ATan(1.0);
    For i% := minsgs% to maxsgs%-1 Do       ' Do for each segment
        If at% = 1 Then
            For k% := 1 to sn%[i%] Do           ' Handling for small areas of threshold
crossing
                If smean[i%][k%] <= smean[i%][k%-1 * minor Then
                    smean[i%][k%-1] += smean[i%][k%];
                    ArrConst(smean[i%][k%-1:],smean[i%][k%:]);
                    sn%[i%] -= 1;
                EndIf
            Next
        EndIf
        If sn%[i%]> 1 Then  ' Only do if more than one segment found (should always be
the case (or falls over if segn%[i%] = 1))
            If ang% = 1 Then ' Handling of angles to allow zero crossing (circular stats)
                ArrConst(x[],smean[i%][0:sn%[i%]-1]);
                ArrConst(y[],smean[i%][0:sn%[i%]-1]);
                ArrDiv(x[0:sn%[i%]-1],360/(2*pi));                  ' Convert to radians
                ArrDiv(y[0:sn%[i%]-1],360/(2*pi));                  ' Convert to radians
                Cos(x[0:sn%[i%]-1]);
        ' x= cos x
                Sin(y[0:sn%[i%]-1]);
        ' y= sin y
                ArrSum(x[0:sn%[i%]-1],meanx);                                   '
mean x= sum(cos x)/n
                ArrSum(y[0:sn%[i%]-1],meany);                                   '
mean y= sum(cos y)/n
                If meanx >0 Then
                    winmean[i%] := atan(meany/meanx);               ' mean angle=
atan(meany/meanx)
                Else
                    winmean[i%] := pi + atan(meany/meanx);          ' if mean x<0 then
mean angle += 180 degrees
                EndIf
                winmean[i%] *=360/(2*pi);
    ' Convert back to degrees<<<<
                winmean[i%] := (winmean[i%] + 360) mod 360;
                winsd[i%] := (pow(meanx,2) + pow(meany,2));     ' r=
(xmean^2+ymean^2)^0.5
                winsd[i%] := 2*(1-winsd[i%]);                                   '
SD= 2(1-r)
                winsd[i%] *=360/(2*pi);
    ' Convert back to degrees<<<<
                If winsd[i%] > 0 Then       ' Will be unless sum of meanx and meany is 1
```

```
                winsd[i%]:= Pow(winsd[i%],0.5);                    ' SD= (1(1-
r))^0.5
            Else
                winsd[i%]:= 0;
                Printlog("Could not calculate SD at time %.3f s in channel %d: sum mean x
and mean y = 1\n",t,ch%); ' #### Temp
            EndIf
        Else
            ArrSum(smean[i%][0:sn%[i%]-1],winmean[i%],winsd[i%]);
        EndIf
    Else
        PrintLog("Could not calculate mean or SD at time %.3f in channel %d in segment
%d (%d segments)\n",t,ch%,i%,sn%[i%]);
        winmean[i%] := 0;
        winsd[i%] := 0;
    EndIf
    View(rh%).Print("%#.4f,%#.4f,",winmean[i%],winsd[i%]);
  Next
End

' ------------------------------------------------------------------
Proc results(ch%,winsize%,stt,v%,rh%,maxt,at%);      'Calculate values and send to text
file
  ' (Channel to process, size of time windows, start time,type of variable to return, handle
  '   of text file, highest threshold crossing time)
  Var mean;                    ' Mean of values read
  Var k%,l%;                   ' Looping variables
  Var firstang%,firstt;        ' Angle and time of first threshold crossing
  Var t1, t2;                  ' Start and end times of segment windows
  Var edgew;                   ' Time of next window edge
  Var winend, endflag$;    ' Last time in window and character flag for end of file (only
used in window size text output to file)
  Var writeang%;               ' Segment angle to assign segment means to
  Var ind%;                    ' Index of threshold times (segments of crank cycle/ which
thresholds between)
  Var minsegs%, maxsegs%;  ' Maximum number of possible segments (360/segments-1
if crank cycle) and minimum segment value to use (don't include crank 0 if doing thresholds)
  Var segmean[36][50000];    ' Array for each mean read for each segment
  Var segn%[36];               ' Number of values returned
  Var vp%;                     ' Analysis type to pass to dosums (mean (2), sum (4) or
RMS (11))
  Var done% := 0;              ' Flag if found lower time

  DoCase
    Case at% = 0 Then   ' Analysis by crank segments
      maxsegs% := 360/segments%-1;
      minsegs% := 0;
    Case at% = 1 Then   ' Analysis by thresholds
      maxsegs% := 2;
      minsegs% := 1;
    Case at% = 2 Then   ' Analysis of peaks
      maxsegs% := 1;
      minsegs% := 0;
  EndCase
  If at% = 0 Then
```

```
    firstang% := Min(thresht[minsegs%:360/segments%][0]);
  Else
    firstang% := minsegs% + Min(thresht[minsegs%:(segments%-minsegs%)][0]);
  EndIf
  firstt := thresht[firstang%][0];
  l% := 0; ' Initialise index of threshold crossing times array
  edgew:=stt;    ' Initialise window edge
  ind% := firstang%;   ' Reset angle to that of first threshold crossing
  t1 := firstt; 'Initialise t1
  t2 := 0; ' Initialise t2
  View(rh%);
  Repeat
                    '<<<<<<<<< Do for each time window
    ArrConst(segn%[],0); ' Reset segment count
    edgew += winsize%; ' Increment by size of time windows
    If edgew > maxt then
      winend := maxt;
      endflag$ := "*";
    Else
      winend := edgew;
      endflag$ := "";
    EndIf
    View(rh%).Print("%.2f,%.2f,%s,",edgew-winsize%,winend,endflag$);
    View(v1%);
    Repeat  '                ' <<<<<<<<<< Do for all segments in time window
      ind%+= 1;
      If ind% > maxsegs% Then ind%:= minsegs%;          EndIf
      While done% =0 And l% > 0 Do        ' Find lower time in next segment
        l% -= 1;
        If thresht[ind%][l%] < t1 And thresht[ind%][l%] > 0 Then
          done% := 1;
        Else
        EndIf
      Wend
      done% := 0;
      Repeat   ' Find next highest time
        If l% >= maxthresh% Then
          Message("ERROR!|Reached end of threshold crossing array\nwith next time
not found\n\nThreshold index %d",ind%);
          leaveall();
        EndIf
        t2 := thresht[ind%][l%];
        l%+=1;
      Until t2 >= t1+View(v1%).BinSize(ch%)*4 Or t2 <0;
      l% -= 1;
      If t2 > 0 Then      ' If haven't reach last threshold crossing
        DoCase
          Case v% = 0 Then       ' Mean
            vp% := 2;
          Case v% = 1 Then       ' Sum
            vp% := 4;
          Case v% = 2 Then       ' RMS
            vp% := 11;
        Else
          Message("Error!|Incorrect analysis type passed (%d)",v%);
```

```
            leaveall();
        EndCase
        mean := dosums(ch%,t1,t2,vp%);
        writeang%:=ind%-1;      ' Write to previous segment or shifts data by one
segment
        If writeang%<minsegs% Then writeang%:= maxsegs%;    EndIf
        segmean[writeang%][segn%[writeang%]]:= mean;
        segn%[writeang%] += 1;
        t1 := t2;
    EndIf
  Until t2 >= edgew Or t2>=maxt Or t2 < 0 ; ' >>>>>>>>> End of time window
  writedata(minsegs%,maxsegs%+1,rh%,segmean[][],segn%[],0,at%,t2-
timew%,ch%); '#### Should maxsegs% be +1 wasn't n-1 in writedata (counting from 0 so
should be)
  View(rh%).Print("\n");
 Until edgew >= maxt;'
 '>>>>> End of channel
End


' ------------------------------------------------------------------
Proc dopeak(rh%,evn%[],crch%,ch%,stt,maxt,tw%,pkcoeff);    'Get the positions and
magnitude of peaks and write these to file
' (text file handle to write to, array holding number of events (crank, rising, falling), crank
channel, active channel, peak coefficient)

 Var ct1, ct2;              ' Crank zero crossing times
 Var ta[2][50000];          ' Array for threshold crossing crank angles
 Var tan%[2];               ' Array for count of threshold crossings
 Var ent;                   ' End time of window
 Var k%:=0;                 ' Looping variable
 Var endflag$;              ' Characher flag if end of window truncated
 Var peakt;                 ' Time of peak

 View(rh%).Print("\n");
 writechhead(rh%,ch%,2,0);
 Repeat
  ent := stt+ timew%;
  If ent > maxt then
   ent := maxt;
   endflag$ := "*";
  Else
   endflag$ := "";
  EndIf
  View(rh%).Print("%.2f,%.2f,%s,",stt,ent,endflag$);
  ArrConst(tan%[],0);  ' Initialise threshold counts to zero
  Repeat
   ct1:=thresht[0][k%];
   ct2:=thresht[0][k%+1];
   If ct2-ct1 > 0.4 And ct2-ct1 < 1.2 Then        ' If CV between 50 and 150 rpm
    ta[0][tan%[0]]:= ChanMeasure(ch%,14,ct1,ct2,er%);       ' Find peak value in
crank cycle
    If er% = 0 Then
     Message("Error!|Error finding peak \nbetween %.3f and %.3f
seconds",ct1,ct2);
```

```
            leaveall();
         EndIf
         peakt := setevent(ta[0][tan%[0]]*pkcoeff,ct1,ct2,ch%,0,0,-1,0);    ' Find time
of peaks (index= -1 so will fall over if called (it shouldn't be!))
         If peakt > 0 Then  ' Will be unless bad data in crank cycle
            ta[1][tan%[1]] := ChanValue(crch%,peakt);
            tan%[1] +=1;
            tan%[0] +=1;
         EndIf
      EndIf
      k% +=1;
   Until thresht[0][k%+2] > ent Or thresht[0][k%+2] <0; '
   ' >>>>>>>>> End of time window
   writedata(0,1,rh%,ta[][],tan%[],0,2,stt,ch%);     ' Do without zero crossing handling
for peaks
   ArrConst(ta[0][],ta[1][]);
   tan%[0] := tan%[1];
   writedata(0,1,rh%,ta[][],tan%[],1,2,stt,ch%);     ' and with for angles
   View(rh%).Print("\n");
   stt := ent;
Until ent > maxt Or thresht[0][k%+2] <0;
End

' ---------------------------------------------------------------------
Proc dothreshpos(rh%,evn%[],crch%,ch%,stt,maxt,tw%);       'Get the positions of
threshold crossings and write these to file
' (text file handle to write to, array holding number of events (crank, rising, falling), crank
channel, active channel)

   Var peakcoeff :=1;       ' Coefficient of peak value that must cross in finding peak
   Var peak;                  ' Threshold peak must fall below to count as peak
   Var peakt;                 ' Timing of peak
   Var ct1, ct2;             ' Crank zero crossing times
   Var ta[2][50000];          ' Array for threshold crossing crank angles
   Var tan%[2];               ' Array for count of threshold crossings
   Var ent;                   ' End time of window
   Var k%:=0,l%;              ' Looping variables
   Var endflag$;              ' Characher flag if end of window truncated
   Var try% := 0;             ' Number of attempts at finding peak
   Var tryback% := 0;         ' Flag if tried going back half a crank cycle to find peak

   While thresht[0][k%] < stt Do       ' Find first crank cycle in time window
      k% += 1;
      If thresht[0][k%] < 0 Then
         Message("Error!|Failed to find first crank cycle in time window\nStart time:
%.3f",stt);
         leaveall();
      EndIf
   Wend
'  View(rh%).Print("\n");
   writechhead(rh%,ch%,3,0);
   Repeat
      ent := stt+ timew%;
      If ent > maxt then
         ent := maxt;
```

```
            endflag$ := "*";
        Else
            endflag$ := "";
        EndIf
        View(rh%).Print("%.2f,%.2f,%s,",stt,ent,endflag$);
        ArrConst(tan%[],0);   ' Initialise threshold counts to zero
        Repeat
            ct1:=thresht[0][k%];
            ct2:=thresht[0][k%+1];
            If er% = 0 Then
                Message("Error!|Error finding peak \nbetween %.3f and %.3f
seconds",ct1,ct2);
                leaveall();
            EndIf
            If ct2-ct1 > 0.4 And ct2-ct1 < 1.2 Then          ' If CV between 50 and 150 rpm
                Repeat
                    Repeat
                        peak:= ChanMeasure(ch%,14,ct1,ct2,er%)*peakcoeff;          ' Find peak
value in crank cycle
                        peakt := setevent(peak,ct1,ct2,ch%,0,0,-1,0);          ' Find time of peaks
(index= -1 so will fall over if called (it shouldn't be!))
                        peakcoeff *= 0.9;     ' reduce by 10% and try again
                        try% +=1;
                    Until peakt >0 Or try% >3;       ' Try five times
                    try% := 0;
                    peakcoeff := 1;
                    If peakt <1 Then          ' Still haven't found peak
                        If k% > 0 Then
                            ct1 := thresht[0][k%-1] + (thresht[0][k%]-thresht[0][k%-1])/2;
                        EndIf
                        If k% < maxthresh% -2 Then
                            ct2 := thresht[0][k%] + (thresht[0][k%+1]-thresht[0][k%])/2;
                        EndIf
                        tryback% += 1;
                    EndIf
                Until tryback% > 1 Or peakt >0;
                tryback% := 0;
                If peakt = 0 Then
                    PrintLog("Data skipped between %.3f and %.3fs in channel %d: Failed to
find peak (%.3f)(%.3f)\n",ct1,ct2,ch%,peak,peakcoeff);
                EndIf
                If peakt <0 Then
                    PrintLog("Data skipped between %.3f and %.3fs in channel %d: Found %d
peaks (%.3f)(%.3f)\n",ct1,ct2,ch%,peakt*-1,peak,peakcoeff);
                EndIf
                If peakt >0 Then   ' Will be -1 if bad data in crank cycle
                    j% := evn%[1];
                    While j% >0 Do ' Find high going threshold prior to peak
                        j% -= 1;
                        If thresht[1][j%] <= peakt Then
                            ta[0][tan%[0]] := ChanValue(crch%,thresht[1][j%]);
                            tan%[0]+=1;
                            j% := 0;
                        EndIf
                    Wend
```

```
                Repeat ' Find low going threshold after peak 1 or 2
                    If thresht[2][j%] >= peakt2 Then
                        ta[1][tan%[1]] := ChanValue(crch%,thresht[2][j%]);
                        tan%[1]+=1;
                        j% := evn%[2];
                    Else
                        j% += 1;
                    EndIf
                Until j% =evn%[2];
            EndIf
        EndIf
        k% +=1;
    Until thresht[0][k%+2] > ent Or thresht[0][k%+2] <0; '
    ' >>>>>>>>> End of time window
    writedata(0,2,rh%,ta[][],tan%[],1,2,ct1,ch%);
    View(rh%).Print("\n");
    stt := ent;
Until ent > maxt Or thresht[0][k%+2] <0;
End

' ------------------------------------------------------------------
Proc getpercthresh(ch%[],thresh);       'Get peak values in channels and calculate % max
(array of channels, % threshold)
    Const wins% := 20;       ' Number of windows to split file into

    Var k%,l%;                  ' Looping variables
    Var ch$[32];            ' Array for channel titles
    Var threshwin[wins%];   ' Array of max values found in each time window
    Var stt,ent;            ' Start and end times of time windows
    Var fv%;                    ' Front view when called

    ChanHide(-1);
    Xrange(0,MaxTime());
    fv% := FrontView();
    FrontView(v1%);
    For k% := 0 To len(ch%[])-1 Do
        ChanShow(ch%[k%]);
        Optimise(ch%[k%]);
        stt := 0;
        l% := 0;
        Repeat
            ent := stt + MaxTime(ch%[k%])/wins%;
            threshwin[l%] := ChanMeasure(ch%[k%],8,stt,ent,er%);
            If er% = 0 Then
                Message("Failed to find max in channel %d",ch%[k%]);
                leaveall();
            EndIf
            stt := ent;
            l% += 1;
        until ent >= MaxTime(ch%[k%]) Or l% >= wins%-1;
        ArrSum(threshwin[],chthresh[k%]);
        ch$[k%] := ChanTitle$(ch%[k%]);
    Next
    ArrMul(chthresh[],thresh/100);
    DlgCreate("Channel max's",0,0,42);
```

```
    For k% := 1 To len(ch%[]) Do
        DlgReal(k%,ch$[k%-1],YLow(ch%[k%-1]),YHigh(ch%[k%-1]),15,k%);
    Next
    er% := DlgShow(chthresh[]);
    If er% = 0 Then
        leaveall();
    EndIf
    FrontView(fv%);
    View(v1%);

End

'=============================================================
===========
' Main routine
'=============================================================
===========

Proc main()
    Var currentch%;              ' Channel number currently processing
    Var timelist%[20];          ' Array for list of time views (assumes no more than 20)
    Var toolbar$;                ' String for messages for toolbar
    Var numchan%;                ' Number of channels in file
    Var level%;                  ' Level to find crossing at
    Var numevent%[3];            ' Number of events found in channel at each threshold
crossing (crank zeros, rising, falling)
    Var analtype%;               ' Type of analysis to be conducted (0: split by crank
segments, 1: thresholds of whole crank cycles)
    Var analtext$;               ' String to hold detials of analysis type for logging
    Var evmode%;                 ' Type of events to find (0: peak, 2: rising, 3: falling)
    Var czero%;                  ' Flag if looking for crank zero crossing (1)
    Var sums%;                   ' Get calculation options for crank segments analysis
    Var resh%;                   ' Handle of text file for results
    Var maxt:=0;                 ' Time of last threshold crossing
    Var ch%;                     ' Index of channel being processed in wavlist
    Var peakcoeff;               ' Percentage of peak that threshold will be detected at
    Var threshty%;               ' Type of thrshold (0: fixed, 1: % max)

    ToolbarText("Running script version " + ver$);
    Viewlist (timelist%[], 1); ' Are there any time views already open
    FrontView(LogHandle());
    If timelist%[0] > 0 Then  'There are some time views
        choosev(timelist%[]);
    Else
        getfile();     ' No time views open go and get one
    EndIf
    View(v1%); ' Set returned view as active
    PrintLog("\n\n======>> FP_extract v%s
<<=====================================>>> %s
<<<=====================================\n\n",ver$,Windowtitle$());
    Repeat
        wavlist%[0]:=getca%();
        numchan% :=  getch%(wavlist%[0]);
        If numchan% <1 Then
            Message("Error!|No channels selected!");
```

```
      EndIf
   until numchan% > 0;
   analtype% := gettype%();
   gettimes(60,0,Maxtime());   ' (Default time window,start and end values)
   resh% := makeres%();
   PrintLog("\nFile split into %d second windows from %.4f to %.4f (%d
windows)\n\n",timew%,startt,endt,Round(((endt-startt)/timew%)+0.49999));
   View(resh%).Print("%d,Time windows\n",Round(((endt-startt)/timew%)+0.49999));
   maxt:= findmaxt();
   For i% := 0 to 35 Do      ' Initialise threshold crossing times array
      ArrConst(thresht[i%][],-1);
   Next
   DoCase
      Case analtype% = 0 Then          ' >>>>>>>>>>>>>>>>> Analysis by segments
of crank cycle
         segments% := getsegs%(10); ' (Default segment size)
         PrintLog("\nAnalysis by segments of crank cycle\n\nFile split into %d degree crank
segments\n",segments%);
         sums% := getsegsums%();
         DoCase
            Case sums% = 0 Then analtext$ :="mean";
            Case sums% = 1 Then analtext$ :="sum";
            Case sums% = 2 Then analtext$ :="RMS";
         EndCase
         View(resh%).Print("Analysis by segments of crank cycle\nExtracting
%s\n",analtext$);
         ToolbarText("Splitting data into segments of crank cycle");
         For i% := 0 to 360-segments% Step segments% Do
            If i% = 0 Then
               evmode% := 3;
               czero% := 1;
            Else
               evmode% :=2;
               czero% := 0;
            EndIf
            numevent%[0] :=
setevent(i%,startt,endt,wavlist%[0],evmode%,czero%,i%/segments%,1);
         Next
         maxt:= findmaxt();
         For ch% := 1 to numchan%-1 Do      ' Do for all channels
            writechhead(resh%,wavlist%[ch%],analtype%,0);
            results(wavlist%[ch%],timew%,startt,sums%,resh%,maxt,analtype%);      '
Send data to text file
         Next
      Case analtype% = 1 Then          ' >>>>>>>>>>>>>>>>> Anaysis by threshold
crossing in source channel
         segments% := 3;
         threshty% := getthresh%();
         If threshty% = 0 Then
            analtext$ :="fixed";
            ArrConst(chthresh[],thresh);
         Else
            analtext$ :="% mean";
            getpercthresh(wavlist%[1:numchan%-1],thresh);
         EndIf
```

```
        PrintLog("\nAnalysis by threshold crossings\n\tThreshold: %.3f (%s)\n\tInclude
sum between thresholds: %d\t(0: no, 1:yes)\n",thresh,analtext$,int%);
        View(resh%).Print("Analysis of threshold crossings\nThreshold at %.3f
(%s)\n",thresh,analtext$);
        ToolbarText("Splitting data into segments of crank cycle");
        numevent%[0] := setevent(0,startt,endt,wavlist%[0],i%,1,0,1);          'Get crank
zero crossings
        For ch% := 1 to numchan%-1 Do       ' Do for all channels
            maxt:= findmaxt();
            PrintLog("Channel %d: %s: Threshold
%.3f\n",wavlist%[ch%],ChanTitle$(wavlist%[ch%]),chthresh[ch%-1]);
            For i% := 2 to 3 Do          ' Find low going then high going threshold crossings
                numevent%[i%-1]:= setevent(chthresh[ch%-
1],startt,endt,wavlist%[ch%],i%,0,i%-1,1);       'Get thresholdcrossings
            Next
            '#### Add routine here to sort thresht's for double peaks!
            If int% = 1 Then
                writechhead(resh%,wavlist%[ch%],analtype%,chthresh[ch%-1]);
                results(wavlist%[ch%],timew%,startt,1,resh%,maxt,analtype%);' Send data
to a text file <><><><><>
            EndIf

    dothreshpos(resh%,numevent%[],wavlist%[0],wavlist%[ch%],startt,endt,timew%); '
Write threshold crossing positions too
        Next
      Case analtype% = 2 Then          ' >>>>>>>>>>>>>>>>> Anaysis of peaks
        segments% := 1;
        peakcoeff := getpeakcoeff(75);
        PrintLog("\nAnalysis of peaks\n\tPeak coefficient at : %.3f\n",peakcoeff);
        View(resh%).Print("Analysis of peaks\nPeak coefficient %.3f\n",peakcoeff);
        ToolbarText("Splitting data into segments of crank cycle");
        numevent%[0] := setevent(0,startt,endt,wavlist%[0],i%,1,0,1);          'Get crank
zero crossings
        For ch% := 1 to numchan%-1 Do       ' Do for all channels

    dopeak(resh%,numevent%[],wavlist%[0],wavlist%[ch%],startt,endt,timew%,peakcoeff/
100);
        Next
      Else
      Message("Error!|How the hell did you get here?");
      leaveall();
    EndCase
    ToolBarText("Dividing data into time windows");       ' >>>> This needs moved!
    ToolBarText("");
    PrintLog("\nResults written to: %s\n",View(resh%).FileName$(0));
    closeres%(resh%,-1);
    leaveall();
    main();
End

main();   ' Gets the thing going!!!
```

Appendix 2: Tables of complete statistical results for the analysis of the data from Chapter 5.

2.1: Static grid

Table 2-1: Full results of Three Way ANOVAs for all points and as *x* and *y* separately for digitising method (digit), with and without the use of the correction method (correct) and the calibration sequence used (calib) for the static grid.

		df	MS	ε	*F*	*p*
calib	*X* and *Y*	1.000	118.671	1.000	4.474	0.040*
	X	1.000	75.150	1.000	4.772	0.039*
	Y	1.000	579.596	1.000	36.078	<0.001*
digit	*X* and *Y*	1.000	1.300	1.000	19.101	<0.001*
	X	1.000	0.549	1.000	9.675	0.005*
	Y	1.000	0.760	1.000	9.279	0.006*
correct	*X* and *Y*	1.000	1266	1.000	110.984	<0.001*
	X	1.000	785.503	1.000	96.897	<0.001*
	Y	1.000	497.057	1.000	34.278	<0.001*
calib x digit	*X* and *Y*	1.000	0.003	1.000	0.082	0.776
	X	1.000	0.192	1.000	6.341	0.019*
	Y	1.000	0.131	1.000	4.415	0.046*
calib x correct	*X* and *Y*	1.000	40.288	1.000	2.001	0.163
	X	1.000	52.925	1.000	3.804	0.063
	Y	1.000	264.106	1.000	16.872	<0.001*
digit x correct	*X* and *Y*	1.000	0.252	1.000	12.601	<0.001*
	X	1.000	0.199	1.000	14.461	<0.001*
	Y	1.000	0.069	1.000	2.639	0.117
calib x digit x correct	*X* and *Y*	1.000	<0.001	1.000	<0.01	0.976
	X	1.000	0.055	1.000	1.934	0.177
	Y	1.000	0.052	1.000	1.989	0.171

2.2: Dynamic sequence

Table 2-2: Full results of Three Way ANOVAs for all points and as *x* and *y* separately for digitising method (digit), with and without the use of the correction method (correct) and the calibration sequence used (calib) for the dynamic pendulum sequence.

		df	MS	*ε*	*F*	*p*
calib	*RA*	1.000	0.050	*1.000*	46.065	0.001*
	VA	1.000	0.004	*1.000*	5.027	0.111
digit	*RA*	1.000	0.008	*1.000*	1.378	0.293
	VA	1.000	1.610	*1.000*	1,238.969	<0.001*
correct	*RA*	1.000	0.046	*1.000*	50.409	<0.001*
	VA	1.000	11.574	*1.000*	197.922	<0.001*
calib x digit	*RA*	1.000	0.006	*1.000*	50.007	<0.001*
	VA	1.000	1.527	*1.000*	684.169	<0.001*
calib x correct	*RA*	1.000	0.007	*1.000*	43.085	0.001*
	VA	1.000	0.886	*1.000*	65.166	0.004*
digit x correct	*RA*	1.000	0.009	*1.000*	39.810	0.001*
	VA	1.000	1.547	*1.000*	717.920	<0.001*
calib x digit x correct	*RA*	1.000	0.007	*1.000*	41.050	0.001*
	VA	1.000	1.499	*1.000*	598.620	<0.001*

Appendix 3: Tables of complete statistical results for the analysis of the data from Chapter 8.

3.1: Resultant, effective and ineffective forces

3.1.1: Resultant force

Table 3-1: Full results of Two Way ANOVAs for the magnitude of peak resultant forces on the left and right pedals

Side		High / low		Time		High / low x time	
		SS1,7 + R1	SS2-2	SS1,7 + R1	SS2-2	SS1,7 + R1	SS2-2
Left	*df*	1.000	1.000	2.246	3.782	4.000	9.000
	MS	341.406	438670	26517	1800	150.668	395.537
	ε	1.000	1.000	1.000	1.000	1.000	1.000
	F	0.165	21.420	62.804	2.398	0.823	1.245
	p	0.696	0.002*	<0.001*	0.075	0.520	0.282
	η^2	0.020	0.728	0.887	0.231	0.093	0.135
Right	*df*	1.000	1.000	1.627	2.756	4.000	9.000
	MS	1151	466178	38201	3928	84.009	259.181
	ε	1.000	1.000	1.000	1.000	1.000	1.000
	F	0.927	28.147	26.885	6.655	0.305	1.452
	p	0.364	<0.001*	<0.001*	0.003*	0.872	0.183
	η^2	0.104	0.779	0.771	0.454	0.037	0.154

Table 3-2: Full results of Two Way ANOVAs for the crank angle at peak resultant forces on the left and right pedals

Side		High / low		Time		High / low x time	
		SS1,7 + R1	SS2-2	SS1,7 + R1	SS2-2	SS1,7 + R1	SS2-2
Left	*df*	1.000	1.000	4.000	9.000	4.000	9.000
	MS	33.599	3898	15.422	57.355	11.476	37.601
	ε	1.000	1.000	1.000	1.000	1.000	1.000
	F	0.746	1.614	0.927	1.083	1.035	0.733
	p	0.413	0.240	0.461	0.386	0.404	0.677
	η^2	0.085	0.168	0.104	0.119	0.115	0.084
Right	*df*	1.000	1.000	4.000	9.000	4.000	9.000
	MS	1516	248.672	130.628	119.950	20.122	132.183
	ε	1.000	1.000	1.000	1.000	1.000	1.000
	F	3.717	0.085	1.325	1.113	0.643	1.382
	p	0.090	0.778	0.282	0.365	0.636	0.212
	η^2	0.317	0.011	0.142	0.122	0.074	0.147

3.1.2: Effective force

Table 3-3: Full results of Two Way ANOVAs for the magnitude of peak effective forces on the left and right pedals

Side		High / low		Time		High / low x time	
		SS1,7 + R1	SS2-2	SS1,7 + R1	SS2-2	SS1,7 + R1	SS2-2
Left	*df*	1.000	1.000	2.253	9.000	4.000	9.000
	MS	500.886	391679	23230	343.346	346.887	522.991
	ε	1.000	1.000	1.000	1.000	1.000	1.000
	F	0.246	40.978	104.138	1.647	1.393	1.676
	p	0.633	<0.001*	<0.001*	0.118	0.259	0.111
	η^2	0.030	0.837	0.929	0.171	0.148	0.173
Right	*df*	1.000	1.000	1.970	9.000	4.000	9.000
	MS	398.919	446993	36347	206.975	191.563	178.612
	ε	1.000	1.000	1.000	1.000	1.000	1.000
	F	0.459	61.706	65.120	1.296	1.230	1.379
	p	0.517	<0.001*	<0.001*	0.254	0.318	0.214
	η^2	0.054	0.885	0.891	0.139	0.133	0.147

Table 3-4: Full results of Two Way ANOVAs for the crank angle at peak effective forces on the left and right pedals

Side		High / low		Time		High / low x time	
		SS1,7 + R1	SS2-2	SS1,7 + R1	SS2-2	SS1,7 + R1	SS2-2
Left	*df*	1.000	1.000	4.000	9.000	4.000	1.909
	MS	5.801	2.807	7.706	20.238	3.111	282.974
	ε	1.000	1.000	1.000	1.000	1.000	1.000
	F	0.179	0.004	0.732	1.839	1.164	2.684
	p	0.683	0.952	0.577	0.076	0.345	0.102
	η^2	0.022	<0.001	0.084	0.187	0.127	0.251
Right	*df*	1.000	1.000	2.797	9.000	4.000	1.538
	MS	28.246	43.618	9.426	9.572	3.468	145.428
	ε	1.000	1.000	1.000	1.000	1.000	1.000
	F	1.121	0.193	2.890	1.054	1.573	2.848
	p	0.321	0.672	0.061	0.407	0.205	0.105
	η^2	0.123	0.024	0.265	0.116	0.164	0.263

3.1.3: Ineffective force

Table 3-5: Full results of Two Way ANOVAs for the magnitude of peak ineffective forces on the left and right pedals

Side		High / low		Time		High / low x time	
		SS1,7 + R1	SS2-2	SS1,7 + R1	SS2-2	SS1,7 + R1	SS2-2
Left	*df*	1.000	1.000	1.424	9.000	4.000	9.000
	MS	22.610	463491	48856	532.612	320.566	371.925
	ε	1.000	1.000	1.000	1.000	1.000	1.000
	F	0.014	15.127	16.236	0.892	0.853	0.421
	p	0.908	0.005*	<0.001*	0.537	0.503	0.920
	η^2	0.002	0.654	0.670	0.100	0.096	0.050
Right	*df*	1.000	1.000	1.493	4.723	4.000	4.793
	MS	564.502	192975	15675	1125	43.033	857.474
	ε	1.000	1.000	1.000	1.000	1.000	1.000
	F	0.576	12.214	12.454	2.930	0.191	2.054
	p	0.470	0.008*	0.002*	0.027*	0.942	0.095
	η^2	0.067	0.604	0.609	0.268	0.023	0.204

Table 3-6: Full results of Two Way ANOVAs for the crank angle at peak ineffective forces on the left and right pedals

Side		High / low		Time		High / low x time	
		SS1,7 + R1	SS2-2	SS1,7 + R1	SS2-2	SS1,7 + R1	SS2-2
Left	*df*	1.000	1.000	1.717	2.802	4.000	9.000
	MS	0.001	829.715	106.668	48.788	0.997	5.197
	ε	1.000	1.000	1.000	1.000	1.000	1.000
	F	<0.01	4.691	8.188	3.896	0.453	0.856
	p	0.995	0.062	0.006*	0.024*	0.770	0.568
	η^2	<0.001	0.370	0.506	0.327	0.054	0.097
Right	*df*	1.000	1.000	1.748	2.739	4.000	5.853
	MS	7.310	1219	144.815	27.820	0.949	13.648
	ε	1.000	1.000	1.000	1.000	1.000	1.000
	F	0.371	6.851	8.288	2.948	0.315	2.160
	p	0.559	0.031*	0.005*	0.059	0.866	0.065
	η^2	0.044	0.461	0.509	0.269	0.038	0.213

Table 3-7: Full results of One Way ANOVAs for the high-fatigue trail for the whole of the second steady state for the resultant, effective and ineffective peak force parameters for the left and right pedals

Variable	Side	*df*	MS	ε	*F*	*p*	η^2
$\bar{x}$ *peak* F_r	Left	18.000	873.546	1.000	1.501	0.098	0.158
	Right	2.708	11239	1.000	4.400	0.017*	0.355
$\bar{x}$ θ_c at peak F_r	Left	1.979	941.734	1.000	1.784	0.200	0.182
	Right	1.353	2422	1.000	2.495	0.138	0.238
$\bar{x}$ *peak* F_{eff}	Left	18.000	383.107	1.000	0.697	0.810	0.080
	Right	18.000	330.242	1.000	0.982	0.484	0.109
$\bar{x}$ θ_c at peak F_{eff}	Left	2.570	408.831	1.000	5.078	0.011*	0.388
	Right	1.380	452.759	1.000	2.033	0.182	0.203
$\bar{x}$ *peak* F_{ineff}	Left	18.000	786.807	1.000	0.469	0.967	0.055
	Right	2.297	15093	1.000	6.651	0.005*	0.454
$\bar{x}$ θ_c at peak F_{ineff}	Left	2.310	130.668	1.000	2.807	0.080	0.260
	Right	2.647	143.166	1.000	5.204	0.009*	0.394

Table 3-8 p-values for *post hoc* pair-wise comparisons of peak resultant force at the right pedal with (un-shaded) and without (least significant difference) (shaded) Bonferroni correction

	8%	13%	18%	24%	29%	34%	39%	45%	50%	55%	61%	66%	71%	76%	82%	87%	92%	97%	
	0.194	0.641	0.077	0.033*	0.046*	0.053	0.016*	0.007*	0.015*	0.050*	0.011*	0.005*	0.006*	0.006*	0.008*	0.008*	0.007*	0.282	**3%**
92%	1.000	0.422	0.209	0.366	0.229	0.250	0.046*	0.036*	0.043*	0.179	0.013*	0.006*	0.007*	0.006*	0.006*	0.008*	0.006*	0.354	**8%**
87%	1.000	1.000	0.059	0.084	0.015*	0.018*	0.007*	0.003*	0.001*	0.018*	0.003*	0.001*	0.003*	0.001*	0.001*	0.003*	0.002*	0.299	**13%**
82%	1.000	1.000	1.000	0.365	0.921	0.916	0.482	0.263	0.127	0.615	0.017*	0.028*	0.019*	0.067	0.019*	0.004*	0.006*	0.662	**18%**
76%	1.000	1.000	1.000	1.000	0.323	0.325	0.040*	0.020*	0.048*	0.185	0.008*	0.004*	0.006*	0.006*	0.006*	0.011*	0.007*	0.521	**24%**
71%	1.000	1.000	1.000	1.000	1.000	0.961	0.466	0.154	0.074	0.483	0.021*	0.017*	0.013*	0.052	0.017*	0.009*	0.008*	0.674	**29%**
66%	1.000	1.000	1.000	1.000	1.000	1.000	0.253	0.110	0.008*	0.182	0.045*	0.013*	0.042*	0.006*	0.008*	0.022*	0.013*	0.670	**34%**
61%	1.000	1.000	1.000	1.000	1.000	1.000	1.000	0.506	0.174	0.835	0.065	0.014*	0.050	0.014*	0.015*	0.022*	0.014*	0.783	**39%**
55%	1.000	1.000	1.000	1.000	1.000	1.000	1.000	1.000	0.288	0.957	0.117	0.037*	0.057	0.079	0.053	0.030*	0.025*	0.853	**45%**
50%	1.000	1.000	1.000	1.000	1.000	1.000	1.000	1.000	1.000	0.367	0.535	0.175	0.336	0.202	0.117	0.063	0.043*	0.983	**50%**
45%	1.000	1.000	1.000	1.000	1.000	1.000	1.000	1.000	1.000	1.000	0.288	0.065	0.202	0.033*	0.043*	0.065	0.032*	0.854	**55%**
39%	1.000	1.000	1.000	1.000	1.000	1.000	1.000	1.000	1.000	1.000	1.000	0.183	0.185	0.573	0.214	0.043*	0.023*	0.819	**61%**
34%	1.000	1.000	1.000	1.000	1.000	1.000	1.000	1.000	1.000	1.000	1.000	1.000	0.674	0.645	0.955	0.193	0.077	0.566	**66%**
29%	1.000	1.000	1.000	1.000	1.000	1.000	1.000	1.000	1.000	1.000	1.000	1.000	1.000	0.963	0.801	0.118	0.092	0.673	**71%**
24%	1.000	1.000	1.000	0.950	1.000	1.000	0.706	1.000	1.000	1.000	1.000	1.000	1.000	1.000	0.600	0.248	0.125	0.673	**76%**
18%	1.000	1.000	0.746	1.000	1.000	1.000	1.000	1.000	1.000	1.000	1.000	1.000	1.000	1.000	1.000	0.199	0.068	0.593	**82%**
13%	1.000	0.298	0.489	0.086	0.151	0.508	0.230	0.478	1.000	0.251	0.524	1.000	1.000	1.000	1.000	1.000	0.725	0.201	**87%**
8%	1.000	1.000	1.000	1.000	1.000	1.000	0.943	1.000	1.000	1.000	1.000	1.000	1.000	1.000	1.000	1.000	1.000	0.165	**92%**
3%	1.000	1.000	1.000	1.000	1.000	1.000	0.864	1.000	1.000	1.000	1.000	1.000	1.000	1.000	1.000	1.000	1.000	1.000	
	97%	**92%**	**87%**	**82%**	**76%**	**71%**	**66%**	**61%**	**55%**	**50%**	**45%**	**39%**	**34%**	**29%**	**24%**	**18%**	**13%**	**8%**	

Table 3-9 *p*-values for *post hoc* pair-wise comparisons of left crank angle at peak effective force with (un-shaded) and without (least significant difference) (shaded) Bonferroni correction

	8%	13%	18%	24%	29%	34%	39%	45%	50%	55%	61%	66%	71%	76%	82%	87%	92%	97%	
	0.318	0.976	0.222	0.609	0.467	0.726	0.576	0.795	0.749	0.369	0.165	0.126	0.311	0.080	0.063	0.015*	0.008*	0.014*	**3%**
92%	1.000	0.483	0.997	0.208	0.705	0.536	0.972	0.523	0.774	0.221	0.098	0.114	0.140	0.051	0.045*	0.016*	0.015*	0.018*	**8%**
87%	1.000	1.000	0.524	0.714	0.429	0.750	0.634	0.855	0.790	0.503	0.272	0.234	0.400	0.170	0.125	0.052	0.038*	0.031*	**13%**
82%	1.000	1.000	1.000	0.053	0.757	0.581	0.977	0.403	0.797	0.109	0.045*	0.066	0.095	0.019*	0.025*	0.008*	0.008*	0.017*	**18%**
76%	1.000	1.000	1.000	1.000	0.216	0.264	0.248	0.404	0.414	0.429	0.118	0.140	0.386	0.059	0.080	0.021*	0.018*	0.034*	**24%**
71%	1.000	1.000	1.000	1.000	1.000	0.285	0.637	0.379	0.455	0.247	0.118	0.136	0.133	0.057	0.069	0.029*	0.026*	0.027*	**29%**
66%	1.000	1.000	1.000	1.000	1.000	1.000	0.650	0.806	0.920	0.260	0.099	0.127	0.149	0.047*	0.061	0.025*	0.023*	0.030*	**34%**
61%	1.000	1.000	1.000	1.000	1.000	1.000	1.000	0.598	0.740	0.243	0.087	0.114	0.071	0.028*	0.027*	0.008*	0.014*	0.018*	**39%**
55%	1.000	1.000	1.000	1.000	1.000	1.000	1.000	1.000	0.808	0.261	0.102	0.110	0.128	0.033*	0.050*	0.018*	0.017*	0.027*	**45%**
50%	1.000	1.000	1.000	1.000	1.000	1.000	1.000	1.000	1.000	0.285	0.114	0.139	0.128	0.050*	0.058	0.025*	0.026*	0.035*	**50%**
45%	1.000	1.000	1.000	1.000	1.000	1.000	1.000	1.000	1.000	1.000	0.078	0.074	0.801	0.047*	0.091	0.038*	0.027*	0.072	**55%**
39%	1.000	1.000	1.000	1.000	1.000	1.000	1.000	1.000	1.000	1.000	1.000	0.293	0.398	0.385	0.296	0.094	0.054	0.109	**61%**
34%	1.000	1.000	1.000	1.000	1.000	1.000	1.000	1.000	1.000	1.000	1.000	1.000	0.233	0.670	0.820	0.287	0.078	0.177	**66%**
29%	1.000	1.000	1.000	1.000	1.000	1.000	1.000	1.000	1.000	1.000	1.000	1.000	1.000	0.040*	0.069	0.032*	0.036*	0.069	**71%**
24%	1.000	1.000	1.000	1.000	1.000	1.000	1.000	1.000	1.000	1.000	1.000	1.000	1.000	1.000	0.403	0.094	0.062	0.123	**76%**
18%	1.000	1.000	1.000	1.000	1.000	1.000	1.000	1.000	1.000	1.000	1.000	1.000	1.000	1.000	1.000	0.078	0.081	0.141	**82%**
13%	1.000	1.000	1.000	1.000	1.000	1.000	1.000	1.000	1.000	1.000	1.000	1.000	1.000	1.000	1.000	1.000	0.127	0.190	**87%**
8%	1.000	1.000	1.000	1.000	1.000	1.000	1.000	1.000	1.000	1.000	1.000	1.000	1.000	1.000	1.000	1.000	1.000	0.454	**92%**
3%	1.000	1.000	1.000	1.000	1.000	1.000	1.000	1.000	1.000	1.000	1.000	1.000	1.000	1.000	1.000	1.000	1.000	1.000	
	97%	**92%**	**87%**	**82%**	**76%**	**71%**	**66%**	**61%**	**55%**	**50%**	**45%**	**39%**	**34%**	**29%**	**24%**	**18%**	**13%**	**8%**	

Table 3-10 *p*-values for *post hoc* pair-wise comparisons of right peak ineffective force with (un-shaded) and without (least significant difference) (shaded) Bonferroni correction

	8%	13%	18%	24%	29%	34%	39%	45%	50%	55%	61%	66%	71%	76%	82%	87%	92%	97%	
	0.838	0.710	0.082	0.080	0.039*	0.010*	0.010*	0.004*	0.009*	0.016*	0.008*	0.005*	0.009*	0.005*	0.004*	0.004*	0.004*	0.154	**3%**
92%	1.000	0.963	0.135	0.215	0.100	0.036*	0.009*	0.010*	0.027*	0.046*	0.004*	0.003*	0.004*	0.003*	0.001*	0.002*	0.003*	0.121	**8%**
87%	1.000	1.000	0.105	0.123	0.028*	0.011*	0.013*	0.007*	0.005*	0.011*	0.008*	0.005*	0.008*	0.003*	0.002*	0.003*	0.003*	0.151	**13%**
82%	1.000	1.000	1.000	0.335	0.730	0.174	0.128	0.172	0.067	0.218	0.024*	0.016*	0.021*	0.017*	0.012*	0.009*	0.007*	0.367	**18%**
76%	1.000	1.000	1.000	1.000	0.082	0.020*	0.024*	0.015*	0.010*	0.033*	0.013*	0.008*	0.015*	0.006*	0.005*	0.005*	0.005*	0.246	**24%**
71%	1.000	1.000	1.000	1.000	1.000	0.184	0.163	0.169	0.021*	0.137	0.042*	0.025*	0.034*	0.016*	0.013*	0.011*	0.009*	0.389	**29%**
66%	1.000	1.000	1.000	1.000	1.000	1.000	0.649	0.459	0.218	0.654	0.120	0.043*	0.070	0.019*	0.017*	0.012*	0.007*	0.534	**34%**
61%	1.000	1.000	1.000	1.000	1.000	1.000	1.000	0.820	0.622	0.964	0.012*	0.003*	0.015*	0.006*	0.003*	0.003*	0.004*	0.574	**39%**
55%	1.000	1.000	1.000	1.000	1.000	1.000	1.000	1.000	0.706	0.828	0.180	0.030*	0.077	0.018*	0.010*	0.007*	0.006*	0.601	**45%**
50%	1.000	1.000	1.000	1.000	1.000	1.000	1.000	1.000	1.000	0.402	0.469	0.207	0.233	0.104	0.068	0.032*	0.017*	0.717	**50%**
45%	1.000	1.000	1.000	1.000	1.000	1.000	1.000	1.000	1.000	1.000	0.201	0.071	0.102	0.024*	0.019*	0.014*	0.011*	0.605	**55%**
39%	1.000	0.602	0.479	0.570	0.971	1.000	0.521	1.000	1.000	1.000	1.000	0.075	0.044*	0.096	0.013*	0.012*	0.023*	0.960	**61%**
34%	1.000	1.000	1.000	1.000	1.000	1.000	1.000	1.000	1.000	1.000	1.000	1.000	0.642	0.518	0.050*	0.011*	0.024*	0.794	**66%**
29%	1.000	1.000	1.000	1.000	1.000	1.000	1.000	1.000	1.000	1.000	1.000	1.000	1.000	0.778	0.047*	0.023*	0.064	0.737	**71%**
24%	1.000	0.772	0.924	0.877	0.987	1.000	1.000	1.000	1.000	1.000	1.000	1.000	1.000	1.000	0.022*	0.034*	0.058	0.669	**76%**
18%	1.000	1.000	1.000	1.000	1.000	1.000	1.000	1.000	1.000	1.000	1.000	1.000	1.000	1.000	1.000	0.253	0.332	0.403	**82%**
13%	1.000	0.547	0.519	0.384	0.452	1.000	0.919	1.000	1.000	0.810	1.000	1.000	1.000	1.000	1.000	1.000	0.602	0.186	**87%**
8%	1.000	0.474	0.359	0.246	0.461	0.650	0.496	0.694	1.000	1.000	1.000	1.000	1.000	1.000	1.000	1.000	1.000	0.142	**92%**
3%	1.000	0.616	0.644	0.617	0.803	1.000	0.872	1.000	1.000	1.000	0.729	1.000	1.000	1.000	1.000	1.000	1.000	1.000	
	97%	**92%**	**87%**	**82%**	**76%**	**71%**	**66%**	**61%**	**55%**	**50%**	**45%**	**39%**	**34%**	**29%**	**24%**	**18%**	**13%**	**8%**	

Table 3-11 *p*-values for *post hoc* pair-wise comparisons of crank angle at right peak ineffective force with (un-shaded) and without (least significant difference) (shaded) Bonferroni correction

	8%	13%	18%	24%	29%	34%	39%	45%	50%	55%	61%	66%	71%	76%	82%	87%	92%	97%	
	0.418	0.434	0.145	0.951	0.859	0.171	0.231	0.136	0.224	0.146	0.028*	0.066	0.071	0.045*	0.020*	0.045*	0.054	0.002*	**3%**
92%	1.000	0.989	0.179	0.391	0.564	0.319	0.367	0.274	0.378	0.221	0.023*	0.074	0.082	0.058	0.019*	0.045*	0.054	0.003*	**8%**
87%	1.000	1.000	0.433	0.423	0.582	0.229	0.528	0.393	0.349	0.270	0.070	0.149	0.178	0.118	0.058	0.089	0.093	0.006*	**13%**
82%	1.000	1.000	1.000	0.092	0.103	0.604	0.824	0.622	0.602	0.307	0.030*	0.129	0.154	0.111	0.040*	0.067	0.077	0.003*	**18%**
76%	1.000	1.000	1.000	1.000	0.856	0.049*	0.126	0.102	0.062	0.057	0.006*	0.049*	0.067	0.043*	0.014*	0.030*	0.033*	0.002*	**24%**
71%	1.000	1.000	1.000	1.000	1.000	0.118	0.105	0.200	0.065	0.013*	0.002*	0.043*	0.061	0.034*	0.019*	0.023*	0.033*	0.002*	**29%**
66%	1.000	1.000	1.000	1.000	1.000	1.000	0.689	0.985	0.935	0.623	0.117	0.179	0.249	0.150	0.072	0.089	0.079	0.004*	**34%**
61%	1.000	1.000	1.000	1.000	1.000	1.000	1.000	0.670	0.686	0.341	0.000*	0.039*	0.072	0.026*	0.017*	0.025*	0.032*	0.001*	**39%**
55%	1.000	1.000	1.000	1.000	1.000	1.000	1.000	1.000	0.957	0.611	0.088	0.095	0.133	0.084	0.012*	0.048*	0.055	0.005*	**45%**
50%	1.000	1.000	1.000	1.000	1.000	1.000	1.000	1.000	1.000	0.426	0.106	0.183	0.249	0.185	0.059	0.065	0.075	0.008*	**50%**
45%	0.895	1.000	1.000	1.000	1.000	1.000	1.000	1.000	1.000	1.000	0.181	0.291	0.398	0.312	0.076	0.087	0.122	0.013*	**55%**
39%	0.180	1.000	1.000	1.000	1.000	1.000	1.000	0.080	1.000	1.000	1.000	0.544	0.787	0.548	0.118	0.167	0.196	0.012*	**61%**
34%	0.744	1.000	1.000	1.000	1.000	1.000	1.000	1.000	1.000	1.000	1.000	1.000	0.498	0.946	0.172	0.044*	0.094	0.032*	**66%**
29%	0.279	1.000	1.000	1.000	1.000	1.000	1.000	0.277	1.000	1.000	1.000	1.000	1.000	0.674	0.141	0.033*	0.068	0.024*	**71%**
24%	0.324	1.000	1.000	1.000	1.000	1.000	1.000	1.000	1.000	1.000	1.000	1.000	1.000	1.000	0.221	0.171	0.212	0.032*	**76%**
18%	0.439	1.000	1.000	1.000	1.000	1.000	1.000	1.000	1.000	1.000	1.000	1.000	1.000	1.000	1.000	0.990	0.936	0.281	**82%**
13%	1.000	1.000	1.000	1.000	1.000	1.000	1.000	1.000	1.000	1.000	1.000	1.000	1.000	1.000	1.000	1.000	0.827	0.237	**87%**
8%	0.489	1.000	1.000	1.000	1.000	1.000	1.000	1.000	1.000	1.000	1.000	1.000	1.000	1.000	1.000	1.000	1.000	0.251	**92%**
3%	0.287	1.000	1.000	1.000	1.000	1.000	1.000	1.000	1.000	1.000	1.000	1.000	1.000	1.000	1.000	1.000	1.000	1.000	
	97%	**92%**	**87%**	**82%**	**76%**	**71%**	**66%**	**61%**	**55%**	**50%**	**45%**	**39%**	**34%**	**29%**	**24%**	**18%**	**13%**	**8%**	

3.2: Work and power

3.2.1: Total, negative and positive work

Table 3-12: Full results of Two Way ANOVAs for total work on the left and right pedals

Side		High / low		Time		High / low x time	
		SS1,7 + R1	SS2-2	SS1,7 + R1	SS2-2	SS1,7 + R1	SS2-2
Left	*df*	1.000	1.000	1.558	9.000	4.000	9.000
	MS	87.675	57815	7717	9.063	4.400	4.929
	ε	1.000	1.000	1.000	1.000	1.000	1.000
	F	0.933	144.007	216.601	1.302	1.144	0.419
	p	0.362	<0.001*	<0.001*	0.251	0.354	0.921
	η^2	0.104	0.947	0.964	0.140	0.125	0.050
Right	*df*	1.000	1.000	1.232	9.000	4.000	9.000
	MS	6.928	45891	7675	3.969	1.452	10.153
	ε	1.000	1.000	1.000	1.000	1.000	1.000
	F	0.138	179.247	177.081	1.492	0.361	1.946
	p	0.720	<0.001*	<0.001*	0.168	0.835	0.059
	η^2	0.017	0.957	0.957	0.157	0.043	0.196

Table 3-13: Full results of Two Way ANOVAs for sum negative work on the left and right pedals

Side		High / low		Time		High / low x time	
		SS1,7 + R1	SS2-2	SS1,7 + R1	SS2-2	SS1,7 + R1	SS2-2
Left	*df*	1.000	1.000	2.241	9.000	4.000	9.000
	MS	4.109	0.418	51.849	10.161	10.632	18.975
	ε	1.000	1.000	1.000	1.000	1.000	1.000
	F	0.306	0.003	4.175	0.917	1.765	1.503
	p	0.595	0.961	0.029*	0.515	0.160	0.163
	η^2	0.037	<0.001	0.343	0.103	0.181	0.158
Right	*df*	1.000	1.000	1.986	9.000	4.000	9.000
	MS	2.795	222.961	22.729	1.648	0.209	1.145
	ε	1.000	1.000	1.000	1.000	1.000	1.000
	F	1.120	7.912	10.039	1.006	0.181	0.697
	p	0.321	0.023*	0.002*	0.443	0.947	0.710
	η^2	0.123	0.497	0.557	0.112	0.022	0.080

Table 3-14: Full results of Two Way ANOVAs for sum positive work on the left and right pedals

Side		High / low		Time		High / low x time	
		SS1,7 + R1	SS2-2	SS1,7 + R1	SS2-2	SS1,7 + R1	SS2-2
Left	*df*	1.000	1.000	1.240	9.000	4.000	9.000
	MS	816.794	52314	8925	215.718	192.828	192.837
	ε	1.000	1.000	1.000	1.000	1.000	1.000
	F	2.551	15.203	5.585	1.021	1.011	0.777
	p	0.149	0.005*	0.035*	0.432	0.417	0.638
	η^2	0.242	0.655	0.411	0.113	0.112	0.089
Right	*df*	1.000	1.000	1.230	9.000	2.600	9.000
	MS	1364	43600	9841	44.350	297.940	51.745
	ε	1.000	1.000	1.000	1.000	1.000	1.000
	F	4.560	16.152	17.662	0.670	2.837	0.535
	p	0.065	0.004*	0.001*	0.733	0.070	0.844
	η^2	0.363	0.669	0.688	0.077	0.262	0.063

3.2.2: Crank angle at which positive work started and ended

Table 3-15: Full results of Two Way ANOVAs for crank angle where positive work started on the left and right pedals

Side		High / low		Time		High / low x time	
		SS1,7 + R1	SS2-2	SS1,7 + R1	SS2-2	SS1,7 + R1	SS2-2
Left	*df*	1.000	1.000	1.734	4.197	4.000	2.634
	MS	67.912	24897	1953	1272	53.871	4102
	ε	1.000	1.000	1.000	1.000	1.000	1.000
	F	0.048	1.281	3.390	2.606	0.641	4.864
	p	0.833	0.290	0.069	0.051	0.637	0.012*
	η^2	0.006	0.138	0.298	0.246	0.074	0.378
Right	*df*	1.000	1.000	1.655	9.000	4.000	9.000
	MS	20.871	20684	286.459	132.803	5.685	269.071
	ε	1.000	1.000	1.000	1.000	1.000	1.000
	F	0.356	6.579	16.577	1.164	1.468	1.410
	p	0.567	0.033*	<0.001*	0.331	0.235	0.200
	η^2	0.043	0.451	0.674	0.127	0.155	0.150

Table 3-16: Full results of One Way ANOVAs for the for crank angle where positive work started for the left leg during the second steady state section (SS2-2) of the high and low fatigue trials separately

Side	Trial	*df*	MS	ε	*F*	*p*	η^2
Left	Low fatigue	7.348	325.869	1.000	2.611	0.019*	0.246
	High fatigue	2.279	6033	1.000	4.100	0.030*	0.339

Table 3-17: Full results of One Way ANOVAs (high/low) at each time window for the crank angle where positive work started for the left leg during the second steady state section (SS2-2) of the fatigue trials.

Time window	*df*	MS	ε	*F*	*p*	η^2
1	1.000	12332	1.000	4.795	0.060	0.375
2	1.000	8835	1.000	5.732	0.044*	0.417
3	1.000	4645	1.000	2.921	0.126	0.267
4	1.000	4260	1.000	2.861	0.129	0.263
5	1.000	1838	1.000	1.038	0.338	0.115
6	1.000	1575	1.000	0.615	0.455	0.071
7	1.000	747.117	1.000	0.339	0.576	0.041
8	1.000	1280	1.000	0.536	0.485	0.063
9	1.000	185.943	1.000	0.065	0.806	0.008
10	1.000	1.432	1.000	<0.01	0.982	<0.001

Table 3-18: Full results of Two Way ANOVAs for crank angle where positive work ended on the left and right pedals

Side		High / low		Time		High / low x time	
		SS1,7 + R1	SS2-2	SS1,7 + R1	SS2-2	SS1,7 + R1	SS2-2
Left	*df*	1.000	1.000	1.323	3.660	4.000	9.000
	MS	10295	8009	23546	57.556	3529	6.387
	ε	1.000	1.000	1.000	1.000	1.000	1.000
	F	1.976	0.440	5.614	3.098	1.596	0.898
	p	0.197	0.526	0.031*	0.034*	0.199	0.532
	η^2	0.198	0.052	0.412	0.279	0.166	0.101
Right	*df*	1.000	1.000	1.383	9.000	4.000	9.000
	MS	82.733	3232	431.417	21.392	3.543	13.868
	ε	1.000	1.000	1.000	1.000	1.000	1.000
	F	1.720	10.413	9.498	1.325	0.812	1.091
	p	0.226	0.012*	0.007*	0.239	0.527	0.380
	η^2	0.177	0.566	0.543	0.142	0.092	0.120

3.2.3: Power

Table 3-19: Full results of Two Way ANOVAs for mean power on the left and right pedals

Side		High / low		Time		High / low x time	
		SS1,7 + R1	SS2-2	SS1,7 + R1	SS2-2	SS1,7 + R1	SS2-2
Left	*df*	1.000	1.000	1.503	9.000	4.000	9.000
	MS	184.814	247858	32470	49.205	43.976	94.367
	ε	1.000	1.000	1.000	1.000	1.000	1.000
	F	0.897	169.775	94.375	1.218	1.016	1.681
	p	0.371	<0.001*	<0.001*	0.298	0.414	0.109
	η^2	0.101	0.955	0.922	0.132	0.113	0.174
Right	*df*	1.000	1.000	1.449	9.000	4.000	9.000
	MS	31.035	179800	25721	41.969	25.778	77.886
	ε	1.000	1.000	1.000	1.000	1.000	1.000
	F	0.113	148.891	94.610	1.752	0.693	1.668
	p	0.746	<0.001*	<0.001*	0.093	0.602	0.113
	η^2	0.014	0.949	0.922	0.180	0.080	0.173

Table 3-20: Full results of One Way ANOVAs for the high-fatigue trail for the whole of the second steady state (SS2-1) for the work and power parameters for the left and right pedals

Variable	Side	*df*	MS	ε	*F*	*p*	η^2
Σ Total work	Left	3.106	560.781	1.000	3.045	0.046*	0.276
	Right	2.029	490.870	1.000	4.230	0.033*	0.346
Σ Negative work	Left	18.000	21.585	1.000	0.835	0.656	0.095
	Right	18.000	3.987	1.000	1.584	0.071	0.165
Σ Positive work	Left	18.000	418.263	1.000	0.756	0.747	0.086
	Right	18.000	150.956	1.000	1.175	0.289	0.128
$\bar{x}$ θ_c at start pos. work	Left	3.170	5853	1.000	2.995	0.047*	0.272
	Right	18.000	2417	1.000	0.898	0.582	0.101
$\bar{x}$ θ_c at end pos. work	Left	18.000	14.020	1.000	1.291	0.202	0.139
	Right	18.000	11.573	1.000	0.567	0.918	0.066
$\bar{x}$ power	Left	2.841	2524	1.000	3.745	0.027*	0.319
	Right	2.302	1908	1.000	3.783	0.037*	0.321

Table 3-21 *p*-values for *post hoc* pair-wise comparisons of left total work with (un-shaded) and without (least significant difference) (shaded) Bonferroni correction

	8%	13%	18%	24%	29%	34%	39%	45%	50%	55%	61%	66%	71%	76%	82%	87%	92%	97%	
	0.848	0.233	0.351	0.091	0.402	0.253	0.079	0.216	0.657	0.475	0.497	0.188	0.247	0.335	0.519	0.183	0.222	0.050*	**3%**
92%	1.000	0.093	0.292	0.057	0.347	0.206	0.038*	0.111	0.631	0.419	0.445	0.132	0.187	0.276	0.488	0.140	0.175	0.037*	**8%**
87%	1.000	1.000	0.847	0.274	0.872	0.547	0.164	0.434	0.997	0.812	0.825	0.280	0.349	0.468	0.752	0.256	0.293	0.057	**13%**
82%	1.000	1.000	1.000	0.193	0.589	0.441	0.080	0.351	0.934	0.713	0.738	0.232	0.337	0.384	0.672	0.189	0.246	0.052	**18%**
76%	1.000	1.000	1.000	1.000	0.410	0.561	0.693	0.826	0.523	0.505	0.434	0.679	0.762	0.822	0.815	0.407	0.489	0.094	**24%**
71%	1.000	1.000	1.000	1.000	1.000	0.736	0.150	0.454	0.890	0.901	0.927	0.302	0.433	0.447	0.797	0.200	0.268	0.052	**29%**
66%	1.000	1.000	1.000	1.000	1.000	1.000	0.195	0.704	0.721	0.852	0.850	0.229	0.407	0.548	0.932	0.259	0.288	0.077	**34%**
61%	1.000	1.000	1.000	1.000	1.000	1.000	1.000	0.489	0.387	0.321	0.336	0.826	0.892	0.917	0.713	0.484	0.559	0.092	**39%**
55%	1.000	1.000	1.000	1.000	1.000	1.000	1.000	1.000	0.408	0.548	0.621	0.522	0.622	0.705	0.910	0.329	0.387	0.057	**45%**
50%	1.000	1.000	1.000	1.000	1.000	1.000	1.000	1.000	1.000	0.671	0.792	0.187	0.183	0.251	0.653	0.062	0.076	0.036*	**50%**
45%	1.000	1.000	1.000	1.000	1.000	1.000	1.000	1.000	1.000	1.000	0.963	0.015*	0.099	0.286	0.762	0.058	0.068	0.060	**55%**
39%	1.000	1.000	1.000	1.000	1.000	1.000	1.000	1.000	1.000	1.000	1.000	0.027*	0.099	0.304	0.745	0.066	0.073	0.067	**61%**
34%	1.000	1.000	1.000	1.000	1.000	1.000	1.000	1.000	1.000	1.000	1.000	1.000	0.954	0.983	0.412	0.343	0.384	0.102	**66%**
29%	1.000	1.000	1.000	1.000	1.000	1.000	1.000	1.000	1.000	1.000	1.000	1.000	1.000	0.997	0.395	0.287	0.264	0.098	**71%**
24%	1.000	1.000	1.000	1.000	1.000	1.000	1.000	1.000	1.000	1.000	1.000	1.000	1.000	1.000	0.150	0.114	0.202	0.080	**76%**
18%	1.000	1.000	1.000	1.000	1.000	1.000	1.000	1.000	1.000	1.000	1.000	1.000	1.000	1.000	1.000	0.008*	0.024*	0.079	**82%**
13%	1.000	1.000	1.000	1.000	1.000	1.000	1.000	1.000	1.000	1.000	1.000	1.000	1.000	1.000	1.000	1.000	0.634	0.136	**87%**
8%	1.000	1.000	1.000	1.000	1.000	1.000	1.000	1.000	1.000	1.000	1.000	1.000	1.000	1.000	1.000	1.000	1.000	0.133	**92%**
3%	1.000	1.000	1.000	1.000	1.000	1.000	1.000	1.000	1.000	1.000	1.000	1.000	1.000	1.000	1.000	1.000	1.000	1.000	
	97%	**92%**	**87%**	**82%**	**76%**	**71%**	**66%**	**61%**	**55%**	**50%**	**45%**	**39%**	**34%**	**29%**	**24%**	**18%**	**13%**	**8%**	

Table 3-22 *p*-values for *post hoc* pair-wise comparisons of right total work with (un-shaded) and without (least significant difference) (shaded) Bonferroni correction

	8%	13%	18%	24%	29%	34%	39%	45%	50%	55%	61%	66%	71%	76%	82%	87%	92%	97%	
	0.129	0.456	0.027*	0.198	0.105	0.039*	0.095	0.125	0.091	0.659	0.034*	0.183	0.051	0.468	0.624	0.679	0.966	0.071	**3%**
92%	1.000	0.306	0.057	0.538	0.360	0.081	0.262	0.422	0.252	0.644	0.145	0.800	0.303	0.757	0.682	0.335	0.306	0.035*	**8%**
87%	1.000	1.000	0.004*	0.175	0.078	0.002*	0.055	0.191	0.012*	0.989	0.059	0.118	0.063	0.709	0.977	0.530	0.581	0.058	**13%**
82%	1.000	1.000	1.000	0.380	0.603	0.824	0.355	0.505	0.785	0.147	0.933	0.143	0.527	0.052	0.173	0.161	0.054	0.027*	**18%**
76%	1.000	1.000	1.000	1.000	0.672	0.180	0.803	0.800	0.410	0.347	0.412	0.755	0.672	0.444	0.435	0.283	0.198	0.047*	**24%**
71%	1.000	1.000	1.000	1.000	1.000	0.411	0.737	0.778	0.895	0.206	0.601	0.362	0.986	0.009*	0.116	0.176	0.056	0.036*	**29%**
66%	1.000	1.000	1.000	1.000	1.000	1.000	0.146	0.367	0.521	0.050	0.946	0.086	0.531	0.018*	0.089	0.143	0.045*	0.032*	**34%**
61%	1.000	1.000	1.000	1.000	1.000	1.000	1.000	0.902	0.430	0.269	0.388	0.604	0.724	0.317	0.370	0.250	0.180	0.036*	**39%**
55%	1.000	1.000	1.000	1.000	1.000	1.000	1.000	1.000	0.708	0.375	0.420	0.616	0.750	0.304	0.336	0.205	0.126	0.035*	**45%**
50%	1.000	1.000	1.000	1.000	1.000	1.000	1.000	1.000	1.000	0.056	0.799	0.224	0.906	0.154	0.261	0.243	0.158	0.040*	**50%**
45%	1.000	1.000	1.000	1.000	1.000	1.000	1.000	1.000	1.000	1.000	0.208	0.354	0.267	0.781	0.971	0.586	0.682	0.086	**55%**
39%	1.000	1.000	1.000	1.000	1.000	1.000	1.000	1.000	1.000	1.000	1.000	0.352	0.590	0.124	0.156	0.126	0.054	0.029*	**61%**
34%	1.000	1.000	1.000	1.000	1.000	1.000	1.000	1.000	1.000	1.000	1.000	1.000	0.319	0.410	0.504	0.333	0.233	0.051	**66%**
29%	1.000	1.000	1.000	1.000	1.000	1.000	1.000	1.000	1.000	1.000	1.000	1.000	1.000	0.087	0.220	0.180	0.064	0.033*	**71%**
24%	1.000	1.000	1.000	1.000	1.000	1.000	1.000	1.000	1.000	1.000	1.000	1.000	1.000	1.000	0.753	0.422	0.357	0.053	**76%**
18%	1.000	1.000	1.000	1.000	1.000	1.000	1.000	1.000	1.000	1.000	1.000	1.000	1.000	1.000	1.000	0.356	0.355	0.070	**82%**
13%	1.000	1.000	1.000	1.000	1.000	1.000	1.000	1.000	1.000	1.000	1.000	1.000	0.310	1.000	1.000	0.659	0.559	0.108	**87%**
8%	1.000	1.000	1.000	1.000	1.000	1.000	1.000	1.000	1.000	1.000	1.000	1.000	1.000	1.000	1.000	1.000	1.000	0.080	**92%**
3%	1.000	1.000	1.000	1.000	1.000	1.000	1.000	1.000	1.000	1.000	1.000	1.000	1.000	1.000	1.000	1.000	1.000	1.000	
	97%	**92%**	**87%**	**82%**	**76%**	**71%**	**66%**	**61%**	**55%**	**50%**	**45%**	**39%**	**34%**	**29%**	**24%**	**18%**	**13%**	**8%**	

Table 3-23 *p*-values for *post hoc* pair-wise comparisons of the crank angle at which positive work started on the left pedal with (un-shaded) and without (least significant difference) (shaded) Bonferroni correction

	8%	13%	18%	24%	29%	34%	39%	45%	50%	55%	61%	66%	71%	76%	82%	87%	92%	97%	
	0.090	0.492	0.196	0.337	0.298	0.067	0.050	0.255	0.173	0.216	0.367	0.124	0.185	0.409	0.284	0.153	0.180	0.218	**3%**
92%	1.000	0.524	0.735	0.833	0.635	0.097	0.088	0.370	0.259	0.425	0.016*	0.026*	0.135	0.272	0.201	0.095	0.119	0.163	**8%**
87%	1.000	1.000	0.460	0.621	0.492	0.147	0.102	0.304	0.238	0.336	0.118	0.112	0.149	0.366	0.243	0.135	0.165	0.198	**13%**
82%	1.000	1.000	1.000	0.933	0.789	0.158	0.142	0.412	0.301	0.519	0.098	0.043*	0.114	0.233	0.174	0.074	0.098	0.142	**18%**
76%	1.000	1.000	1.000	1.000	0.616	0.049*	0.043*	0.371	0.248	0.467	0.087	0.048*	0.123	0.234	0.170	0.072	0.097	0.138	**24%**
71%	1.000	1.000	1.000	1.000	1.000	0.226	0.030*	0.352	0.259	0.543	0.138	0.084	0.089	0.221	0.126	0.075	0.096	0.106	**29%**
66%	1.000	1.000	1.000	1.000	1.000	1.000	0.402	0.735	0.589	0.849	0.022*	0.009*	0.047*	0.052	0.057	0.014*	0.023*	0.046*	**34%**
61%	1.000	1.000	1.000	1.000	1.000	1.000	1.000	0.937	0.776	0.328	0.019*	0.009*	0.019*	0.036*	0.022*	0.008*	0.014*	0.015*	**39%**
55%	1.000	1.000	1.000	1.000	1.000	1.000	1.000	1.000	0.863	0.385	0.193	0.152	0.056	0.173	0.076	0.072	0.082	0.029*	**45%**
50%	1.000	1.000	1.000	1.000	1.000	1.000	1.000	1.000	1.000	0.177	0.116	0.083	0.052	0.094	0.060	0.031*	0.037*	0.010*	**50%**
45%	1.000	1.000	1.000	1.000	1.000	1.000	1.000	1.000	1.000	1.000	0.134	0.081	0.050	0.158	0.078	0.054	0.069	0.039*	**55%**
39%	1.000	1.000	1.000	1.000	1.000	1.000	1.000	1.000	1.000	1.000	1.000	0.475	0.324	0.572	0.434	0.209	0.244	0.281	**61%**
34%	1.000	1.000	1.000	1.000	1.000	1.000	1.000	1.000	1.000	1.000	1.000	1.000	0.310	0.638	0.447	0.190	0.240	0.303	**66%**
29%	1.000	1.000	1.000	1.000	1.000	1.000	1.000	1.000	1.000	1.000	1.000	1.000	1.000	0.576	0.514	0.570	0.583	0.569	**71%**
24%	1.000	1.000	1.000	1.000	1.000	1.000	1.000	1.000	1.000	1.000	1.000	1.000	1.000	1.000	0.669	0.121	0.234	0.365	**76%**
18%	1.000	1.000	1.000	1.000	1.000	1.000	1.000	1.000	1.000	1.000	1.000	1.000	1.000	1.000	1.000	0.391	0.449	0.465	**82%**
13%	1.000	1.000	1.000	1.000	1.000	1.000	1.000	1.000	1.000	1.000	1.000	1.000	1.000	1.000	1.000	1.000	0.720	0.778	**87%**
8%	1.000	1.000	1.000	1.000	1.000	1.000	1.000	1.000	1.000	1.000	1.000	1.000	1.000	1.000	1.000	1.000	1.000	0.882	**92%**
3%	1.000	1.000	1.000	1.000	1.000	1.000	1.000	1.000	1.000	1.000	1.000	1.000	1.000	1.000	1.000	1.000	1.000	1.000	
	97%	**92%**	**87%**	**82%**	**76%**	**71%**	**66%**	**61%**	**55%**	**50%**	**45%**	**39%**	**34%**	**29%**	**24%**	**18%**	**13%**	**8%**	

Table 3-24 *p*-values for *post hoc* pair-wise comparisons of mean power at left pedal with (un-shaded) and without (least significant difference) (shaded) Bonferroni correction

	8%	13%	18%	24%	29%	34%	39%	45%	50%	55%	61%	66%	71%	76%	82%	87%	92%	97%	
	0.036*	0.928	0.624	0.138	0.678	0.833	0.592	0.655	0.936	0.767	0.948	0.552	0.580	0.611	0.871	0.219	0.243	0.033*	**3%**
92%	1.000	0.067	0.131	0.014*	0.162	0.291	0.139	0.234	0.411	0.521	0.553	0.181	0.210	0.257	0.443	0.115	0.123	0.018*	**8%**
87%	1.000	1.000	0.736	0.030*	0.672	0.892	0.542	0.597	0.892	0.784	0.975	0.456	0.476	0.540	0.823	0.212	0.234	0.034*	**13%**
82%	1.000	1.000	1.000	0.031*	0.334	0.900	0.404	0.527	0.789	0.929	0.922	0.373	0.431	0.442	0.715	0.158	0.175	0.029*	**18%**
76%	1.000	1.000	1.000	1.000	0.294	0.048*	0.198	0.450	0.374	0.089	0.197	0.533	0.672	0.761	0.467	0.410	0.469	0.059	**24%**
71%	1.000	1.000	1.000	1.000	1.000	0.536	0.909	0.867	0.841	0.470	0.737	0.719	0.732	0.684	0.963	0.231	0.265	0.027*	**29%**
66%	1.000	1.000	1.000	1.000	1.000	1.000	0.144	0.462	0.811	0.754	0.958	0.175	0.292	0.398	0.740	0.174	0.180	0.035*	**34%**
61%	1.000	1.000	1.000	1.000	1.000	1.000	1.000	0.892	0.767	0.241	0.531	0.652	0.698	0.738	0.908	0.250	0.273	0.040*	**39%**
55%	1.000	1.000	1.000	1.000	1.000	1.000	0.730	1.000	0.636	0.296	0.460	0.808	0.784	0.803	0.866	0.266	0.304	0.031*	**45%**
50%	1.000	1.000	1.000	1.000	1.000	1.000	1.000	1.000	1.000	0.543	0.856	0.482	0.438	0.480	0.886	0.169	0.188	0.025*	**50%**
45%	1.000	1.000	1.000	1.000	1.000	1.000	1.000	1.000	1.000	1.000	0.765	0.004*	0.044*	0.144	0.529	0.109	0.108	0.027*	**55%**
39%	1.000	1.000	1.000	1.000	1.000	1.000	1.000	1.000	1.000	1.000	1.000	0.141	0.184	0.324	0.688	0.109	0.116	0.033*	**61%**
34%	1.000	1.000	1.000	1.000	1.000	1.000	1.000	1.000	1.000	1.000	1.000	1.000	0.837	0.869	0.609	0.229	0.242	0.048*	**66%**
29%	1.000	1.000	1.000	1.000	1.000	1.000	1.000	1.000	1.000	1.000	1.000	1.000	1.000	0.946	0.548	0.240	0.245	0.049*	**71%**
24%	1.000	1.000	1.000	1.000	1.000	1.000	1.000	1.000	1.000	1.000	1.000	1.000	1.000	1.000	0.291	0.205	0.207	0.036*	**76%**
18%	1.000	1.000	1.000	1.000	1.000	1.000	1.000	1.000	1.000	1.000	1.000	1.000	1.000	1.000	1.000	0.061	0.057	0.036*	**82%**
13%	1.000	1.000	1.000	1.000	1.000	1.000	1.000	1.000	1.000	1.000	1.000	1.000	1.000	1.000	1.000	1.000	0.499	0.125	**87%**
8%	1.000	1.000	1.000	1.000	1.000	1.000	1.000	1.000	1.000	1.000	1.000	1.000	1.000	1.000	1.000	1.000	1.000	0.116	**92%**
3%	1.000	1.000	1.000	1.000	1.000	1.000	1.000	1.000	1.000	1.000	1.000	1.000	1.000	1.000	1.000	1.000	1.000	1.000	
	97%	**92%**	**87%**	**82%**	**76%**	**71%**	**66%**	**61%**	**55%**	**50%**	**45%**	**39%**	**34%**	**29%**	**24%**	**18%**	**13%**	**8%**	

Table 3-25 *p*-values for *post hoc* pair-wise comparisons of mean power at right pedal with (un-shaded) and without (least significant difference) (shaded) Bonferroni correction

	8%	13%	18%	24%	29%	34%	39%	45%	50%	55%	61%	66%	71%	76%	82%	87%	92%	97%	
	0.037*	0.224	0.018*	0.192	0.092	0.018*	0.055	0.100	0.060	0.131	0.025*	0.025*	0.009*	0.104	0.221	0.686	0.846	0.072	**3%**
92%	1.000	0.316	0.160	0.731	0.871	0.111	0.404	0.759	0.650	0.946	0.250	0.523	0.176	0.847	0.698	0.307	0.293	0.025*	**8%**
87%	1.000	1.000	0.031*	0.477	0.291	0.039*	0.190	0.364	0.040*	0.245	0.098	0.055	0.086	0.398	0.752	0.482	0.539	0.055	**13%**
82%	1.000	1.000	1.000	0.126	0.331	0.423	0.902	0.792	0.719	0.356	0.659	0.672	0.766	0.250	0.377	0.261	0.236	0.028*	**18%**
76%	1.000	1.000	1.000	1.000	0.641	0.022*	0.220	0.577	0.346	0.817	0.183	0.235	0.125	0.876	0.867	0.392	0.402	0.038*	**24%**
71%	1.000	1.000	1.000	1.000	1.000	0.191	0.564	0.864	0.759	0.830	0.369	0.720	0.338	0.670	0.621	0.331	0.322	0.033*	**29%**
66%	1.000	1.000	1.000	1.000	1.000	1.000	0.149	0.084	0.220	0.037*	0.664	0.086	0.301	0.006*	0.099	0.170	0.136	0.019*	**34%**
61%	1.000	1.000	1.000	1.000	1.000	1.000	1.000	0.176	0.677	0.314	0.502	0.570	0.915	0.187	0.307	0.226	0.205	0.021*	**39%**
55%	1.000	1.000	1.000	1.000	1.000	1.000	1.000	1.000	0.941	0.637	0.189	0.920	0.472	0.524	0.505	0.272	0.269	0.027*	**45%**
50%	1.000	1.000	1.000	1.000	1.000	1.000	1.000	1.000	1.000	0.166	0.465	0.996	0.567	0.436	0.532	0.322	0.322	0.042*	**50%**
45%	1.000	1.000	1.000	1.000	1.000	1.000	1.000	1.000	1.000	1.000	0.180	0.258	0.235	0.903	0.749	0.364	0.377	0.049*	**55%**
39%	1.000	1.000	1.000	1.000	1.000	1.000	1.000	1.000	1.000	1.000	1.000	0.372	0.657	0.102	0.151	0.174	0.147	0.019*	**61%**
34%	1.000	1.000	1.000	1.000	1.000	1.000	1.000	1.000	1.000	1.000	1.000	1.000	0.375	0.239	0.443	0.280	0.267	0.031*	**66%**
29%	1.000	1.000	1.000	1.000	1.000	1.000	1.000	1.000	1.000	1.000	1.000	1.000	1.000	0.045*	0.242	0.220	0.189	0.022*	**71%**
24%	1.000	1.000	1.000	1.000	1.000	1.000	1.000	1.000	1.000	1.000	1.000	1.000	1.000	1.000	0.739	0.346	0.347	0.033*	**76%**
18%	1.000	1.000	1.000	1.000	1.000	1.000	1.000	1.000	1.000	1.000	1.000	1.000	1.000	1.000	1.000	0.260	0.232	0.033*	**82%**
13%	1.000	1.000	1.000	1.000	1.000	1.000	1.000	1.000	1.000	1.000	1.000	1.000	1.000	1.000	1.000	1.000	0.406	0.098	**87%**
8%	1.000	1.000	1.000	1.000	1.000	1.000	1.000	1.000	1.000	1.000	1.000	1.000	1.000	1.000	1.000	1.000	1.000	0.065	**92%**
3%	1.000	1.000	1.000	1.000	1.000	1.000	1.000	1.000	1.000	1.000	1.000	1.000	1.000	1.000	1.000	1.000	1.000	1.000	
	97%	**92%**	**87%**	**82%**	**76%**	**71%**	**66%**	**61%**	**55%**	**50%**	**45%**	**39%**	**34%**	**29%**	**24%**	**18%**	**13%**	**8%**	

3.3: Instantaneous index of effectiveness

Table 3-26: Full results of Two Way ANOVAs for mean Instantaneous Index of Effectiveness (*IIE*) on the left and right pedals

Side		High / low		Time		High / low x time	
		SS1,7 + R1	SS2-2	SS1,7 + R1	SS2-2	SS1,7 + R1	SS2-2
Left	*df*	1.000	1.000	1.256	6.985	2.231	3.112
	MS	40.952	2392	1175	93.719	73.804	402.246
	ε	1.000	1.000	1.000	1.000	1.000	1.000
	F	0.165	4.344	9.214	2.215	2.318	3.813
	p	0.695	0.071	0.010*	0.047*	0.123	0.021*
	η^2	0.020	0.352	0.535	0.217	0.225	0.323
Right	*df*	1.000	1.000	2.004	3.617	4.000	7.243
	MS	94.905	4909	1089	88.194	13.424	41.016
	ε	1.000	1.000	1.000	1.000	1.000	1.000
	F	1.287	25.805	15.485	4.139	0.732	2.457
	p	0.289	<0.001*	<0.001*	0.011*	0.577	0.027*
	η^2	0.139	0.763	0.659	0.341	0.084	0.235

Table 3-27: Full results of One Way ANOVAs for the instantaneous index of effectiveness (*IIE*) in the left and right legs during the second steady state section (SS2-2) of the high and low fatigue trials separately

Side	Trial	*df*	MS	ε	*F*	*p*	η^2
Left	Low fatigue	7.925	58.276	1.000	2.373	0.027*	0.229
	High fatigue	2.517	573.868	1.000	3.365	0.046*	0.296
Right	Low fatigue	7.245	53.636	1.000	2.637	0.018*	0.248
	High fatigue	3.478	65.428	1.000	4.495	0.008*	0.360

Table 3-28: Full results of One Way ANOVAs (high/low) at each time window for mean instantaneous index of effectiveness for the left and right legs during the second steady state section (SS2-2) of the fatigue trials.

Side	Time window	*df*	MS	ε	*F*	*p*	η^2
Left	1	1.000	1441	1.000	31.306	<0.001*	0.796
	2	1.000	835.409	1.000	16.576	0.004*	0.674
	3	1.000	271.872	1.000	2.506	0.152	0.239
	4	1.000	435.321	1.000	5.698	0.044*	0.416
	5	1.000	185.101	1.000	1.605	0.241	0.167
	6	1.000	148.872	1.000	1.345	0.280	0.144
	7	1.000	180.029	1.000	1.442	0.264	0.153
	8	1.000	141.367	1.000	1.860	0.210	0.189
	9	1.000	1.361	1.000	0.021	0.889	0.003
	10	1.000	3.377	1.000	0.032	0.863	0.004
Right	1	1.000	1175	1.000	54.199	<0.001*	0.871
	2	1.000	582.318	1.000	27.130	<0.001*	0.772
	3	1.000	154.323	1.000	4.936	0.057	0.382
	4	1.000	500.172	1.000	10.693	0.011*	0.572
	5	1.000	587.031	1.000	11.790	0.009*	0.596
	6	1.000	547.856	1.000	23.216	0.001*	0.744
	7	1.000	621.385	1.000	14.759	0.005*	0.648
	8	1.000	359.492	1.000	13.857	0.006*	0.634
	9	1.000	333.718	1.000	20.990	0.002*	0.724
	10	1.000	345.341	1.000	10.575	0.012*	0.569

3.4: Crank velocity

Table 3-29: Full results of Two Way ANOVA for crank velocity

Side		High / low		Time		High / low x time	
		SS1,7 + R1	SS2-2	SS1,7 + R1	SS2-2	SS1,7 + R1	SS2-2
N/A	*df*	1.000	1.000	2.471	9.000	4.000	2.505
	MS	0.002	42.711	2.616	0.035	0.122	0.367
	ε	1.000	1.000	1.000	1.000	1.000	1.000
	F	0.007	32.639	18.608	1.023	1.423	2.261
	p	0.933	<0.001*	<0.001*	0.430	0.249	0.121
	η^2	<0.001	0.803	0.699	0.113	0.151	0.220

Table 3-30: Full results of One Way ANOVAs for the high-fatigue trail for the whole of the second steady state (SS2-1) for the instantaneous index of effectiveness (*IIE*) and for the left and right pedals and crank velocity (ω_c)

Variable	Side	*df*	MS	ε	*F*	*p*	η^2
$\bar{x}$ IIE	Left	18.000	103.552	1.000	1.623	0.062	0.169
	Right	3.644	174.937	1.000	3.472	0.022*	0.303
$\bar{x}$ ω_c	N/A	18.000	0.074	1.000	1.486	0.103	0.157

Table 3-31: *p*-values for *post hoc* pair-wise comparisons of Instantaneous Index of Effectiveness at the right pedal with (un-shaded) and without (least significant difference) (shaded) Bonferroni correction

	8%	13%	18%	24%	29%	34%	39%	45%	50%	55%	61%	66%	71%	76%	82%	87%	92%	97%	
	0.206	0.168	0.383	0.015*	0.121	0.088	0.215	0.329	0.566	0.298	0.911	0.809	0.525	0.988	0.536	0.504	0.321	0.039*	**3%**
92%	1.000	0.555	0.733	0.867	0.583	0.315	0.394	0.837	0.610	0.763	0.597	0.550	0.946	0.384	0.921	0.266	0.054	0.006*	**8%**
87%	1.000	1.000	0.340	0.497	0.970	0.200	0.978	0.462	0.126	0.763	0.207	0.197	0.565	0.108	0.549	0.088	0.002*	0.000*	**13%**
82%	0.230	1.000	1.000	0.764	0.266	0.194	0.418	0.584	0.899	0.521	0.764	0.765	0.770	0.495	0.865	0.217	0.054	0.009*	**18%**
76%	0.639	1.000	1.000	1.000	0.449	0.284	0.543	0.786	0.669	0.744	0.686	0.671	0.902	0.496	0.979	0.297	0.093	0.011*	**24%**
71%	0.104	0.682	1.000	1.000	1.000	0.426	0.965	0.536	0.236	0.763	0.338	0.278	0.672	0.121	0.413	0.095	0.009*	0.000*	**29%**
66%	1.000	1.000	1.000	1.000	1.000	1.000	0.565	0.113	0.124	0.312	0.142	0.048*	0.257	0.040*	0.270	0.053	0.002*	0.000*	**34%**
61%	0.743	1.000	1.000	1.000	1.000	1.000	1.000	0.634	0.345	0.688	0.284	0.142	0.706	0.049*	0.552	0.138	0.010*	0.001*	**39%**
55%	0.313	1.000	1.000	1.000	1.000	1.000	1.000	1.000	0.465	0.888	0.315	0.195	0.894	0.060	0.721	0.106	0.005*	0.000*	**45%**
50%	0.998	1.000	1.000	1.000	1.000	1.000	1.000	1.000	1.000	0.548	0.739	0.837	0.606	0.627	0.832	0.280	0.039*	0.006*	**50%**
45%	0.031*	0.901	1.000	1.000	1.000	1.000	1.000	1.000	1.000	1.000	0.419	0.068	0.867	0.015*	0.650	0.112	0.012*	0.002*	**55%**
39%	0.148	1.000	1.000	1.000	1.000	1.000	1.000	1.000	1.000	1.000	1.000	0.902	0.197	0.863	0.695	0.299	0.114	0.004*	**61%**
34%	0.053	0.381	1.000	1.000	1.000	1.000	1.000	1.000	1.000	1.000	1.000	1.000	0.367	0.499	0.631	0.255	0.043*	0.007*	**66%**
29%	0.048*	1.000	1.000	1.000	1.000	1.000	1.000	1.000	1.000	1.000	1.000	1.000	1.000	0.249	0.862	0.105	0.004*	0.001*	**71%**
24%	1.000	1.000	1.000	1.000	1.000	1.000	1.000	1.000	1.000	1.000	1.000	1.000	1.000	1.000	0.303	0.297	0.070	0.004*	**76%**
18%	1.000	1.000	1.000	1.000	1.000	1.000	1.000	1.000	1.000	1.000	1.000	1.000	1.000	1.000	1.000	0.146	0.048*	0.001*	**82%**
13%	0.038*	0.375	1.000	1.000	1.000	1.000	1.000	1.000	1.000	1.000	1.000	1.000	1.000	1.000	1.000	1.000	0.898	0.158	**87%**
8%	1.000	1.000	1.000	1.000	1.000	1.000	1.000	1.000	1.000	1.000	1.000	1.000	1.000	1.000	1.000	1.000	1.000	0.039*	**92%**
3%	1.000	1.000	1.000	1.000	1.000	1.000	1.000	1.000	1.000	1.000	1.000	1.000	1.000	1.000	1.000	1.000	1.000	1.000	
	97%	**92%**	**87%**	**82%**	**76%**	**71%**	**66%**	**61%**	**55%**	**50%**	**45%**	**39%**	**34%**	**29%**	**24%**	**18%**	**13%**	**8%**	

3.5: Segment angular displacement

3.5.1: Thigh

Table 3-32: Full results of Two Way ANOVAs for the minimum thigh angle for the left and right legs

Side		High / low		Time		High / low x time	
		SS1,7 + R1	SS2-2	SS1,7 + R1	SS2-2	SS1,7 + R1	SS2-2
Left	*df*	1.000	1.000	1.527	3.000	4.000	3.000
	MS	<0.001	94.308	<0.001	0.488	<0.001	0.134
	ε	1.000	1.000	1.000	1.000	1.000	1.000
	F	2.157	7.663	5.562	0.606	2.557	0.319
	p	0.185	0.028*	0.028*	0.619	0.061	0.812
	η^2	0.236	0.523	0.443	0.080	0.268	0.044
Right	*df*	1.000	1.000	1.182	3.000	4.000	3.000
	MS	<0.001	150.519	<0.001	0.461	<0.001	0.987
	ε	1.000	1.000	1.000	1.000	1.000	1.000
	F	0.034	4.465	10.621	0.655	0.223	1.686
	p	0.859	0.079	0.012*	0.590	0.923	0.206
	η^2	0.006	0.427	0.639	0.098	0.036	0.219

Table 3-33: Full results of Two Way ANOVAs for the maximum thigh angle for the left and right legs

Side		High / low		Time		High / low x time	
		SS1,7 + R1	SS2-2	SS1,7 + R1	SS2-2	SS1,7 + R1	SS2-2
Left	*df*	1.000	1.000	4.000	3.000	4.000	3.000
	MS	<0.001	20.498	<0.001	0.338	<0.001	0.542
	ε	1.000	1.000	1.000	1.000	1.000	1.000
	F	0.062	1.619	27.666	0.140	0.148	0.737
	p	0.811	0.244	<0.001*	0.935	0.962	0.542
	η^2	0.009	0.188	0.798	0.020	0.021	0.095
Right	*df*	1.000	1.000	2.094	3.000	4.000	3.000
	MS	<0.001	519.843	<0.001	1.298	<0.001	0.599
	ε	1.000	1.000	1.000	1.000	1.000	1.000
	F	1.144	1.956	4.626	0.814	0.297	0.739
	p	0.326	0.211	0.030*	0.503	0.877	0.543
	η^2	0.160	0.246	0.435	0.119	0.047	0.110

Table 3-34: Full results of Two Way ANOVAs for the crank angle at which minimum thigh angle occurred for the left and right legs

Side		High / low		Time		High / low x time	
		SS1,7 + R1	SS2-2	SS1,7 + R1	SS2-2	SS1,7 + R1	SS2-2
Left	*df*	1.000	1.000	4.000	3.000	4.000	3.000
	MS	0.008	15800	<0.001	17931	0.002	7207
	ε	1.000	1.000	1.000	1.000	1.000	1.000
	F	3.372	0.460	0.120	1.215	0.717	1.001
	p	0.109	0.519	0.974	0.329	0.587	0.412
	η^2	0.325	0.062	0.017	0.148	0.093	0.125
Right	*df*	1.000	1.000	4.000	3.000	4.000	3.000
	MS	<0.001	39.581	<0.001	1.531	<0.001	7.840
	ε	1.000	1.000	1.000	1.000	1.000	1.000
	F	0.955	0.673	1.301	0.356	0.144	1.958
	p	0.373	0.443	0.303	0.785	0.963	0.156
	η^2	0.160	0.101	0.207	0.056	0.028	0.246

Table 3-35: Full results of Two Way ANOVAs for the crank angle at which maximum thigh angle occurred for the left and right legs

Side		High / low		Time		High / low x time	
		SS1,7 + R1	SS2-2	SS1,7 + R1	SS2-2	SS1,7 + R1	SS2-2
Left	*df*	1.000	1.000	1.088	3.000	4.000	3.000
	MS	<0.001	120.259	<0.001	5.032	<0.001	0.477
	ε	1.000	1.000	1.000	1.000	1.000	1.000
	F	0.335	2.252	4.459	1.380	0.907	0.151
	p	0.581	0.177	0.067	0.276	0.473	0.928
	η^2	0.046	0.243	0.389	0.165	0.115	0.021
Right	*df*	1.000	1.000	4.000	3.000	4.000	3.000
	MS	<0.001	57.368	<0.001	3.488	<0.001	7.819
	ε	1.000	1.000	1.000	1.000	1.000	1.000
	F	0.364	1.067	0.662	1.373	2.584	3.082
	p	0.568	0.342	0.624	0.283	0.063	0.054
	η^2	0.057	0.151	0.099	0.186	0.301	0.339

3.5.2: Shank

Table 3-36: Full results of Two Way ANOVAs for the minimum shank angle for the left and right legs

Side		High / low		Time		High / low x time	
		SS1,7 + R1	SS2-2	SS1,7 + R1	SS2-2	SS1,7 + R1	SS2-2
Left	*df*	1.000	1.000	1.237	3.000	4.000	3.000
	MS	<0.001	27.997	<0.001	1.128	<0.001	1.139
	ε	1.000	1.000	1.000	1.000	1.000	1.000
	F	0.987	0.725	21.329	0.308	0.960	2.131
	p	0.353	0.423	<0.001*	0.819	0.445	0.127
	η^2	0.124	0.094	0.753	0.042	0.121	0.233
Right	*df*	1.000	1.000	4.000	3.000	4.000	3.000
	MS	<0.001	450.028	<0.001	5.801	<0.001	5.928
	ε	1.000	1.000	1.000	1.000	1.000	1.000
	F	0.817	2.135	1.265	2.019	0.338	3.015
	p	0.401	0.194	0.311	0.147	0.850	0.057
	η^2	0.120	0.262	0.174	0.252	0.053	0.334

Table 3-37: Full results of Two Way ANOVAs for the maximum shank angle for the left and right legs

Side		High / low		Time		High / low x time	
		SS1,7 + R1	SS2-2	SS1,7 + R1	SS2-2	SS1,7 + R1	SS2-2
Left	*df*	1.000	1.000	4.000	3.000	4.000	3.000
	MS	<0.001	72.101	<0.001	1.326	<0.001	2.737
	ε	1.000	1.000	1.000	1.000	1.000	1.000
	F	1.986	1.630	2.402	0.669	0.127	2.484
	p	0.202	0.242	0.074	0.581	0.971	0.089
	η^2	0.221	0.189	0.255	0.087	0.018	0.262
Right	*df*	1.000	1.000	1.529	3.000	4.000	1.275
	MS	<0.001	129.170	<0.001	3.965	<0.001	18.220
	ε	1.000	1.000	1.000	1.000	1.000	1.000
	F	0.029	3.399	6.969	2.168	0.652	4.386
	p	0.871	0.115	0.019*	0.127	0.631	0.065
	η^2	0.005	0.362	0.537	0.265	0.098	0.422

Table 3-38: Full results of Two Way ANOVAs for the crank angle at which minimum shank angle occurred for the left and right legs

Side		High / low		Time		High / low x time	
		SS1,7 + R1	SS2-2	SS1,7 + R1	SS2-2	SS1,7 + R1	SS2-2
Left	*df*	1.000	1.000	4.000	3.000	4.000	3.000
	MS	<0.001	12.452	<0.001	5.921	<0.001	9.894
	ε	1.000	1.000	1.000	1.000	1.000	1.000
	F	1.918	0.512	0.522	1.013	1.683	2.085
	p	0.209	0.497	0.720	0.407	0.182	0.133
	η^2	0.215	0.068	0.069	0.126	0.194	0.230
Right	*df*	1.000	1.000	4.000	3.000	4.000	3.000
	MS	<0.001	2.133	<0.001	4.257	<0.001	2.308
	ε	1.000	1.000	1.000	1.000	1.000	1.000
	F	0.558	0.043	1.163	0.857	0.967	0.497
	p	0.483	0.843	0.352	0.481	0.444	0.689
	η^2	0.085	0.007	0.162	0.125	0.139	0.076

Table 3-39: Full results of Two Way ANOVAs for the crank angle at which maximum shank angle occurred for the left and right legs

Side		High / low		Time		High / low x time	
		SS1,7 + R1	SS2-2	SS1,7 + R1	SS2-2	SS1,7 + R1	SS2-2
Left	*df*	1.000	1.000	2.080	3.000	4.000	3.000
	MS	<0.001	0.405	<0.001	2.830	<0.001	3.953
	ε	1.000	1.000	1.000	1.000	1.000	1.000
	F	0.415	0.012	9.219	0.463	1.255	0.671
	p	0.540	0.915	0.002*	0.711	0.311	0.579
	η^2	0.056	0.002	0.568	0.062	0.152	0.087
Right	*df*	1.000	1.000	1.736	3.000	4.000	3.000
	MS	<0.001	158.323	<0.001	3.369	<0.001	0.555
	ε	1.000	1.000	1.000	1.000	1.000	1.000
	F	0.160	3.074	3.144	1.203	1.059	0.212
	p	0.703	0.130	0.090	0.337	0.398	0.887
	η^2	0.026	0.339	0.344	0.167	0.150	0.034

3.5.3: Foot

Table 3-40: Full results of Two Way ANOVAs for the minimum foot angle for the left and right legs

Side		High / low		Time		High / low x time	
		SS1,7 + R1	SS2-2	SS1,7 + R1	SS2-2	SS1,7 + R1	SS2-2
Left	*df*	1.000	1.000	1.281	3.000	4.000	3.000
	MS	<0.001	52.944	<0.001	7.074	<0.001	3.341
	ε	1.000	1.000	1.000	1.000	1.000	1.000
	F	0.174	1.193	11.135	1.188	1.242	1.490
	p	0.689	0.311	0.007*	0.338	0.316	0.246
	η^2	0.024	0.146	0.614	0.145	0.151	0.175
Right	*df*	1.000	1.000	1.966	3.000	4.000	3.000
	MS	<0.001	5.143	<0.001	2.588	<0.001	4.965
	ε	1.000	1.000	1.000	1.000	1.000	1.000
	F	2.959	0.086	4.520	1.759	0.336	2.124
	p	0.136	0.779	0.035*	0.191	0.851	0.133
	η^2	0.330	0.014	0.430	0.227	0.053	0.261

Table 3-41: Full results of Two Way ANOVAs for the maximum foot angle for the left and right legs

Side		High / low		Time		High / low x time	
		SS1,7 + R1	SS2-2	SS1,7 + R1	SS2-2	SS1,7 + R1	SS2-2
Left	*df*	1.000	1.000	4.000	3.000	4.000	3.000
	MS	<0.001	0.907	<0.001	15.272	<0.001	7.578
	ε	1.000	1.000	1.000	1.000	1.000	1.000
	F	0.178	0.013	0.140	2.756	1.806	3.009
	p	0.686	0.914	0.966	0.068	0.156	0.053
	η^2	0.025	0.002	0.020	0.282	0.205	0.301
Right	*df*	1.000	1.000	2.148	3.000	4.000	3.000
	MS	<0.001	21.021	<0.001	5.292	<0.001	9.582
	ε	1.000	1.000	1.000	1.000	1.000	1.000
	F	0.012	0.116	6.164	3.248	0.569	3.052
	p	0.915	0.745	0.012*	0.046*	0.687	0.055
	η^2	0.002	0.019	0.507	0.351	0.087	0.337

Table 3-42: Full results of Two Way ANOVAs for the crank angle at which minimum foot angle occurred for the left and right legs

Side		High / low		Time		High / low x time	
		SS1,7 + R1	SS2-2	SS1,7 + R1	SS2-2	SS1,7 + R1	SS2-2
Left	*df*	1.000	1.000	1.384	3.000	4.000	3.000
	MS	<0.001	30.223	<0.001	7.051	<0.001	3.102
	ε	1.000	1.000	1.000	1.000	1.000	1.000
	F	0.001	1.233	56.633	0.930	0.299	0.554
	p	0.978	0.303	<0.001*	0.444	0.876	0.651
	η^2	<0.001	0.150	0.890	0.117	0.041	0.073
Right	*df*	1.000	1.000	4.000	3.000	4.000	3.000
	MS	<0.001	30.415	<0.001	8.806	<0.001	10.507
	ε	1.000	1.000	1.000	1.000	1.000	1.000
	F	0.394	0.172	0.383	1.105	0.611	0.829
	p	0.553	0.692	0.819	0.373	0.659	0.495
	η^2	0.062	0.028	0.060	0.156	0.092	0.121

Table 3-43: Full results of Two Way ANOVAs for the crank angle at which maximum foot angle occurred for the left and right legs

Side		High / low		Time		High / low x time	
		SS1,7 + R1	SS2-2	SS1,7 + R1	SS2-2	SS1,7 + R1	SS2-2
Left	*df*	1.000	1.000	1.659	3.000	4.000	3.000
	MS	<0.001	15.152	<0.001	7.656	<0.001	21.428
	ε	1.000	1.000	1.000	1.000	1.000	1.000
	F	0.354	0.290	6.187	0.367	0.099	1.474
	p	0.570	0.607	0.018*	0.777	0.982	0.250
	η^2	0.048	0.040	0.469	0.050	0.014	0.174
Right	*df*	1.000	1.000	4.000	3.000	4.000	1.927
	MS	<0.001	312.323	<0.001	11.688	<0.001	164.762
	ε	1.000	1.000	1.000	1.000	1.000	1.000
	F	0.891	0.520	0.412	0.412	0.300	5.348
	p	0.382	0.498	0.798	0.747	0.875	0.023*
	η^2	0.129	0.080	0.064	0.064	0.048	0.471

Table 3-44: Full results of One Way ANOVAs for the crank angle at maximum foot angle in the right leg during the second steady state section (SS2-2) of the high and low fatigue trials separately

Trial	*df*	MS	ε	*F*	*p*	η^2
Low fatigue	3.000	1.294	1.000	0.669	0.582	0.100
High fatigue	1.847	24.283	1.000	5.904	0.017*	0.458

Table 3-45: Full results of One Way ANOVAs (high/low) at each time window for the crank angle at which maximum foot angle of the right leg occurred during the second steady state section (SS2-2) of the fatigue trials.

Time window	*df*	MS	ε	*F*	*p*	η^2
1	1.000	0.778	1.000	0.004	0.949	0.001
2	1.000	14.592	1.000	0.094	0.768	0.013
3	1.000	205.421	1.000	0.927	0.368	0.117
4	1.000	124.378	1.000	0.912	0.371	0.115

Table 3-46: Full results of One Way ANOVAs for the high-fatigue trail for the whole of the second steady state (SS1-1) for each segmental angular displacement variable for the left and right pedals

Variable	Side	*df*	MS	ε	*F*	*p*	η^2
Thigh min	Left	4.000	0.499	1.000	0.707	0.594	0.092
	Right	4.000	0.284	1.000	0.475	0.754	0.063
Thigh max	Left	4.000	0.522	1.000	0.504	0.733	0.067
	Right	4.000	0.486	1.000	1.504	0.228	0.177
θ_c at thigh min	Left	4.000	4252	1.000	0.651	0.631	0.085
	Right	4.000	3.310	1.000	0.992	0.428	0.124
θ_c at thigh max	Left	4.000	5.934	1.000	0.762	0.559	0.098
	Right	1.866	45.029	1.000	3.545	0.061	0.336
Shank min	Left	4.000	1.561	1.000	0.438	0.780	0.059
	Right	4.000	10.824	1.000	1.980	0.125	0.221
Shank max	Left	4.000	7.228	1.000	1.910	0.136	0.214
	Right	1.115	56.817	1.000	3.465	0.098	0.331
θ_c at shank min	Left	4.000	4.595	1.000	1.029	0.409	0.128
	Right	4.000	2.570	1.000	0.292	0.881	0.040
θ_c at shank max	Left	4.000	4.656	1.000	1.175	0.343	0.144
	Right	4.000	6.020	1.000	2.187	0.096	0.238
Foot min	Left	2.181	42.196	1.000	6.035	0.010*	0.463
	Right	1.683	42.539	1.000	6.858	0.013*	0.495
Foot max	Left	2.112	47.740	1.000	5.300	0.017*	0.431
	Right	2.155	35.813	1.000	6.471	0.008*	0.480
θ_c at foot min	Left	4.000	6.879	1.000	0.947	0.452	0.119
	Right	4.000	6.946	1.000	0.742	0.571	0.096
θ_c at foot max	Left	4.000	10.500	1.000	0.841	0.511	0.107
	Right	4.000	32.693	1.000	1.440	0.247	0.171

Table 3-47 *p*-values for *post hoc* pair-wise comparisons of the segmental angular displacement variables with significant ($p<0.05$) (i.e. foot minimum and maximum angles) main effects with (BON) and without (least significant difference (LSD)) Bonferroni correction

Left foot minimum angle

	2	3	4	5	
	0.013*	0.013*	0.023*	0.013*	1
4	1.000	0.066	0.280	0.082	2
3	1.000	1.000	0.271	0.497	3
2	0.824	1.000	0.662	0.243	4
1	0.126	0.231	0.134	0.132	
	5	4	3	2	

Right foot minimum angle

	2	3	4	5	
	0.005*	0.016*	0.009*	0.017*	1
4	1.000	0.478	0.112	0.134	2
3	1.000	0.376	0.038*	0.163	3
2	1.000	1.000	1.000	0.900	4
1	0.167	0.093	0.163	0.048*	
	5	4	3	2	

Left foot maximum angle

	2	3	4	5	
	0.270	0.044*	0.070	0.023*	1
4	1.000	0.021*	0.105	0.006*	2
3	1.000	1.000	0.583	0.488	3
2	0.056	1.000	0.214	0.188	4
1	0.233	0.699	0.445	1.000	
	5	4	3	2	

Right foot maximum angle

	2	3	4	5	
	0.280	0.036*	0.089	0.009*	1
4	0.476	0.027*	0.167	0.008*	2
3	0.200	1.000	0.553	0.020*	3
2	0.080	1.000	0.272	0.048*	4
1	0.093	0.892	0.355	1.000	
	5	4	3	2	

3.6: Joint angular displacement

3.6.1: Hip

Table 3-48: Full results of Two Way ANOVAs for the maximum hip flexion for the left and right legs

Side		High / low		Time		High / low x time	
		SS1,7 + R1	SS2-2	SS1,7 + R1	SS2-2	SS1,7 + R1	SS2-2
Left	*df*	1.000	1.000	1.029	3.000	4.000	3.000
	MS	<0.001	<0.001	<0.001	0.002	<0.001	0.001
	ε	1.000	1.000	1.000	1.000	1.000	1.000
	F	0.397	0.008	10.488	0.832	0.359	0.676
	p	0.549	0.932	0.013*	0.491	0.835	0.577
	η^2	0.054	0.001	0.600	0.106	0.049	0.088
Right	*df*	1.000	1.000	4.000	3.000	4.000	3.000
	MS	<0.001	0.161	<0.001	0.001	<0.001	0.002
	ε	1.000	1.000	1.000	1.000	1.000	1.000
	F	0.129	0.822	2.104	0.334	1.158	0.835
	p	0.732	0.399	0.112	0.801	0.354	0.492
	η^2	0.021	0.121	0.260	0.053	0.162	0.122

Table 3-49: Full results of Two Way ANOVAs for the maximum hip extension for the left and right legs

Side		High / low		Time		High / low x time	
		SS1,7 + R1	SS2-2	SS1,7 + R1	SS2-2	SS1,7 + R1	SS2-2
Left	*df*	1.000	1.000	4.000	3.000	4.000	3.000
	MS	<0.001	0.003	<0.001	<0.001	<0.001	<0.001
	ε	1.000	1.000	1.000	1.000	1.000	1.000
	F	0.628	0.096	1.486	0.721	1.184	0.895
	p	0.454	0.766	0.233	0.551	0.339	0.460
	η^2	0.082	0.014	0.175	0.093	0.145	0.113
Right	*df*	1.000	1.000	4.000	3.000	4.000	3.000
	MS	<0.001	0.139	<0.001	<0.001	<0.001	<0.001
	ε	1.000	1.000	1.000	1.000	1.000	1.000
	F	0.510	0.921	2.240	0.400	1.604	1.032
	p	0.502	0.374	0.095	0.755	0.206	0.402
	η^2	0.078	0.133	0.272	0.062	0.211	0.147

Table 3-50: Full results of Two Way ANOVAs for the crank angle at which maximum hip flexion occurred for the left and right legs

Side		High / low		Time		High / low x time	
		SS1,7 + R1	SS2-2	SS1,7 + R1	SS2-2	SS1,7 + R1	SS2-2
Left	*df*	1.000	1.000	1.014	3.000	4.000	3.000
	MS	<0.001	0.004	0.001	<0.001	<0.001	<0.001
	ε	1.000	1.000	1.000	1.000	1.000	1.000
	F	0.908	2.402	12.386	1.438	0.416	0.008
	p	0.372	0.165	0.009*	0.260	0.795	0.999
	η^2	0.115	0.255	0.639	0.170	0.056	0.001
Right	*df*	1.000	1.000	4.000	3.000	4.000	3.000
	MS	<0.001	0.142	<0.001	0.007	<0.001	0.022
	ε	1.000	1.000	1.000	1.000	1.000	1.000
	F	0.364	0.860	0.662	1.046	2.584	3.072
	p	0.568	0.390	0.624	0.396	0.063	0.054
	η^2	0.057	0.125	0.099	0.148	0.301	0.339

Table 3-51: Full results of Two Way ANOVAs for the crank angle at which maximum hip extension occurred for the left and right legs

Side		High / low		Time		High / low x time	
		SS1,7 + R1	SS2-2	SS1,7 + R1	SS2-2	SS1,7 + R1	SS2-2
Left	*df*	1.000	1.000	4.000	3.000	4.000	3.000
	MS	0.008	1.539	0.002	4.926	0.002	3.131
	ε	1.000	1.000	1.000	1.000	1.000	1.000
	F	1.784	0.455	0.926	1.242	0.685	1.266
	p	0.223	0.522	0.463	0.320	0.609	0.312
	η^2	0.203	0.061	0.117	0.151	0.089	0.153
Right	*df*	1.000	1.000	4.000	3.000	4.000	3.000
	MS	<0.001	0.001	<0.001	<0.001	<0.001	<0.001
	ε	1.000	1.000	1.000	1.000	1.000	1.000
	F	0.509	0.658	1.186	0.350	0.181	1.961
	p	0.502	0.448	0.342	0.790	0.946	0.156
	η^2	0.078	0.099	0.165	0.055	0.029	0.246

3.6.2: Knee

Table 3-52: Full results of Two Way ANOVAs for the maximum knee extension for the left and right legs

Side		High / low		Time		High / low x time	
		SS1,7 + R1	SS2-2	SS1,7 + R1	SS2-2	SS1,7 + R1	SS2-2
Left	*df*	1.000	1.000	1.328	3.000	4.000	3.000
	MS	<0.001	0.001	<0.001	0.003	<0.001	0.002
	ε	1.000	1.000	1.000	1.000	1.000	1.000
	F	2.669	0.018	3.291	2.544	1.327	1.679
	p	0.146	0.896	0.095	0.084	0.284	0.202
	η^2	0.276	0.003	0.320	0.267	0.159	0.193
Right	*df*	1.000	1.000	1.276	3.000	4.000	3.000
	MS	<0.001	0.006	<0.001	0.003	<0.001	0.004
	ε	1.000	1.000	1.000	1.000	1.000	1.000
	F	0.166	0.198	11.705	2.081	0.335	2.225
	p	0.698	0.672	0.008*	0.139	0.852	0.120
	η^2	0.027	0.032	0.661	0.257	0.053	0.270

Table 3-53: Full results of Two Way ANOVAs for the maximum knee flexion for the left and right legs

Side		High / low		Time		High / low x time	
		SS1,7 + R1	SS2-2	SS1,7 + R1	SS2-2	SS1,7 + R1	SS2-2
Left	*df*	1.000	1.000	1.044	3.000	4.000	3.000
	MS	<0.001	<0.001	<0.001	<0.001	<0.001	<0.001
	ε	1.000	1.000	1.000	1.000	1.000	1.000
	F	0.378	0.034	28.989	0.650	0.333	0.774
	p	0.558	0.858	<0.001*	0.592	0.853	0.522
	η^2	0.051	0.005	0.805	0.085	0.045	0.100
Right	*df*	1.000	1.000	4.000	3.000	4.000	3.000
	MS	<0.001	0.001	<0.001	<0.001	<0.001	<0.001
	ε	1.000	1.000	1.000	1.000	1.000	1.000
	F	1.138	0.692	1.785	1.273	1.221	1.506
	p	0.327	0.437	0.165	0.314	0.328	0.247
	η^2	0.159	0.103	0.229	0.175	0.169	0.201

Table 3-54: Full results of Two Way ANOVAs for the crank angle at which maximum knee extension occurred for the left and right legs

Side		High / low		Time		High / low x time	
		SS1,7 + R1	SS2-2	SS1,7 + R1	SS2-2	SS1,7 + R1	SS2-2
Left	*df*	1.000	1.000	2.093	3.000	4.000	3.000
	MS	<0.001	<0.001	<0.001	<0.001	<0.001	<0.001
	ε	1.000	1.000	1.000	1.000	1.000	1.000
	F	0.346	0.525	3.960	0.611	1.296	1.748
	p	0.575	0.492	0.041*	0.615	0.296	0.188
	η^2	0.047	0.070	0.361	0.080	0.156	0.200
Right	*df*	1.000	1.000	4.000	3.000	4.000	3.000
	MS	<0.001	0.003	<0.001	<0.001	<0.001	<0.001
	ε	1.000	1.000	1.000	1.000	1.000	1.000
	F	0.163	1.623	0.685	0.239	0.384	2.295
	p	0.700	0.250	0.609	0.868	0.818	0.112
	η^2	0.026	0.213	0.102	0.038	0.060	0.277

Table 3-55: Full results of Two Way ANOVAs for the crank angle at which maximum knee flexion occurred for the left and right legs

Side		High / low		Time		High / low x time	
		SS1,7 + R1	SS2-2	SS1,7 + R1	SS2-2	SS1,7 + R1	SS2-2
Left	*df*	1.000	1.000	4.000	3.000	4.000	3.000
	MS	<0.001	0.008	<0.001	<0.001	<0.001	<0.001
	ε	1.000	1.000	1.000	1.000	1.000	1.000
	F	0.064	5.882	2.456	0.743	0.474	2.111
	p	0.808	0.046*	0.069	0.539	0.755	0.129
	η^2	0.009	0.457	0.260	0.096	0.063	0.232
Right	*df*	1.000	1.000	4.000	3.000	4.000	3.000
	MS	<0.001	16.390	<0.001	0.105	<0.001	1.890
	ε	1.000	1.000	1.000	1.000	1.000	1.000
	F	0.315	1.339	1.501	0.082	0.840	1.945
	p	0.595	0.291	0.233	0.969	0.513	0.159
	η^2	0.050	0.182	0.200	0.014	0.123	0.245

3.6.3: Ankle

Table 3-56: Full results of Two Way ANOVAs for the maximum ankle plantar-flexion for the left and right legs

Side		High / low		Time		High / low x time	
		SS1,7 + R1	SS2-2	SS1,7 + R1	SS2-2	SS1,7 + R1	SS2-2
Left	*df*	1.000	1.000	4.000	3.000	4.000	3.000
	MS	<0.001	0.027	<0.001	0.001	<0.001	0.001
	ε	1.000	1.000	1.000	1.000	1.000	1.000
	F	0.030	1.550	1.440	0.481	2.663	1.137
	p	0.867	0.253	0.247	0.699	0.053	0.357
	η^2	0.004	0.181	0.171	0.064	0.276	0.140
Right	*df*	1.000	1.000	4.000	3.000	4.000	3.000
	MS	<0.001	0.095	<0.001	<0.001	<0.001	<0.001
	ε	1.000	1.000	1.000	1.000	1.000	1.000
	F	5.178	11.426	2.883	0.803	0.595	0.696
	p	0.063	0.015*	0.044*	0.509	0.670	0.567
	η^2	0.463	0.656	0.325	0.118	0.090	0.104

Table 3-57: Full results of Two Way ANOVAs for the maximum ankle dorsiflexion for the left and right legs

Side		High / low		Time		High / low x time	
		SS1,7 + R1	SS2-2	SS1,7 + R1	SS2-2	SS1,7 + R1	SS2-2
Left	*df*	1.000	1.000	4.000	3.000	4.000	3.000
	MS	<0.001	0.011	<0.001	0.002	<0.001	<0.001
	ε	1.000	1.000	1.000	1.000	1.000	1.000
	F	0.003	0.886	1.468	0.938	1.702	1.346
	p	0.961	0.378	0.238	0.440	0.178	0.286
	η^2	<0.001	0.112	0.173	0.118	0.196	0.161
Right	*df*	1.000	1.000	4.000	3.000	4.000	3.000
	MS	<0.001	0.090	<0.001	<0.001	<0.001	<0.001
	ε	1.000	1.000	1.000	1.000	1.000	1.000
	F	1.282	7.983	1.200	0.458	1.146	0.963
	p	0.301	0.030*	0.336	0.715	0.359	0.432
	η^2	0.176	0.571	0.167	0.071	0.160	0.138

Table 3-58: Full results of Two Way ANOVAs for the crank angle at which maximum ankle plantar-flexion occurred for the left and right legs

Side		High / low		Time		High / low x time	
		SS1,7 + R1	SS2-2	SS1,7 + R1	SS2-2	SS1,7 + R1	SS2-2
Left	*df*	1.000	1.000	4.000	3.000	4.000	3.000
	MS	0.004	1.330	0.001	0.617	0.002	0.203
	ε	1.000	1.000	1.000	1.000	1.000	1.000
	F	1.691	0.208	1.435	0.434	1.173	0.273
	p	0.235	0.662	0.248	0.731	0.344	0.844
	η^2	0.195	0.029	0.170	0.058	0.143	0.038
Right	*df*	1.000	1.000	4.000	3.000	4.000	3.000
	MS	<0.001	0.423	<0.001	0.003	<0.001	0.002
	ε	1.000	1.000	1.000	1.000	1.000	1.000
	F	0.233	1.020	1.759	1.069	0.308	0.870
	p	0.647	0.352	0.170	0.387	0.870	0.475
	η^2	0.037	0.145	0.227	0.151	0.049	0.127

Table 3-59: Full results of Two Way ANOVAs for the crank angle at which maximum ankle dorsiflexion occurred for the left and right legs

Side		High / low		Time		High / low x time	
		SS1,7 + R1	SS2-2	SS1,7 + R1	SS2-2	SS1,7 + R1	SS2-2
Left	*df*	1.000	1.000	3.266	3.000	4.000	3.000
	MS	<0.001	0.014	<0.001	<0.001	<0.001	<0.001
	ε	1.000	1.000	1.000	1.000	1.000	1.000
	F	0.017	3.536	2.902	0.277	0.381	0.762
	p	0.899	0.102	0.053	0.842	0.821	0.528
	η^2	0.002	0.336	0.293	0.038	0.052	0.098
Right	*df*	1.000	1.000	2.149	3.000	4.000	3.000
	MS	0.005	4.457	<0.001	0.063	<0.001	0.059
	ε	1.000	1.000	1.000	1.000	1.000	1.000
	F	1.160	3.026	21.483	2.303	1.066	1.838
	p	0.323	0.133	<0.001*	0.112	0.395	0.176
	η^2	0.162	0.335	0.782	0.277	0.151	0.235

Table 3-60: Full results of One Way ANOVAs for the high-fatigue trail for the whole of the second steady state (SS2-1) for each joint angular displacement variable for the left and right pedals

Variable	Side	*df*	MS	ε	*F*	*p*	η^2
Hip min	Left	4.000	<0.001	1.000	0.127	0.972	0.018
	Right	4.000	<0.001	1.000	0.095	0.983	0.013
Hip max	Left	4.000	<0.001	1.000	0.287	0.884	0.039
	Right	4.000	<0.001	1.000	0.057	0.994	0.008
θ_c at hip min	Left	4.000	<0.001	1.000	0.787	0.543	0.101
	Right	2.371	0.110	1.000	3.797	0.038*	0.352
θ_c at hip max	Left	4.000	0.981	1.000	0.582	0.678	0.077
	Right	4.000	<0.001	1.000	0.984	0.432	0.123
Knee min	Left	1.395	0.028	1.000	4.945	0.042*	0.414
	Right	1.231	0.055	1.000	3.881	0.077	0.357
Knee max	Left	4.000	<0.001	1.000	0.362	0.833	0.049
	Right	4.000	<0.001	1.000	1.970	0.127	0.220
θ_c at knee min	Left	4.000	<0.001	1.000	0.438	0.780	0.059
	Right	4.000	<0.001	1.000	0.773	0.552	0.099
θ_c at knee max	Left	4.000	<0.001	1.000	2.427	0.071	0.257
	Right	4.000	0.498	1.000	0.427	0.788	0.057
Ankle min	Left	2.244	0.005	1.000	3.059	0.071	0.304
	Right	4.000	0.002	1.000	1.410	0.257	0.168
Ankle max	Left	4.000	0.002	1.000	2.558	0.061	0.268
	Right	4.000	<0.001	1.000	1.542	0.217	0.181
θ_c at ankle min	Left	4.000	0.740	1.000	1.122	0.366	0.138
	Right	4.000	0.035	1.000	2.199	0.095	0.239
θ_c at ankle max	Left	2.652	0.002	1.000	3.155	0.054	0.311
	Right	4.000	0.013	1.000	1.912	0.136	0.215

Table 3-61 p-values for *post hoc* pair-wise comparisons of the joint angular displacement variables with significant ($p<0.05$) (i.e. crank angle at maximum right hip flexion and maximum left knee extension) main effects with (BON) and without (least significant difference (LSD)) Bonferroni correction

Right θ_c at max hip flex.

	2	3	4	5	
	0.206	0.204	0.112	0.038*	1
4	1.000	0.490	0.165	0.021*	2
3	0.434	1.000	0.243	0.043*	3
2	0.205	1.000	1.000	0.105	4
1	0.384	1.000	1.000	1.000	
	5	4	3	2	

Maximum left knee ext.

	2	3	4	5	
	0.095	0.110	0.079	0.017*	1
4	0.521	0.221	0.165	0.016*	2
3	0.275	1.000	0.652	0.028*	3
2	0.156	1.000	1.000	0.052	4
1	0.175	0.786	1.000	0.949	
	5	4	3	2	

3.7: Joint velocity kinematic data

3.7.1: Hip

Table 3-62: Full results of Two Way ANOVAs for the minimum hip angular velocity for the left and right legs

Side		High / low		Time		High / low x time	
		SS1,7 + R1	SS2-2	SS1,7 + R1	SS2-2	SS1,7 + R1	SS2-2
Left	*df*	1.000	1.000	2.081	3.000	4.000	3.000
	MS	1901	14671	39941	321.224	207.000	255.891
	ε	1.000	1.000	1.000	1.000	1.000	1.000
	F	1.262	8.811	10.189	1.977	0.212	1.848
	p	0.298	0.021*	0.002*	0.148	0.930	0.170
	η^2	0.153	0.557	0.593	0.220	0.029	0.209
Right	*df*	1.000	1.000	4.000	3.000	4.000	3.000
	MS	6413	624.446	2986	224.494	1102	71.161
	ε	1.000	1.000	1.000	1.000	1.000	1.000
	F	1.372	0.370	2.629	1.382	1.369	0.256
	p	0.286	0.565	0.059	0.280	0.274	0.856
	η^2	0.186	0.058	0.305	0.187	0.186	0.041

Table 3-63: Full results of Two Way ANOVAs for the maximum hip angular velocity for the left and right legs

Side		High / low		Time		High / low x time	
		SS1,7 + R1	SS2-2	SS1,7 + R1	SS2-2	SS1,7 + R1	SS2-2
Left	*df*	1.000	1.000	1.268	2.350	2.280	2.253
	MS	25347	19846	60926	1839	14520	1121
	ε	1.000	1.000	1.000	1.000	1.000	1.000
	F	54.293	9.519	13.290	4.970	22.361	4.868
	p	<0.001*	0.018*	0.004*	0.017*	<0.001*	0.020*
	η^2	0.886	0.576	0.655	0.415	0.762	0.410
Right	*df*	1.000	1.000	1.911	3.000	1.938	3.000
	MS	317.157	320.643	20823	315.000	15671	150.976
	ε	1.000	1.000	1.000	1.000	1.000	1.000
	F	0.110	0.125	13.737	1.036	13.679	0.749
	p	0.751	0.735	<0.001*	0.400	<0.001*	0.537
	η^2	0.018	0.020	0.696	0.147	0.695	0.111

Table 3-64: Full results of One Way ANOVAs for the maximum hip angular velocity in the left leg during the second steady state section (SS2-2) of the high and low fatigue trials separately

Trial	*df*	MS	ε	*F*	*p*	η^2
Low fatigue	3.000	189.708	1.000	0.912	0.452	0.115
High fatigue	2.292	2740	1.000	8.213	0.003*	0.540

Table 3-65: Full results of One Way ANOVAs (high/low) at each time window for the maximum hip angular velocity in the left leg during the second steady state section (SS2-2) of the fatigue trials.

Time window	*df*	MS	ε	*F*	*p*	η^2
1	1.000	6521	1.000	8.414	0.023*	0.546
2	1.000	9073	1.000	12.067	0.010*	0.633
3	1.000	5968	1.000	6.847	0.035*	0.494
4	1.000	812.250	1.000	3.952	0.087	0.361

3.7.2: Knee

Table 3-66: Full results of Two Way ANOVAs for the minimum knee angular velocity for the left and right legs

Side		High / low		Time		High / low x time	
		SS1,7 + R1	SS2-2	SS1,7 + R1	SS2-2	SS1,7 + R1	SS2-2
Left	*df*	1.000	1.000	1.502	1.559	1.577	1.858
	MS	13755	15098	20521	2247	15529	826.494
	ε	1.000	1.000	1.000	1.000	1.000	1.000
	F	13.016	11.919	3.776	7.634	9.128	4.130
	p	0.009*	0.011*	0.067	0.011*	0.006*	0.043*
	η^2	0.650	0.630	0.350	0.522	0.566	0.371
Right	*df*	1.000	1.000	1.854	3.000	1.790	3.000
	MS	654.229	3120	17779	157.357	14756	86.500
	ε	1.000	1.000	1.000	1.000	1.000	1.000
	F	0.151	1.075	6.571	1.516	14.091	0.516
	p	0.711	0.340	0.014*	0.244	0.001*	0.677
	η^2	0.025	0.152	0.523	0.202	0.701	0.079

Table 3-67: Full results of One Way ANOVAs for the minimum knee angular velocity in the left leg during the second steady state section (SS2-2) of the high and low fatigue trials separately

Trial	*df*	MS	ε	*F*	*p*	H^2
Low fatigue	3.000	252.250	1.000	2.195	0.119	0.239
High fatigue	2.224	1926	1.000	8.811	0.002*	0.557

Table 3-68: Full results of One Way ANOVAs (high/low) at each time window for the maximum hip velocity in the left leg during the second steady state section (SS2-2) of the fatigue trials.

Time window	*df*	MS	ε	*F*	*p*	η^2
1	1.000	15098	1.000	11.919	0.011*	0.630
2	1.000	5256	1.000	9.370	0.018*	0.572
3	1.000	3600	1.000	10.080	0.016*	0.590
4	1.000	930.250	1.000	2.721	0.143	0.280

Table 3-69: Full results of Two Way ANOVAs for the maximum knee angular velocity for the left and right legs

Side		High / low		Time		High / low x time	
		SS1,7 + R1	SS2-2	SS1,7 + R1	SS2-2	SS1,7 + R1	SS2-2
Left	*df*	1.000	1.000	1.614	1.890	2.096	3.000
	MS	18271	23948	65695	911.710	12799	113.438
	ε	1.000	1.000	1.000	1.000	1.000	1.000
	F	11.495	11.352	31.460	3.078	27.041	1.520
	p	0.012*	0.012*	<0.001*	0.082	<0.001*	0.239
	η^2	0.622	0.619	0.818	0.305	0.794	0.178
Right	*df*	1.000	1.000	1.703	3.000	1.768	3.000
	MS	7592	3210	16874	92.024	16014	35.762
	ε	1.000	1.000	1.000	1.000	1.000	1.000
	F	2.053	0.729	8.408	0.841	19.662	0.423
	p	0.202	0.426	0.008*	0.489	<0.001*	0.739
	η^2	0.255	0.108	0.584	0.123	0.766	0.066

3.7.3: Ankle

Table 3-70: Full results of Two Way ANOVAs for the minimum ankle angular velocity for the left and right legs

Side		High / low		Time		High / low x time	
		SS1,7 + R1	SS2-2	SS1,7 + R1	SS2-2	SS1,7 + R1	SS2-2
Left	*df*	1.000	1.000	1.463	3.000	1.696	3.000
	MS	6661	203.062	15944	830.854	12357	366.604
	ε	1.000	1.000	1.000	1.000	1.000	1.000
	F	5.524	0.120	3.449	2.499	10.983	1.233
	p	0.051	0.740	0.082	0.087	0.003*	0.323
	η^2	0.441	0.017	0.330	0.263	0.611	0.150
Right	*df*	1.000	1.000	1.941	3.000	2.019	3.000
	MS	3023	129.018	12298	409.113	14509	25.113
	ε	1.000	1.000	0.485	1.000	0.505	1.000
	F	1.228	0.059	3.021	1.610	8.252	0.069
	p	0.310	0.816	0.089	0.222	0.005*	0.976
	η^2	0.170	0.010	0.335	0.212	0.579	0.011

Table 3-71: Full results of Two Way ANOVAs for the maximum ankle angular velocity for the left and right legs

Side		High / low		Time		High / low x time	
		SS1,7 + R1	SS2-2	SS1,7 + R1	SS2-2	SS1,7 + R1	SS2-2
Left	*df*	1.000	1.000	1.220	3.000	1.633	3.000
	MS	14072	5439	91378	30.292	11747	82.604
	ε	1.000	1.000	1.000	1.000	1.000	1.000
	F	28.206	3.864	19.830	0.205	15.827	1.177
	p	0.001*	0.090	0.001*	0.891	<0.001*	0.342
	η^2	0.801	0.356	0.739	0.029	0.693	0.144
Right	*df*	1.000	1.000	2.321	3.000	1.713	3.000
	MS	16173	1586	12172	17.214	20834	96.452
	ε	1.000	1.000	1.000	1.000	1.000	1.000
	F	11.739	1.109	21.519	0.172	20.495	0.510
	p	0.014*	0.333	<0.001*	0.914	<0.001*	0.680
	η^2	0.662	0.156	0.782	0.028	0.774	0.078

Table 3-72: Full results of One Way ANOVAs for the high-fatigue trail for the whole of the second steady state for each joint velocity variable for the left and right pedals

Variable	Side	*df*	MS	ε	*F*	*p*	η^2
Hip min	Left	4.000	206.725	1.000	2.352	0.078	0.252
	Right	4.000	268.288	1.000	0.739	0.573	0.095
Hip max	Left	4.000	1622	1.000	7.008	<0.001*	0.500
	Right	4.000	257.287	1.000	0.688	0.606	0.090
Knee min	Left	2.461	2157	1.000	5.319	0.012*	0.432
	Right	4.000	148.662	1.000	1.095	0.378	0.135
Knee max	Left	3.116	526.703	1.000	3.972	0.020*	0.362
	Right	4.000	171.875	1.000	1.648	0.190	0.191
Ankle min	Left	4.000	155.213	1.000	0.865	0.497	0.110
	Right	4.000	158.500	1.000	0.313	0.866	0.050
Ankle max	Left	4.000	206.275	1.000	1.325	0.285	0.159
	Right	4.000	82.900	1.000	0.440	0.778	0.059

Table 3-73 *p*-values for *post hoc* pair-wise comparisons of the joint velocity variables with significant ($p<0.05$) (i.e. right hip maximum and left knee minimum and maximum) main effects with (BON) and without (least significant difference (LSD)) Bonferroni correction

Left hip max

	2	3	4	5	
	0.366	0.633	0.681	0.002*	1
4	0.426	0.619	0.183	0.003*	2
3	0.081	1.000	0.309	0.008*	3
2	0.035*	1.000	1.000	0.043*	4
1	0.018*	1.000	1.000	1.000	
	5	4	3	2	

Left knee min

	2	3	4	5	
	0.773	0.248	0.390	0.018*	1
4	0.204	0.027*	0.007*	0.001*	2
3	0.850	1.000	0.471	0.085	3
2	0.013*	0.067	0.265	0.020*	4
1	0.181	1.000	1.000	1.000	
	5	4	3	2	

Left knee max

	2	3	4	5	
	0.961	1.000	0.961	1.000	1
4	0.163	1.000	0.163	1.000	2
3	0.197	1.000	0.197	1.000	3
2	0.011*	0.108	0.011*	0.108	4
1	0.136	1.000	0.136	1.000	
	5	4	3	2	

Appendix 4: Figures for all variables in Chapter 8.

4.1: Kinematic data

4.1.1: Segment angular displacement

4.1.1.1: Thigh angular displacement

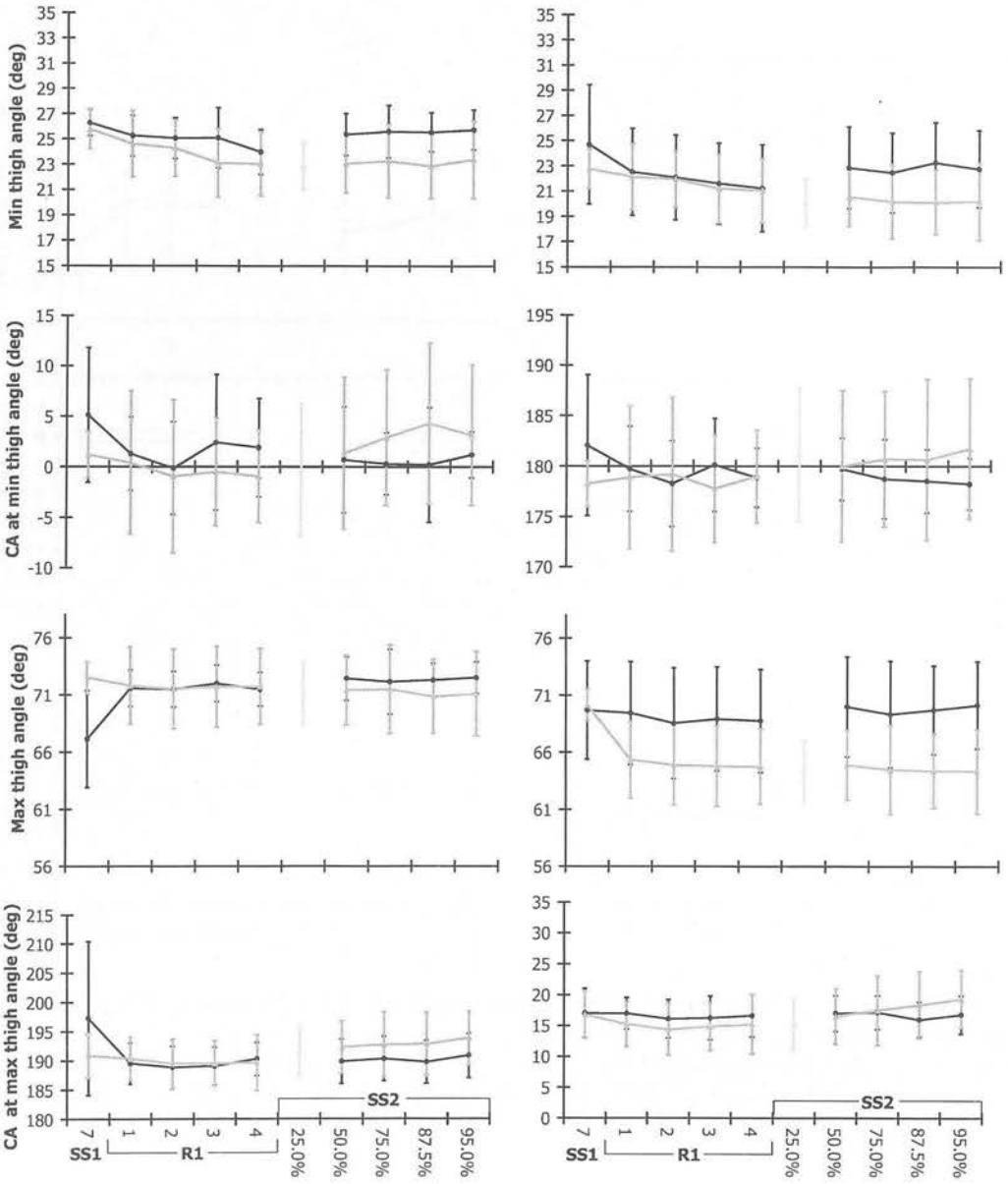

Figure 4-1: Group mean (±SD) minimum and maximum thigh angles and the crank angles (CA) at which they occurred (left column: left leg, right column, right leg). (black diamonds: low fatigue trial, grey triangles: high fatigue trial, lighter grey 25% in SS2-1 in high fatigue; SS1 & R1: minutes, SS2: % time to failure)

4.1.1.2: Shank angular displacement

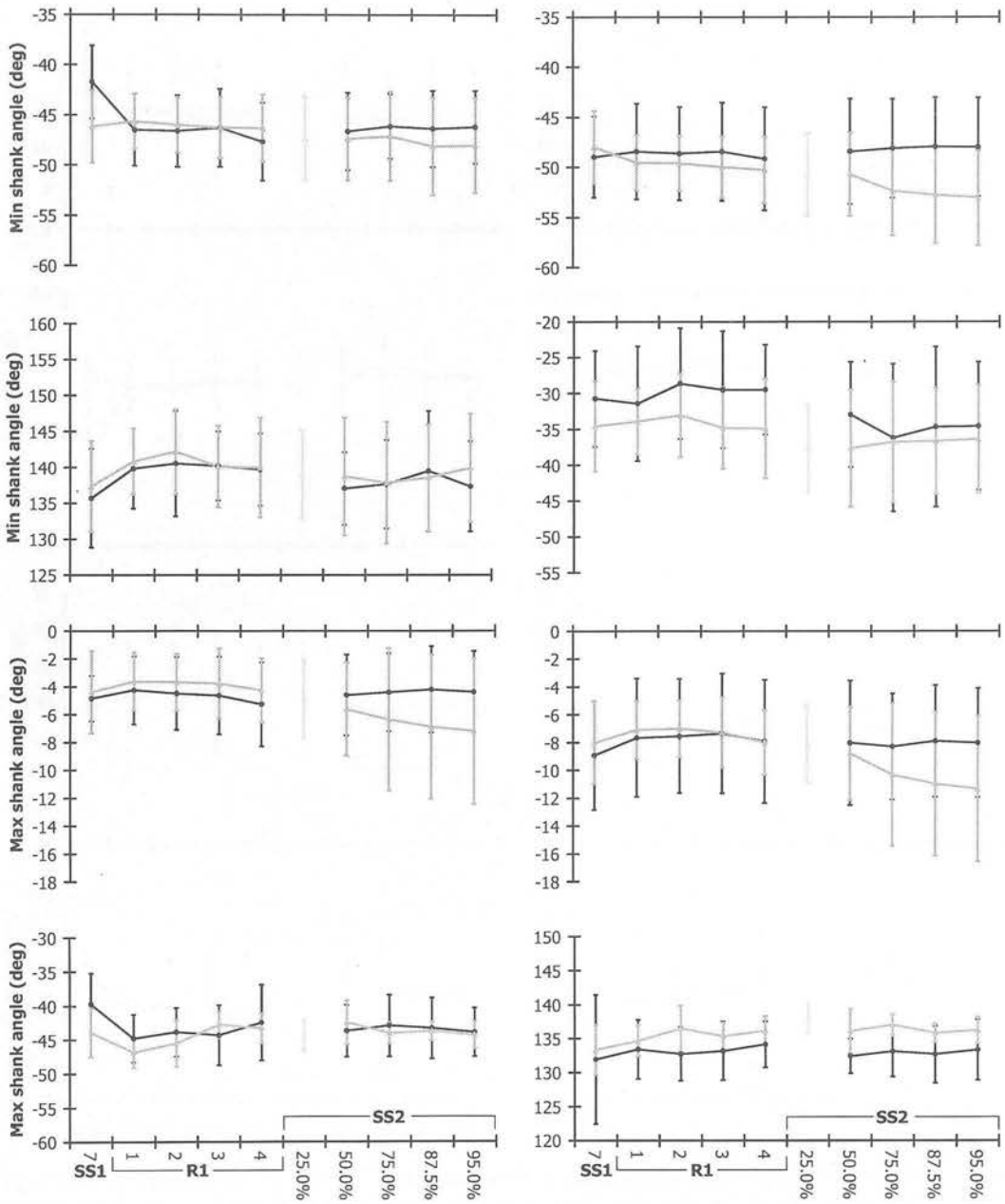

Figure 4-2: Group mean (±SD) minimum and maximum shank angles and the crank angles (CA) at which they occurred (left column: left leg, right column, right leg). (black diamonds: low fatigue trial, grey triangles: high fatigue trial, lighter grey 25% in SS2-1 in high fatigue; SS1 & R1: minutes, SS2: % time to failure)

4.1.1.3: Foot angular displacement

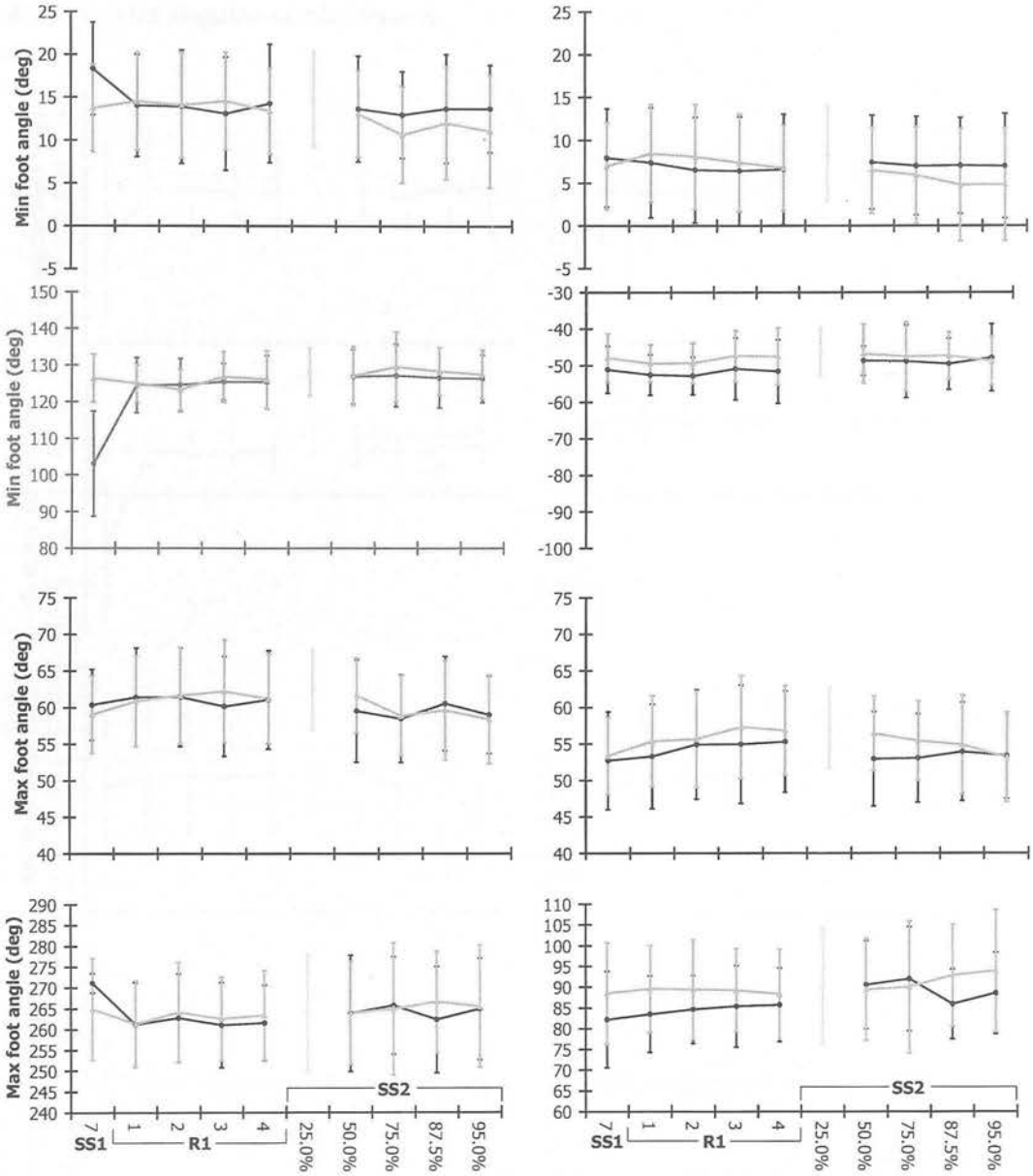

Figure 4-3: Group mean (±SD) minimum and maximum foot angles and the crank angles (CA) at which they occurred (left column: left leg, right column, right leg). (black diamonds: low fatigue trial, grey triangles: high fatigue trial, lighter grey 25% in SS2-1 in high fatigue; SS1 & R1: minutes, SS2: % time to failure)

4.1.2: Joint angular displacement

4.1.2.1: Hip angular displacement

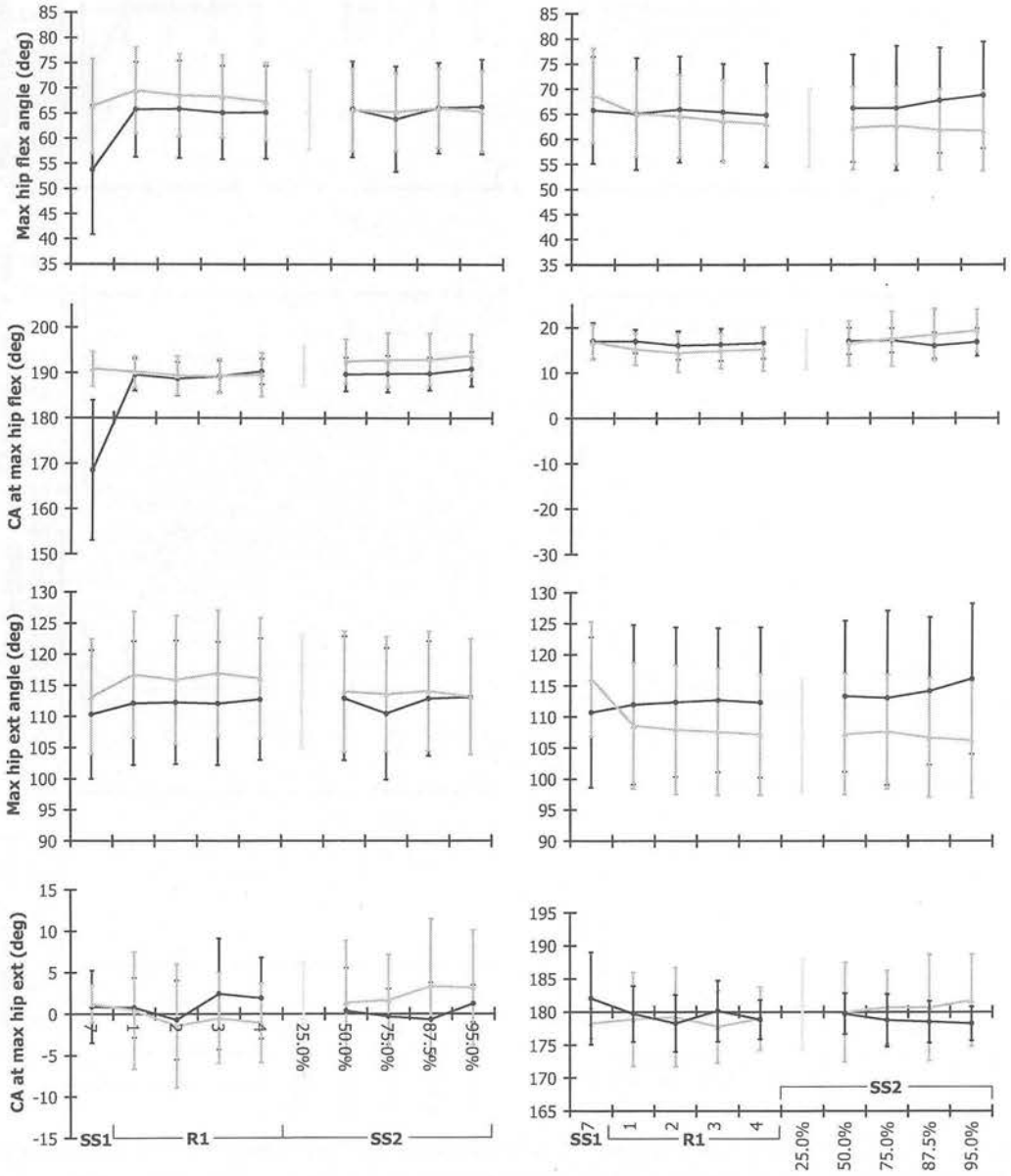

Figure 4-4: Group mean (±SD) maximum hip flexion and extension angles and the crank angles (CA) at which they occurred (left column: left leg, right column, right leg). (black diamonds: low fatigue trial, grey triangles: high fatigue trial, lighter grey 25% in SS2-1 in high fatigue; SS1 & R1: minutes, SS2: % time to failure)

4.1.2.2: Knee angular displacement

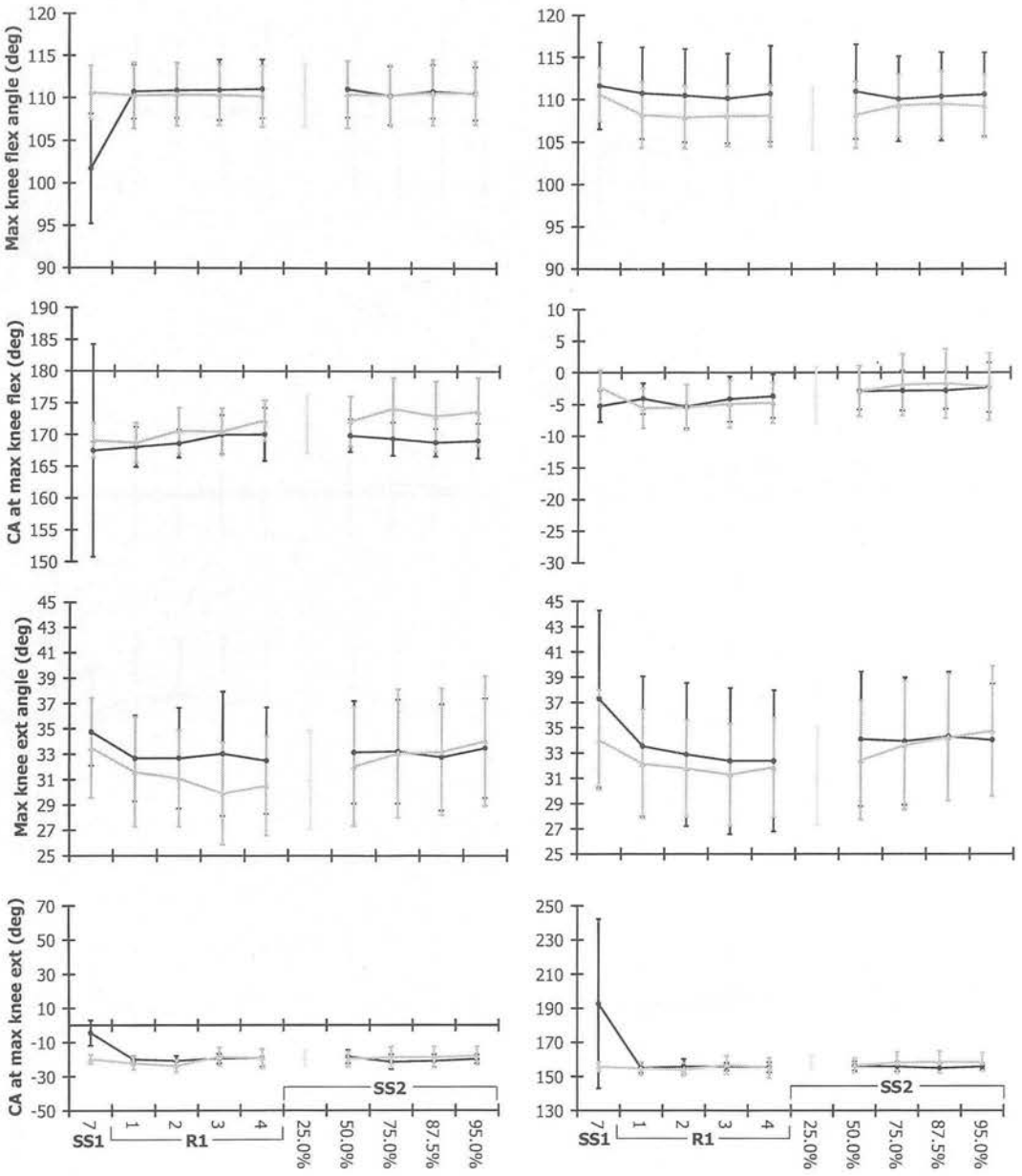

Figure 4-5: Group mean (±SD) maximum knee flexion and extension angles and the crank angles (CA) at which they occurred (left column: left leg, right column, right leg). (black diamonds: low fatigue trial, grey triangles: high fatigue trial, lighter grey 25% in SS2-1 in high fatigue; SS1 & R1: minutes, SS2: % time to failure)

4.1.2.3: Ankle angular displacement

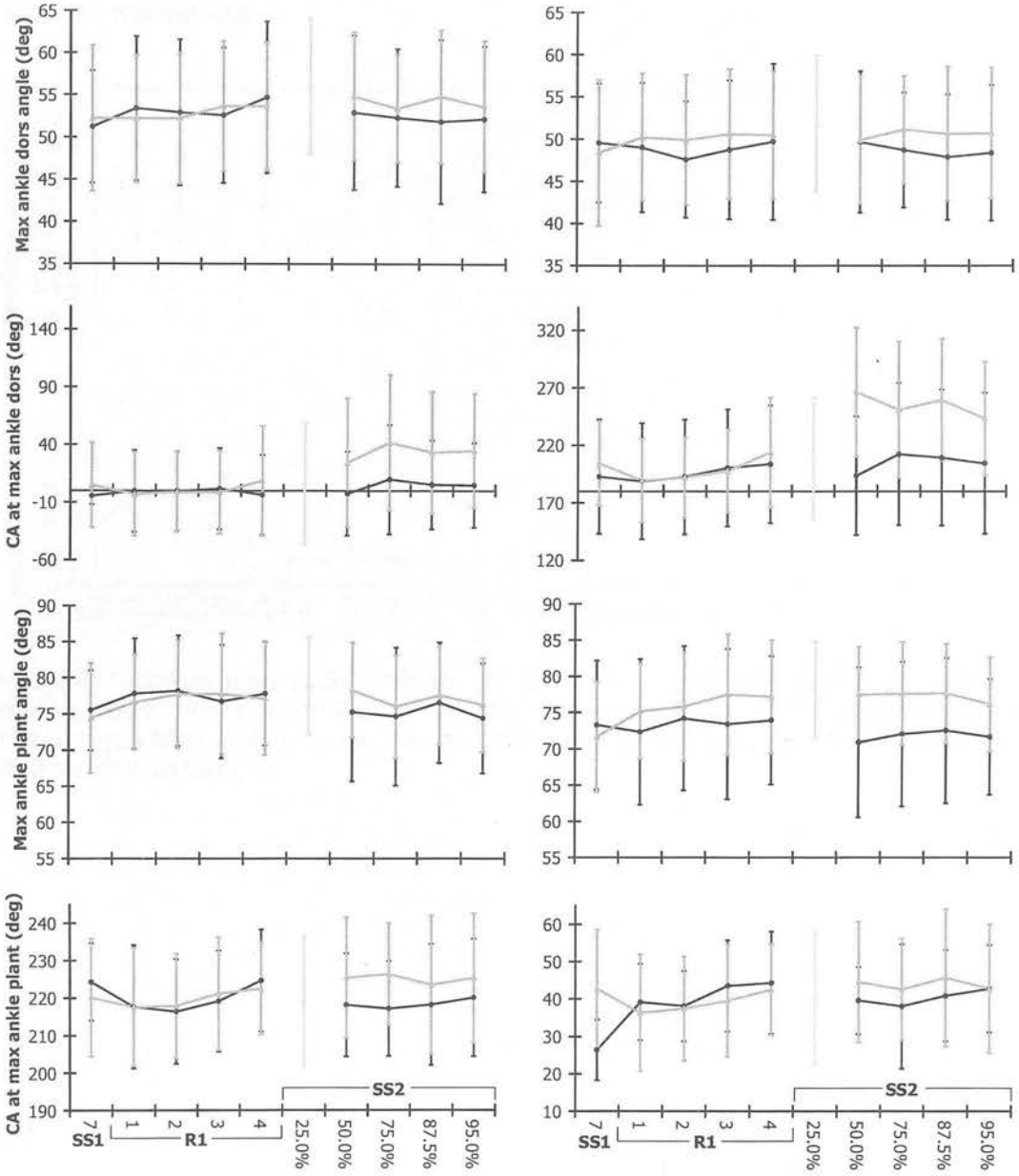

Figure 4-6: Group mean (±SD) maximum ankle plantar-flexion and dorsiflexion angles and the crank angles (CA) at which they occurred (left column: left leg, right column, right leg). (black diamonds: low fatigue trial, grey triangles: high fatigue trial, lighter grey 25% in SS2-1 in high fatigue; SS1 & R1: minutes, SS2: % time to failure)

4.1.3: Joint velocity

4.1.3.1: Hip velocity

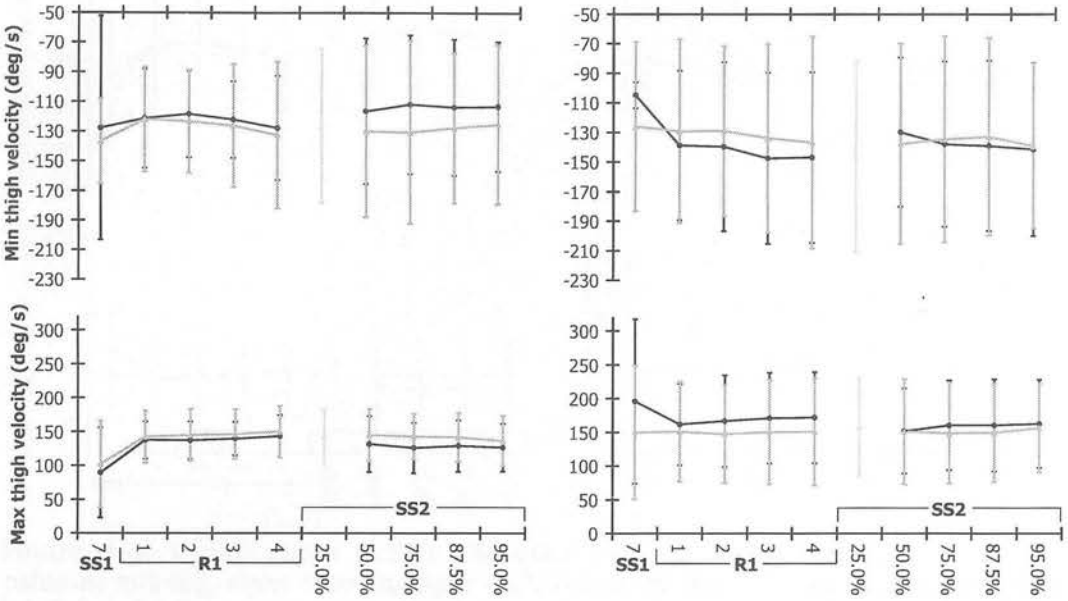

Figure 4-7: Group mean (±SD) minimum and maximum hip velocities (left column: left leg, right column, right leg). (black diamonds: low fatigue trial, grey triangles: high fatigue trial, lighter grey 25% in SS2-1 in high fatigue; SS1 & R1: minutes, SS2: % time to failure)

4.1.3.2: Knee velocity

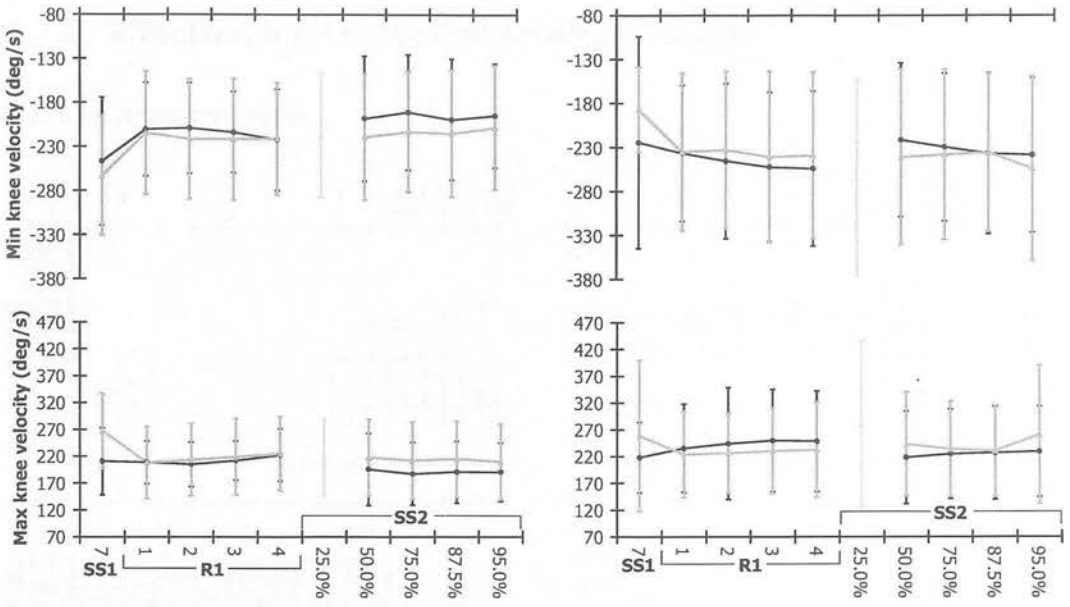

Figure 4-8: Group mean (±SD) minimum and maximum knee velocities (left column: left leg, right column, right leg). (black diamonds: low fatigue trial, grey triangles: high fatigue trial, lighter grey 25% in SS2-1 in high fatigue; SS1 & R1: minutes, SS2: % time to failure)

4.1.3.3: Ankle velocity

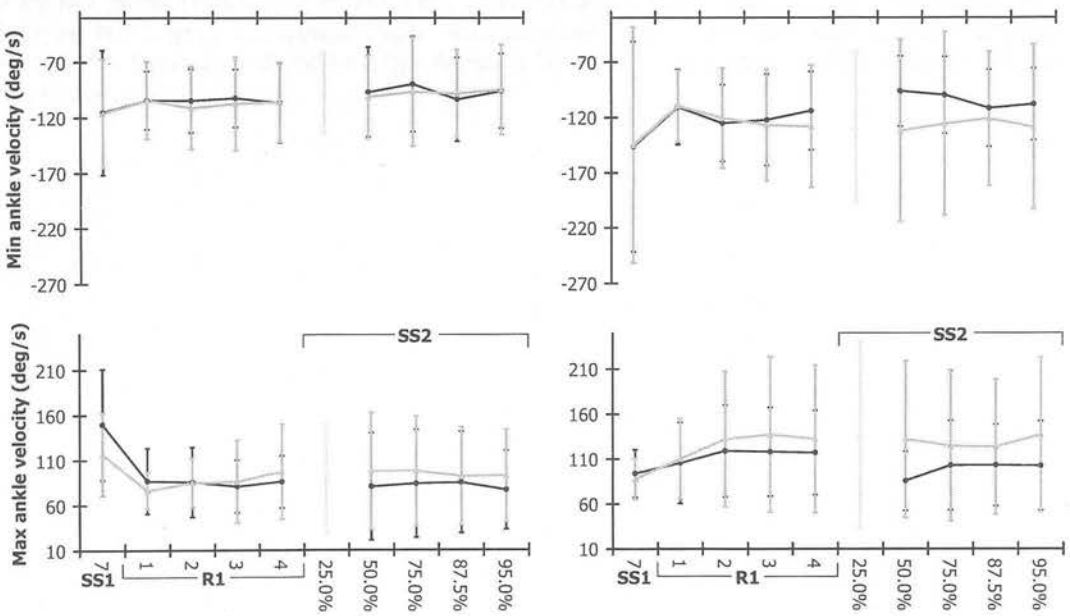

Figure 4-9: Group mean (±SD) minimum and maximum ankle velocities (left column: left leg, right column, right leg). (black diamonds: low fatigue trial, grey triangles: high fatigue trial, lighter grey 25% in SS2-1 in high fatigue; SS1 & R1: minutes, SS2: % time to failure)

4.2: Kinetic data

4.2.1: Effective, ineffective and resultant forces

4.2.1.1: Resultant force

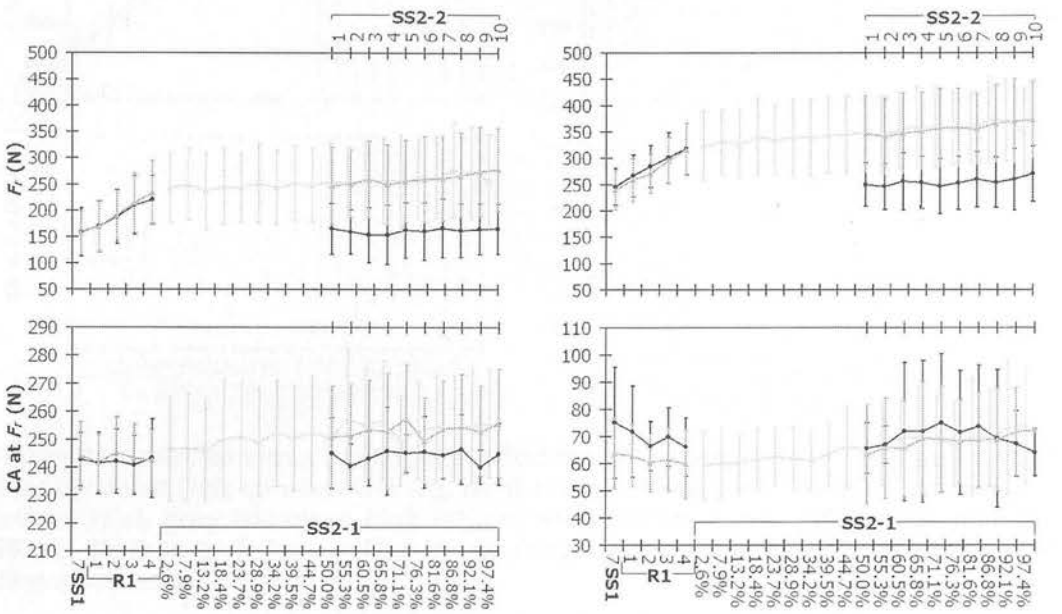

Figure 4-10: Group mean (±SD) peak resultant forces and the crank angle at which they occurred (left column: left leg, right column, right leg). (black diamonds: low fatigue trial, grey triangles: high fatigue trial) (lower x-axis: SS1 & R1: minutes, SS2-1: % time to failure in high fatigue trial (lighter grey), upper x-axis: SS2-2: time windows)

4.2.1.2: Effective force

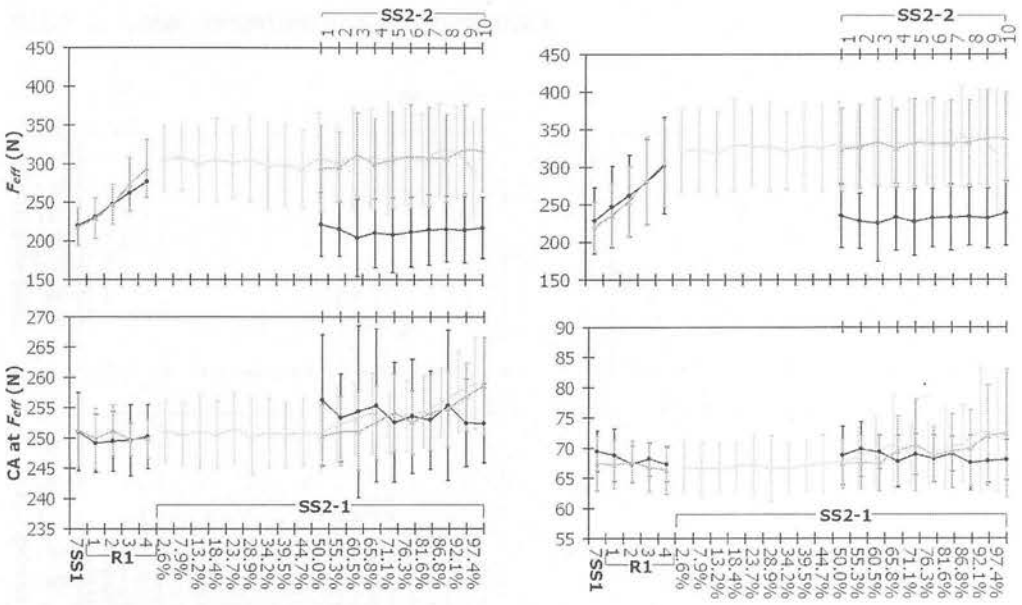

Figure 4-11: Group mean (±SD) peak effective forces and the crank angle at which they occurred (left column: left leg, right column, right leg). (black diamonds: low fatigue trial, grey triangles: high fatigue trial) (lower x-axis: SS1 & R1: minutes, SS2-1: % time to failure in high fatigue trial (lighter grey), upper x-axis: SS2-2: time windows)

4.2.1.3: Ineffective force

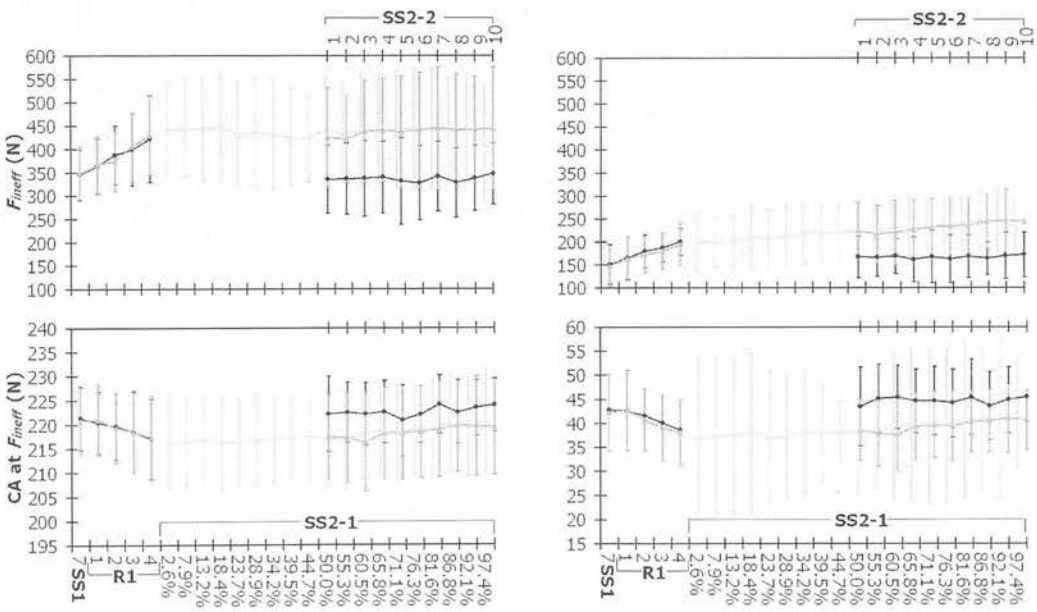

Figure 4-12: Group mean (±SD) peak ineffective forces and the crank angle at which they occurred (left column: left leg, right column, right leg). (black diamonds: low fatigue trial, grey triangles: high fatigue trial) (lower x-axis: SS1 & R1: minutes, SS2-1: % time to failure in high fatigue trial (lighter grey), upper x-axis: SS2-2: time windows)

4.2.2: Work and power

4.2.2.1: Total, negative and positive work

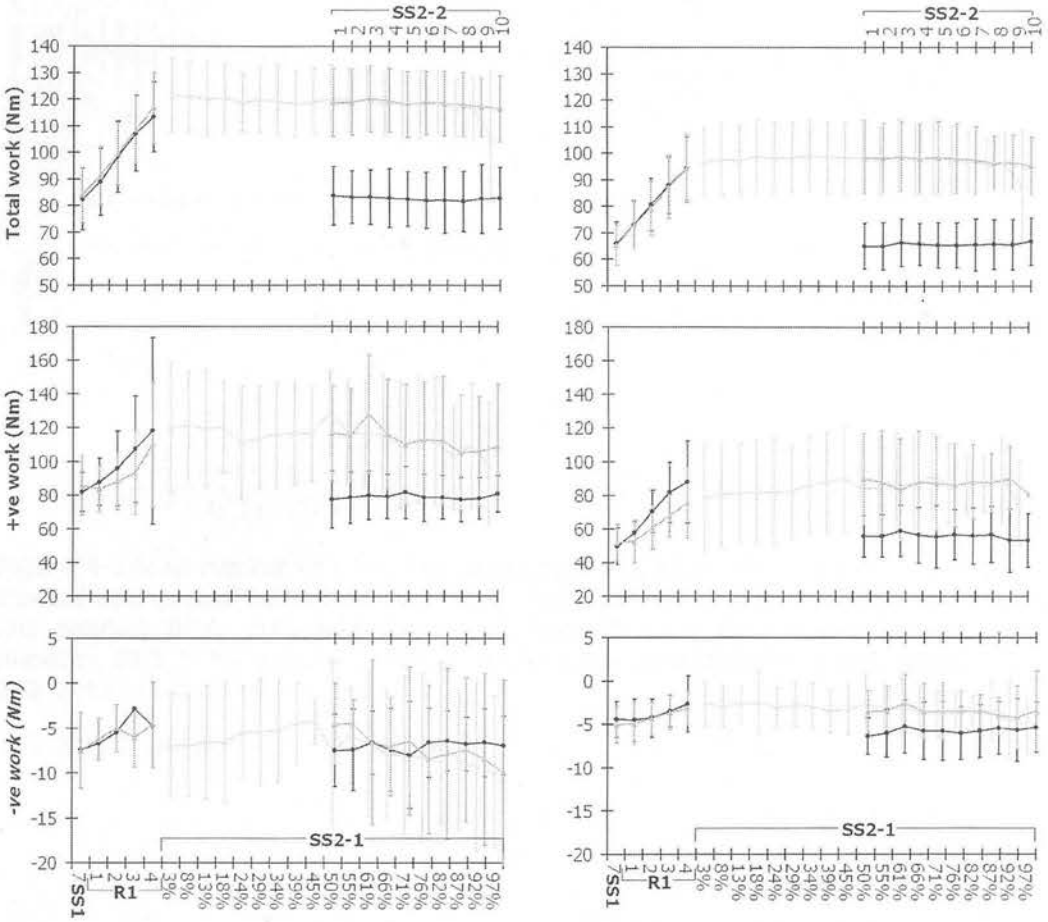

Figure 4-13: Group mean (±SD) sum total, positive and negative work (left column: left leg, right column, right leg). (black diamonds: low fatigue trial, grey triangles: high fatigue trial) (lower x-axis: SS1 & R1: minutes, SS2-1: % time to failure in high fatigue trial (lighter grey), upper x-axis: SS2-2: time windows)

4.2.2.2: Crank angle at which positive work started and ended

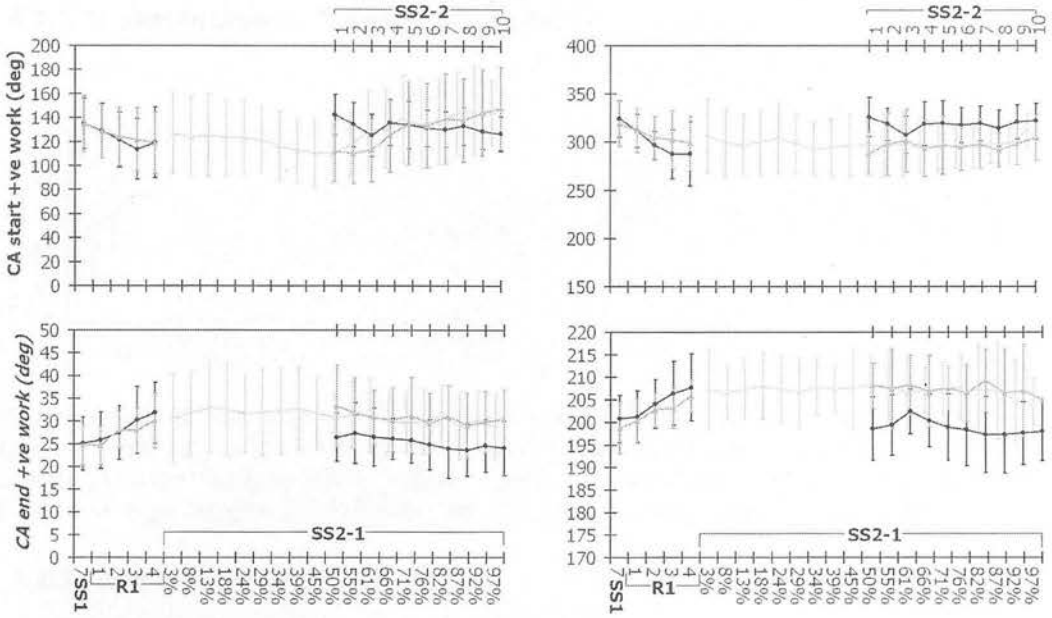

Figure 4-14: Group mean (±SD) of crank angle (CA) at which positive (+ve) work started and ended (left column: left leg, right column, right leg). (black diamonds: low fatigue trial, grey triangles: high fatigue trial) (lower x-axis: SS1 & R1: minutes, SS2-1: % time to failure in high fatigue trial (lighter grey), upper x-axis: SS2-2: time windows)

4.2.2.3: Mean power

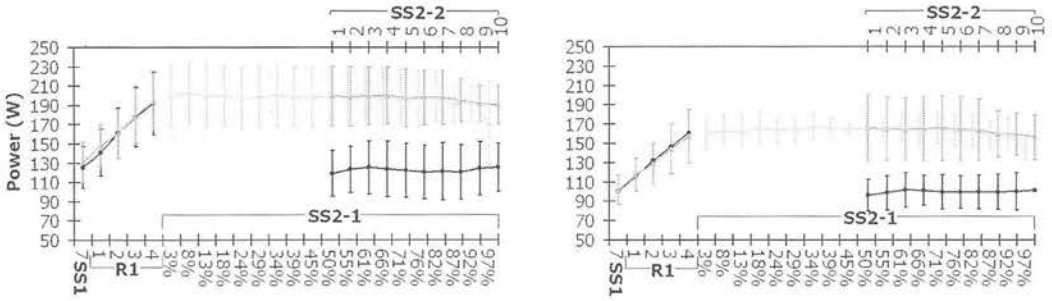

Figure 4-15: Group mean (±SD) mean power (left column: left leg, right column, right leg). (black diamonds: low fatigue trial, grey triangles: high fatigue trial) (lower x-axis: SS1 & R1: minutes, SS2-1: % time to failure in high fatigue trial (lighter grey), upper x-axis: SS2-2: time windows)

4.2.3: Instantaneous Index of Effectiveness and crank velocity

4.2.3.1: Instantaneous Index of Effectiveness

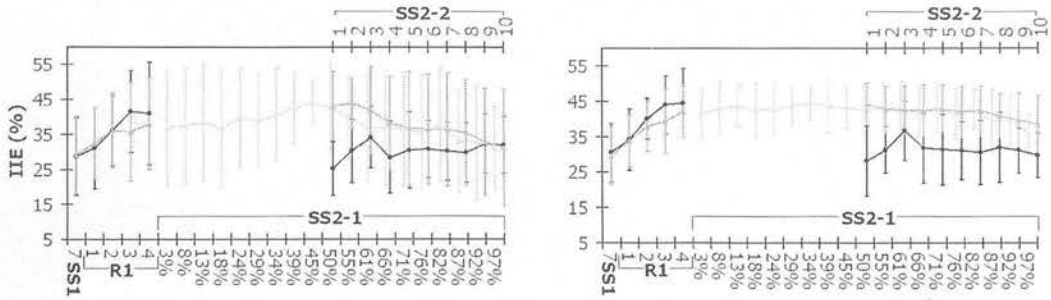

Figure 4-16: Group mean (±SD) Instantaneous Index of Effectiveness (IIE) (left column: left leg, right column, right leg). (black diamonds: low fatigue trial, grey triangles: high fatigue trial) (lower x-axis: SS1 & R1: minutes, SS2-1: % time to failure in high fatigue trial (lighter grey), upper x-axis: SS2-2: time windows)

4.2.3.2: Crank velocity

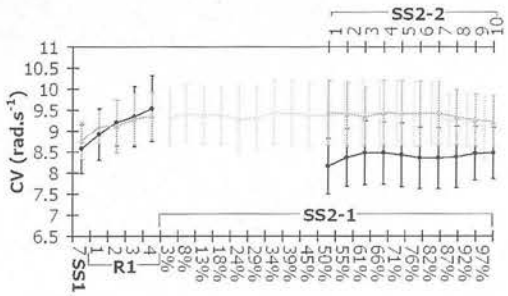

Figure 4-17: Group mean (±SD) mean crank velocity (left column: left leg, right column, right leg). (black diamonds: low fatigue trial, grey triangles: high fatigue trial) (lower x-axis: SS1 & R1: minutes, SS2-1: % time to failure in high fatigue trial (lighter grey), upper x-axis: SS2-2: time windows)